UNIVERSITY OF Southampton

University of Southampton Research Repository
ePrints Soton

UNIVERSITY OF SOUTHAMPTON

FACULTY OF SOCIAL AND HUMAN SCIENCES

School of Geography

Quantifying the Impacts of Climate and Land Use Changes on the Hydrological Response of a Monsoonal Catchment

by

Nor Aizam Adnan

Thesis for the degree of Doctor of Philosophy

October 2010

UNIVERSITY OF SOUTHAMPTON

ABSTRACT
FACULTY OF SOCIAL AND HUMAN SCIENCES
SCHOOL OF GEOGRAPHY
Doctor of Philosophy

QUANTIFYING THE IMPACTS OF CLIMATE AND LAND USE CHANGES ON
THE HYDROLOGICAL RESPONSE OF A MONSOONAL CATCHMENT
by Nor Aizam Adnan

The effect of climate change and land use change on runoff generation and flooding has received great attention in many hydrological modelling studies. However, currently many hydrologists are still uncertain how much these two factors contribute to runoff generation, particularly in monsoon catchments. The river Kelantan is in one of the states in Malaysia, which experiences monsoon flooding, was used to investigate these two factors in effecting hydrologic response changes. Therefore, this study tries to provide a framework mainly to i) *identify trends in the River Kelantan streamflow and explore the possible causes of that change, including precipitation change and land use changes*; ii) *disentangle and quantify the precipitation and land use and change effects on hydrological response and potential flooding in the River Kelantan catchment using past and current hydrological events*; iii) *simulate the future runoff scenarios (i.e. 2020s, 2050s and 2080s) using precipitation and land use changes projections.*

Historical data on the streamflow of the River Kelantan and precipitation in the Kelantan catchment were investigated for trends using the Mann-Kendall non-parametric method. In summary, a general pattern has been revealed in which streamflow is increasing in all seasons upstream, but is decreasing in the dry season downstream. The pattern in streamflow downstream is fairly well matched by increases in precipitation in the wet season and decreases in precipitation in the dry season. In the upstream area, the increases in streamflow are not matched by universal increases in precipitation, but rather by increases in the wet season only and decreases in the dry season, as for the downstream sub-catchment. The increases in streamflow in the dry season are, thus, more difficult to explain and land use change been performed and has been proven to cause a partial contribution of such observed trend in the upstream area. Subsequently, a study using the lumped HEC-HMS model to disentangle these two factors in causing hydrologic response changes (i.e. peak discharge and runoff volume) was performed. The results demonstrate that for the upstream area precipitation and land use changes led to the greatest increases in peak discharge and runoff volume. In contrast, in the downstream area the results suggest that precipitation trends may have led to significant increases in runoff generation. The simulation of hydrologic response in the future (i.e. 2020s, 2050s and 2080s) showed that climate change (i.e. precipitation change) has positive links with the peak discharge and runoff volume. If precipitation estimated to decrease using PRECIS A1B storyline from the SRES scenario, runoff was predicted to decrease and *vice-versa*. For the land use change impact, the scenario involved reducing the forested area, increasing the agricultural and built-up land caused runoff estimated to increase from 2020s to 2080s. The combined scenario demonstrated that precipitation change coupled with land use change has a significant impact to changes in peak discharge and runoff volume for the study area compared to climate change and land use change studies alone.

Table of Contents

List of Figures

List of Tables

DECLARATION OF AUTHORSHIP

I, **Nor Aizam Adnan,** declare that the thesis entitled **Quantifying the Impacts of Climate and Land Use Changes on the Hydrological Response of a Monsoonal Catchment** and the work presented in the thesis are both my own, and have been generated by me as the result of my own original research. I confirm that:

- this work was done wholly or mainly while in candidature for a research degree at this University;

- where any part of this thesis has previously been submitted for a degree or any other qualification at this University or any other institution, this has been clearly stated;

- where I have consulted the published work of others, this is always clearly attributed;

- where I have quoted from the work of others, the source is always given. With the exception of such quotations, this thesis is entirely my own work;

- I have acknowledged all main sources of help;

- where the thesis is based on work done by myself jointly with others, I have made clear exactly what was done by others and what I have contributed myself;

- parts of this work have been published as:

i) Adnan NA, Atkinson PM. 2010. Exploring the impact of climate and land use changes on streamflow trends in a monsoon catchment. *International Journal of Climatology* 31 (6): 815 -831.

ii) Adnan NA, Atkinson PM. 2009. Exploring the causes of increasing streamflow trends in a monsoon catchment. In, Proceedings 8th International Symposium and Exhibition on Geoinformation (Joint 8th International Symposium and Exhibition on Geoinformation 2009 & ISPRS Symposium on Spatial Decision Support System and LBS 2009, Crown Plaza Mutiara Hotel, 10 – 11 August, 2009. Kuala Lumpur.

Signed: …………………………………………………………………..

Date:……………………………………………………………………….

Acknowledgements

First and foremost, Alhamdulillah, all praises to the Almighty Allah for his merciful and giving me the strength and making this possible. I also owe my gratitude to all those people who have made this dissertation possible and because of whom my PhD research experience has been one that I will cherish forever.

Special thanks to Ministry of Higher Education and MARA University of Technology (UiTM), Malaysia for the scholarships and providing me with this great opportunity to pursue my PhD in United Kingdom.

My deepest gratitude is to my supervisor, Professor Peter M. Atkinson. I have been amazingly fortunate to have a supervisor who gave me the freedom to explore on my own, and at the same time the guidance to recover when my steps faltered. He has also been commenting on my views and helping me understand and enrich my ideas. His patience and support helped me overcome many crisis situations and finish this dissertation. I would also like to express my special thanks to Professor Ted Milton, Professor Paul Carling and Dr Ellois Biggs for generously given their time, expertise and useful advises to better my work. I thank them for their contribution and their good-natured support.

Many friends have helped me stay sane through these difficult years. Special thanks to Noreha, Moon and Sis Zaharah.Their support and care helped me overcome setbacks, enlightened, and help me to stay focused on my study over the many years of our friendship. They have consistently helped me keep perspective on what is important in life and shown me how to deal with reality. I am also grateful to the Keluarga_Soton, MSA and ISOC communities that helped me adjust to a new country.

Most importantly, none of this would have been possible without the love and patience of my family. I would like to express my heart-felt gratitude to my mom, *Jamaliah Zainal* and my brothers and sisters. Finally, gratitude also goes to my beloved husband, *Mohamed Adnan Idris* and my son, *Ahmad FakhrulRazi*. They have been a constant source of love, concern, support and strength all these years.

Abbreviations

ADB	Asian development bank
AMC	Antecedent moisture condition
AOGCMs	Atmospheric-ocean general circulation models
ASTER	Advanced Spaceborne Thermal Emission and Reflection Radiometer
ATCOR	Atmospheric and Topographic Correction
AVHRR	Advanced Very High Resolution Radiometer
BMRC	Bureau of Meterological Research Centre
CCC	Canadian Climate Centre
CCIRG	Climate Change Impacts Review Group
CGCM	Canadian General Circulation Model
CGIAR-CSI	Consultative Group for International Agriculture Research–Consortium for Spatial Information
CLUE	Conversion of Land Use Change and its Effects
CO_2	Carbon dioxide
CSIRO	Commonwealth Scientific and Industrial Research Organisation
DEM	Digital elevation model
DID	Department of Irrigation and Drainage, Malaysia
DN	Digital number
DSM	Digital surface model
DTM	Digital terrain model
ERS	Earth Resources System
ET	Evapotranspiration
ETM^+	Enhanced Thematic Mapper
GCM	General circulation model
GCP	Ground control point
GHG	Greenhouse gases
GIS	Geographical information system
HadCM	Hadley Centre coupled model
HEC-HMS	Hydrologic Engineering Centre – Hydrologic Modelling System
IPCC	Intergovermental Panel on Climate Change
IRS	India Remote Sensing
LiDAR	Light detection and ranging

LULC	Land use and land cover
MACRES	Malaysian Remote Sensing Centre
MMD	Malaysia Meteorological Department
MODIS	Moderate-Resolution Imaging Spectrometer
MPI	Max-Planck Institute for Meteorology
MRI	Meteorological Research Institute of Japan
MSS	Multispectral Scanner
NAHRIM	National Hydraulics Research Institute of Malaysia
NE	North-east
NSGEV	Non-stationary generalized extreme value model
PDM	Probability-distributed model
PET	Potential evaporation
PFE	Permanent forest estate
PM	Peninsular Malaysia
PRECIS	Providing Regional Climates for Impact Studies
RCM	Regional climate model
RegHCM-PM	Regional physically-based hydrological-atmospheric model
RMSE	Root mean square error
SAR	Synthetic Aperture Radar
SCS CN	Soil Conservation Service Curve number
SEA	Southeast Asian
SPOT	Satellite Pour l'Observation de la Terre
SRES	Special report on the emission scenarios
SRTM	Shuttle Radar Topographic Mapping
SWAT	Soil and Water Assessment Tool
TCPD	Malaysia Department of Town, Country and Regional Planning
TM	Thematic Mapper
TR 55	Technical Reports 55
UH	Unit hydrograph
UKMOH	United Kingdom Meteorological Office high resolution model
USACE	United States Army Corps of Engineers
USGS	United State Geological Survey
UTM	Universal Transverse Mercator
VIC	Variable Infiltration Capacity

Chapter 1
Introduction

1.1 RESEARCH CONTEXT

Flooding is an environmental hazard that can occur almost all around the world. In general, flooding is defined as an overflowing of water onto land that is normally dry (Junk, 1997; Mays, 2001). Based on a report by the World Meteorological Organization (WMO), flooding was found to be the third most common natural disaster contributing to high numbers of deaths and loss of properties. Floods occur almost every year in tropical countries, whereas for other basins the frequency of occurrence may vary dramatically. Although floods are an integral part of the dynamics of any river channel, floods have created hazards for human communities for many years (Wohl, 2000). Historical records of flooding have shown that the impacts of flooding on people's livelihoods are unavoidable (Tapsell et al., 2002; Jonkman and Kelman, 2005; Grothmann and Reusswig, 2006).

Floods affect all aspects of life and may have discouraged economic development in highly flood-prone areas (Chan and Parker, 1996). For example, flood events that have been recorded in India have killed up to 1,000 people per year and damaged millions of hectares of crop land (De et al., 2005). Furthermore, it can be a major hazard to human health and well-being as well as to the society's infrastructure (Foody et al., 2004). Another example is the flooding in the autumn of 2000, triggered by monsoon rainfall, which caused extensive damage in several Southeast Asian (SEA) countries of $251 million. Further, four million people were made homeless and were at risk for diarrhea, cholera, dengue fever, and malaria. Based on the report from Malaysia's National

Register of River Basins Study in the year 2003, about 29,000 km^2 or 9% of the total land area and more than 4.82 million people (22%) in Malaysia are affected by flooding annually (Shafiee et al., 2004). Table 0-1 adapted from Wohl (2000) shows a partial listing of historical devastating floods and estimated losses.

Table 0-1. Partial listing of historical devastating floods.

Location	Date	Cause	Damages
Nile River, Egypt	Ca. 747 B.C	Rainfall	Unspecific
Mississippi River	March 1543	Rainfall	Unspecific
China	1642	Rainfall	300,000 dead
James River, USA	May 1771	Rainfall	City of Richmond, Virginia destroyed, 150 drowned
Connecticut River, USA	May 1874	Reservoir failure	$1 million damages, 143 dead
Yangtze River, China	1911	Rainfall	100,000 dead
Texas, USA	Dec. 1913	Rainfall	$9 million damages, 177 dead
Lower Mississippi River basin, USA	March 1927	Rainfall	$300 million damages, 313 dead
Yellow River, China	1933	Dike failure	18,000 dead
Kazvin District, Iran	Aug. 1954	Not stated	2000+dead

1.2 FLOODING IN A MONSOON CATCHMENT

Floods occur almost every year in tropical countries due to the high magnitude and intensity of rainfall. Based on historical records, almost all natural rivers are characterized by floods. There are several types of flooding in Asia: extensive basin flooding due to riverbank overflow, inundation basin flooding backwater effects from tidal influence affecting lower reaches, inland floodi

ng which is caused by poor drainage from inland flood prone areas and urban flash flooding which is caused by inadequate drainage and storage systems to cater for rapid urbanization (Hamzah, 2005). In Malaysia, there are two major types of flooding seriously impacting human life and the environment, which are flash flooding and monsoon flooding (Chan and Parker, 1996; Shafiee et al., 2004).

Flood events have become more frequent in the 1990s to 2000s due to several factors. Climate change and changes in land use pattern have been attributed as causes of increases in flood frequency and magnitude as well as changes in hydrological response (Pinter et al., 2006; Guo et al., 2010). Climate change may lead to higher rainfall

2

intensities and prolonged rainfall (Nyarko, 2002), which may cause increases in flood frequency, magnitude and duration in the affected area (Wilson, 2004) especially for monsoon catchment areas (Zehe et al., 2006). On the other hand, rapid urbanization leads to changes in the land use pattern due to associated activities such as deforestation, agriculture, mining, road construction, reservoir construction (Wohl 2000; Hassan et al., 2005; Mustafa et al., 2005) encroachment of settlements into floodplain areas (Kundzewich and Takeuchi, 1999; Islam and Sado, 2000) and improper management. Such changes have caused disturbance of the natural water flow (Nawaz, 2001) as well as the hydrological response.

In order to deal with the above changes, there is an urgent need for reliable modelling of flood events to quantify how these changes affect the hydrologic response as well as the frequency and magnitude of floods (Foody et al., 2004). Much research has been undertaken to mitigate different types of floods, but limited research has been done on monsoon flooding. Hydrological models coupled with a geographical information system (GIS), remote sensing and climate change models (i.e. regional climate models) are potentially useful tools for assessing the changes in hydrological response (i.e. peak flow and runoff volume) and flooding.

1.3   RESEARCH PROBLEM AND JUSTIFICATION

Flooding in Malaysia has been reported since the 1800s, with specific attention paid to monsoon flooding and flash floods. The first reported severe flood event took place in 1886 and caused extensive damage in Kelantan, one of the states of Malaysia (Chan & Parker, 1996). In 1926, flooding affected most of Peninsular Malaysia, resulting in extensive damage to property, road systems and agricultural land and crops (Malaysia National Committee, 1976; DID, 2008). In 1967, disastrous floods surged across the Kelantan, Terengganu and Perak river basins, taking 55 lives (Chan, 1995). Again, in 1971, a flood swept across many parts of the country (Chan, 1997; Chan, 2002).

The River Kelantan is important because it is subject to the most severe monsoon flooding in Malaysia (DID, 2004). Further, it is perceived that flooding is increasing along the river, presenting a significant management problem. Flooding appears to be increasing in Kelantan in terms of frequency as well as magnitude (Sooryanayana,

1988; DID, 1992; MMD, 2007). For example, intense and prolonged precipitation in 2002 caused flooding of a total area of 1,640 km^2 with an affected population of 714,287. Again, in the year 2004 flooding also occurred and the frequency increased in 2006 and 2007 when the study area experienced flooding twice per year: in 2006 flooding occurred on 12 February and 19 December, and in 2007 flooding occurred on 08 January and 13 December. The history of flooding in Kelantan and its impact is shown in Table 0-2. However, little research has been conducted to understand and quantify how these factors contribute to flooding and hydrological response in the River Kelantan monsoon catchment.

The River Kelantan has become prone to flood disasters, and this is potentially due to meteorological factors (i.e. climate change), rapid changes in land use, and weaknesses in development planning and monitoring. Increases in population, coupled with urbanization, may contribute to residential and industrial development in the floodplain. Rapid land use changes from the 1970s to 2000s, especially in relation to deforestation (due to logging activities) and conversion to agricultural land (rubber and oil palm) have been reported, especially in the upstream catchment area (Wan, 1996; Jamaliah, 2007). For example, in Kelantan, the rate of urbanization from the 1970s to 1990s was 7% but slowed in the 2000s to 1.4% (Hassan, 2004) revealing that substantial land use changes have occurred in the area. Furthermore, human activities such as unplanned rapid settlement development, uncontrolled construction of buildings and problems in relation to drainage management are factors, which may cause increases in runoff (Pradhan, 2009). These changes may lead to higher peak flow and runoff volume when coupled with heavy rainfall in the monsoon season (October to March) as normally experienced in the study area. However, currently no study has been performed to quantify the effects of land use changes (e.g., deforestation, urbanisation) and precipitation changes on increased runoff and flooding in the River Kelantan catchment, and this uncertainty currently hampers land use planning and water resource management activities.

Land use change due to human activities may influence hydrological processes such as evapotranspiration and infiltration (Wooldridge et al., 2001). Deforestation may cause increases in overland and river flow due to lower evapotranspiration capacity (Niehoff et al., 2002). In contrast, urbanization may lead to a greater impervious surface area

(e.g., pavements, roads, car parks and buildings) and may cause infiltration excess to occur when poor infiltration conditions are coupled with high rainfall intensities (Moussa et al., 2002; Chahinian et al., 2005). Several studies have found that changes of land use from forest to other land uses (e.g., built-up, agricultural or bare land) may cause increases in runoff volume, frequency of flooding and peak discharge (Bronstert et al., 2002; Xiaoming et al., 2007; Wang et al., 2008).

Table 0-2. Flood impact in Kelantan from the year 1983 to 2004 with total number of evacuees, total amount of damage in Ringgit Malaysia (RM) and in USD.

Year	Total number of evacuees	Total amount of damage (in Ringgit Malaysia)	Total amount of damages (in USD)
2004	10476	14317800	3767842
2003	2228	5554400	1461684
2002	No record	1420000	373684
2001	5800	8462700	2227026
2000	506	4940620	1300163
1999	No record	1924440	506432
1998	136	1628455	428541
1997	No record	922020	242637
1996	No evacuation	735795	193630
1995	1172	1485095	390814
1994	441	2413922	635243
1993	13587	1512816	398110
1992	743	329256	86646
1991	No record	1427872	375756
1990	4581	1036100	272658
1989	No record	-	-
1988	41059	-	-
1987	402	3336589	878576
1986	7968	6092454	1603277
1985	No record	-	-
1984	7177	1998268	525860
1983	33816	-	-

It is important to quantify these perceived changes in runoff generation and flooding. Further, it is important to quantify the extent to which these changes are due to changes in precipitation (which themselves may be due to global climate change), to known land use changes or both. The answer will determine future land use planning policy in the area, as well as flood management policy and decisions. Thus, the River Kelantan was chosen as a site of some environmental importance.

1.4 AIMS OF THE STUDY

This study focuses on understanding past and future hydrological responses, which have led or may lead to flooding in a monsoon catchment (i.e. the River Kelantan catchment). The specific objectives of the study are as follows:

1. **To identify trends in streamflow and explore the possible causes of that change, including precipitation change due to climate change and, to a lesser extent, land use change factors.**

Historical data for not more than 31 years on the stream flow of the River Kelantan and precipitation in the Kelantan catchment were investigated for trends using the Mann-Kendall non-parametric method (Man, 1945; Kendall, 1975). In addition the non-parametric Sen's slope test was used to determine the magnitude of changes exhibited in the area (Salmi, 2002).

Land use classification maps were also derived from two multi-temporal satellite sensor images (Landsat Thematic Mapper (TM) imagery of 7 August 1988 and 28 May 2000). Land use change analysis was then performed and its plausible effect on streamflow changes was assessed.

The questions which need to be answered for this objective are:

    i)   Is there any trend exhibited in streamflow and precipitation (annual, seasonal and monthly) within the River Kelantan catchment? If yes, where and how much?

    ii)   Is the observed streamflow trend accompanied by a similar trend in precipitation as well as by land use changes?

2. **To develop a hydrological semi-distributed model to quantify runoff for previous (i.e. 1988) and current (i.e. 2004) storm events.**

An event-based runoff model for the River Kelantan catchment was developed using the semi-distributed HEC-HMS model. The runoff model was developed for both historic (1988) and more recent (2004) hydrological events to represent the specific

characteristics of the hydrologic response during each period. The 1988 event represents conditions prior to, and the 2004 event represents conditions after, significant deforestation, afforestation and expansion of agricultural land. The sensitivity analysis was done prior to the model calibration. The model validation was done using 1990 and 2006 events. The analysis tries to answer the following question:

    i)   Is the semi-distributed rainfall-runoff model adequate to represent the observed hydrograph of the River Kelantan catchment?

3. To disentangle and quantify the land use and precipitation changes effects on the hydrological response and flooding in the River Kelantan catchment.

This study attempts to quantify the relative contributions of precipitation and land use changes to hydrological response in the River Kelantan catchment. The effects of precipitation and land use changes, both singly and in combination, on peak flow and runoff volume were investigated using a storm event in 2004 as a baseline. Attention was given to differences in peak discharge and runoff volume resulting from the replacement of land use and precipitation data for 2004 with the equivalent data of 1988. This knowledge is currently missing, but is important because presently planners and decision-makers can only speculate about the causes of increased streamflow and flooding in the river Kelantan catchment. The analysis tries to answer the followings questions:

    i)   How much of the change in hydrological response between 2004 and 1988 is due to precipitation changes?

    ii)   How much of the change in hydrological response between 2004 and 1988 is due to land use changes?

    iii)   How much change in hydrological response between 2004 and 1988 is expected due to a combination of precipitation and land use changes?

4. **To simulate flooding in the future (i.e. 2020s, 2050s and 2080s) using what-if scenarios of precipitation and land use changes in the River Kelantan catchment.**

The 2004 runoff model that was developed in the second objective was used and considered as a current model (or baseline model) to run what-if analysis for future scenarios. The what-if analysis is used to simulate what happens to flooding in the future (i.e. in the year 2020s, 2050s and 2080s) by evaluating changes in peak discharge and runoff volume. Land use change scenarios were predicted from the observed land use change that has occured previously in the study area. Precipitation changes were adopted from the model developed by the Hadley Centre, United Kingdom known as Providing Regional Climates for Impact Studies (PRECIS HadCM3).

Chapter 2
Understanding the hydrological response and flooding through climate change, land use change and rainfall-runoff modelling

2.1 INTRODUCTION

In general, flooding is a result of heavy or continuous rainfall exceeding the absorptive capacity of soil and the flow capacity of rivers, streams, and coastal areas. In other perspectives, flooding results in the inundation of an area by a rise of water by both dam failure or extreme rainfall duration and intensity in which life and properties in the affected area are under risk (Nyarko, 2002). Rainfall can produce very widespread surface flooding where water encounters dry ground and infiltrates, raising the groundwater volumes (Gumbricht et al., 2004). This phenomenon has produced a large impact, which has destroyed livelihoods and altered environments, particularly in Asian countries (i.e. China, Bangladesh, India, Malaysia and Indonesia). Much research has been done and is still going on to understand flood characteristics and how to control flooding (Chan and Parker, 1996; Bates et al., 1997; Mertes, 2000; Horrit et al., 2001; Brivio et al., 2002).

This chapter specifically deals with hydrological modelling, and the climate variability and land use change factors that influence the flooding phenomenon with emphasis on the role played by each of the factors on hydrological response and flooding.

2.2 CLIMATE VARIABILITY AND ITS EFFECT ON FLOODING

The climate variability, includes all forms of climate inconsistency (i.e. deviations from long-term statistics) and can be considered as a natural phenomenon and happens occasionally from time to time. Such changes are reversible and non-permanent such as the El Nino and La Nina phenomena. Others form of climate variability such as temperature, precipitation and discharge (Schulze, 2000). The present study of a River Kelantan time-series focused on the climate variability of precipitation and discharge.

In general, understanding of observational and historical hydroclimatological data (i.e. temperature, precipitation, evapotranspiration, discharge, etc.) associated with climate change is important, especially, for water resource planning and management. Changes in river discharge and precipitation patterns can be important climatic indicators for environmental risk problems such as global warming and flooding (Chang, 2007). In monsoon areas associated with annual flooding due to high intensity of rainfall, knowledge about changes in hydrological data (i.e. streamflow and precipitation) is very important to understand flooding risk and to allow preparation for mitigation.

The first comprehensive review of climate change and its effects on flooding and runoff was reported by the Intergovermental Panel on Climate Change (IPCC) (1996). The report suggested that in some regions predicted increases in precipitation are likely to cause higher runoff. Again, the IPCC (2007) reported that Southeast Asia (SEA) countries may be at the greatest risk of increased flooding due to increased sea levels and flooding from rivers. Furthermore, several studies also suggested that the mean temperature had increased by $0.1 - 0.3^{\circ}$ C per decade between 1951 and 2000, with rainfall showing a decreasing trend during $1960 - 2000$ and sea levels rising between $1 - 3$ mm per year in SEA (IPCC, 2007; ADB, 2009). The same studies also reported that although rainfall showed decreased trends in several SEA countries, environmental problems such as floods, droughts and tropical cyclones have become more intense and frequent and led to extensive damage to human life. The possible climate change effects on global water resources in the 21st century simulated by IPCC (2007) are shown in Table 2-1.

Several studies state that increases in temperature have caused increases in evapotranspiration in rivers, dams and other water reservoirs, which have led to

decreased water availability for agricultural irrigation, domestic and non-domestic usage as well as hydropower generation (Boer and Dewi, 2008; Cuong, 2008; Perez, 2008). Furthermore, decreases in precipitation have caused decreases in streamflow and water level in many dams, especially during El Nino years which subsequently have led to decreased water availability and increased water stress for SEA populations. Meanwhile, during La-Nina years increases in streamflow were observed which have led to runoff and flooding. Similar flooding events have also been experienced in the River Kelantan catchment, for example, heavy flooding in 1988 and 2000 during La-Nina periods.

Table 2-1 Possible impact of climate change on water resources as predicted by IPCC, 2007.

Phenomenon and direction of trend	Likelihood of future trends based on projections for 21st century using SRES* scenarios	Projected impact on water resources
Over most land areas, warmer and fewer cold days and nights, warmer and more frequent hot days and nights	Virtually certain	Effects on water resources relying on snow melt; effects on some water supplies
Warm spells/heat waves. Frequency increases over most land areas	Very likely	Increased water demand; water quality problems, e.g., algal blooms
Heavy precipitation events. Frequency increases over most areas	Very likely	Adverse effects on quality of surface and groundwater; contamination of water supply; water scarcity may be relieved
Area affected by drought increases	Likely	More widespread water stress
Intense tropical cyclone activity increases	Likely	Power outages causing disruption of public water supply
Increased incidence of extreme high sea level (excludes tsunamis)	Likely	Decreased freshwater availability due to saltwater intrusion

*SRES – Special report on the emission scenarios

It has been demonstrated that changes in the magnitude and frequency of flooding can be attributed to climate change, particularly due to precipitation, temperature, evapotranspiration and sea level change (Esteban et al., 1998; Meehl et al., 2000; Bronstert, 2003; Haylock et al., 2005; Ntegeka and Willems, 2007; Oudin et al., 2008). More intense precipitation may lead to increases in flood peaks and may subsequently cause increases in the extent of flood inundation. Much research has been carried out to demonstrate how variations in precipitation, temperature and land use may contribute to changes in flood frequency (Meehl et al., 2000; Wang et al., 2008). Three widely used methods are normally adopted to understand and quantify the effects of climate change on flooding; the first is based on an analysis of time-series trends exhibited in the historical hydrological data, secondly, analysis of historical or current meteorological data coupled with hydrological models and, thirdly a combination of climate models (i.e. a general circulation model, GCM and regional climate models, RCMs) with hydrological data for future projections (Bronstert et al., 2002; Prudhomme et al., 2002). The same three broad approaches are adopted in this thesis.

2.3 STATISTICAL TIME-SERIES TRENDS OF STREAMFLOW AND PRECIPITATION

Statistical methods have been implemented widely to detect time-series trends exhibited in hydrometeorological data such as temperature, precipitation and streamflow. Understanding trends exhibited in hydrological data is crucial for guiding water resource planning and management, and assessing climate variability and change impacts on water resources (Xia et al., 2004; Chen et al., 2006). Linear trends of a hydrological time series can be detected using non-parametric statistical tests such as the Spearman's rho, Seasonal Kendall and Mann-Kendall tests (Kahya and Kalayci, 2004). In particular, the Mann-Kendall test has received great attention because it is the only non-parametric test suitable to be used in climatic and hydrologic studies (Yu et al., 1993). This monotonic time-series model was used due to its advantages: simplicity, capability of handling non-normal and missing data distributions and robustness to the effects of outliers and gross data errors (Kahya and Kalayci, 2004; Xu et al., 2005; Modarres and daSilva, 2007). Many researchers from all over the world have used these parametric and non-parametric methods to detect trends in hydrometeorological data.

Two tests (i.e. Mann-Kendall and stationary versus deterministic trend) were applied to detect trends in annual and seasonal precipitation for north, central and south of Italy (Yu et al., 1993). Meteorological time-series data covering the period 1961 to 2006 were used. Yu et al. (1993) found that on annual cumulated precipitation, no significant trend was detected using a 90% confidence level. However, in northern Italy, a decreasing trend was detected in winter at a rate of -1.47mm year^{-1}. A study by Kahya and Kalayci (2004) used five tests (Sen's T, Spearman's Rho, Mann-Kendall, seasonal Kendall and Sen's estimator of slope). They found that a decreased trend was detected in western Turkey, whereas, no trend was exhibited in the eastern area. They also concluded that the first four tests provide the same findings in identifying the existence of a trend.

A study to quantify long-term trends in annual precipitation and runoff in the Korean river basins was done by Bae et al. (2008) using the Mann-Kendall test. They found that in the spring season, runoff decreased and associated with decreases in precipitation, accompanied by rising temperatures which subsequently reduced soil moisture. Similarly Birsan et al. (2005) using the Mann-Kendall test attributed increased streamflow trend within 48 watersheds in Switzerland as probably due to air temperature changes in the mountain basins (i.e. due to the fact that this area is the most vulnerable to temperature changes which affect rainfall) and no association with precipitation was found. The result was strengthened with a good correlation between streamflow trends and basins characteristics such as mean basin elevation, glacier coverage and mean soil depth.

Cheung et al. (2008) used the *t*-test parametric method and regression for annual time-series and found no significant changes in rainfall within an Ethiopian watershed. For the seasonal rainfall the test found significant decreases in June to September rainfall. Observation at gauge level showed that rainfall experienced changes over time in Ethiopia, suggesting that the parametric test was not successful in detecting rainfall trends in the study area. However, Longobardi and Villani (2009) have used the Student *t*-test and Mann-Kendall test to detect precipitation trends in Southern Italy. Both tests managed to find significant positive and negative trends over the 30 year data period used. Linear regression analysis and the Mann-Kendall test were also used to assess the relationship between rainfall, land use and runoff changes in a Southern Malawi

catchment and trends in precipitation and temperature in an Iranian catchment (Rahimzadeh et al., 2008; Mbano et al., 2009). The method found that rainfall and forest area have decreased significantly which led to decreases in streamflow. Although trends in precipitation and temperature were found in the Iranian catchment (Rahimzadeh et al., 2008), no explanation of the relationship between these two datasets was reported. According to Onoz and Bayazit (2003) the parametric t-test has less power than the non-parametric Mann–Kendall test when the probability distribution is skewed, but, in many practical applications, they can be used interchangeably, with identical results in most cases.

Delgado et al. (2010) used a parametric test which accounts for the skewness of the data (i.e. non-stationary generalized extreme value model (NSGEV)) and non-parametric methods (i.e. Mann-Kendall test) together with linear regression to detect trends in discharge data for the Mekong River in SEA countries. They had found that the NSGEV was the most powerful method to detect trends in average flood, followed by the Mann-Kendal test and finally linear regression. The NSGEV was the most powerful method in trend detection due to its power of detection in the presence of changing variance. Although Mann-Kendall is not as powerful as NSGEV, it does show that the method was competent and widely implemented in many studies for trend detection in hydrometeorological data (discharge, flooding, etc.).

At the national scale, a study by Tangang et al. (2007) investigated temperature warming trends and interannual variability in Malaysia using linear regression and the Student's t-test. The study revealed that the temperature records for most regions in Malaysia are positively influenced by global warming. The study used seasonal temperature data records for over 41 years (i.e. 1961-2002) and found that on a seasonal basis, the temperature has increased by $2.7\,\text{C} - 4.0^{\text{o}}\text{C}$ over 100 years. Moreover, a study related to long-term trend analysis of precipitation in the Asian Pacific was carried out by Xu et al. (2005). From the 30 rivers studied, four rivers including the Johor River located in southeast Peninsular Malaysia indicated significant increasing precipitation trends at the 95% significance level. Furthermore, the study suggested that, in general, catchments from tropical monsoon regions (i.e. Malaysia, Indonesia and Thailand) exhibited significant precipitation trends due to climate change compared to humid and

temperate zones. However, no regional trend analysis was performed due to lack of available data.

2.4 CLIMATE CHANGE MODELS

Natural and anthropogenic factors are known to cause global warming (IPCC, 2007). Natural forcing has occurred over thousands of years and involves interactions between the ocean and atmosphere and has caused climate variations on yearly, decadal and century time scales. In contrast, anthropogenic factors are due to human intervention activities (i.e. deforestation, agriculture, urbanization) which have contributed, amongst other effects, to increases in greenhouse gases (GHG) concentration in the atmosphere (MMD, 2009). At present, many climate models have been developed to understand the impact of climate change for the future. Two widely implemented climate change models are the Atmosphere-Ocean General Circulation Models, also known as global climate models (GCM) and regional climate models (RCM).

A GCM simulates the whole Earth's climate for long periods (i.e. decades, centuries) based on the laws of physics of the oceans, and the exchange processes between the Earth's surface and/or the atmosphere and biosphere. The model attempts to mathematically simulate 3-D grid processes of the Earth system as a consequences of an increase in atmospheric CO_2 (i.e. instantaneous doubling of CO_2 equilibrium simulations as well as increases of CO_2 incrementally over a number of model years) on the mean global climate (IPCC, 1995; Shackley et al., 1998; Bronstert, 2003; Chen et al., 2006). Due to its role in representing climate change for the whole Earth the spatial resolution used is generally coarse (i.e. 300-600 km in the horizontal direction and around 1 km in the vertical direction). GCMs have been developed by many researchers and scientists in different countries such as Australia (i.e. Commonwealth Scientific and Industrial Research Organisation (CSIRO-MK3.0) (Gordon et al., 2002), the National Center for Atmospheric Research, USA (CCSM3) (Smith and Gent, 2002; Collins et al., 2004; Collins et al., 2006), the United Kingdom Meteorological Office high resolution model (UKMO-HadCM3 and UKMO-HadGEM1) (Pope et al., 2000; Lipscomb, 2001; Johns et al., 2006), the Canadian Centre for Climate Modelling and Analysis (CGCM3.1(T47)) (Kim et al., 2002; Flato, 2005), the the Meteorological Research Institute of Japan (MRI-CGCM2.3.2) (Yukimoto and Noda, 2003) and Max-

Planck Institute for Meteorology (ECHAM5/MPI-OM) (Roeckner et al., 2003; Jungclaus et al., 2005).

Although many GCMs are available, comparison between these GCMs for future climate changes are difficult to evaluate simultaneously due to the fact that each GCM result can differ significantly. Furthermore, the GCM climate change models and climate change impacts models for future scenarios propagate uncertainties in the available input data and knowledge (Shackley et al., 1998). For example, a study by Maurer and Duffy (2005) have used ten different GCMs with multiple emission scenarios (i.e. unchanging CO_2 and 1% per year increasing CO_2) for the Sacramento-San Joaquin Basin, California. The study found that uncertainties in projected streamflow for the period of 21 to 40 years, and 51 to 70 years from the observed period of 1960 – 1999 were due to inter-model variability between the 10 GCMs. However, significant detection of changes in streamflow due to climate change were found (i.e. streamflow increases in winter and decreases in summer). Furthermore, a study by Gosling et al. (2010) found that considerable uncertainty in the magnitude and the sign of regional runoff changes using different GCMs modesl. However, runoff changes for regions that experience large runoff increases and decreases (i.e. Central Asia and the Mediterranean) have much less uncertainty. Uncertainty was also found to be higher for all three GCM models (i.e. HadCM3, CCGCM2 and CSIRO-Mk2) compared to two emission scenarios (A2 and B2) for future climate uncertainty simulations of Thrushel catchment, Cornwall UK (Prudhomme and Davies, 2005). All the scenarios showed a decreased in annual mean flow (ANN) with median changes between 3.9% (CSIRO-Mk2) to 14.4% (CCGCM2)) because all the GCMs used underestimated ANN during current conditions and this underestimation is propagated to future projections (Prudhomme and Davies, 2005).

Despite the above, the use of different GCM models may assist in evaluating the impact of climate change scenarios because future scenarios are not highly dependent on the result of a single GCM (Chiew et al., 1995). Hence, while a diversity of models may introduce uncertainties, the approach is reasonable to increase the precision of estimation and account for model-specific variations (Shackley et al., 1998).

Another disadvantage of models is their demand for massive computing and personal resources as well as their coarse spatial resolutions (i.e. 500 x 500 km) which provide

insufficient details on regional impacts, and hence, generate unreliable data for regional hydrologic change and flood analysis due to averaged information on topographic features and land surface characteristics at the subregion scale (Arora, 2001; Kavvas et al., 2006; Jiang et al., 2007).). In addition, GCMs also have limited capabilities or are unable to model the profound causes of the climatic warming pattern, such as human induced aerosols. These aerosols are highly variable spatially and vary significantly from region to region and cannot be modelled by coarse resolution GCMs (Kavvas et al., 2006). Another disadvantage of coarse resolution GCMs is on the impact of land use changes on climate; GCMs are unable to incorporate the spatial variation of land use patterns at regional scales which are deemed to play a significant role in climate change studies (Kavvas et al., 2006). Despite the low spatial resolutions for regional climate purposes, it does not compromise the validity of the global response to CO_2 forcing as simulated in many GCM models (Shackley et al., 1998).

In contrast, RCMs try to represent climate change at a finer resolution which only covers a small section of the globe. Thus, a finer spatial resolution is used of approximately 50 km or less. However, the GCMs were used as climatic conditions at the boundaries of the regional sections in the regional models. Hence, this error (i.e. atmospheric dynamics) is transferred to RCMs (Fowler and Ekström, 2009). In spite of its finer resolution, which is appropriate to represent large-scale precipitation patterns, the RCMs are insufficient to represent small scale, convective precipitation (Lahmer, 2001; Bronstert, 2003).

Many studies have been done to link downscaling GCM climate change models and their impact on the hydrological system. The downscaling techniques were developed to establish statistical links between the observed large-scale circulation and the regional scale climate variability such as precipitation (Trigo and Palutikof, 2001). A study done by Fowler et al. (2007) has reviewed GCM downscaling methods. The two most prominent techniques for downscaling GCMs into finer spatial resolution climate change models are dynamical and statistical approaches. The dynamical approach is where a higher-resolution climate model such as RCM is coupled with a GCM model to produce a higher resolution result (i.e. at the ~0.5^0 latitude and longitude scale) (Fowler et al., 2007). The advantages using dynamic downscaling methods are this technique can realistically simulate regional climate features (i.e. regional scale climate anomalies,

extreme climate events) (Fowler et al., 2007), able to simulate meso-scale precipitation processes, thus, producing more plausible climate change scenarios for climate events at a regional scale (Schmidli et al., 2006) and also takes in account the fundamental impact of topography and land surface conditions on its local climate (Chen et al., 2006). However, the techniques also has disadvantages such as the model produced depends on biases in the GCM climate conditions used and also is affected by regional scale conditions such as land cover/use changes, temperature and precipitation conditions variability due to topographic effects (Wang et al., 2004) and it also requires a high computational cost (Ghosh and Mujumdar, 2008).

The second technique is statistical downscaling which involves a two-step approach consisting of i) deriving empirical relationships between observed small-scale variables such as from station level (i.e. temperature, precipitation and stream flow) and larger scale variables (GCM) either using analysis such as regression analysis or neural network methods (Ghosh and Mujumdar, 2008; Fowler et al., 2007; Zorita and Storch, 1999) and ii) application of derived empirical relationships to the GCM output projection results to project the regional climate features (Kavvas et al., 2006). To use this method, three assumptions need to be considered which are, firstly, the GCM variables are relevant and realistically modeled by the host GCM. Secondly, the empirical relationship is valid also under altered climatic conditions. Thirdly, the variables from the GCM fully represent the climate change signal (Ghosh and Mujumdar, 2008). The advantages of statistical downscaling are that this technique is more straightforward compared to dynamic downscaling (Fowler et al., 2007). Furthermore, this technique is computionally efficient and can be easily applied to output from different GCM experiments (Wilby et al., 2004) and can be re-run to generate large ensembles of daily precipitation series at the catchment scale for uncertainty assessment (Prudhomme and Davies, 2005). However, this technique has disadvantages such as the tendency to underestimate climate variability because only part of the regional and local climate variability is related to large-scale climate variations (Fowler et al., 2007). For example, that the mean annual runoff estimates are fundamentally dependent upon precipitation projections is questionable since the future precipitation projections by GCMs at regional scale are unable to represent spatially varying topography appropriately (Kavvas et al., 2006). Moreover, this technique is not suitable to be used to represent extreme events (Murphy, 1999). Detailed explanation of

the GCM downscaling methods can be found in many previous studies (Fowler et al., 2007; Schmidli et al., 2006; Murphy, 2000; Murphy, 1999; Wilby and Wigley, 1997; Hewitson and Crane, 1996).

According to the IPCC (2007), global warming is mostly due to human activities (i.e. land use, industrialization, transportation, agricultural) which has caused increases in GHG emission, particularly, carbon dioxide (CO_2). Assumptions about future emissions of GHG and aerosols and the proportion of emissions remaining in the atmosphere are used to project anthropogenic climate change in the future. The IPCC developed several scenarios of future emissions based on assumptions concerning economic, policy factors, demographic, land use, energy availability, fuel mix and technological changes for the period 1990 – 2100. Two main parameters were used to represent climatic change known as 'emission scenarios' representing CO_2 concentrations in the atmosphere and 'climatic sensitivity' representing the assumption of doubling in CO_2 concentration and its climatic system response from the 1961-1990 period. The summary of climate change processes, characteristics and threats adopted from UNEP/GRID-Arendal (2005) as shown in Figure 2-1.
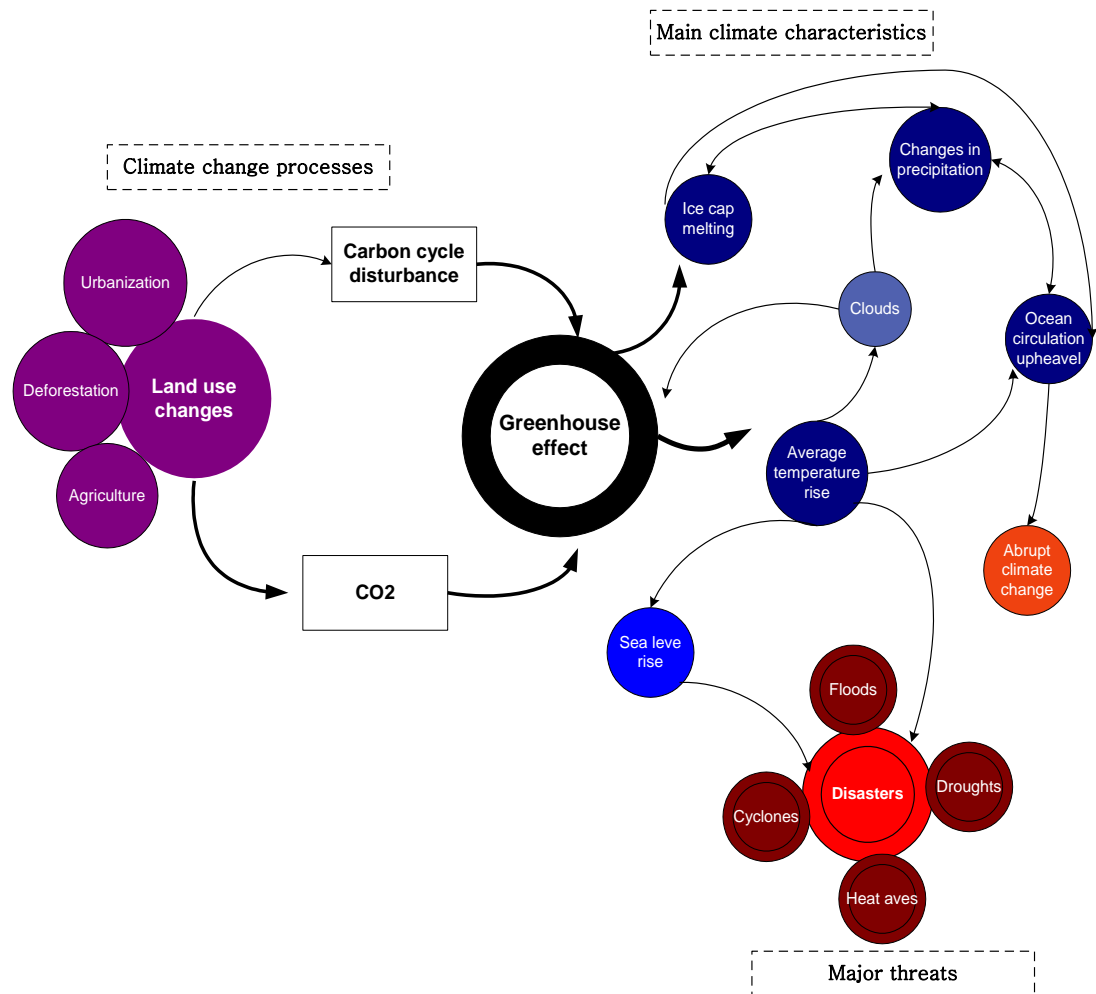
Figure 2-1 Summary of greenhouse effect due to climate change processes, characteristics and threats adopted from UNEP/GRID-Arendal (2005).

The IPCC Fourth Asseement Report (AR4) observed that extreme rainfall events have increased over most land areas, which is consistent with increases in temperature and atmospheric water vapor (IPCC, 2007). Furthermore, the IPCC Special Report on Emission Scenarios (SRES) generated four main hypotheses or storylines and emission scenarios. These scenarios describe future based on assumptions of economic growth, global population change and changes in energy-technology and lifestyle (IPCC, 2007; ADB, 2009; MMD, 2009). Four emission scenarios describe the different rates of GHG known as A1, A2, A1B and B2. The descriptions of each emission storyline and scenario are shown in Table 2-2. The A1B storyline or medium scenario was used in this research to run precipitation scenario for the periods of 2020s, 2050s and 2080s since it provides continued practice of present day standards in regard to socioeconomic activities and fuel type usage.

Table 2-2 The IPCC SRES emission storyline scenarios and descriptions.

Storyline	Assumption descriptions	
	Economy growth	Global population
A1	Very rapid economic growth	Peaks mid-century and declines thereafter
A2	Regionally oriented and per capita economic growth	Very slow fertility pattern across regions and expected continuous increasing in the world's population
B1	Rapid change in economic structures toward a service and information economy, with reductions in material intensity	Same as A1
B2	Intermediate levels of economic development	Continuously increasing global population, at a rate lower than A2

An investigation of climate change effects on regional water resources generally consists of three different stages (Xu et al., 2005; Jiang et al., 2007). The first is using climate models to simulate the climatic effects of increasing atmospheric concentration of GHGs. Secondly, a downscaling technique from a GCM to RCM is derived to provide a regional catchment scale climate scenario and later used as an input to a hydrological model. Finally, a hydrological model is used to demonstrate the hydrological impacts of climate change. However, the present study of the River Kelantan catchment used only the result of climate change predicted from a RCM and subsequently simulates how the climate change scenario affected hydrological response in the study area.

2.5   RAINFALL-RUNOFF MODELLING

According to Pramanik et al. (1992), Asian countries suffer the most from flooding impacts because of their lack of preparedness and preventative measures available in the countries. Understanding which factors cause increases in the frequency and magnitude of flooding is important in order to minimize the impact of flooding on floodplain areas. Hydrological modelling is one way to deal with the flooding problem because it can provide information on the interaction of different processes within a catchment under investigation.

A hydrological model is a mathematical simulation of the complex hydrological cycle and is a powerful tool to understand and to approximate the hydrological response of a basin (Perrin et al., 2001; Bourletsikas et al., 2006). The hydrologic model development process can be divided into three stages (Thompson and Polet, 2000). The first stage is comprised of gaining data to depict the topographical relief of the watershed basin. The second involves model parameterization, which includes acquisition of necessary data to allow accurate renditions of real world activity within the model. Finally, it involves running model scenarios that permit "what if" situations to be investigated with resulting findings displayed in the form of flood maps.

Hydrologic models are used commonly for runoff estimation. The runoff system is initiated by precipitation on a watershed. Before the water can run down to the channel stream and towards downstream, there are certain processes which take place. Some of the rainfall water from precipitation returns to the atmosphere through evaporation from land surfaces, vegetation and water bodies and transpiration from plants. A portion of it may infiltrate into the soil depending on soil type, ground cover, antecedent moisture and watershed properties. Some of the water will be stored and some of it will rise again by capillary action, become interflow, or percolate to groundwater aquifers. Eventually, the interflow and water from aquifers will move slowly and return to the stream channel as base flow (USACE, 2000) (Figure 2-2).
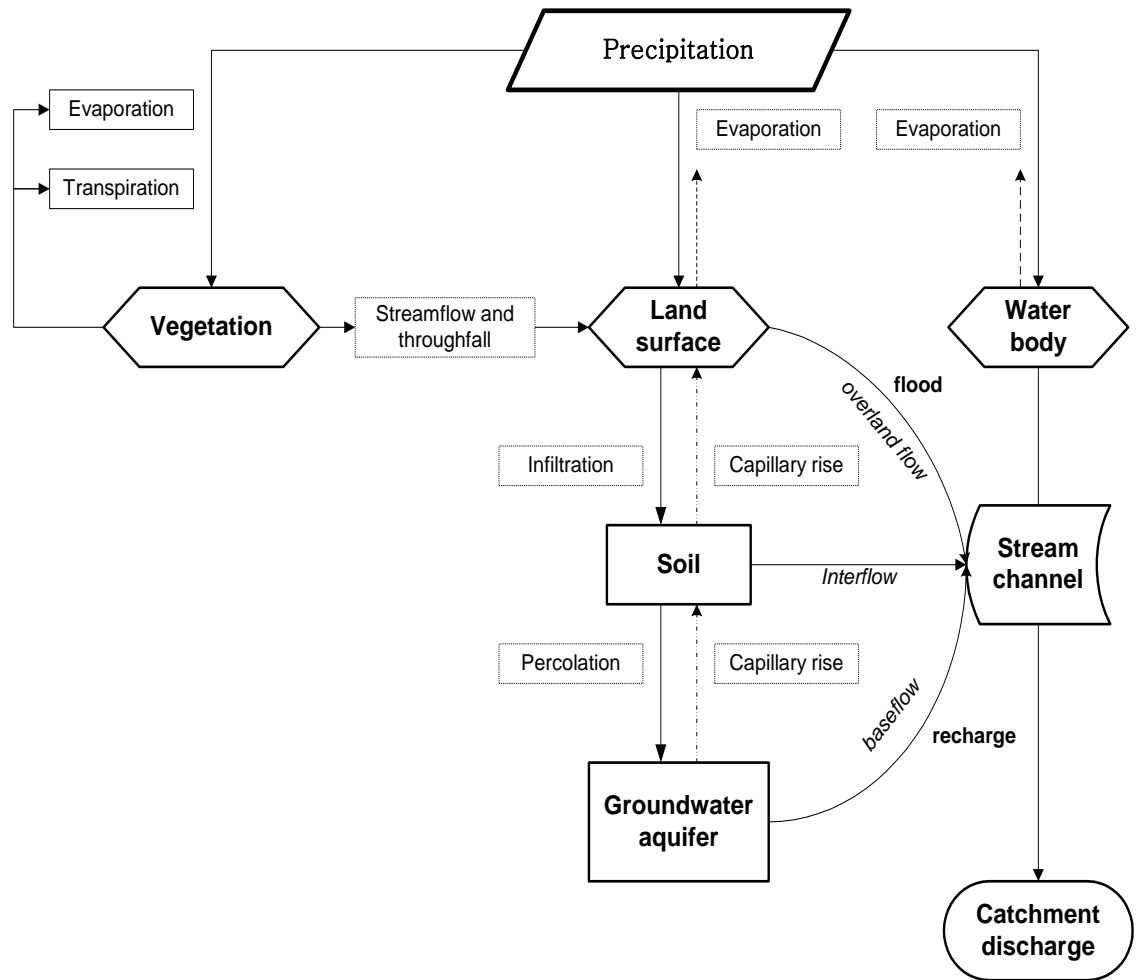
Figure 2-2 Runoff system and processes (adapted from USACE, 2000).

Many hydrological models have been developed to quantify the runoff, direct surface flows, baseflow calculation, water balance and flooding estimation. The models developed include distributed hydrologic models (Abbott et al., 1986; Quinn et al., 1991; Chappell et al., 1998; Legesse et al., 2003; Bingeman et al., 2006), conceptual models (Winsemius et al., 2005) and semi-distributed models (Moliová et al., 1997; Koutsoyannis and Manetas, 1998; Durand et al., 2002). According to Seth (1999), most hydrological problems can be mitigated by using physically-based distributed models. Such models require understanding of the physics of hydrological processes and use exhaustive equations to describe the processes. They are, therefore, considered as complex models due to theirs structure and input requirements. On the other hand, simpler models which can yield adequate results, provided a suitable objective function

is given, are known as lumped models. Lumped models are different from distributed models because the models do not consider in much detail the spatial distribution of physical properties such as soil, land use or topography. The advantages of lumped models compared to distributed models are that lumped models require less data, limited number of parameters and are less prone to equifinality (Beven, 1997; Montanari et al., 2006). However, the model can only be applied to basins with measurements and they need long-term historical data for calibration purposes (Montanari et al., 2006; Nurmohamed et al., 2006). On the other hand, distributed models require numerous parameters because they represent space by sub-basins or grids. Such models are suitable to be applied for large catchment areas, due to the variety of topographic and climatic variation in time and space. According to Chow et al. (1988) the abstract or mathematical form of hydrologic models can be classified based on functions of randomness, spatial variation and time variation (Figure 2-3).
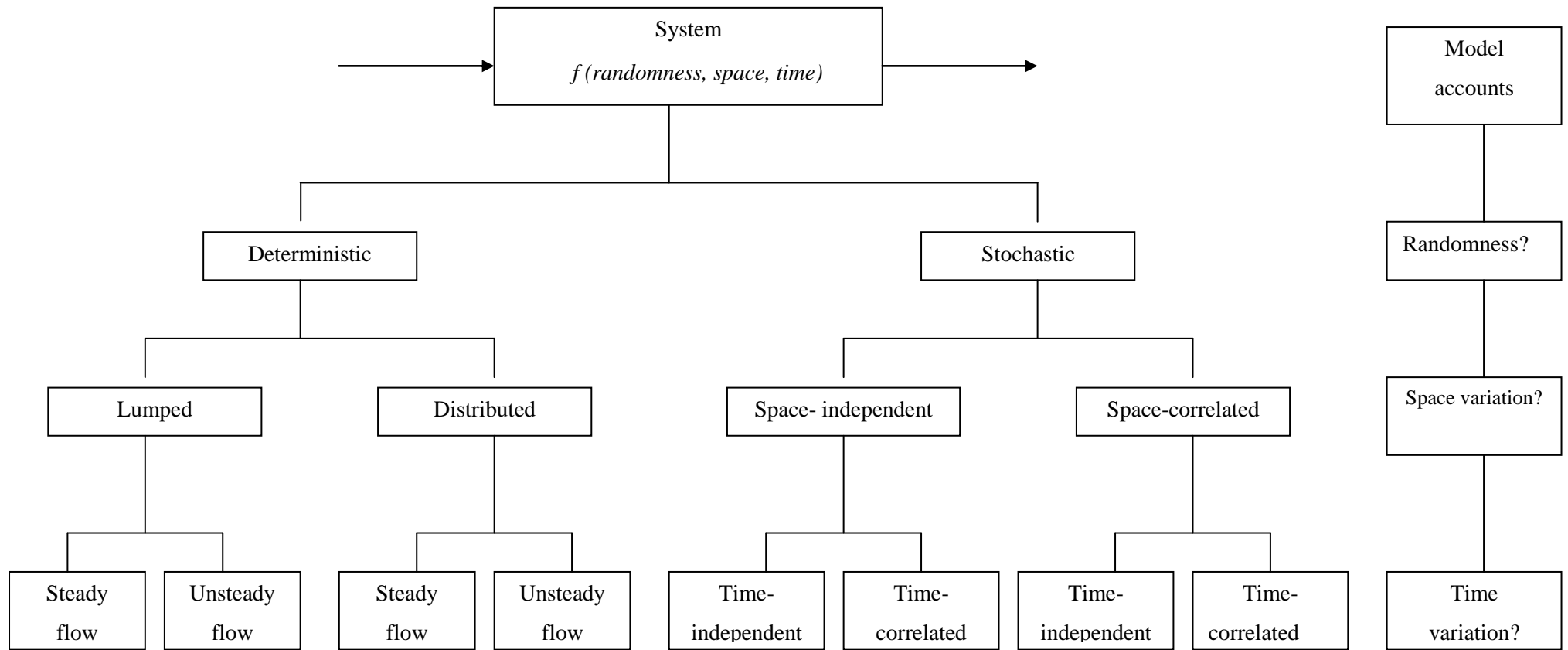
Figure 2-3   Classification of mathematical hydrologic models based on randomness, space and time variation.

Adapted from Chow et al. (1988).

2.5.1 GIS and remote sensing applications to hydrological modelling

Several mathematical models (i.e. loss model, transform model, baseflow model) have been developed for the investigation of the runoff system and processes. Recently, such models have been integrated with GIS and satellite remote sensing data (Scawthorn et al., 2006). GIS provides representations of spatial features of the Earth, while hydrologic modeling is concerned with the flow of water and its constituents over the land surface and subsurface environments. Furthermore, for flood management purposes, Clark (1998) stated that the main advantage of using GIS is to generate a visualization of flooding and allow for practical estimation of the probable hazard due to flood.

Integration of GIS and hydrological modelling has become more important because this combination of techniques offers a treasure of spatially distributed information and analysis. For example, the accuracy of parameters extracted from DEMs are as reliable as derived by manual methods with much less processing time (Wang and Yin, 1998; Islam, 2004; Rumman et al., 2005). The integration of GIS and hydrological models can be done through distributed or lumped parameter hydrologic models (Hellweger and Maidment, 1999). Raster GIS data can be used for distributed parameter hydrologic models using finite-difference or finite-element methods (Saghafian, 1996). On the other hand, for the lumped parameter hydrologic models, GIS normally plays the role of a preprocessor which involves translations of GIS data structure to the hydrologic model such as HEC-GeoHMS preprocessor tools (Olivera et al., 1997; Olivera and Maidment, 1998a; Rumman et al., 2005). It can be used to identify and parameterize relevant hydrological processes over small and large catchment areas (Winsemius et al., 2005) such as basin size, basin slope, main channel length and stream length. GIS is a very useful platform that can be used for the production of digital elevation models (DEMs), that is, the division of the watershed into grid-cells, in order to characterize its terrain (Bourletsikas et al., 2006). A study by Seth et al. (1999) stated that the greatest advantage of using GIS and remote sensing data for hydrological modeling and monitoring is their ability to generate information in the spatial and temporal domain, which is crucial for model analysis, prediction and validation.

GIS has commonly been integrated with remote sensing, hydrological and hydraulic models. This is because GIS functionalities allow manipulating and combining multiscale, multitemporal, multithematic data layers and can be used to minimize the impacts of flood events and forecast such events by two techniques: i) by observing and learning lessons from past events and, ii) by trying to understand such phenomena in order to model them and hence simulate such potential hydrological events (Tholey et al., 1997). For real-time forecasting perspectives, morphological and biophysical characteristics of the region under investigation can be estimated from remote sensor images. Variables such as altitude, slope, orientation, and basins and sub-basins, which represent morphological characteristics, can be extracted from a DEM constructed from optic or radar remote sensing data. For biophysical parameters, land cover (i.e. hydrography, vegetation cover or urban areas) also can be derived from optical imagery (Tholey et al., 1997). Via GIS modelling and the utilization of multithematic information, information pertinent to hydrological models can be estimated and the identification of risk areas under flood hazard designation can be performed (i.e. surface runoff can be described based on slopes and vegetation cover of the region of interest).

Rainfall-runoff modelling involves a large number of datasets, especially those related to hydrology data (river depth, catchment area, watershed topology, evaporation, infiltration, etc.), meteorology data (rainfall data, runoff coefficient), remote sensing data (for land use map purposes), and others such as topography (e.g., contour map), elevation, geology, soil type and infrastructure (Berne et al., 2004; Croke et al., 2004; Ivanov et al., 2004; Liu et al., 2004; Ashagrie et al., 2006; Grapes et al., 2006). For many hydrological purposes, hydrological data alone are not sufficient and need to be merged with data from other sources, for example, with a multitude of spatially related 2-D or 3-D data such as DEMs and digital surface model (DSM) data. The DEMs are different from DSMs because they are a representation of the Earth's surface, excluding features such as vegetation, buildings, bridges, etc.

DEMs are increasingly becoming the focus of attention within the larger realm of digital topographic data. They provide a digital representation of a portion of the Earth's terrain over a 2-D surface. According to Shibasaki and Ochi (1998), DEMs can be derived from GOTO30 and Shuttle Radar Topographic Mapping (SRTM), one of

the most precise mesh elevation datasets covering the entire world land area. DEMs can be very efficient in extracting hydrological data (especially the basin characteristics) by analyzing different topographical attributes, for example, elevation, slope, aspect, relief and curvature for modeling purposes (Seth et al., 1999). Furthermore, DEMs can be utilized to derive the flow direction and the computational sequence for flow routing for each of the discretized cells of the catchment represented as a proper hydrologic cascading system (Jain and Singh, 2005).

Besides DEM data, other datasets play an important role for flood study including Digital Surface Models (DSMs). Research by Zulkarnain and Alkema (2006) discovered that the 2-D terrain model helps understanding of rainfall and runoff and also flood behaviour especially for flood simulation purposes. Remote sensing is able to provide elevation models from airborne remotely-sensed data such as light detection and ranging (LiDAR) data. However, these data are quite limited or non-existent, especially for Asian countries (Wilson, 2004).

Remote sensing can contribute to mapping topography such as DEM generation and defining surface roughness and land use/ cover. Data from satellite observations such as from the Earth Resources System (ERS), RADARSAT, Satellite Pour l'Observation de la Terre (SPOT) and India Remote Sensing (IRS) sensors can provide DEM data at spatial resolutions of about 30 m. Land use information can be derived from the Advanced Very High Resolution Radiometer (AVHRR), Landsat, SPOT and IRS satellite sensor imagery datasets. Synthetic Aperture Radar (SAR) has powerful advantages for flood mapping and hydrology parameter estimation due to its capability of achieving regular observation of the Earth's surface even in the presence of cloud cover since hydrology requires a regularly acquired image for monitoring purposes. SAR data were used for estimation of soil moisture and for identifying open water by dark tone backscatter reflectance. By combining these data with optical and infrared photography, extremely accurate and detailed digital maps can be obtained for flood mapping purposes.

Several studies have been conducted showing the advantages of using satellite sensor imagery for hydrologic modelling and mapping purposes (Schmugge et al., 2002; Boegh et al., 2004; Zwenzner and Voigt, 2009). Remotely sensed datasets can be used for estimation of flood extent and inundation or the land–flood boundary, and are

suitable for describing surface properties, topography, rainfall, evaporation rate and soil moisture (Rango and Anderson, 1974; Ormsby, 1985; Townsend and Walsh, 1998; Ivanov et al., 2004) which are known to be important parameters in hydrologic models. Most flood modelling studies use microwave or radar remote sensing data such as from ERTS, NEXRAD, ERS-SAR, and optical remote sensing datasets such as the Landsat Multispectral Scanner (MSS), the Landsat Thematic Mapper (TM), the Landsat Enhanced Thematic Mapper (ETM$^+$), AVHRR, SPOT, the Advanced Spaceborne Thermal Emission and Reflection Radiometer (ASTER), Moderate-Resolution Imaging Spectrometer (MODIS) and IKONOS (Imhoff et al., 1987; Schultz, 1988; Bates, 1997; Smith, 1997; Horrit et al., 2001). Although a wide range of remotely sensed images are available at different spatial, spectral and temporal scales, due to the cost to acquire data, especially for a large catchment with fine spatial resolution and also due to computer processing demand and time consuming, not all the available data are suitable to be used for rainfall-runoff modelling purposes.

Rapid developments in computer technology and GIS help to process remote sensing data and GIS layers to provide new forms of valuable information through spatial visualization and give tremendous potential for identification, monitoring and assessment of natural hazards such as flooding. Remote sensing and GIS have recently become powerful tools for disaster management activities such as related to floods. According to Jeyaseelan (2003), disaster management activities (i.e. related to floods) can be grouped into three major phases as follows: the preparedness phase: including prediction and risk zone identification activities long before the event occurs, the prevention phase: including activities such as early warning or forecasting, monitoring and preparation of contingency plans before or during the event and the response or mitigation phase: including activities undertaken just after the event which include damage assessment and relief management. However, most runoff modeling lies in the first phase which is for prediction. In addition, in SEA countries (e.g., Malaysia), the lack of availability of data, data sharing and integration has caused flood early warning and forecasting systems to be poorly developed.

The magnitude of flooding and the extent of flood-affected areas depends on the intensity of rainfall, its duration, the watershed topography and its conditions at the time of heavy rainfall (Brivio et al., 2002). Nevertheless, appropriate land use planning,

which requires accurate knowledge of flood extent for locating flood prone areas, is a key tool to improve flood management and to mitigate its potentially catastrophic effects. Accurate information on the extent of water bodies is important for flood prediction, monitoring and relief (Jain et al., 2005).

2.6   EFFECTS OF LAND USE CHANGE AND CLIMATE VARIABILITY ON RAINFALL-RUNOFF MODELS

Flooding generation and runoff processes are highly nonlinear systems and depend on many factors such as; natural and spatial or temporal variability of meteorology, topography, climate, soil, vegetation, groundwater conditions and channel drainage (Bronstert, 2003). In particular, climate change is due to GHG and global warming, which subsequently alter temperature, precipitation, evapotranspiration, and streamflow volumes. Climatic changes are considered a primary cause of alteration to basic components of hydrologic processes (i.e. soil moisture, groundwater conditions, magnitude and timing of runoff). For developing countries (such Malaysia, Africa) inter-seasonal climate variability may be more important than at decadal time scales (Schulze, 2000). On the other hand, human-made activities have caused land use change, and alterations to drainage and river structure. Furthermore, land use is a main boundary condition, in addition to elevation, which may have direct and indirect influences on runoff generation and flooding (Dooge, 1992).

The interaction of the land surface and the atmosphere is important in hydrological processes such as infiltration, evapotranspiration and runoff generation and flooding. However, over time the behaviour of a natural catchment system may change due to several factors. Increased growth in human populations has caused increases in demand for residential areas and has led to urbanization. At the same time, increases in food demand have caused deforestation with forests being replaced by other land uses such as agriculture and industry. For example, over-exploitation of resources due to an increase in population and demand for food supply has caused land degradation in western Kenya (Githui et al., 2009). However, deforestation and land development for agriculture have not necessarily led to an equal increase in food production, but rather has often led to land erosion in the upstream area and triggered heavy floods in the downstream area (Vandaele and Poesen, 1995).

Changes in land surfaces can cause changes in climatic conditions (Pielke et al., 2002). For example, a decrease in tropical primary forest through conversion of forest to agriculture may change the hydrological response (e.g., a decrease in transpiration, decrease in thunderstorm activity and warmer conditions generally) (Lawton et al., 2001). In the United States, crop vegetation that has replaced broad leaf deciduous trees and needle leaf evergreen trees has caused changes to ecological properties and subsequently affected precipitation (Bonan, 1997). Generally, crop vegetation is shorter than forest vegetation, which causes roughness length to decrease leading to decreases in momentum, sensible heat and latent heat fluxes for a given set of conditions (wind, temperature, humidity gradient and surface wind). As a result, a decrease in precipitation was observed of 1 to 2 mm day^{-1} along the East Coast of the US and this became more obvious with increasing proportion of agriculture (Bonan, 1997).

Land use changes and variability in climate have received much attention in relation to explaining changes in discharge over time. Several studies reported that as a result of deforestation, landscape moisture that would normally be recycled to the atmosphere through evapotranspiration or retained in vegetation is instead quickly released as increased runoff or subsurface flow (IPCC, 1996; Laurance, 1998).

The energy and water cycles are closely interrelated systems with mutual impact. At the global scale, an increase in temperature will cause intensification of the hydrological cycle (Bronstert, 2003). Climate change evident through increases in the frequency and/or duration of precipitation can lead to increases in discharge and runoff volume. High intensity and prolonged precipitation can cause flooding to occur when a river's capacity is exceeded due to a high volume of water flow (Bronstert, 2003). In urban areas, high intensity precipitation of short duration can cause flooding due to rapid direct runoff from highly impervious surface areas. Furthermore, Mitchell (1989) estimated that if global temperature increased between 2.8 to 5.2^{o} the commensurate increases in global evaporation and precipitation rates would be between 7% to 15%. A study by Jones et al. (2006) focused on sensitivity of mean annual flow (for 22 catchments across Australia) due to changes in precipitation and potential evaporation. They have used potential evaporation rather than temperature because potential evaporation is a more direct measure of moisture loss from water-limited regions rather than energy limited. (Walsh et al., 2001). They have found that mean annual flow was

3- 5 times more sensitive to changes in precipitation than changes in potential evaporation for each 1% change in climate using two lumped simple conceptual daily rainfall-runoff models (i.e SIMHYD and AWBM) and one simple top-down two parameters model (i.e Zhang01). The emphasis of their study was to explore a wide range of climatic and hydrological uncertainty and to develop a simple systematic method that can be applied to make rapid estimates of potential changes in runoff under climate change, rather than to evaluate the precision of each single climate change scenario (Jones et al., 2006).

In a study of global runoff changes, a combination of land air temperature anomalies and sea surface anomalies was used to quantify their correlation to global runoff (Labat et al., 2004) for two different periods of 1875 - 1925 and 1925 - 1994. In the first period (i.e 1875 -1925) a positive correlation was established with global runoff decreased due to temperature decreases and an inverse correlation was found in the second period (i.e 1925 – 1994) (Labat et al., 2004). The analysis suggests that the global runoff increases by 4% if global temperature increases by 1^0C. According to them, this may be due to complexity of the hydrological consequences and feedbacks of recent climate changes. A similar result also found by Berner and Kothavala (2001) which found a 3.8% increase in global runoff due to change of global temperature. Apart from that, a spatial difference of precipitation and temperature trends was found in Yangtze basin, China. A study conducted by Zhang et al. (2005) found that the middle and lower Yangtze basin showed a negative relationship of increase precipitation trend with decrease temperature trend from 1950 – 2002 and floods are in upward trend. Inversely, the upper Yangtze basin showed a decreasing precipitation trend with increasing temperature trend for the same period and floods showed a downward trend. They attributed these findings to increasing precipitation and cloud coverage, hence, causing ground surface temperature to decrease (Zhang et al., 2005).

Many studies have indicated that land use changes such as deforestation and expansion in agricultural land may lead to increases in peak discharge and runoff volume. Rainfall-runoff models have been used widely to study the impact of deforestation and agricultural expansion on runoff generation in hydrological catchments. Saghafian et al. (2008) used the HEC-HMS hydrological model to show that land use change from forest and rangelands to cultivated areas over hill slopes caused substantial land

degradation and increased the outflow peak and total runoff volume observed. Githui et al. (2009), using the CLUE-S model, demonstrated that a "worst" scenario of deforestation and expansion in unsustainable agriculture led to increases in runoff, baseflow and total streamflow. They attributed such changes to decreases in the evapotranspiration rate (due to a reduction in forest area) and infiltration capacity (due to soil compaction caused by agriculture). Eckhardt et al. (2003) simulated a structured artificial catchment with four land use types consisting of two forest types (i.e. deciduous and coniferous), pasture and arable land. They found that arable land produced the largest contribution to streamflow due to lower evapotranspiration followed by pasture and forest land use.

The effect of a combination of land use change and climate change on runoff generation has been the focus of several studies. In most studies, future climate change scenarios were derived from regional climate models (RCM) which provide finer spatial resolution data compared to global atmosphere-ocean circulation models (GCM) (Lahmer, 2001; Bronstert, 2003). Some studies found that land use change is a dominant factor while other studies found that climate change affects the hydrological response more than land use change. In particular, Hejazi and Markus (2009) used present land use and precipitation conditions as inputs to a historical runoff model to show that urbanization was the dominant factor in explaining increases in flood peaks (34% higher than the parallel increase in precipitation) in northeastern Illinois watersheds. Moreover, Saghafian et al. (2008) stated that a larger return period (i.e. 100 year flood peak) reduced the relative effect of land use change on the flood peak discharge due to higher intensity storms.

Ward et al. (2007) attempted to differentiate between climate change and land use change effects on mean discharge, flood frequency and flood magnitude for the period 4000-3000 BP and 1000-2000 AD. The study found that it was difficult to differentiate between natural fluctuation and human activities on flooding in the Meuse River, Germany using a GCM model coupled with the STREAM hydrological model. However, they concluded that simulated daily discharge was higher in 1000-2000 AD compared to 3000-4000 BP and almost all of the increases were ascribed to land use changes due to deforestation and in the 20th century, increases in mean discharge and flood frequency were attributed to increases in annual and winter precipitation.

Similarly, climate change and land use change simulation on the Severn and Thames rivers showed an increase of 47% and 28% respectively, in peak daily discharge compared to only 28% and 16% alone in precipitation change for 50 year flood frequency. Furthermore, Crooks and Davies (2001) found that the effect of land use change on flood frequency on the Thames river from 1961 to 1996 was very small compared to rainfall.

A study which coupled a hydrological model (IHACRES) and a conceptual crop model (CATCHCROP) was performed by Croke et al. (2004) to evaluate the impacts of land cover change on stream flow in the mountainous regions of Thailand. The crop model was used to study the land use effects on infiltration and runoff and augmented to the hydrologic model in order to predict land use effects on hydrologic response. The study used 12 scenarios for forest conversion, which correspond to slope (i.e. 16^0 to 35^0) (the study area is dominated by steep topography upstream). These scenarios were used to illustrate its effects on mean annual, wet season and dry season discharge with the same climatic condition for the periods of eight years (1985 – 1993). They found that an increase in forest cover of 70% with slope greater than 35° caused a decrease in mean annual discharge (2.4%) and deforestation of 50% caused an increase in mean annual discharge of 3.9%. This result occurs because forest evaporates more water than any other land cover or land use such as agricultural crops. In wet climates forests play a role to evaporate intercepted water more than short crops due to their rough surfaces, which can help the aerodynamic transport of water vapour into the atmosphere. Meanwhile, in drier climates, deeper forest root systems help in maintaining transpiration and may lead to higher evaporation rates of forest compared to agricultural crops (Legesse et al., 2003).

2.6.1 HEC-HMS model

The choice of hydrologic model is dependent on the purpose of the study and data availability (Ng and Marsalek, 1992; Jiang et al., 2007). The HEC-HMS model was developed by the US Army Corps of Engineers (USACE) Hydrologic Engineering Center's (HEC) and is known one of the most widely used rainfall-runoff models, particularly in United States and has been further adopted by many researchers from other countries to study applications related to the hydrological system.

HEC-HMS was designed to simulate the rainfall-runoff process of a dendritic watershed system (USACE, 2000). The model is suitable for small and larger catchment hydrologic applications in addition to lumped and distributed rainfall-runoff modeling (Fleming and Neary, 2004; Chu and Steinman, 2009; Verma et al., 2009) such as water balance studies (Moghadas, 2009), flood studies (i.e. flood-frequency studies, flood-loss reduction studies, flood-warning system planning, urban flooding studies) (Wurbs et al., 2001; USACE, 2008; Razi et al., 2010), impact of land use and climate change on runoff generation and flooding (Kang and Ramirez, 2007; McColl and Aggett, 2007; Hejazi and Markus, 2009; Yimer et al, 2009). The HEC-HMS model can be classified into two categories, which are an events model and continuous model. The events model is associated with short periods of rainfall event, while, the continuous model is associated with longer periods of time (i.e. months, seasonal and annual, etc.).

The HEC-HMS has three components to build the full model known as basin model, meteorological model and control specifications. The basin model component is capable of representing a variety of watersheds by subdividing the hydrological system into smaller and manageable pieces with seven types of hydrologic elements as shown in Table 2-3 and Figure 2-4. The meteorological model includes precipitation and evapotranspiration (ET) for continuous runoff modeling and evapotranspiration is negligible for the event model due to the intensity of the storm being modeled, continuous saturation of the air and because ET volume is negligible compared to runoff volume (Knebl et al., 2005; Cunderlik and Simonovic 2007; McColl and Aggett, 2007). The control specifications are for time span of a simulation which includes a starting date and time, ending date and time and computation time step.

Table 2-3 Hydrologic elements used in HEC-HMS models.

Element/Symbol	Description
Sub-basin	A physical watershed or a region of space enclosed by a single boundary line following natural drainage divides which precipitation falls and only one outflow (i.e. excess precipitation) is transforming to outlet which located at the most downstream point in the basin.
Reach	A single line which carries flow downstream from one or many upstream hydrologic elements in the basin model. All inflow is added together and the outflow terminates at the watershed outlet.
Junction	A location where multiple streamflow from upstream hydrologic elements are joint together (i.e. at a confluence) to form one downstream reach, or where the drainage from a sub-basin enters a channel reach.
Diversion	A location where one upstream reach splits to form two downstream reaches, or where water is withdrawn from the channel and may be discharged to a canal or downstream.
Reservoir	An area of impounded water bounded by lines, which have one or more inflow (which add together) and only one computed outflow. It is normally used to model the detention and attenuation of a hydrograph caused by a reservoir or detention pond.
Source	An inlet location where a river discharges water derived from a drainage area lying outside the study watershed. Source elements are particularly useful for partitioning a large region into smaller study areas using gauged flows at the source locations to describe the contribution of upstream tributary areas, thus outflow from the source element is defined by the user.
Sink	An outlet location where a river discharge leaves the watershed. There is one or many inflows that come from upstream hydrologic elements and no outflow from the sink element.
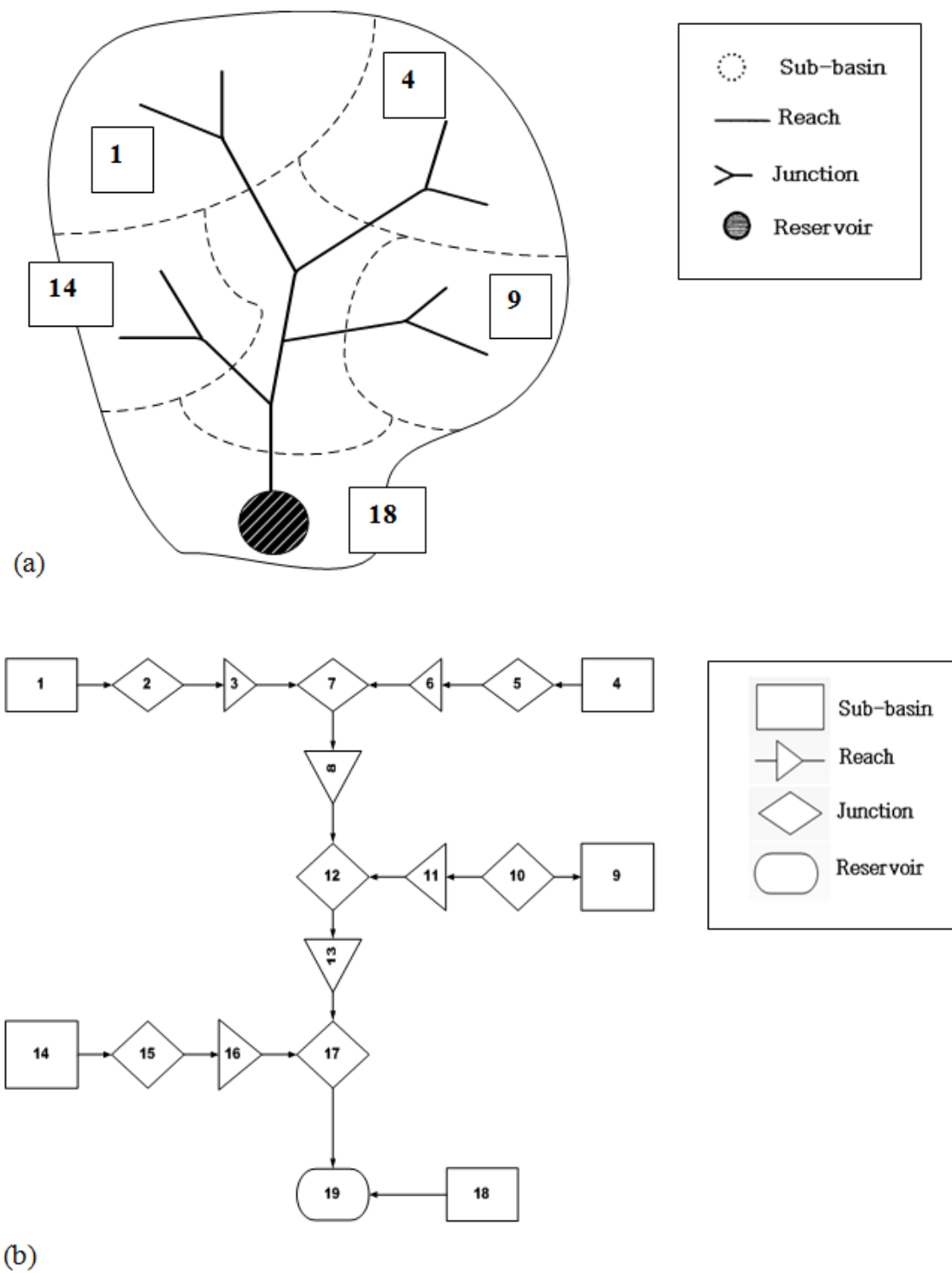
Figure 2-4　Example of (a) physical watershed and (b) HEC-HMS hydrologic
elements associated with physical watershed.

2.7   FUTURE PROJECTIONS AND EFFECTS ON RAINFALL-RUNOFF MODELS

2.7.1 General climate change projections

Hydrological modeling and climate change models (i.e. GCMs and RCMs) are normally used to study runoff generation and flooding in future scenarios. Research has indicated that the predominant factor, which contributes to change in the hydrological cycle and runoff, is climatic variability or climate change effects. Climate change effects such as increasing temperature, precipitation and evaporation may lead to fluctuations in river discharge and eventually cause flooding events to occur (Ashagrie et al., 2006). However, it is uncertain by how much and at which spatial scale these environmental changes are likely to affect the generation of storm runoff and consequently, flood discharge of rivers (Bronstert et al., 2002) many researchers have used hydrological and climate models in combination to provide insight into hydrological response, runoff generation and flooding in the future (Bergstrom et al, 2001).

A conceptual daily rainfall-runoff model (i.e. Probability-distributed model, PDM) coupled with two climate change scenarios developed for the UK Climate Change Impacts Review Group (CCIRG) were used by Arnell and Reynard (1996). The calibrated-validated runoff model from 1980-1989 was used as a baseline for future runoff scenarios (i.e. 2050). The study found that climate change (i.e. change in temperature, precipitation and evaporation) may have a significant impact on streamflow regime in 21 catchments in the UK with prediction of higher flows in winter and lower flows in summer. Similarly, a climate change study by Reynard et al. (2001) for the Thames and Severn rivers, UK has shown that climate change effects will contribute increases in the frequency and magnitude of flooding events by the year 2050. In addition, Walsh and Kilsby (2007) found that using UKC1P02 climate change scenarios, they predicted that warmer climate (increase in temperature of 2.5 - 3.0 C) and more precipitation in winter and drier conditions in summer seasons is likely in the future (2070-2100) for the UK. The study used two climate scenarios, which are first, change in both precipitation and potential evaporation, and secondly only change in precipitation. These climate scenarios were applied to identify the relative effects of those changes on runoff. They concluded that changes in precipitation caused greater increases in runoff

than potential evaporation changes (PET) with the aid of SHETRAN 3D surface/subsurface physically-distributed hydrological modelling. However, the results from these studies were subjective to the climate model used due to the fact that different climate change scenarios will generate different streamflow, runoff or flooding magnitude results.

More comprehensive coupling of climate change modelling with hydrological modelling was undertaken by Cherkauer and Sinha (2010). The Variable Infiltration Capacity (VIC) large scale hydrology model with two climate models and three future scenarios were presented for the years of 2009 to 2100. The results also suggested that in Lake Michigan winter and spring precipitation are expected to increase. However, summer precipitation is expected to decrease or stay the same with an increase in warmer air temperature that will cause an increase in ET and hence, streamflow also showed a similar decreasing trend. Similarly, Chiew et al. (1995) demonstrated changes in runoff and soil moisture using conceptual hydrological modeling (i.e. MODHYDROLOG) with five GCMs (CSIRO09, BMRC, IPCC, UKMOH and GFDLH) for 28 catchments in Australia. They found that for a future scenario (i.e. 2030) the GCM model was able to predict changes in summer and winter runoff and soil moisture (i.e. between -20% to 100%) for different regions in Australia (i.e. North-east coast, South-east coast, Murray-Darling, Tasmania, South Australian Gulf, South-west coast, West coast and North Australia).

Meanwhile, a study by Booij (2005) indicated that the impact of climate on flooding can be studied by using spatially and temporally changed climate patterns and a hydrological model with three different spatial resolutions on a daily basis. Furthermore, he mentioned that important processes in the context of climate change impacts on river flooding were found to be precipitation, evapotranspiration, infiltration excess overland flow, saturation excess overland flow, subsurface storm flow, subsurface flow and river flow. The advantage of the study was that land use information (variable of 5 km) was included since land use change also has important effects on runoff apart from climate change alone.

2.7.2 Malaysia climate change projections.

The impact of climate change on hydrology in Malaysia has been examined using both GCMs and RCMs. The GCMs from nine coupled Atmospheric-Ocean General Circulation Models (AOGCMs) developed by France, Japan, China, USA, UK, Germany and Canada were used by Malaysian Meteorological Department to study projections of future changes in rainfall and temperature in Malaysia (MMD, 2009). These nine AOGCMs are from the Coupled Model Inter-comparison Project as presented in the IPCC 4th Assessment Report. In the study, the 1990-1999 data were used as a control period and the SRES A1B scenario was run for the future periods of 2020-2029, 2050-2059 and 2090-2099. The result showed that all nine models simulated an increase in temperature for Peninsular Malaysia (PM); however, with different degrees of increases as shown in Figure 2-5. However, rainfall was projected to increase over the West-coast and to decrease in the East-coast states of PM (Figure 2-6) (MMD, 2009).

Due to the coarse resolution of the GCMs, RCMs were used since they can provide high-resolution information on climate change projections for smaller regions. A regional climate-modelling tool used by the Malaysian Meteorological Department is known as Providing Regional Climates for Impact Studies (PRECIS) (Marengo et al., 2009; Marengo and Ambrizzi, 2006). The model is a RCM derived using dynamical downscaling approach which uses meteorological boundary conditions from the Hadley Centre HadCM3 AOGCM. The model was developed by the Hadley Centre, United Kingdom. Observational data (i.e. temperature and rainfall) of 60 km resolution from the Climate Research Unit of the University of East Anglia, United Kingdom were used to validate the baseline (1961 – 1990) regional climate simulation at 50 km resolution. The regional simulation for PM used the SRES A1B scenario for the period from 2001 to 2099. The PRECIS results showed that temperature was predicted to increase by $1.1\,^{O}C$, $1.7\,^{O}C$ and $2.9\,^{O}C$ for the period of 2020-2029, 2050-2059 and 2090-2099 respectively for North-East PM where the River Kelantan catchment is situated (Figure 2-7) (MMD, 2009). The result is in good agreement with the nine GCM outputs as described earlier.

(a)
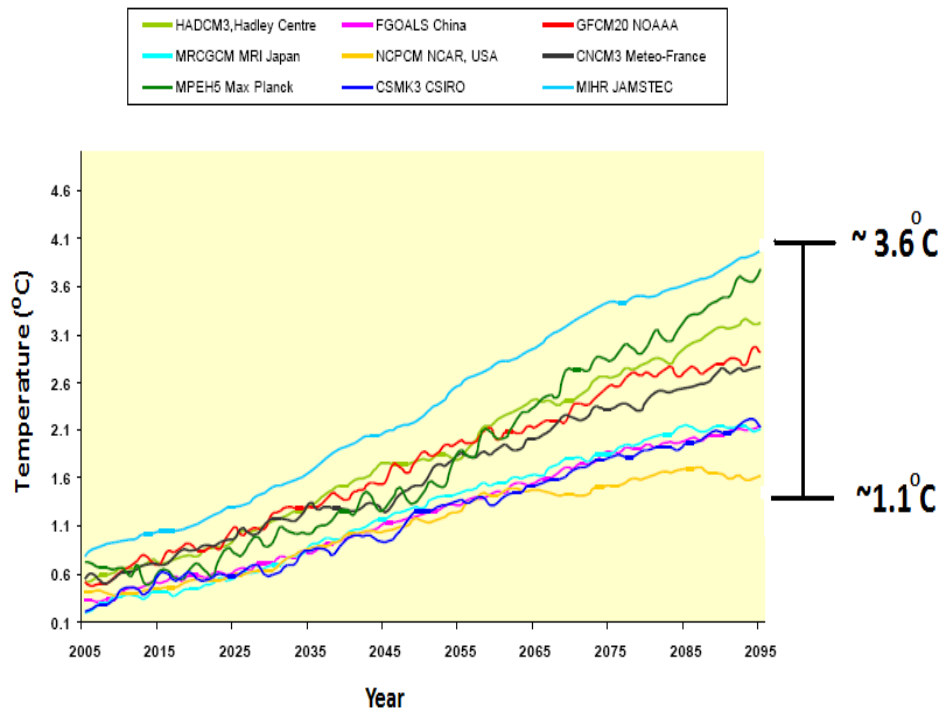
(b)
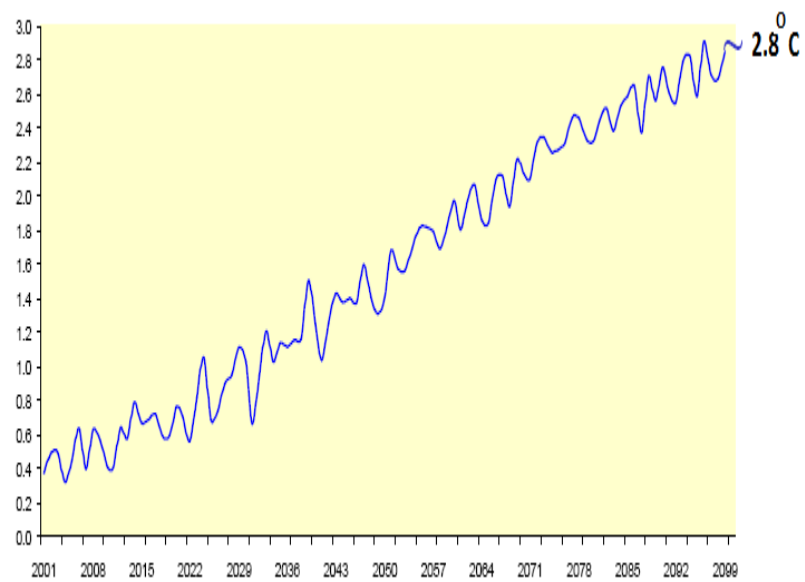
Figure 2-5   Future projections of temperature for Peninsular Malaysia (PM)using (a) nine GCMs based on the SRES A1B and (b) ensemble mean (adapted from MMD, 2009).
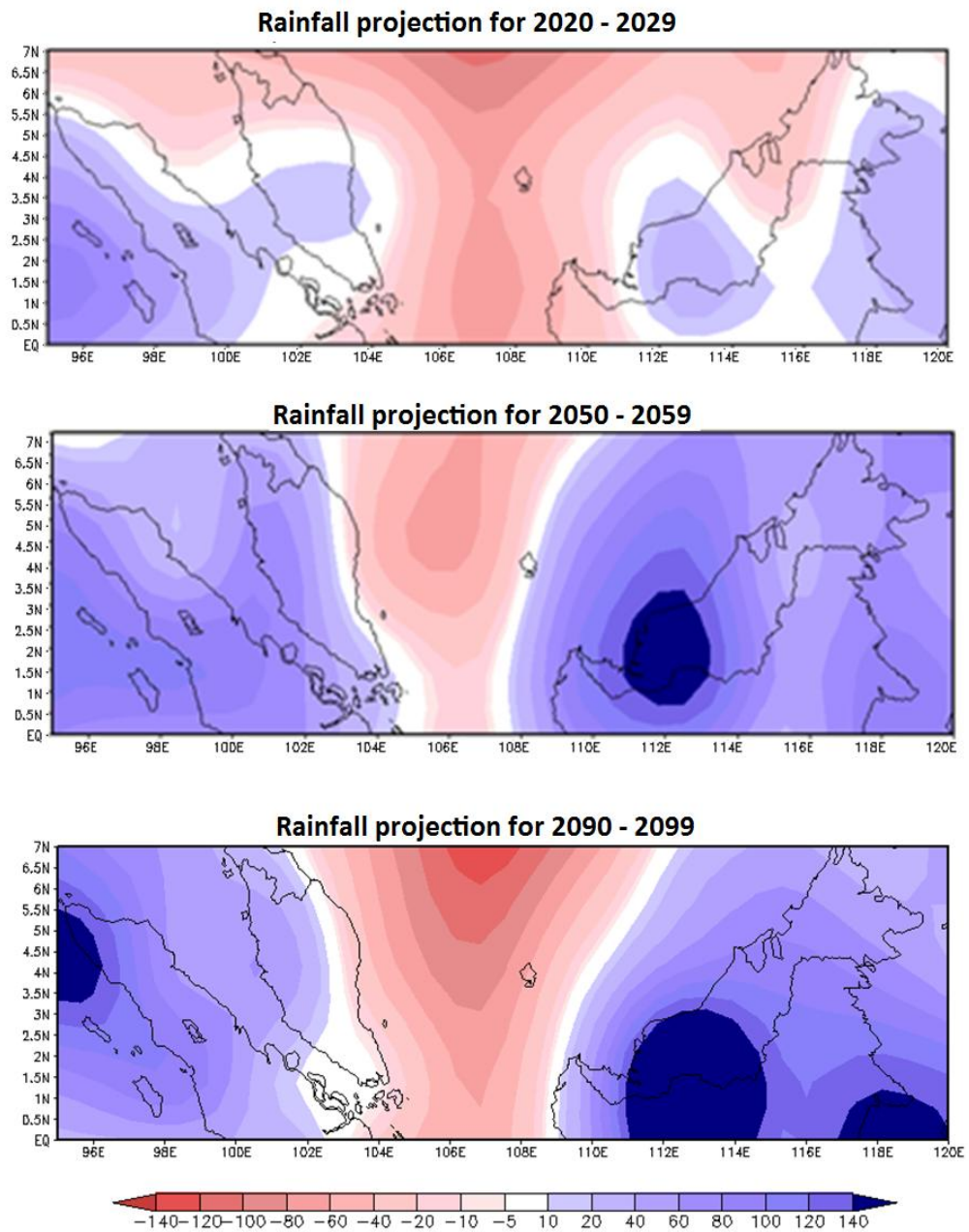
Figure 2-6   Future projections of rainfall changes for PM for the period of (upper) 2020-2029, (middle) 2050-2059 and (bottom) 2090-2099 from the nine AOGCM ensemble. (Adapted from MMD, 2009).

(a)

(b)
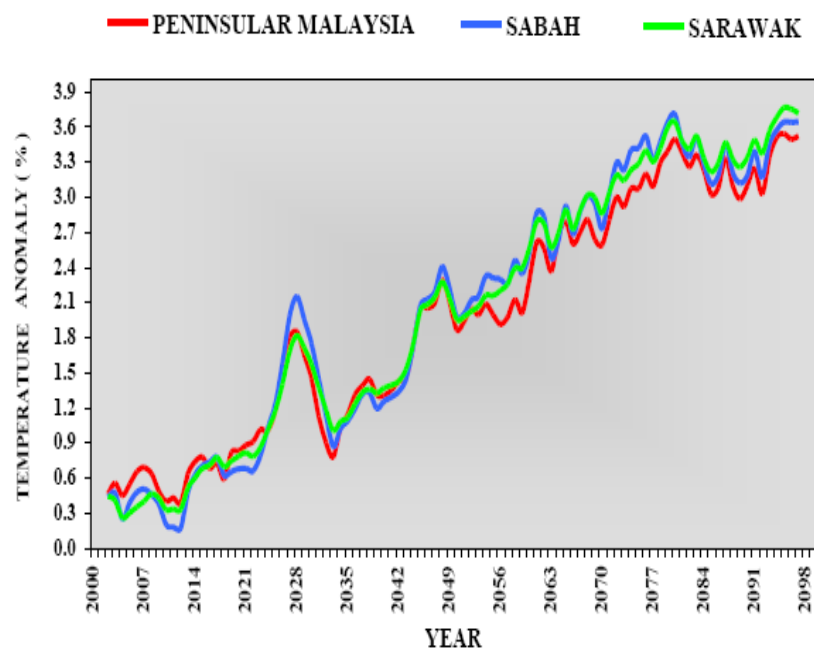
Figure 2-7 The Malaysia map show (a) Peninsular Malaysia, Sabah and Sarawak and (b) the PRECIS annual temperature projections for Peninsular Malaysia, Sabah and Sarawak driven by HadCM A1B for the period of 2001-2099 (adapted from MMD, 2009).

The rainfall simulation using PRECIS model projected that PM will experience increased rainfall towards the end of the century (i.e. the year 2080 onwards) (Figure 2-8). A comparison between temperature and rainfall demonstrated that increases in annual temperature simulated for 2028, 2048, 2061 and 2079 were associated with decreases in annual rainfall simulated for the same years, generally found during El-Nino events. The model also showed that the highest temperature increase in 2028 corresponded to the highest rainfall decrease for the same year. An increase in annual rainfall was simulated during 2030 to 2031, 2055 to 2058 and 2084 to 2091 which is associated with strong La Nina events (MMD, 2009). The future projections of rainfall changes (in %) were calculated from comparison between validated hydroclimatic conditions in baseline perios od 1961-1990 and future simulated periods (i.e 2001 – 2099) using assumption of future emission GHG scenarios. The PRECIS model simulated that annual rainfall changes (%)for the North-east PM are -18.7%, -6% and 4.1% for the periods of 2020-2029, 2050-2059 and 2090-2099 respectively (Figure 2-9) (MMD, 2009). These precipitation changes projected by PRECIS were later used in the River Kelantan study for the latter part of the analysis (i.e. what-if future land use and climate change study).
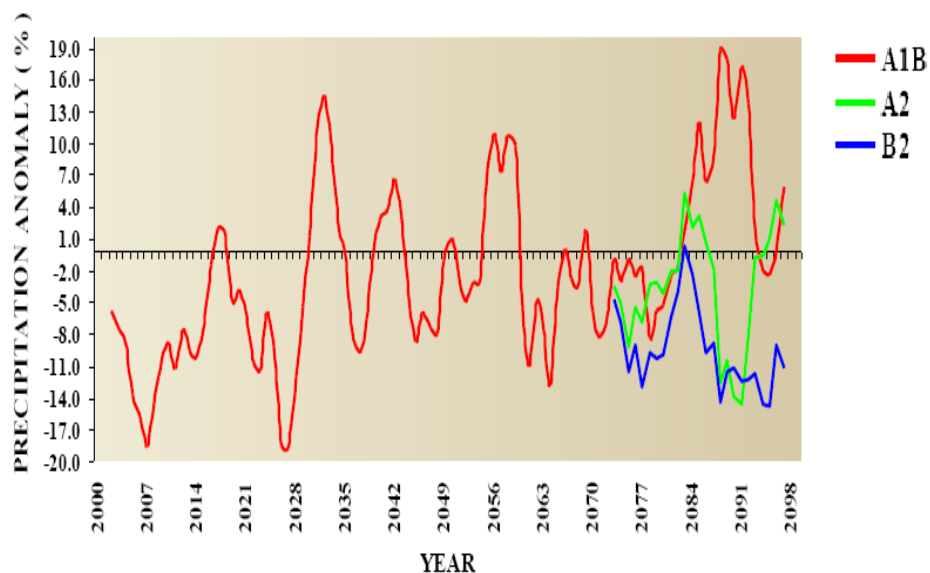
Figure 2-8 The PRECIS annual rainfall anomaly projection of Peninsular Malaysia using A1B and comparison to A2 and B2 scenarios for the period of 2001-2099 from baseline period of 1961 -1990.
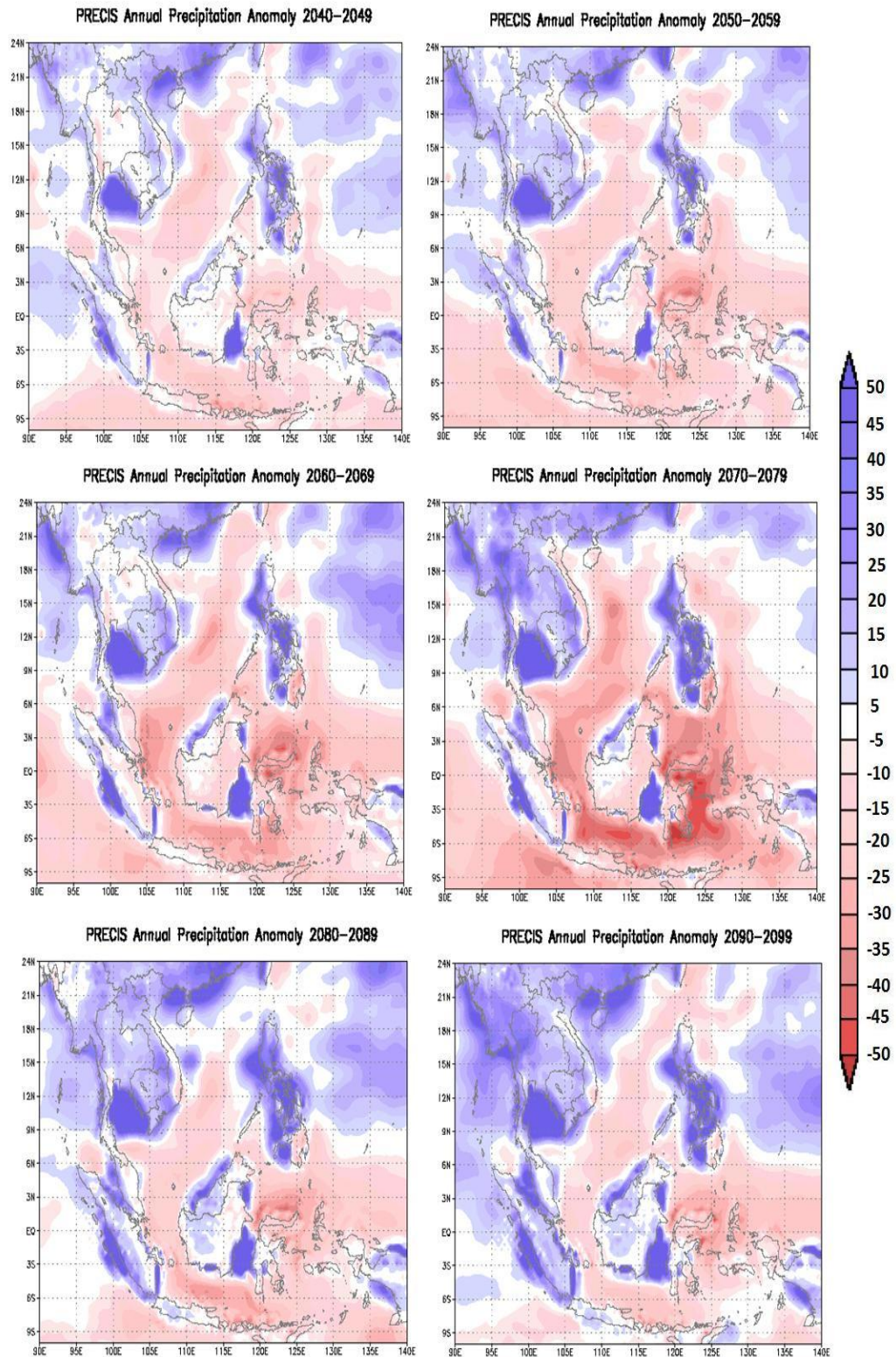
Figure 2-9 The PRECIS annual mean rainfall anomaly from baseline period
of 1961 -1990 simulation for the period of (upper) 2040-2049 and 2050-2059,
(middle) 2060-2069 and 2070-2079 and (bottom) 2080-2089 and 2090-2099
using A1B scenario (adapted from MMD, 2009).

Apart from PRECIS, Malaysia also has another RCM model developed for future hydrological and climate change studies. A regional physically-based hydrological-atmospheric model (RegHCM-PM) of Peninsular Malaysia (PM) was developed using dynamical downscaling from the Canadian General Circulation Model (CGCM1) with coarse-resolution (~410 km) to the PM region at a fine grid resolution (~9 km) to assess the impact of future climate changes on the hydrologic regime and water resources of PM (Chen et al, 2006; Kavvas et al, 2007). The model was able to quantify the impacts of soil water flow, soil heat flow, evapotranspiration, sensible heat flux, short wave and long wave radiation and topography (i.e. steep topography) on the climate of Peninsular Malaysia (Shaaban, 2008; Zakaria and San, 2008; Johar, 2010). It was calibrated using existing land databases, and was validated by historical hydroclimatic data over PM during the 1984-1993 periods (Chen et al. 2006). The climate simulation data for the historical period, produced by CGCM1, were used for initial and boundary conditions for RegHCM-PM simulations of the historical hydroclimate over PM during this period, and compared against ground observations for the validation of the RegHCM-PM model. Once the RegHCM-PM model was validated, it was then used for downscaling the 2041 – 2050 future climate simulations of CGCM1 onto the PM region, during which the CGCM1 data of the IPCC IS92a Scenario Run corresponds to a gradual yearly 1% increase in CO_2 after 1993.
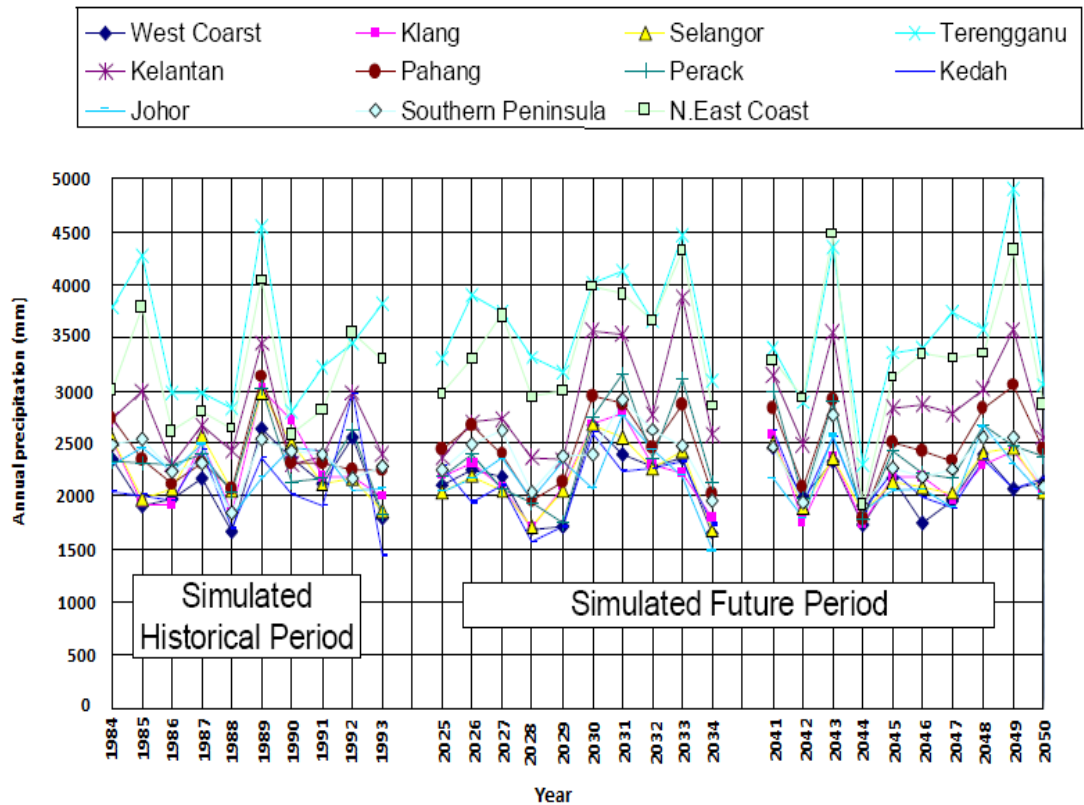
Figure 2-10 Annual precipitation for historical (1984-1993) and simulated future projection of the Peninsular Malaysia states (2025-2034 and 2041-2050) using RegHCM-PM.

2.7.3 Future land use projection studies

In recent years, there has been an increasing amount of literature to determine the impact of land use change on surface runoff, water balance components and evapotranspiration (Reynard et al., 2001; Miller et al., 2002; Ashagrie et al., 2006). Tollan (2002) stated that modelling land-use change impacts within the "Floodware" programme confirmed findings that flood sensitivity to land-use changes such as replacement of grassland into urban areas or increase in corn crops diminished with increasing flood return period. The explanation given is that during large floods, the surface is more saturated over large parts of the catchment, and acts as an impermeable cover. In addition, Wang et al. (2008) used the SWAT hydrologic model and simulated land use change and climate change in a basin of northwest China. They used three land use change scenarios in which area conversion of grassland to forestland was the dominant land use change in the study area. SCS curve number was employed to examine the land use change impact on surface runoff. They found in a sensitivity

analysis that SCS runoff curve number was the most sensitive parameter for simulating streamflow. Mean annual stream flow was reduced by 2.3% under the scenario that all current grassland was converted to forestland, only 0.01% if only 25% grassland was converted to forestland and total deforestation caused increases in streamflow (3.4%). This happened because forest uses more water compared to grassland; hence, less runoff will be produced from a forested catchment (Legesse et al., 2003).

A land use scenario using low and high growth of residential density was carried out by using the *What-if?* software and integrated with HEC-HMS hydrologic model to simulate change in peak discharge due to residential density for the Washington river basin (McColl and Aggett, 2007). They found that increases in both low and high density of residential area produced increases in peak discharge for the period 1995 to 2050 of 3.7% and 9.7%, respectively. A similar result of an increase in peak discharge and runoff volume was found by using an integration of the Conversion of Land Use Change and its Effects (CLUE) land use model with the same hydrologic model in a subtropical monsoon basin in China (Chen et al., 2009). The CLUE model was used because of its capabilities to translate land use demands into land use changes at various locations within the study area according to its drivers (i.e. major roads, altitude, slope, population density, etc.). They also found that the highest urbanization rate in the sub-basin has the most significant effect on estimated hydrologic response with an increase in peak discharge of 10.9% and runoff volume of 12.4% between 2001 and 2050. These two studies suggest a positive relationship: increases in runoff volume and peak discharge are related to the expansion rate of urbanization areas. A similar land use model (CLUE) was used by Lin et al. (2008). They used historical SPOT images between 1990 to 2000 to predict urban sprawl and land use change in a Taiwan watershed and further the result was used as an input to a hydrologic model to analyze the impacts of land use change on watershed hydrology. They found that urbanization impacts on hydrology in terms of streamflow, surface runoff, groundwater discharge and evapotranspiration were proportional to the degree of urbanization.

A hydrologic physically-based distributed model is able to represent explicitly the spatial variability of a catchment (i.e. topographic elevation, slope, vegetation, soil and evapotranspiration). Legesse et al. (2003) used such a model to estimate how much land use change and climate change affected annual runoff and potential

evapotranspiration (PET). An arbitrary value of a 10% change in precipitation and 1.5^0 C temperature change were chosen for climate change scenarios. Land use change scenarios, involved conversion from cultivated land to woodland for the part of catchment between 2000 to 3000 m above mean sea level, which represents 50% of the study area. They found that a decrease in rainfall caused a decrease in runoff with the highest decrease in summer (i.e. August and September), and temperature decreases also caused decreases in PET and increases in mean annual discharge. However, the study only used arbitrary values for rainfall, temperature and land use change, which do not represent actual climate or land use changes that have occurred recently orfuture scenario from climate models in the study area, and the aim of the study was just to show plausible and possible scenarios to simulate potential impacts on hydrology.

2.8   SUMMARY

This chapter has described several studies and techniques relating to flooding and hydrological response in various countries and, particularly, in Malaysia. Understanding the changes in hydrological data such as precipitation and stream flow plays an important role as an indicator of possible causes of changes in runoff generation and floods in a catchment. Several methods were widely implemented as described earlier (i.e. statistical time-series trend analysis, rainfall-runoff models, climate change models, integration of many tools (i.e. geographical information system and data manipulations and remotely sensed image and digital image processing) and have great advantages for hydrological modelling studies.

Combination of rainfall-runoff models with land use/cover and climate change models have received great attention in studying the effects of land use and climate changes on hydrological response in the past and for the future (i.e. changes in peak discharge, runoff volume, etc.). From these various observations of factors relating to changes in hydrological response and floods, methods to study the effects of land use and climate change on hydrological response were formulated for the monsoon catchment of the River Kelantan catchment, Malaysia. The relevant methods are described next.

Chapter 3
Methods

This chapter discusses methods that were used in this study. The methods used involved statistical time-series analysis, remote sensing image classification, hydrologic modelling using HEC-HMS software, and what-if scenarios for climate change and land use change analyses.

3.1   TREND ANALYSIS

The models used widely to examine statistical trends in hydrological data are non-parametric methods. This is due to hydrological datasets such as stream flow and precipitation being characterized by non-normal data distributions. The Mann-Kendall test was chosen in this study to analyze trends in precipitation and streamflow data in the River Kelantan catchment, Malaysia. Additionally, a land use change was also taken into consideration to understand its link to detected trends in stream flow data.

3.1.1 Testing for normality

Data normality test have to be performed to determine the type of data distribution. A data normality check was performed using the Anderson-Darling test, with skewness and kurtosis statistics used to test further the distribution of the data. The Anderson-Darling test (Anderson and Darling, 1952) is used to examine whether the data used come from a population with a specific distribution (normality or non-normality of the data distribution). The Anderson-Darling test statistic is defined using two hypotheses. The H_o states that the data has a normal distribution while H_1 as an alternative

hypothesis states that the data has a non-normal distribution. The Anderson-Darling test statistic assesses if data (Y_1, Y_2, …, Y_n) in the ordered data comes from a distribution with cumulative distribution function (F) :

$$A^2 = -n - S \tag{3-1}$$

Where n is the sample size.

$$S = -n - \frac{2i-1}{n}\left(\ln\left(F(Y_i)\right)\right) + \ln\left(1 - F(Y_{N+1-i})\right) \tag{3-2}$$

An approximate adjustment, A^{*2} is calculated using

$$A^{*2} = A^2\left(1 + \frac{0.75}{n} + \frac{2.25}{n^2}\right) \tag{3-3}$$

If A^{*2} exceeds 0.632 for a 90% significance level then the hypothesis of normality is rejected.

The value of skewness for a perfectly symmetrical distribution is zero; negative values equal negative skewness and positive values equal positive skewness. Kurtosis is the degree of peakedness of a frequency distribution. It is related to deviation away from a perfectly symmetrical curve. A highly peaked distribution is termed leptokurtic, moderate peakedness is known as mesokurtic and a distribution which is relatively flat-topped is known as playkurtic (Shaw and Wheeler, 1985). The result from these two tests will determine whether a non-parametric test is appropriate to be used for the time-series analysis.

3.1.2 Autocorrelation

Autocorrelation or serial correlation may cause an increase in the expected number of false-positive trends. If autocorrelation exists in the time-series data, an approach to remove this trend needs to be performed. The approach used to detect lag k autocorrelation is based on the equation:

$$r_1 = \sum_{t=1}^{N-1} \frac{\left(x_t - \overline{x}\right)\left(x_{t+1} - \overline{x}\right)}{\sum_{t=1}^{N} \left(x_t - \overline{x}\right)^2} \qquad (3\text{-}4)$$

where xt is the time-series data value at time t and N is the number of samples for a constant sampling interval. The values of $r1$ are $0 \leq r1 \leq 1$ with a value of 0 meaning that the time-series is independent, a value of 1 meaning that autocorrelation exists (Box and Jenkins, 1976). The analysis used a significance level of 95%. The most common approach for removing the impact of serial correlation in time-series data is the pre-whitening method (Burn and Hag Elnur, 2002) as follows:

$$xp_t = x_{t+1} - rx_t \qquad (3\text{-}5)$$

where, xpt is the pre-whitened series for time interval t , xt is the original variable x for time interval t, and r is the estimated serial correlation coefficient.

3.1.3 Meteorological time-series trend analysis

The Mann-Kendall test has been used widely for trend detection in hydrological time-series. The alternative hypothesis H_1 of a two-sided test is that the distribution of x_k and x_j are not identical for all, $k\, j \leq$ n with $k \neq j$ (Salmi et al., 2002; Franke et al., 2004; Cheng et al., 2007; Karabork, 2007). The Mann-Kendall test statistic S is calculated using the equation below:

$$S = \sum_{k=1}^{n-1} \sum_{j=k+1}^{n} \text{sgn}\,(x_j - x_k) \qquad (3\text{-}6)$$

Where x_j and x_k are the annual values in years j and k, $j > k$, respectively, and

$$\text{Sgn}\,(x_j - x_k) = \begin{cases} 1 & \text{If } x_j - x_k > 0 \\ 0 & \text{If } x_j - x_k = 0 \\ -1 & \text{If } x_j - x_k < 0 \end{cases} \qquad (3\text{-}7)$$

The statistic $S = 0$ and a variance of S, $Var(S)$, is calculated by

$$Var\,(S) = \frac{1}{18}\left[n(n-1)(2n+5) - \sum_{p=1}^{q} t_p\,(t_p-1)(2t_p+5)\right]$$

(3-8)

Where q is the number of tied groups and t_p is the number of data values in the pth group.

The values of S and $Var(S)$ are used to compute the test statistic Z as follows:

$$Z = \begin{cases} \dfrac{S-1}{\sqrt{Var(S)}} & \text{If } S > 0 \\ 0 & \text{If } S = 0 \\ \dfrac{S+1}{\sqrt{Var(S)}} & \text{If } S < 0 \end{cases}$$

(3-9)

The presence of a statistically significant trend is evaluated using the Z value. Thus, in a two-sided test for the trend, H_1 should be accepted if $|Z| > Z_{\alpha/2}$, where $F_n\,(Z_{\alpha/2}) = \alpha/2$, F_n being the standard normal cumulative distribution function and α being the significance level for the test. Positive values of Z indicate an upward trend and negative values indicate a downward trend.

3.1.4 Sen's non-parameter estimator of slope

The Sen's slope method, used to estimate the magnitude of change, requires a time-series of equally spaced data (Changnon and Demissie, 1996; Burn and Hag Elnur, 2002; Salmi, 2002). This non-parametric test can be used where the trend is expected to be linear, based on the following equation:

$$f\,(s) = Qt + D$$

(3-10)

Where Q is the slope and D is a constant. To estimate the slope Q in Equation (3-10), the slope Q_i of all data pairs are first calculated:

$$Qi = \frac{x_{j-}x_k}{j-k}\ ,\ i = 1,\ldots N$$

(3-11)

Where j and k are times and $j > k$, x_j is a measurement at time j and x_k is a measurement at time k. Q is then estimated as the median of all Q_i (Salmi, 2002)

In addition, to estimate the range of ranks for the specified confidence interval, C needs to be calculated using following equation:

$$C^\alpha = Z_{1-\alpha/2} * \sqrt{Var(S)} \tag{3-12}$$

Subsequently, the ranks of the lower ($M1$) and upper ($M2 + 1$) confidence limits derived by:

$$M1 = \frac{N' - C_\alpha}{2}$$

$$M2 = \frac{N' + C_\alpha}{2}$$

$$\tag{3-13}$$

Where $M1$ and $M2+1$ are the lower and upper confidence limits. The median slope is defined as statistically different from zero (for the selected confidence interval) if the zero does not lie between the upper and lower confidence limits.

3.2 LAND USE CLASSIFICATION AND CHANGE ANALYSIS

3.2.1 Atmospheric correction

The signal recorded by the satellite sensor (e.g., Landsat TM) constitutes errors such as scattering and absorption due to gases and aerosols, which alter the signal amount that is received by the sensor. In many applications using remotely sensed images, atmospheric correction might be necessary to be perform first before continuing with further image processing and analysis. According to Song et al. (2001), atmospheric correction is important to ensure that multitemporal data have same radiometric scale to monitor change of the Earth's surface over time. The atmospheric correction in this thesis was performed using ATCOR 2 software.

3.2.2 Image registration

Image registration is a preprocessing step of image processing and essential for remotely sensed image analysis. It was done to remove geometric distortion to render each pixel in its proper planimetric map location (i.e. x, y). The geometric relationship between the input pixel coordinates (column and row) and the associated map coordinates of the same point (x^1, y^1) usually measured in degrees of latitude and longitude needs to be identified. A number of ground control point (GCP) pairs were used to rectify every pixel in the output image (x, y) with a value from a pixel in the unrectified input image (x^1, y^1) (Lillesand and Kiefer, 1994).

A GCP is a location on the Earth's surface that can be identified on the imagery and located accurately on a map. The structures or features that are permanent or show little change over time and are recognisable are highly recommended to be used as GCPs; an example is a road intersection. The pairs of coordinates from a number of GCPs, (suggested at least 20) (Kardoulas et al., 1996; Riaño et al., 2003; Toutin, 2004), can be modelled to derive the geometric transformation coefficients. The root mean square error (RMSE) was used to measure the goodness of fit between the input and output coordinates for each of the GCPs. The Landsat TM needs to have an RMSE less than one pixel or 30 m.

A procedure known as resampling was performed after collecting GCPs with known RMSE. The resampling was done to ensure that the reflectance from the uncorrected image (i.e. input) was placed correctly in the rectified image (i.e. output). The nearest neighbour resampling method was used in this study. The method was chosen because it does not alter the original reflectance values which are very suitable, especially to detect changes of land use over time. However, it has the disadvantages that it may result in some pixels values being duplicated while others may be lost.

3.2.3 Land use classification (Supervised classification)

Image classification needs to be performed using a remotely-sensed image to make use of its multispectral and multitemporal information and convert it to meaningful information such as the type of land use in the study area. Two main approaches to classify remotely sensed data are unsupervised and supervised classifications. In unsupervised classification the system automatically groups the similar spectral classes based solely on the numerical information in the data. Later the user matches the information classes to several land use classes.

The supervised classification approach is a process of using samples of known identity to classify pixels of unknown identity. In this process, the user has to be familiar with the study area under investigation and 'assist' the system to recognize each pixel of unknown identity (Campbell, 1996). The user needs to have some input that may derive from fieldwork, air photos, topographical maps or reports prior to performing supervised classification. This research used supervised classification since the user was familiar with the study area and was assisted by existing topographical maps.

The maximum likelihood algorithm was used because the algorithm takes variability of the classes into account using the variance-covariance matrix. The algorithm also assumes that the statistics for each class in each band are normally distributed and calculates the probability that a given pixel belongs to a specific land use class. All pixels in the image are classified to a land use class, unless the analyst selects a probability threshold.

The land use and land cover (LULC) classification system developed by Anderson et al. (1976) was used. The system used a hierarchical structure with up to four levels of land land use classification. Level I is the broadest level which divides land use into nine categories, and level II subdivides each category from level I into more detailed land uses. This research adopted the level I class (Table 3-1) only.

Table 3-1 Land use classification system adapted from Anderson et al. (1976).

Level I	Level II
1. Urban or Built-up land	11 Residential 12 Commercial and services 13 Industrial 14 Transportation, communications and Utilities 15 Industrial and commercial complexes 16 Mixed urban or built-up land 17 Other urban or built-up land
2. Agricultural land	21 Cropland and pasture 22 Orchards, groves, vineyards, nurseries and ornamental horticultural areas 23 Confined feeding operations 24 Other agricultural land
3. Rangeland	31 Herbaceous rangeland 32 Shrub and brush rangeland 33 Mixed rangeland
4. Forest land	41 Deciduous forest land 42 Evergreen forest land 43 Mixed forest land
5. Water	44 Streams and canals 45 Lakes 46 Reservoirs 47 Bays and estuaries
6. Wetland	61 Forested wetland 62 Non-forested wetland
7. Barren land	71 Dry salt flats 72 Beaches 73 Sandy and gravel other than beaches 74 Bare exposed rock 75 Strip mines, quarries and gravel pits 76 Transitional areas 77Mixed barren land
8. Tundra	81 Shrub and brush tundra 82 Herbaceous tundra 83 Bare ground 84 Wet tundra 85 Mixed tundra
9. Perennial snow or ice	91 Perennial snowfields 92 Glaciers

Upon completion of supervised classification, accuracy assessment was undertaken to quantify the degree of pixel misclassification.

3.2.4 Accuracy assessment

Accuracy assessment measured the agreement between a standard assumed to be correct and a classified image of known quality (Campbell, 1996). Stratified random samples of reference data (i.e. topographic map) and classification image (i.e. supervised classification) were selected. This approached was used since it provided adequate cover for the entire map and also produced enough pixels for each of the

classes in the classification map. The results of accuracy assessment are normally in the form of a matrix, for example, as in Table 3-2.

Table 3-2. Example of matrix accuracy assessment result.

		Ground classes			No. classified pixels
		A	B	C	
Classification map pixels	A	20	2	2	24
	B	2	19	2	23
	C	3	4	16	23
		25	25	20	70

An overall accuracy and Kappa coefficient were used to assess the accuracy of land use classification that was derived (Lillesand and Kiefer, 1994). The overall accuracy takes into account the correct classification for each class divided by the total pixels used for accuracy assessment.

$$O_a = \frac{\sum t_c}{\sum n_c}$$
(3-14)

Where O_a is the overall accuracy; t_c is the total number of correct classification and n_c is the total number of classifications. Meanwhile, the Kappa coefficient measures the proportional (or percentage) improvement by the classifier over a purely random assignment to classes.

$$K_c = \frac{NA^{'} - B^{'}}{N^2 - B^{'}}$$

(3-15)

Where N is the total sample size, $A^{'}$ is the total number of correctly classified pixels for each class, and $B^{'}$ is the total number of classified pixels multiplied by the total number of each classes of ground data pixels.

3.3   HEC-HMS HYDROLOGIC MODEL

The Hydrologic Modeling System (HMS), developed by the Hydrologic Engineering Center (HEC) of the United States Army Corps of Engineers (USACE), is a lumped, semi-distributed software package used to model rainfall-runoff processes in a

watershed or region. The HEC-HMS hydrological model was used in this research. The model is well-known and used widely for rainfall-runoff modeling (USACE, 2000). The HEC HMS model was chosen due to its flexibility of package with seven infiltration, six stream flow routing, and three baseflow methods. The flexibility of this software allows the user to represent appropriate hydrological processes that need to be modelled, and hence estimate desired outputs adequately.

HEC-HMS requires three input components: (i) a *basin* component, which is a description of the different elements of the hydrologic system (sub-basins, channels, junctions, sources, sinks, reservoirs and diversions) including their hydrologic parameters and topology, (ii) a *meteorologic* component, which is a description in space and time, of the precipitation event to be modeled, and consists of time series of precipitation at specific points or areas and their relation to the hydrologic elements, (iii) *control specifications* component, which defines the time window for the precipitation event and for the calculated flow hydrograph (Francisco and Maidment, 1999; USACE, 2000). HEC-HMS has specific hydrologic elements, which represent how rainfall may convert to runoff.

3.3.1 Basin Model

The basin model contains data, which represent the physical system of the catchment. In basin model preparation, utilization of DEM data and GIS processing enable the basin model to be produced efficiently. The accuracy of the DEM will determine the reliability of the derived basin model. Relatively, for a large catchment area, basin delineation preparation is less time consuming as compared to traditional methods. The model utilized DEM grids of regularly spaced elevation data as a source for derived basic basin parameters such as watershed boundary, flow paths, slope, reach length, etc. (Hoblit and Curtis, 2001).

Recently available GIS software which can be integrated with hydrologic models has made the DEM an important data input. According to USACE (2000), a DEM can be used to derive hydrologic parameters for HEC-HMS such as cross-section data, reach length, flow paths, and hydraulic structures such as bridges, levees and spillways. Accurate and high quality DEM data are needed to represent stream channel and floodplain areas.

The descriptive data are entered by the user or imported from processing done by using HEC-GeoHMS tools embedded in the ARCGIS software. The data include specification of the hydrologic elements of which the basin model is comprised, information on how the hydrologic elements are connected and values of parameters for the hydrologic elements.

3.3.2 Loss volume calculation

Following Horton's equation, the transformation of precipitation into surface runoff is controlled by the independent interaction of many spatially variable processes. The equation considers the excess of precipitation intensity over soil infiltration rate at a given point. This defines infiltration rate:

$$f_t = f_c + (f_o - f_c) \, e^{-kt} \qquad (3\text{-}16)$$

Where f_t is the infiltration at time t (mm hr^{-1}), f_o is the initial infiltration rate (mm hr^{-1}), f_c is the constant infiltration rate (mm/hr) and k is a decay constant.

The cumulative infiltration $F(t)$, without taking into account interception and evapotranspiration, at time t can be expressed as the difference between the cumulative precipitation, $P(t)$ and the sum of the cumulative runoff, $Q(t)$ and the initial abstraction, I_a.

$$F\,(t) = P\,(t) - Q\,(t) - I_a \qquad (3\text{-}17)$$

Surface runoff due to precipitation excess can be derived from rainfall-runoff schemes. A method to estimate precipitation excess and antecedent moisture is based on the Soil Conservation Service (SCS) Curve Number (CN) (USACE, 2000), as a function of cumulative precipitation, soil types, antecedent moisture and land use. This is the command method widely used in hydrologic models. The CN method can be applied for large regions and for the evaluation of spatial variability at various resolutions by implementation of GIS. The equation for the SCS curve number is as in (3-18) (Knebl et al., 2005):

$$Q(t) = \frac{\left(P(t) - I_a\right)^2}{P(t) - I_a + S}$$

$$I_a = 0.2S \qquad\qquad\qquad\qquad (3\text{-}18)$$

$P(t)$ is the accumulated precipitation, and I_a is the initial abstraction before ponding, the maximum amount of rainfall that can be retained on the surface before runoff occurs. S is the potential maximum retention, which measures the ability of a watershed to abstract and retain storm precipitation. The runoff will be zero unless the accumulated rainfall exceeds the initial abstraction. The potential maximum retention S is defined as:

$$S = \frac{25400 - 254CN}{CN} \qquad\qquad\qquad (3\text{-}19)$$

Where CN is curve number. The cumulative runoff, $Q(t)$ at time t is shown in the equation below (USACE, 2000; Knebl et al., 2005):

$$Q(t) = \frac{(P - 0.2S)^2}{P + 0.8S} \qquad\qquad\qquad (3\text{-}20)$$

3.3.3 Estimating the CN

The CN for the study area catchment was estimated as a function of land use, soil types and antecedent moisture of the catchment. It was used in this research to predict the cumulative precipitation excess versus the cumulative losses or abstraction. The CN values published in Technical Report 55 by SCS were used as reference. The CN is a function of three factors: the antecedent moisture condition (AMC) or soil wetness, the land cover/use, and the soil group. The soil wetness is a function of the total rainfall in the 5 day period antecedent to the storm (McCuen, 1982). According to SCS, AMC can be classified into three levels as follows:

AMC 1: represents dry soil with a dormant season rainfall (5 days) of less than 12.7 mm and a growing season rainfall (5 days) of less than 35.6 mm.

AMC II: represents average soil moisture conditions with dormant season rainfall averaging from 12.7 to 27.9 mm and growing season rainfall from 35.6 to 53.3 mm.

AMC III: represents saturated soil with dormant season rainfall of over 27.9 mm and growing season rainfall over 53.3 mm.

3.3.4 Identifying the hydrological soil group

As mentioned earlier, CN is function of land use, AMC as well as soil group. The information on soil group was derived from the available soil map which was produced by the Malaysia Department of Agriculture. By understanding the physical characteristics of the main soil types, their infiltration properties can be estimated according to their soil group as shown in Table 3-3.

From the information on soil types, AMC and land use, a composite CN is calculated as:

$$CN_{composite} = \frac{\sum_{i=1}^{n} A_i CN_i}{\sum_{i=1}^{n} A_i} \qquad (3-21)$$

Where $CN_{composite}$ is the composite CN used for runoff calculations with HEC-HMS; i is the index of the watershed (subdivisions of uniform land use and soil type); CN_i is the CN for subdivision i, and A_i is the drainage area of subdivision i.

Table 3-3 Soil group and infiltration rates (USDA, 1986)

Soil group	Description	Infiltration rate (mm/h)
A	Lowest runoff potential. Coarse texture includes deep sand or gravel with very little silt and clay also deep rapidly permeable loess	>8
B	Moderately low runoff potential. Moderately fine to moderately coarse textures. Mostly sandy soil less deep or less aggregated than A	4 - 8
C	Moderately high runoff potential. Moderately fine to fine texture comprises shallow solid and soil containing considerable clay and colloids. Though less than of those of group D	1 - 4
D	Highest runoff potential includes mostly clays of high swelling percent, but the group also includes some shallow soils with nearly impermeable sub-horizon near the surface.	0 - 1

3.4 TRANSFORMATION OF EXCESS PRECIPITATION TO RUNOFF

In HEC-HMS the transformation of excess precipitation to runoff is to simulate the process of direct runoff across a watershed. The empirical model unit hydrograph (UH) also referred to as a system theoretic model was used in this research. The unit hydrograph model was used due to the well known and widely-used relationship of direct runoff to excess precipitation. The model attempts to establish a causal linkage between runoff and excess precipitation without taking into account much of the internal processes. The equation and the parameters of the model have limited physical significance, and instead, the parameters are selected through optimization of some goodness-of-fit criterion.

The fundamental concept of the UH is that the runoff process is linear, so the runoff from greater or less than one unit is simply a multiple of the unit runoff hydrograph. The SCS UH model was used in this research. The SCS UH method states that the peak and time of UH are expressed by the following (USACE, 2000):

$$U_p = C \frac{A}{T_P} \qquad (3\text{-}22)$$

Where A is the watershed area, and C is the conversion constant (2.08 in SI). The time of peak which represents the duration of the unit of excess precipitation is calculated as:

$$T_p = \frac{\Delta t}{2} + t_{lag} \qquad (3\text{-}23)$$

Where Δt is the excess precipitation duration and t_{lag} is the basin lag or the time difference between the centre of mass of rainfall excess and the peak of the UH.

3.5 ROUTING MODEL

A routing model is used to calculate the conversion of rainfall flow to channel flow for a river. Channel flow computes a downstream hydrograph based on upstream hydrograph as a boundary condition. This research uses a lag model to represent channel flow. The model states that the outflow hydrograph is the inflow hydrograph,

however, with all ordinates translated or lagged in time by a specific duration. The flows are not attenuated, so the shape is not changed. The lag can be estimated from the observed hydrograph as the elapsed time between the time of the centroid of areas of the two hydrographs (i.e. between the time of hydrograph peaks, or between the time of the midpoints of the rising limbs). Downstream ordinates are represented by:

$$O_T = \begin{Bmatrix} I_t & t < lag \\ I_{t-lag} & t \geq lag \end{Bmatrix} \tag{3-24}$$

Where O_t is the outflow hydrograph ordinate at time t, I_t is the inflow hydrograph ordinate at time t and lag is the time by which the inflow ordinates are to be lagged.

3.6   SENSITIVITY ANALYSIS

Sensitivity analysis is a method to determine which parameters of the model have the greatest impact on the runoff hydrograph results. Local sensitivity analysis was chosen. Using local analysis the effects of each input parameter are calculated separately with the other parameters kept constant or at their initial values. The analysis was done by adjusting the input model parameters using $\pm 10\%$, $\pm 20\%$ and $\pm 30\%$ from the initial model input (i.e. calibrated model parameters) parameters. Relative variation in the model output was calculated as:

$$\text{Output variation} = \frac{O_t - O_b}{O_b} \times 100 \tag{3-25}$$

Where O_t is a value of the output variable for a given simulation and O_b is the value of the initial output. Then the model was run again and simulations using initial input parameters and different values according to the percentage values as described above were compared. Based on the derived results, the sensitivity index is calculated for each sub-basin according to its effect on the peak flow, runoff volume, total direct runoff, total baseflow and total loss. The sensitivity index was calculated as follows (Al-Abed and Whitley, 2002):

$$S_{i=} \left(\frac{O_2 - O_1}{I_2 - I_1} \right) \frac{I_{AVG}}{O_{AVG}} \tag{3-26}$$

Where S_i is the sensitivity index, O_1 and O_2 are the model output values corresponding to I_1 and I_2 which represent the smallest and largest input values (which in this study were $\pm 30\%$ for a given parameter), and I_{AVG} and O_{AVG} are the averages of I_1, I_2 and O_1, O_2 respectively.

Subsequently, the rank of parameters (R_p) from the most sensitive to least sensitive to the hydrograph output was performed using the absolute average sensitivity index as shown in equation (3-27):

$$R_p = \frac{1}{n} \sum_{i=1}^{n} |S_i| \tag{3-27}$$

From the parameter rank, model calibration was performed as described in the next section.

3.7   MODEL CALIBRATION

Model calibration is a systemic approach for adjusting model parameters values to derive an acceptable match between the simulated and observed hydrographs. In the HEC-HMS model, the objective function is used to measure quantitatively the degree of difference between observed and simulated runoff. The process tries to find the optimum values for parameters, which cannot be estimated through measurement or observation of catchment characteristics. Automated calibration was used in the HEC-HMS model by iteratively adjusting the parameter values until the minimum value of the selected objective function was achieved.

3.7.1 Objective function

There are seven objective functions within the HEC-HMS model (USACE, 2000) to optimize the parameter values which are; the sum of squared residuals, peak-weighted

RMS error, percent error peak, percent error volume, RMS log error, sum of absolute residuals and time weighted error. However, only two widely used objective functions are adopted in the analyses which are the sum of squared residuals and peak-weighted RMS error.

The sum of squared residuals (SSR) gives greatest weight to overestimates and underestimates between observed and simulated runoff ordinate. The equation is as follows:

$$Z = \sum_{i=1}^{NQ} [q_o(i) - q_s(i)]^2 \qquad (3\text{-}28)$$

Where, q_o is the observed flow value at a time i, q_s is the simulated flow value at a time i and NQ is the number of flow samples.

The peak-weighted RMS error (PWRMSE) uses a weighting factor. It assigns greater overall weight to error near the peak discharge. Peak-weighted RMS error was calculated using equation (3-29):

$$Z = \sqrt{\frac{\sum_{i=1}^{NQ} [q_o(i) - q_s(i)]^2 \dfrac{q_o(i) + \overline{q_o}}{2\overline{q_o}}}{N}} \; ; \overline{q_o} = \frac{1}{N} \sum_{i=1}^{NQ} q_o(i) \qquad (3\text{-}29)$$

Where $\overline{q_o}$ is the average value of the observed flow.

3.7.2 Model efficiency

Simulated hydrographs may also be subjected to model efficiency tests. Model efficiency is measured using a mathematical equation to assess the closeness between simulated and observed hydrographs. Model efficiency can be assessed using: (i) Nash Sutcliffe efficiency index (E_f); (2) coefficient of determination (R^2); (3) root mean square error (RMSE); (4) mean of absolute error (MAE); and (5) %BIAS. The methods

are used because these measurements are primarily concentrated on the peaks and are very sensitive to high flows of the hydrograph (Krause et al., 2005).

The Nash Sutcliffe efficiency index (E_f) method is widely used to measure goodness of fit of hydrological models (Nash and Sutcliffe, 1970). It is calculated as:

$$E = 1 - \frac{\sum_{i=1}^{n}[Q_s(i) - Q_o(i)]^2}{\sum_{i=1}^{n}(Q_o(i) - \overline{Q_o})^2} \qquad (3\text{-}30)$$

Where, n is the number of flow samples, Q_o represents the observed hydrograph and, Q_s represents the simulated hydrograph. The result of the Nash and Sutcliffe index is within a range of 1 to $-\infty$. A perfect fit is represented by value of 1 and an efficiency value of lower than zero denotes that the mean value of the observed time series would have been a better predictor than the model (Krause et al., 2005).

The coefficient of determination (R^2) is defined as the sum of squared errors divided by the total sum of the square of the deviation of the observed values from the overall mean. The r^2 is calculated using the following equation:

$$r^2 = 1 - \frac{\sum_{i=1}^{n}(y_i - x_i)^2}{\sum_{i=1}^{n}(y_i - \overline{y})^2} \qquad (3\text{-}31)$$

where y_i is the observed value, x_i is the simulated value and $\overline{y}$ is the observed mean value. The range of R^2 lies between 0 and 1 which describes how much of the observed dispersion is explained by the prediction. A value of 1 means that the observed and simulated hydrographs perfectly fit, whereas zero means that no correlation exists between the observed and simulated hydrographs.

Another two methods to measure goodness of fit are the root mean square error (RMSE) which gives particular emphasis to differences of large absolute values and mean absolute error (MAE). These are formulated as:

$$RMSE = \sqrt{\frac{1}{n}\sum_{i=1}^{n}(\frac{x_i - y_i}{y_i})^2} \qquad (3\text{-}32)$$

$$MAE = \frac{1}{n}\sum_{i=1}^{n}\frac{\left|y_i - \overline{y_i}\right|}{y_i} \qquad (3\text{-}33)$$

and the terms of the models are described in Equation   (3-31).

The %BIAS represents the relative percentage differences between the observed and simulated hydrographs as given in Equation   (3-34) :

$$\%BIAS = \frac{\sum_{i=1}^{n}[q_o(i) - q_s(i)]}{\sum_{i=1}^{n}q_o(i)} \times 100\% \qquad (3\text{-}34)$$

3.8   MODEL VALIDATION

Validation is a process of testing the model's ability to simulate observed data different than used for the calibration within acceptable accuracy. The process used constant model parameters obtained from an earlier calibration process as described in section 3.6. The degree of difference between observed and simulated hydrographs is calculated to assess the efficiency of the validated model. Five model efficiency quantitative measures can be used as described in section 3.6 (Equations (3-30); (3-31); (3-32); (3-33) and (3-34)).

3.9   CLIMATE CHANGE SCENARIOS

Future climate change scenarios are used in this research based on the combination of two RCM outputs of future precipitation changes as simulated by the 'Regional Hydroclimate Model of Peninsular Malaysia (RegHCM-PM)' used by the National Hydraulics Research Institute of Malaysia (NAHRIM) (Shaaban, 2008) and secondly, the Providing Regional Climates for Impact Studies (PRECIS) used by the Malaysian Meteorological Department. These two models projected that more extreme hydrological conditions in the future may be expected since higher maximum and

lower minimum precipitation is projected (Shaaban, 2008; MMD, 2009). A precipitation climate scenario for Kelantan using an annual precipitation projection (in percentage change) from the two RCM models for 2020s, 2050s and 2080s was used. Subsequently, the observed precipitation event in 2004 (i.e. baseline model) was scaled by the simulated percentage change (i.e. from RCM models) to represent the precipitation event *as if* in the future and this was input to the runoff model calibrated to the 2004 event.

3.10 LAND USE MAP AND LAND USE SCENARIO

Two hypothetical scenarios for land use were adapted; the first one using an arbitrary land use change scenario and the second using land use projections as estimated from various sources (Goh, 2000; Hai, 2000; Abdullah, 2003; Atan, 2005, ADB, 2009). The first land use scenario, later known as *what-if scenario,* was simulated to quantify the magnitudes of the effect of possible land use changes on the hydrological response in the River Kelantan catchment. The second land use scenario, later known as a *likely projected scenario*, was used because it was assumed that it is likely to happen to land use in the future. There are some justifications for the second land use change scenario. Observed previous land use change (i.e. in the year 1988 to 2000), future agricultural production projections (i.e. oil palm and rubber plantations), availability of suitable land for agriculture and population growth rate are some factors taken into consideration. The projection values will be used as an input for basin modelling particularly through changes to the CN value and percentage of impervious surface.

3.11 SUMMARY

The methods presented in this chapter will then be used for three separate analyses, primary to quantify trends in streamflow data of the River Kelantan catchment, followed by development of rainfall–runoff models of the study area and how precipitation change and land use changes affect hydrological response for the past, current and future runoff events.

Chapter 4

Study Area and Data

4.1 INTRODUCTION

This chapter introduces the location and physiography of the study area. Kelantan is one of the largest states in Malaysia and is affected annually by monsoon flooding, especially in the months of October to March. The description of the dataset used in the research is also presented.

4.2 STUDY AREA

Kelantan is one of the largest states in Peninsular Malaysia apart from Pahang, Terengganu, occupying the huge River Kelantan basin. It is situated in the middle of Peninsular Malaysia which is bordered to the north by Thailand, to the west by Perak, Selangor, Negri Sembilan, and to the south by Terengganu, Pahang and Johor and to the east by the South China Sea (Figure 4-1). The total area of Kelantan is 15,022 km^2 or 4.4% of the Malaysia area with a total population of 1.63 million (Malaysia Statistics Department, 2006). It consists of ten districts namely Bachok, Gua Musang, Jeli, Kuala Krai, Machang, Pasir Mas, Pasir Puteh, Tanah Merah, Tumpat and Kota Bharu which has become the state capital. The River Kelantan catchment is located in the north eastern part of Peninsular Malaysia between the latitudes 4^0 40' and 6^0 12' North, and longitudes 101^0 20' and 102^0 20' East. About 68.5% of the population lives in the Kelantan River Basin. The others are found in the Golok and Kemubu River basins and in the northern coastal plain of the State. The major economic activities in Kelantan

70

State are agricultural based, mainly the cultivation of paddy rice, rubber, oil palm and tobacco. Fishing and livestock farming are also important occupations found in this area. About two thirds of the State is covered by rich tropical forest. Palm oil, rubber and cocoa are cultivated extensively in large land development schemes. Moreover, the establishment of several industrial estates has enhanced the manufacturing sector as a major contributor towards the State's economy. This research will focuses on the River Kelantan area for flood modelling and land use change scenario analysis.

The River Kelantan or Sungai Kelantan was chosen to perform the time series analysis. It is situated in northeast Peninsular Malaysia and is one of the major rivers in Malaysia, frequently affected by flooding events (Awadalla and Noor, 1991; Chan, 1995; Chan, 2002; DID, 2004). It is the longest river in Kelantan State at 248 km and drains an area of 13,100 km^2. The river originates in the Tahan mountain ranges and flows northwards draining into the South China Sea.

The River Kelantan has two tributary rivers: River Galas and River Lebir. River Galas has two other tributaries known as the River Nenggiri and River Pergau which contribute about 8,000 km^2 or 54% from the total Kelantan's catchment (i.e. 13,100 km^2). Meanwhile, River Lebir has one tributary known as River Relai which contributes about 2,500 km^2 or 17% from the total catchment (DID, 1995). The River Kelantan system flows northward passing through major towns as Kuala Krai, Tanah Merah, Pasir Mas and Kota Bharu and finally discharging into the South China Sea (Figure 4-2). The average width of the River Kelantan is between 180 to 300 m. From the total catchment area, approximately 95% is dominated by steep mountainous country (mostly covered with virgin jungle) rising to a height of 2,135 m while the remainder is undulating land (mostly covered by rubber and paddy).

Towns such as Pasir Mas, Kuala Krai, Machang and Kota Bharu are worst affected annually by flooding. According to a flood report in 2005/2006, estimated damage to drainage and irrigation structures during flooding which occurred in November and December 2005 was RM12.1 million. In Kelantan, there are four catchments: River Kelantan, River Kemasin, River Semerak and River Golok. However, only the River Kelantan was used in the research to quantify trends in climate and land cover/land use time series.
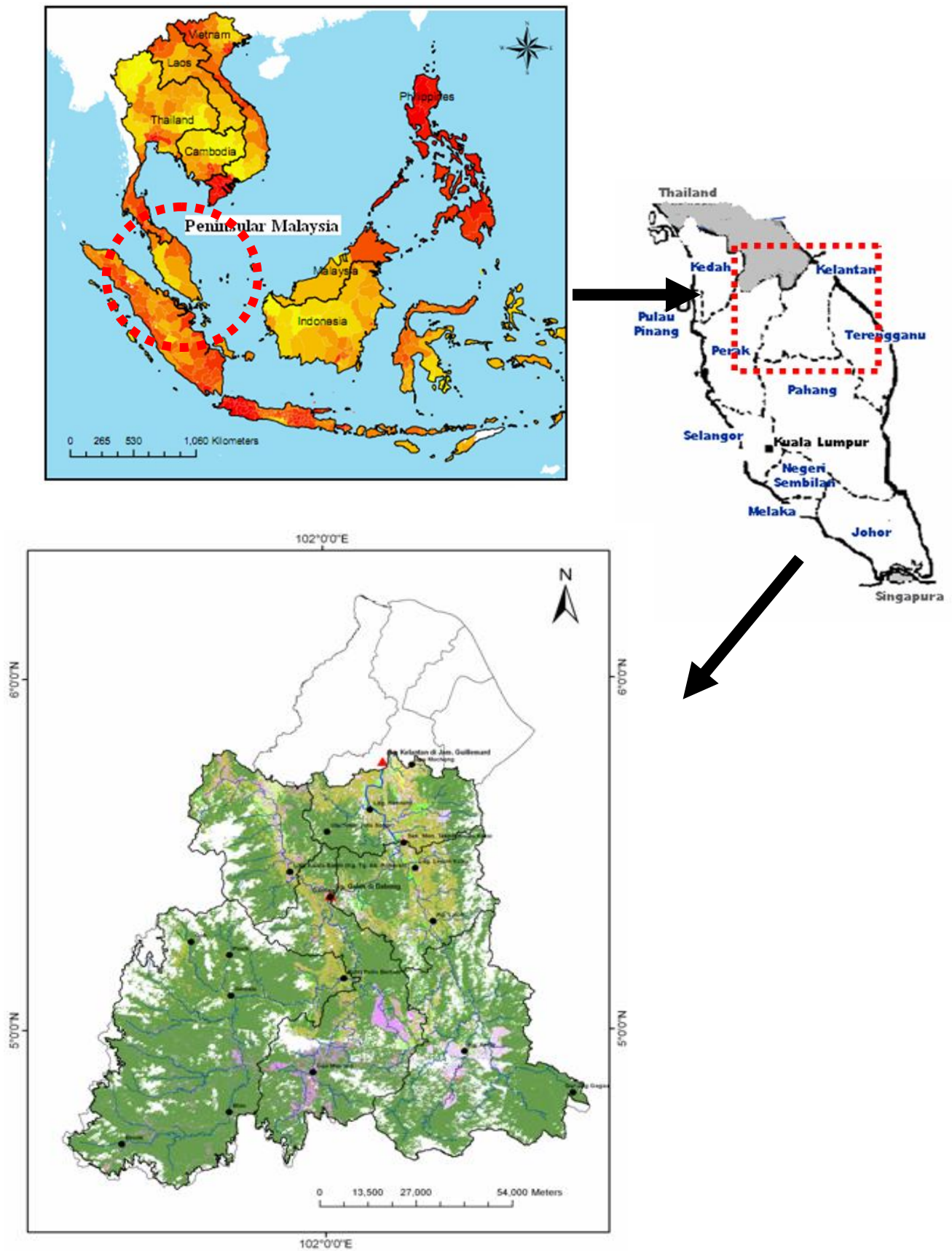
Figure 4-1 (Upper left) Malaysia location, (Upper right) Malaysian states and (Lower left) Kelantan Map.
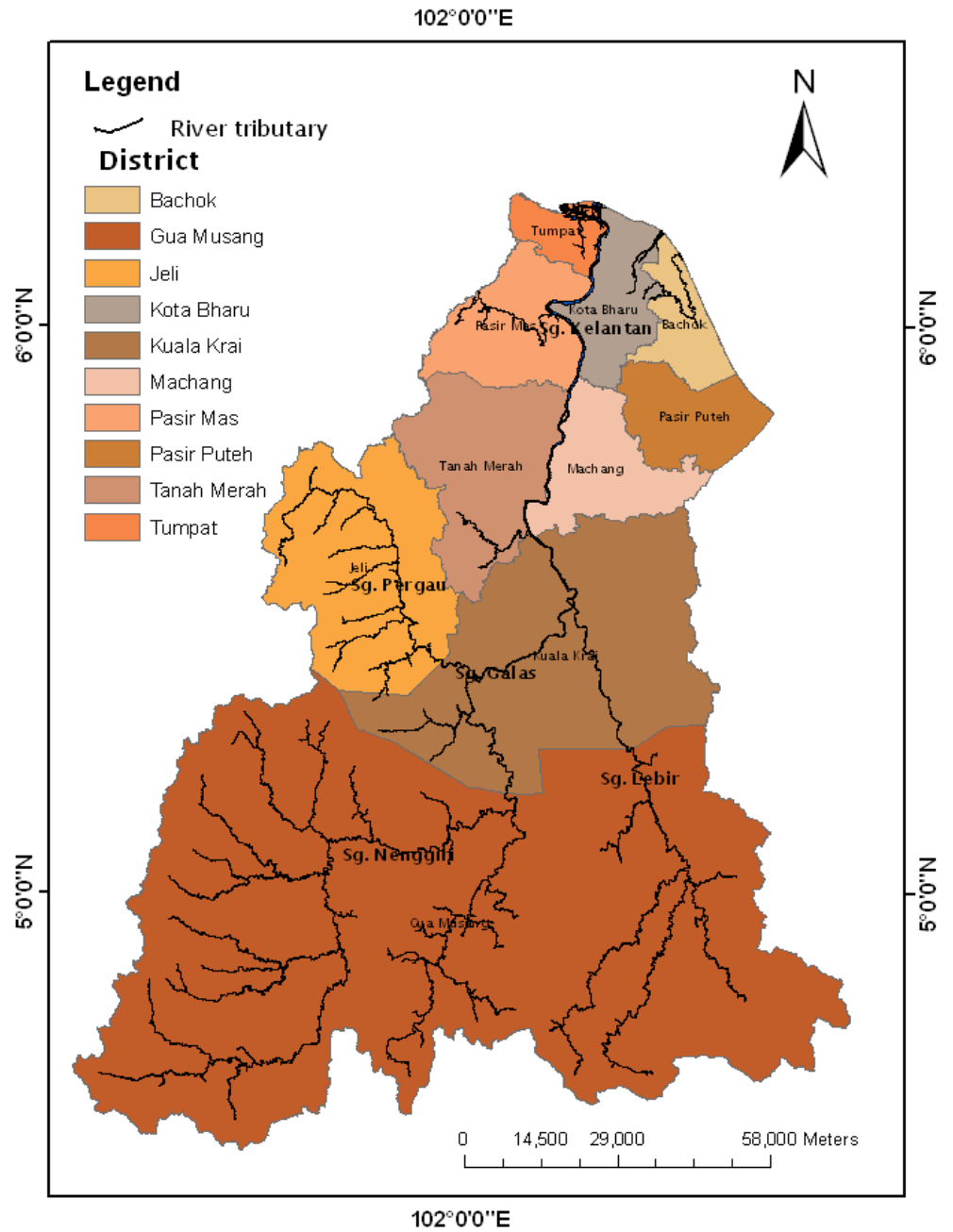
Figure 4-2 River Kelantan tributaries and Kelantan district map.

Approximately, 400 residences (i.e. district, village and town) are located along the
River Kelantan. During the NE monsoon season the downstream area between the

Rivers Galas and Lebir are mostly affected by flooding (i.e. Kuala Krai and Kota Bharu districts) before the discharge water drains to South China Sea.

4.2.1 Land use

Kelantan land use has been dominated by forest reserves which cover an area of 1,078,398.4 ha (71.8% of Kelantan total land area) mainly located in the upstream area or Gua Musang province. It is followed by agriculture which covers an area of 309,279.3 ha (20.6%). Paddy cultivation covers 71,134.0 ha (4.7%), while built up areas only cover 22,146.3 ha (1.5%) of which 28% is located in the district of Kota Bharu. The distribution of land use by district in Kelantan for the year 2002 is shown in Table 4-1. Land use change in terms of urban growth has been changing progressively from the 1970s to 1990s with 7% growth and after the 1990s there were very slow developments in the area with only 1.4% growth (Hassan, 2004).

Table 4-1 Present land use by Kelantan district in the year of 2002 (in hectare).

District	Land Use Categories (hectare)				Total Land Area (hectare)
	Built Up	Agriculture	Forest Reserve & Water Body	Others	
Kota Bharu	6,288.4	32,743.4	854.0	54.0	39,939.00
Tumpat	2,630.3	12,869.3	2,065.0	558.0	18,122.6
Pasir Mas	2,546.9	44,626.0	10,206.3	141.4	57,520.6
Machang	861.8	25,472.3	25,525.3	1,096.0	52,955.4
Pasir Puteh	308.1	29,901.7	11,535.8	533.8	42,279.4
Bachok	4,125.0	19,691.4	2,960.6	763.0	27,540.0
Gua Musang	1,506.0	82,921.4	730,663.1	1,261.0	816,351.5
Jeli	661.5	18,500.4	114,097.2	72.6	133,331.7
Kuala Krai	988.3	59,350.6	165,393.1	413.2	266,145.2
Tanah Merah	2,230.0	54,202.8	29,593.2	1,127.0	87,153.0
Total	*22,146.3*	*380,279.3*	*1,092,893.6*	*6,020.0*	*1,502,600.6*

Source : Adapted fom Technical Report of RSN Kelantan, 2003-2020

Based on forecasted growth of the population and future needs for other sectors, the projection of land requirements for development in Kelantan for the period 2000-2020 is as shown in Table 4-2. This information is important for the present research which focuses on land use change scenarios. The information from projected development

will be used to develop land use change to study its potential impact on runoff for hydrological modelling using the HEC-HMS model.

Table 4-2.Projected development land requirement by category, Kelantan, 2000-2020.

Category		2000 - 2010		2010-2020		Total	
		Ha.	%	Ha.	%	Ha.	%
1.	Residential	12,760	76.9	11,100	82.1	23,860	78.4
2.	Commercial	80	0.5	210	1.6	290	1.0
3.	Industrial	3,760	22.6	2,210	16.3	5,970	19.6
Total		16,600	100.0	13,520	100.0	30,420	100.0

Source : RSN Kelantan, 2003 – 2020

Overall, the projected land requirement for development involves residential, industrial and commercial, with a total required land area of 30,420 ha for the period 2000-2020. The residential development area required is 23,860 ha.

4.2.2 Climate

Malaysia lies entirely in the equatorial zone. The climate is governed by the regime of the northeast (NE) and southwest (SW) monsoons. According to Tangang (2007), October-November-December (OND) represents the early and January-February-March (JFM) represents the late stages of the winter monsoon in Malaysia, also known as the NE monsoon. The April-May-June (AMJ) and July-August-September (JAS) seasons represent the early and late stages of the summer monsoon, respectively, also known as the SW monsoon. The NE monsoon is responsible for the heavy rains which hit the east coast of the peninsula and frequently cause widespread flooding. The SW monsoon is a drier period for the whole country.

 The period between these two monsoons is marked by heavy precipitation which are in December to February. Precipitation patterns in the River Kelantan catchment have been divided into two regions known as the "coastal rainfall" region which is located in the downstream catchment area and the "inlands rainfall" region which dominates the upstream catchment area. Annual precipitation over the area varies between 0 mm to 200 mm in the dry season to 3000 mm in the wet or monsoon season. The estimated runoff for the River Kelantan catchment is 500 m^3s^{-1} during 1950 to 1990 (DID, 2000). Due to the NE monsoon which brings along heavy rainfall, the River Kelantan often

overflows in the period, causing an almost annual recurrence of flood to the State between the end of November till early January (DID, 2006).

The average temperature throughout the year is very stable (26°C), and the mean annual rainfall varies as described earlier. Regional variations in temperature and rainfall are mainly due to relief. For example, the east part of Peninsular Malaysia has a mean temperature of 18°C and an annual rainfall of over 2500 mm, compared to West part of Peninsular Malaysia of 27°C and 2400 mm. The humidity is high (80 %) due to the high evaporation rate in the dry season. The total surface runoff is 566 km³, and about 64 km³/yr (7 % of the total annual rainfall) contribute to groundwater recharge (Zakaria, 1975; Awaldalla and Nor, 1991). However, about 80% of the groundwater flow returns to the rivers and is, therefore, not considered an additional resource. The total internal water resources of Malaysia are estimated at 580 km³yr^{-1} (Zakaria, 1975; Awaldalla and Nor, 1991).

The state of Kelantan is characterized by relative humidity, mild wind and heavy monsoonal rainfall in the NE monsoon season when the high velocity NE winds bring heavy rain to this area. About 40% of annual rainfall is received in the Kelantan state during the NE monsoon. On a macro scale the Kelantan catchment can be divided into two climate regions according to its land elevation surface and effect of rainfall. The first is North region climate and secondly, Middle Highland region. The North region climate is normally associated with relatively warm weather and stable climate conditions (i.e. dry and wet conditions through the year). Meanwhile, the Middle Highland region is associated with relatively cool climate and less rainfall than experienced in the North region (Figure 4-3).

Precipitation in the Kelantan state is not uniformly distributed thoroughout the year. Two weather conditions are experienced in this area which are the wet period and dry period. As described earlier, wet conditions coincide with the NE monsoon. In the extreme NE monsoon season rainfall has been recorded of about 100 to 300 mm per day (DID, 2004). The dry period normally is characterized by weak prevailing winds or usually by calm atmospheric conditions. In 2006, the mean annual rainfall for Kelantan was recorded as 3296.7 mm, with maximum rainfall received of 654.4 mm in December (during NE monsoon) and minimum rainfall of 114.2 mm in March. The

temperature, precipitation and evaporation for the period of 1952 to 1997 of Kota Bharu observation stations are represented in Table 4-3.
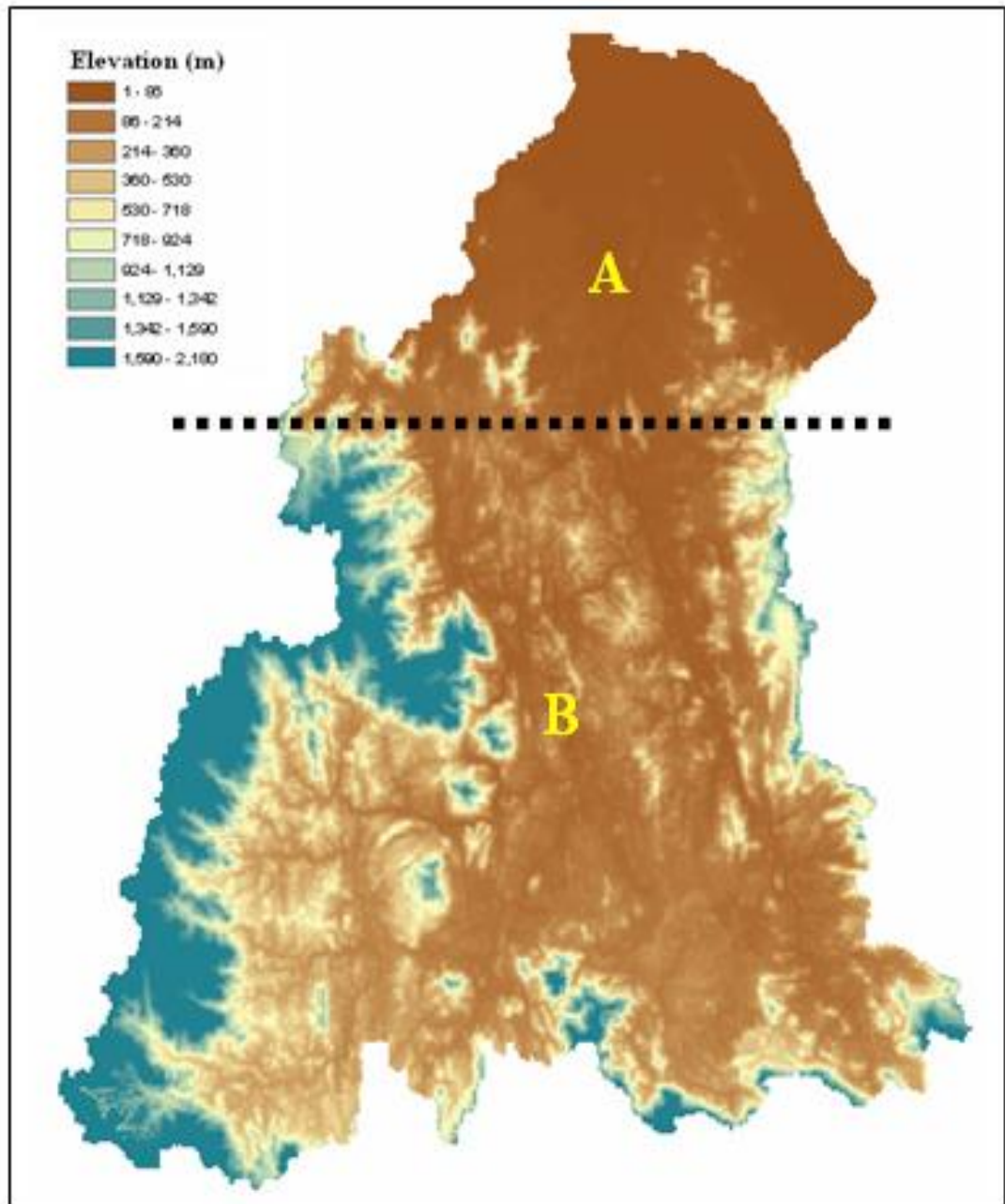
Figure 4-3 Two climate region sub-divisions (approximately) representing by dash line
(**----**) for River Kelantan catchment of (A) North region climate and (B) Middle
highland region climate overlaid with elevation map of Kelantan area.

Table 4-3 The monthly mean temperature and precipitation of Kota Bharu station for the period of 1952-1997.

Month	Temperature (^{0}C)	Precipitation (mm)
Jan	25.7	169
Feb	26.2	74
Mar	27.9	87
Apr	28.1	83
May	27.7	178
June	27.2	187
July	27.0	212
Aug	26.8	257
Sep	26.7	280
Oct	26.0	302
Nov	25.8	640
Dec	26.8	618
Annual	26.8	3086

4.2.3 Geology/Soil

Geology structure in the Kelantan states is comprised of about 25% granite and intermediate intrusive rocks (Zakaria, 1975). The remainder geology are sedimentary rocks (i.e. argillaceous, arenaceous, rudaceous and calcareous) as shown in Figure 4-4. The granite and intermediate intrusive rocks are located with a steep gradient while the other rocks are situated with a gentle gradient. In the lower gradient of the main river tributaries of Nenggiri, Galas, Lebir and Pergau, extensive floodplains and low river terraces are formed.

Most of the northern area of the Kelantan state is covered by Quarternary alluvium (i.e. gravel, sand, silt and clay) and topographically is dominated by the coastal plain with elevation less than 75 m above mean sea level. While the eastern and western granitic masses consist of various types of rock (i.e. shales, sandstones, conglomerate, quartzite, limestone, siltstone and mudstone) and metamorphic rocks of the Paleozoic age (Awaldalla and Nor, 1991), its depth seldom exceeds a few metres. In the steep land area, particularly in the mountainous area, acid igneous rock formations exist and also soils such as alluvium, clay-loam–sand soil which support the growth of thick tropical forest in this area. The soil cover is a metre or so deep but depths of more than 18 m may be encountered in localized areas. The southern parts of the Kelantan state consist of Silurian-Ordovician formations (i.e. schists, phyllite, slate and calcium carbonate,

sand and volcanic rocks). The remaining portion, comprising almost one-third of the catchment, is cloaked by a variable soil cover that varies in depth from a few metres to more than 9 m (Zakaria, 1975; Awaldalla and Nor, 1991).

According to DID (2000), the upstream area until the Guillemard Bridge streamflow gauge station consists of soil from lithosil types on high slopes area. Meanwhile, the low slope areas are dominated by podzoil red-yellow mixed with podzoil yellow-grey soil (i.e. from granite rock formation) and also sediment rocks and laterite soil. These rocks have low baseflow level. However, during heavy rainfall baseflow increases and causes river velocities to change rapidly. Subsequently, flooding can happen due to changing water level conditions (KFD, 2006).
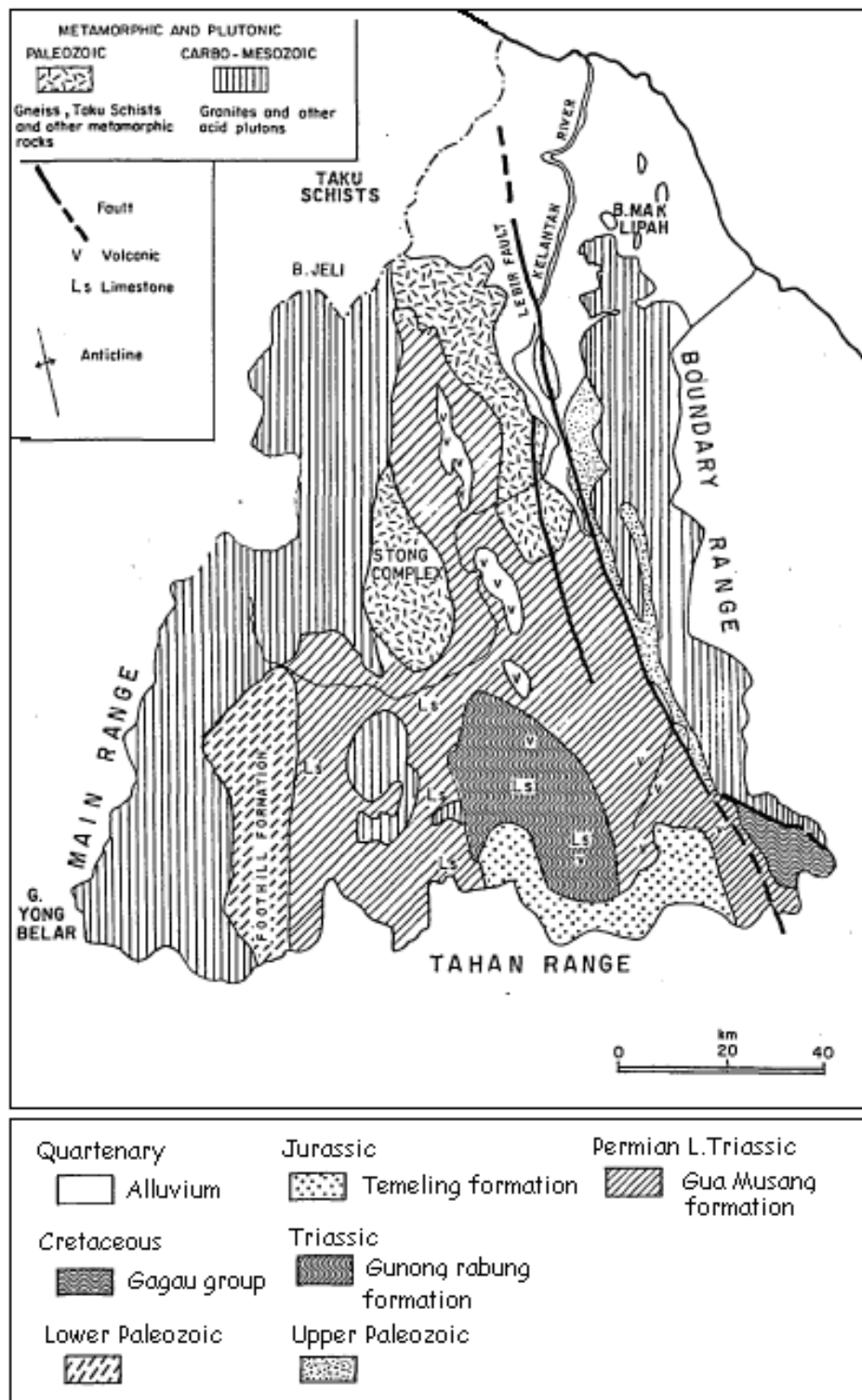
Figure 4-4 Geological map of Kelantan (adapted from Awaldalla and Nor, 1991).

4.3 DATA

4.3.1 Meteorological data

The hydrological data used in the study comprises precipitation and stream flow records for a period of 16 to 44 years. The historical data were extracted from the hydrological data network of the Malaysian Department of Irrigation and Drainage (DID). The data were divided into annual, seasonal and monthly time-series for stream flow and precipitation for the whole River Kelantan catchment. For seasonal trend analysis, the year was divided into four main seasons: JFM (January-February-March), AMJ (April-May-June), JAS (July-August-September) and OND (October-November-December) (Tangang et al., 2007). Total precipitation was calculated for every three month period and trends fitted to these data for each rain gauge station.

The data provided good continuity and were chosen based on having few missing data records. A brief description of each gauge is presented in Table 4-4. Overall, approximately 19% of the data were missing from the time-series.

Table 4-4 Spatial and temporal information of 15 River Kelantan rain gauge stations and two streamflow stations comprised of latitude, longitude, altitude (m), and period of records.

Precipitation Station	Latitude	Longitude	Altitude (m)	Period of records
River Galas catchment precipitation gauge stations (upstream)				
Brook	4^0 40 N	101^0 29 E	153	1984-2006
Blau	4^0 46 N	101^0 45 E	165	1984-2006
Gua Musang	4^0 52 N	101^0 58 E	93	1975-2006
Gemala	5^0 05 N	101^0 45 E	91	1984-2006
BP Bertam	5^0 08 N	102^0 02 E	71	1975-2006
Gob	5^0 15 N	101^0 39 E	270	1984-2005
Dabong	5^0 22 N	102^0 00 E	82	1975-2006
Ladang Kuala Balah	5^0 27 N	101^0 54 E	50	1975-2006
River Kelantan catchment precipitation gauge stations (downstream)				
Gunung Gagau	4^0 45 N	102^0 39 E	1067	1984-2006
Kg Aring	4^0 56 N	102^0 21 E	73	1975-2006
Kg Laloh	5^0 18 N	102^0 16 E	48	1975-2006
Ladang Lepan Kabu	5^0 27 N	102^0 13 E	50	1975-2006
Kuala Krai	5^0 31 N	102^0 12 E	29	1975-2006
Ulu Sekor	5^0 33 N	102^0 00 E	91	1984-2006
Ladang Kenneth	5^0 37 N	102^0 O7 E	30	1975-2006
JPS Machang	5^0 47 N	102^0 13 E	31	1975-2006
Stream flow Station	**Latitude**	**Longitude**	**Altitude (m)**	**Period of records**
River Kelantan	5^0 45 N	102^0 09 E	23	1975-2006
River Galas	5^0 22 N	102^0 00 E	82	1975-2006

Only two streamflow gauges were used, one for upstream (River Galas) and another one located downstream (River Kelantan) (Figure 4-5). Brief information on the two streamflow gauges is given in Table 4-4. From 34 precipitation gauge stations, only 16 stations were used due to data completeness, with the record length ranging from 1975 to 2006 (Table 4-4).
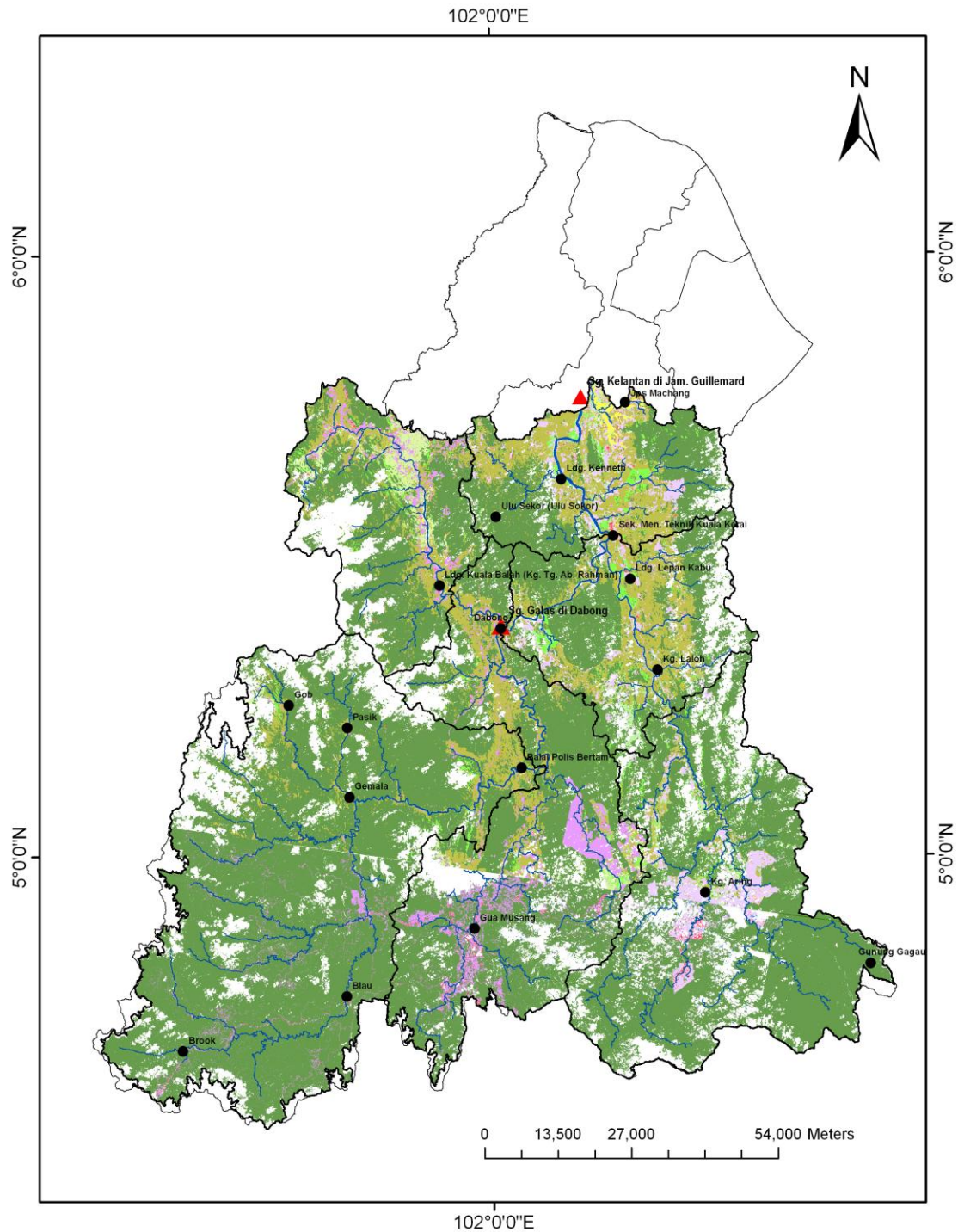
Figure 4-5 Map of Kelantan catchment showing precipitation stations (●) and streamflow stations (▲) with Landsat TM satellite sensor images overlaid corresponding to the upstream and downstream areas.

4.3.2 Remotely sensed images

To derive land use classification, Landast TM remotely-sensed images were used. Landsat TM is fully owned by United States government starting with Landsat 1-

Multispectral Scannning System (MSS) and until today Landsat 7- Landsat Enhanced Thematic Mapper (ETM$^+$). For this study Landsat 5 – Thematic Mapper (TM) was used to map land use in the study area.

Two multi-temporal satellite sensor images were used. Landsat Thematic Mapper (TM) imagery of 7 August 1988 and 28 May 2000 were supplied by the Malaysian Remote Sensing Agency (Remote Sensing Malaysia). These dates were chosen because the temporal difference was relevant to the study and sufficient to perform land use change analysis in the area. The satellite sensor images have 30 m spatial resolution, 8-bit radiometric resolution and six spectral channels denoted by TM1 (blue waveband), TM2 (green), TM3 (red), TM4 (near-infra red) TM5 (mid-infrared) and TM6 (far-infrared). The TM3, TM4 and TM5 bands were used to discriminate land use in the study area (Price et al., 2002; Cingolani et al., 2004). The original uncorrected images of the years 1988 and 2000 before atmospheric and geometric corrections are as shown in Figure 4-6 and Figure 4-7.
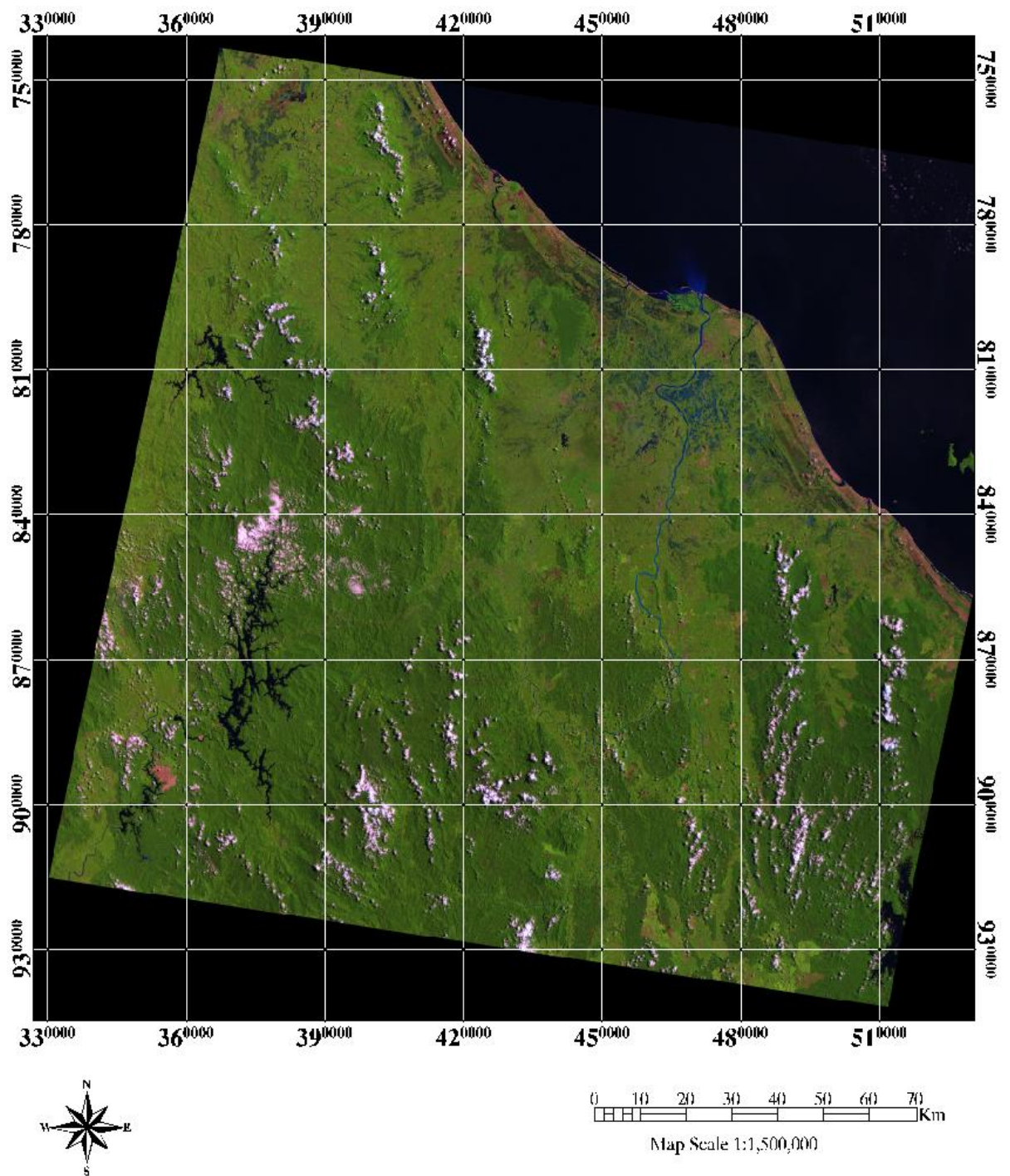
Figure 4-6   The 1988 false color composite atmospherically-corrected image of Landsat TM path 127/56 covering the northern part of Peninsular Malaysia and the Kelantan state: Red= TM5 (MIR), Green = TM4 (NIR) and Blue = TM3 (Red).
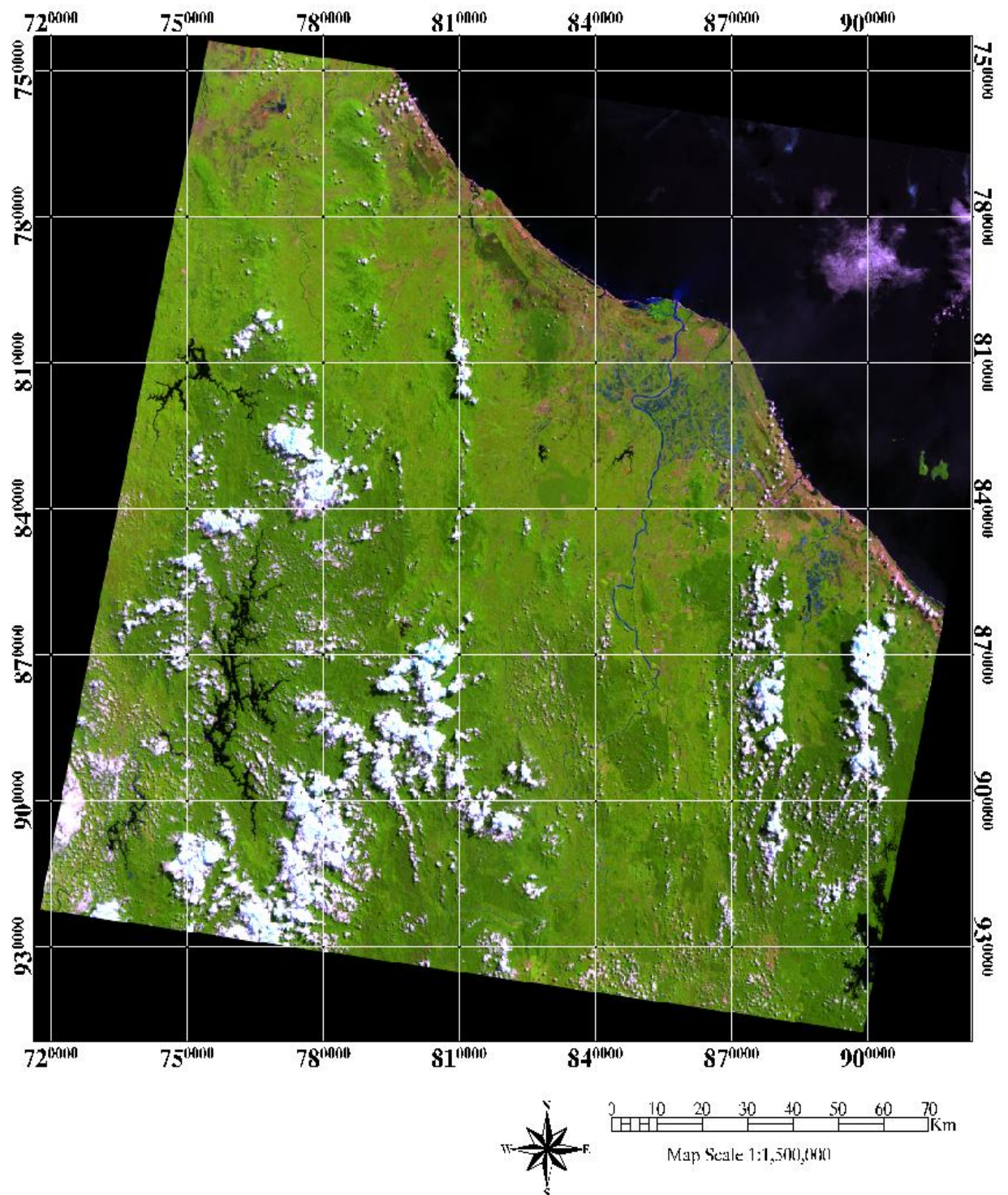
Figure 4-7   The 2000 false color composite atmospherically-corrected image of Landsat TM path 127/56 covering the northern part of Peninsular Malaysia and the Kelantan state: Red= TM5 (MIR), Green = TM4 (NIR) and Blue = TM3 (Red).

4.3.3 GIS layers

A digital land use map of 2002 provided by the Malaysia Department of Town, Country and Regional Planning (TCPD) was used to aid the land use classification. Additionally, other GIS layers representing the Kelantan catchment were obtained from DID, Malaysia. The layers comprise of a grid data structure of digital elevation model (DEM) with 30 m spatial resolution, river network, rainfall gauge stations and streamflow gauge stations (Figure 4-8).

The most crucial data for catchment delineation is a DEM. A DEM consists of a matrix of square grid cells with the mean cell elevation stored in a 2-D array of numbers representing the spatial distribution or topography of elevations above some arbitrary datum in a landscape (Garbrecht and Martz, 2000). DEMs have become important data to derive drainage network structures based on automatic procedures such as provided by the HEC-GeoHMS tool (USACE, 2000b) as is used in this research. Detailed description of catchment delineation using HEC-GeoHMS tool will be discussed in its own chapter.
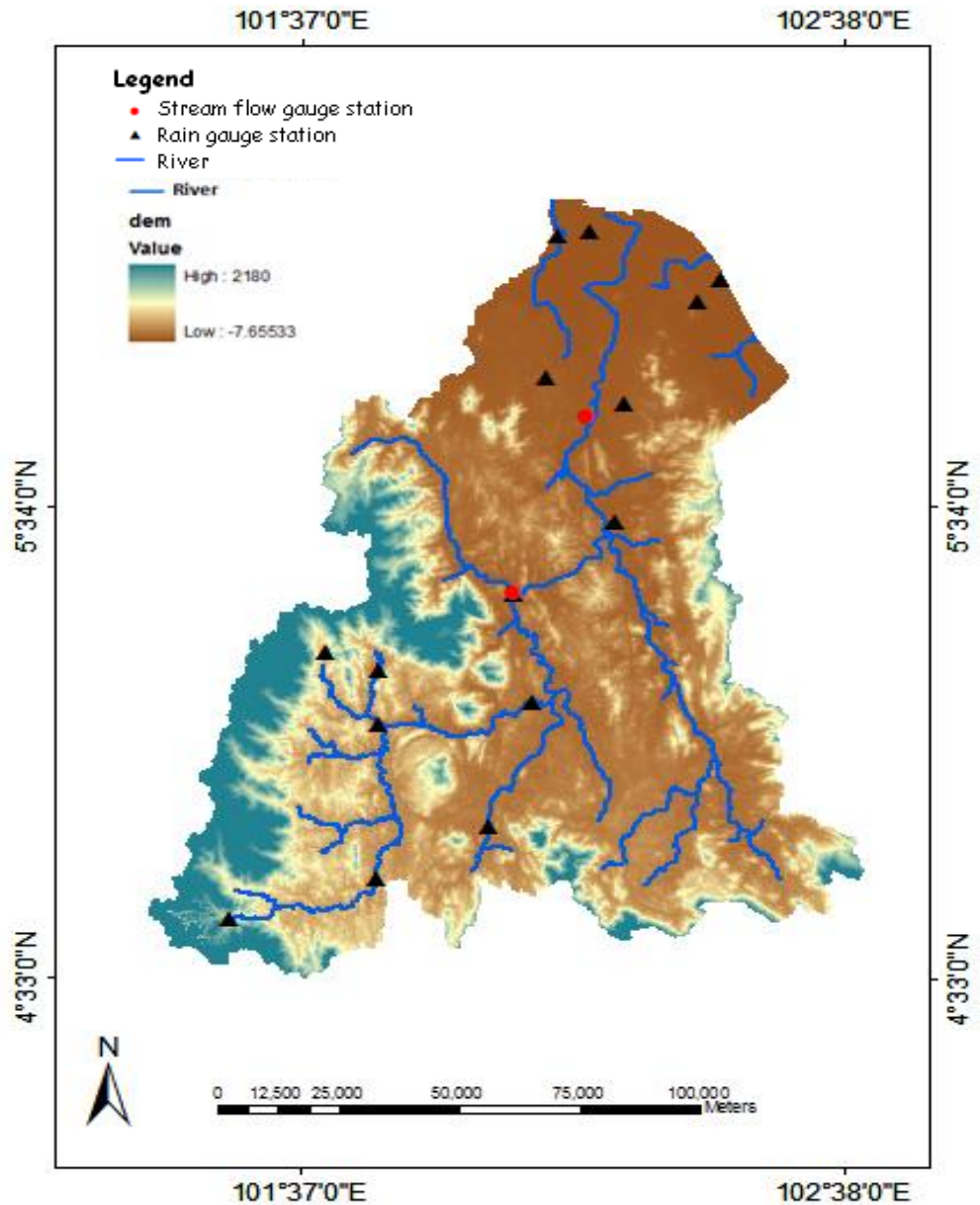
Figure 4-8 GIS layers consisting of 30 m DEM, streamflow gauge stations, rain gauge stations and River Kelantan network.

4.4   SUMMARY

This chapter has given details of the study site and data used for the whole work in this study. Data was obtained from various sources which represent hydrologic data, remotely-sensed images and GIS layers. All data were integrated later in different analyses as shown in the three next chapters (Chapter 5, 6 and 7).

Chapter 5

Trend Detection for Hydrological Time-series Data

5.1 INTRODUCTION

In this study, the method using historical hydrological data was used to investigate streamflow and precipitation trends for the River Kelantan for a 31 year period. The Mann-Kendall non-parametric method was used to investigate the trends (Burn and Hag Elnur, 2002; Franke et al., 2004; Kahya and Kalayci, 2004; Karabork, 2007). The study aims were to identify any trends in streamflow and explore the possible causes of that change including precipitation change due to climate change and land use change factors. In addition, the spatial and temporal patterns of streamflow and precipitation are discussed in order to gain further knowledge and determine their significance. The study attempted to determine the linkages between these factors which might lead to an understanding of change in flooding magnitude and frequency in the River Kelantan catchment.

5.2 TIME SERIES ANALYSIS

The Anderson-Darling test, skewness and kurtosis statistics were estimated to test the normality of the streamflow and precipitation time-series data distributions. The Anderson-Darling test showed that non-normality of data distribution existed at a confidence level of 90%. For streamflow, skewness was positive for both streamflow

stations indicating distributions with an asymmetric tail extending to larger values. Kurtosis was negative. Most of the precipitation gauges in the River Kelantan catchment have negative skewness indicating a distribution with an asymmetric tail extending towards smaller values. Small positive values of kurtosis indicate a relatively peaked distribution. The non-normality of the data distributions suggests that the Mann-Kendall test is a suitable method.

The autocorrelation function showed that white noise or independence of data existed in the streamflow time series for the River Galas and River Kelantan (Figure 5-1). Thus, the procedure for removing serially correlated data was not applied.

(a)
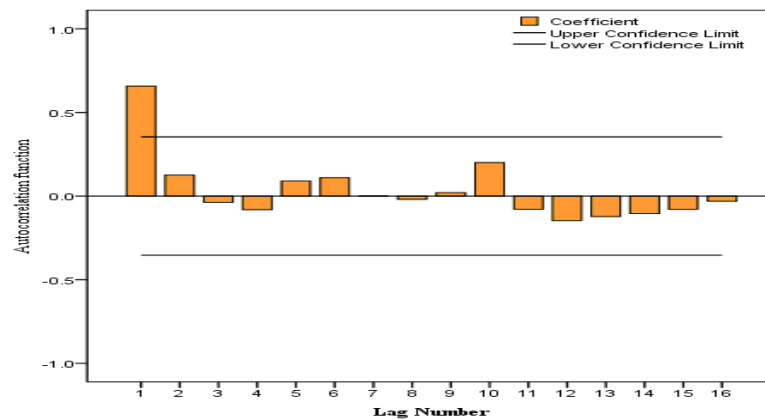
(b)
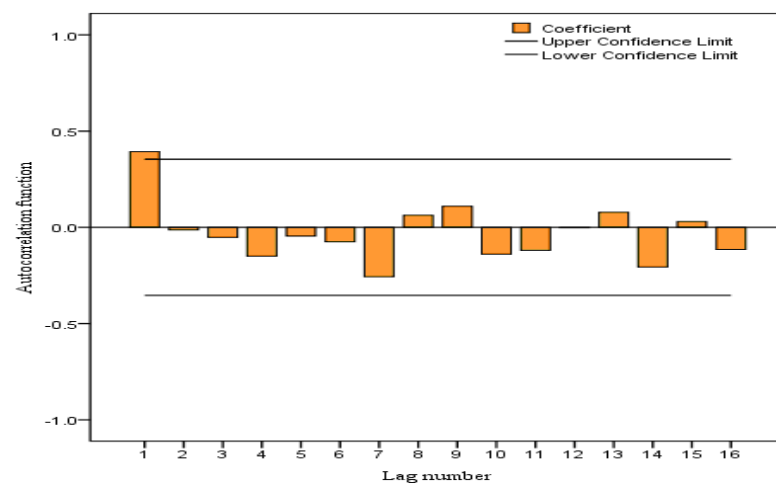
Figure 5-1 Autocorrelation plot for the (a) River Galas and (b) for the River Kelantan. The plots show that white-noise exist in the streamflow data for both rivers.

Statistical descriptions of the time-series of streamflow (m^3s^{-1}) and precipitation (mm) are presented in Table 5-1 and Table 5-2. Based on the Mann-Kendall test, the presence and significance of a trend was evaluated using a 90% confidence level. The analysis attempts to detect time-series trends on an annual, seasonal and monthly basis for stream flow and precipitation. The Sen's Slope was used to indicate the magnitude of change in the time-series trend.

Table 5-1 Statistics of the annual streamflow time-series for the River Kelantan and River Galas stations. F_m, discharge minimum; F_x, discharge maximum; F_e, discharge mean; SD, standard deviation; C_s, skewness; C_k, kurtosis; AD, Anderson Darling statistic; α, AD critical value. The AD statistic demonstrates the non-normality of the time-series for both streamflow stations at 0.632 critical values (90% significance level).

Station	F_m (m^3s^{-1})	F_x (m^3s^{-1})	F_e (m^3s^{-1})	SD	C_s	C_k	AD	α
River Kelantan	246.35	771.11	488.4	126.7	0.47	-0.01	0.692	0.632
River Galas	158.83	845.75	417.94	158.02	0.69	0.26	0.84	0.632

5.2.1 Spatial and temporal Mann-Kendall trend analysis

The hydrological data used in the study comprised streamflow and precipitation records. The historical data were extracted from the hydrological data network of the Malaysian Department of Irrigation and Drainage (DID). The data were divided into three hydrological variables known as annual, seasonal and monthly time-series for stream flow and precipitation for the whole River Kelantan catchment. These hydrological variables were chosen in time-series analysis since no attempt has been made to study streamflow and precipitation trend in Malaysia with monsoon climate conditions. Therefore, no further hyrological variables such as maximum annual, extreme flow or number of rainy days were taken into consideration at this stage. For seasonal trend analysis, the year was divided into four main seasons: JFM (January-February-March), AMJ (April-May-June), JAS (July-August-September) and OND (October-November-December) (Tangang et al., 2007). Total precipitation was calculated for every three month period and trends fitted to these data for each rain gauge station. As described earlier in Chapter 4, the hydrological data used in the study

comprise precipitation and stream flow records for a period of 16 (1984-2006) to 44 years (1975 – 2006). The data starting from year 1975 were chosen solely due to the most data available provided with good continuity and having few missing data records. A brief description of each gauge is presented in Table 4-4. Overall, approximately 19% of the data were missing from the time-series.

Two different periods of records were used to provide adequate temporal and spatial coverage. The first period, providing greater temporal coverage, is 1975–2006 (31 years) and the second period, providing greater spatial coverage, is 1984-2006 (22 years).

Streamflow and precipitation gauges with less than 20% missing data in each of the annual, seasonal and monthly time-series records were selected for analysis. Only two stream flow gauges were used, one for upstream (River Galas) and one for downstream (River Kelantan). A separate analysis was conducted for each of these two sub-catchments, providing a spatial element to the investigation. Brief information on the two streamflow gauges is given in Table 4-4. From 24 available precipitation gauge stations, only 16 stations were selected for further analysis due to data completeness (Figure 4-5). For the 31 year period, 10 precipitation stations (four upstream and six downstream) were used while for the 22 year period 16 precipitation stations (eight upstream and eight downstream) were used.

Table 5-2 Statistics of the annual precipitation (in mm) time-series for 15 stations of River Kelantan catchments. P_m, precipitation minimum; P_x, precipitation maximum; P_e, precipitation mean; *SD*, standard deviation; C_s, skewness; C_k, kurtosis; *AD*, Anderson Darling statistic; α, AD critical value

| **Upstream** | | | | | | | | |
Station	P_m(mm)	P_x(mm)	P_e(mm)	SD(mm)	C_s	C_k	AD	α
Brook	2.26	11.57	6.49	1.89	0.47	2.79	0.853	0.632
Blau	1.92	7.66	5.64	1.26	-1.51	3.67	1.244	0.632
Gua Musang	4.03	8.43	6.293	0.89	-0.1	0.8	0.644	0.632
Gemala	2.48	9.57	5.44	1.72	0.544	1.13	0.728	0.632
BP Bertam	2.23	8.15	5.69	1.46	-0.35	-0.14	0.798	0.632
Gob	5.04	8.9	6.97	1.11	-0.17	-0.3	0.803	0.632
Dabong	3.72	9.16	6.6	1.18	-0.18	0.22	0.655	0.632
Ladang Kuala Balah	1.03	10.27	7.92	1.65	-1.67	5.36	0.864	0.632

| **Downstream** | | | | | | | | |
Station	P_m(mm)	P_x(mm)	P_e(mm)	SD(mm)	C_s	C_k	AD	α
Gunung Gagau	5.76	15.36	10.89	2.1	-0.47	1.3	0.698	0.632
Kg Aring	4.64	8.53	6.92	1	-0.43	-0.18	0.632	0.632
Kg Laloh	4.66	9.77	6.8	1.28	0.65	-0.24	0.81	0.632
Ladang Lepan Kabu	3.45	9.3	6.21	1.4	0.304	-0.27	0.844	0.632
Kuala Krai	3.49	8.68	6.47	1.49	-0.61	-0.29	0.805	0.632
Ulu Sekor	4.55	10.02	7.44	1.69	0.19	-1.01	0.663	0.632
Ladang Kenneth	4.13	12.2	7.15	1.82	0.45	0.07	0.644	0.632
JPS Machang	0.3	12.47	6.9	2.38	-0.37	1.17	0.682	0.632

5.2.2 Upstream catchment trend analysis (1975-2006)

The mean value of annual, seasonal and monthly streamflow time-series for the 31 year period was tested for trends. For the upstream area, represented by the River Galas, all variables showed statistically significant increasing trends. Seasonal streamflow exhibited significant increasing trends for all seasons (Table 5-3). The late wet season (JFM) showed the largest magnitude of 16.01 m^3s^{-1} followed by the early dry season (AMJ) with 13.4 m^3s^{-1}. The trends and magnitudes of streamflow are in good

agreement with the flooding report for the River Kelantan (DID, 2003). Additionally, the early wet season (OND) trend (12.52 m^3s^{-1}) was of greater magnitude compared to the late dry season (JAS) trend (11.88 m^3s^{-1}). This is well understood because the OND season is normally associated with intense rainfall and wet conditions dominate in the region. Overall, streamflow for the River Galas exhibits a significant trend with a magnitude of 13.72 m^3s^{-1}.

Table 5-3 The Mann-Kendall test result for the River Galas streamflow station based on annual, seasonal and monthly analysis from 1975 to 2006 and 1984 to 2006.

1975-2006			
Streamflow	**Annual**	**Seasonal**	**Monthly**
River Galas	S^+	S^+ (JFM, AMJ, JAS, OND)	S^+ (Jan, Feb, Mar, Apr, May, June, July, Aug, Sept, Oct, Nov, Dec.)
Precipitation	**Annual**	**Seasonal**	**Monthly**
Gua Musang	NS	NS	NS
BP Bertam	NS	NS	NS
Dabong	NS	NS	S^+ (Mar, Dec)
Ladang Kuala Balah	S^+	S^+ (JFM, AMJ, OND)	S^+ (Jan, June, Oct)
1984-2006			
Streamflow	**Annual**	**Seasonal**	**Monthly**
River Galas	S^+	S^+ (JFM, AMJ, JAS, OND)	S^+ (Jan, Feb, Mar, Apr, May, June, July, Aug, Sept, Oct, Nov)
Precipitation	**Annual**	**Seasonal**	**Monthly**
Brook	NS	S^+ (OND)	S^+ (Jan, Sept, Nov, Dec)
Blau	NS	NS	S^+ (Dec)
			S^- (Feb)
Gua Musang	NS	S^- (AMJ)	S^- (Apr)
Gemala	NS	NS	S^- (Feb)
BP Bertam	S^-	S^- (JAS)	S^- (Sept)
Gob	NS	NS	S^+ (Jan)
Dabong	NS	NS	S^+ (Dec)
Ladang Kuala Balah	NS	NS	NS

Note: NS is a not significant trend, S^+ is a significant increasing trend, S^- is a significant decreasing trend.

For the monthly analysis, the strongest trend was detected for April streamflow with a magnitude of 14.86 m^3s^{-1} at the 90% confidence level (Table 5-3), followed by February

streamflow of 16.33 m^3s^{-1}. However, the month of January showed the largest magnitude discharge of 17.82 m^3s^{-1}.

Precipitation stations corresponding to the River Galas streamflow stations were also subjected to the Mann-Kendall trend analysis (Figure 5-4). The analysis showed that only Ladang Kuala Balah exhibited a significant increasing annual trend with a small magnitude of 0.09 mm. For the seasonal time series, again, only Ladang Kuala Balah exhibited a significant increasing trend for the JFM, AMJ and OND seasons. OND showed the largest magnitude trend of 0.20 mm. Monthly analysis showed that two stations (i.e. Dabong and Ladang Kuala Balah) exhibited significant increasing trends. The stations showed an increasing trend for the months of January, March, June, October and December (Table 5-3). Based on the above results, for the upstream sub-catchment it can be suggested that changes to precipitation are likely to have contributed to increasing streamflow.

5.2.3 Downstream catchment trend analysis (1975 -2006)

For the downstream catchment the pattern exhibited in streamflow was different compared to the upstream area (Table 5-4). For the annual time series, no statistically significant trend was detected in the downstream area. In contrast, for the seasonal analysis, two of the seasons exhibited significant decreasing trends in AMJ and JAS (i.e. the dry season). For the monthly time-series four significant decreasing trends were detected in the months of May, July, September and November. The month of September exhibited the strongest decreasing trend with a magnitude of -5.75 m^3s^{-1}. It shows that the study area is experiencing drier conditions than before for the dry months, which are well represented by the AMJ and JAS seasons.

For the annual time series, none of the stations showed a significant trend in precipitation at the 90% confidence level (Figure 5-3). However, seasonal analysis showed three precipitation stations exhibiting significant trends. For the Kg Aring station, one increasing trend (JFM) and one decreasing trend (JAS) was detected. Meanwhile, the Ladang Kenneth station has two significant increasing trends for the JFM and OND (i.e. the wet season). The JPS Machang station has a decreasing trend for the AMJ season.
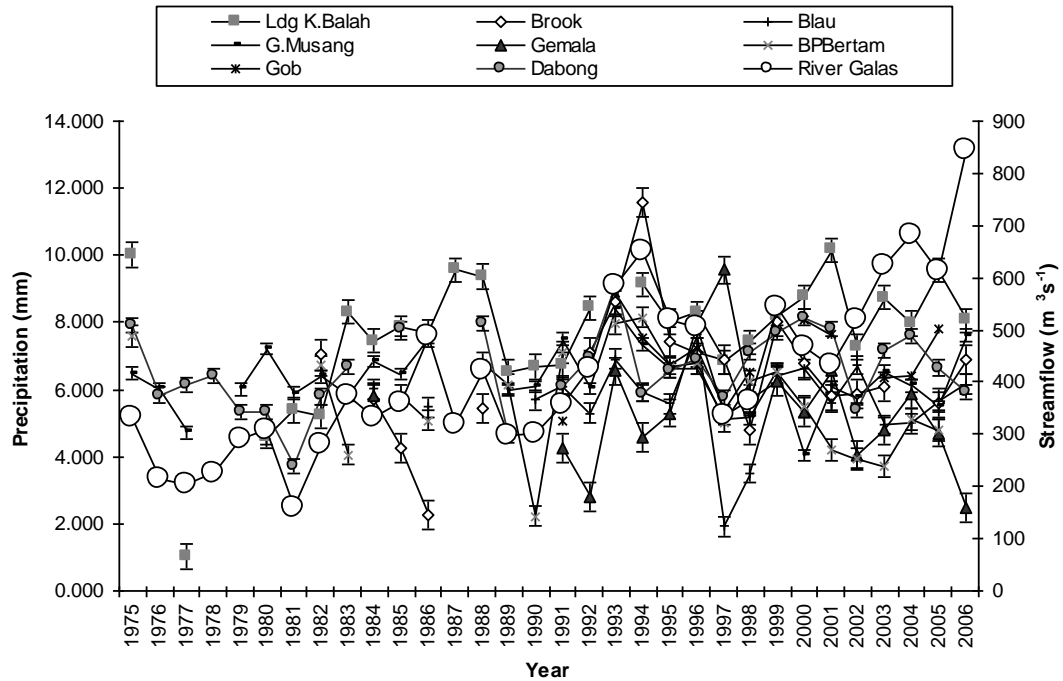
Figure 5-2 Plot of discharge (o) against year for the River Galas station for 1975-2006. The mean precipitation (■) for all rain gauge stations flowing into the River Galas station are shown along with standard error bars. The plot shows a clear upward trend for discharge and a less obvious trend for precipitation.

Monthly analysis revealed similar trends for particular months. The Kg Aring station has five months with significant trends, with two increasing trends (i.e. January and March) and three decreasing trends (i.e. May, July and September). The Kuala Krai station has one significant decreasing trend (i.e. September) and the Ladang Kenneth station has three significant increasing trends in the months of January, March and December (Table 5-4). From the trends, it is clear that for the River Kelantan sub-catchment, rainfall is increasing in the wet months such as January, March and December. Additionally, rainfall is decreasing and causing drier conditions during the dry months, especially for the month of September.

Table 5-4 The Mann-Kendall test result for the River Kelantan streamflow station based on annual, seasonal and monthly analysis from 1975 to 2006 and 1984 to 2006.

1975-2006			
Streamflow	**Annual**	**Seasonal**	**Monthly**
River Kelantan	NS	S$^-$ (AMJ, JAS)	S$^-$ (May, July, Sept, Nov)
Precipitation	**Annual**	**Seasonal**	**Monthly**
Kg Aring	NS	S$^+$ (JFM)	S$^+$ (Jan, Mar)
		S$^-$ (JAS)	S$^-$ (May, July, Sept)
Kg Lalok	NS	NS	NS
Ldg Lepan Kabu	NS	NS	NS
Kuara Krai	NS	NS	S$^-$ (Sept)
Ldg Kenneth	NS	S$^+$ (JFM, OND)	S$^+$ (Jan, Mar, Dec)
JPS Machang	NS	S$^-$ (AMJ)	NS
1984-2006			
Streamflow	**Annual**	**Seasonal**	**Monthly**
River Kelantan	S$^-$	S$^-$ (AMJ, JAS)	S$^-$ (Mar, May, June, July, Sept, Oct.)
Precipitation	**Annual**	**Seasonal**	**Monthly**
Gunung Gagau	S$^-$	S$^-$ (OND)	S$^-$ (May, Nov)
Kg Aring	NS	S$^+$ (JFM)	S$^+$ (Jan)
		S$^-$ (JAS)	S$^-$ (Sept)
Kg Lalok	NS	NS	NS
Ldg Lepan Kabu	NS	NS	S$^-$ (Sept)
Kuara Krai	NS	NS	NS
Ulu Sekor	NS	NS	S$^+$ (Aug)
Ldg Kenneth	NS	S$^+$ (JFM)	S$^+$ (Jan, June, Aug, Dec)
JPS Machang	NS	NS	S$^-$ (July)

Note: NS is a not significant trend, S$^+$ is a significant increasing trend, S$^-$ is a significant decreasing trend.
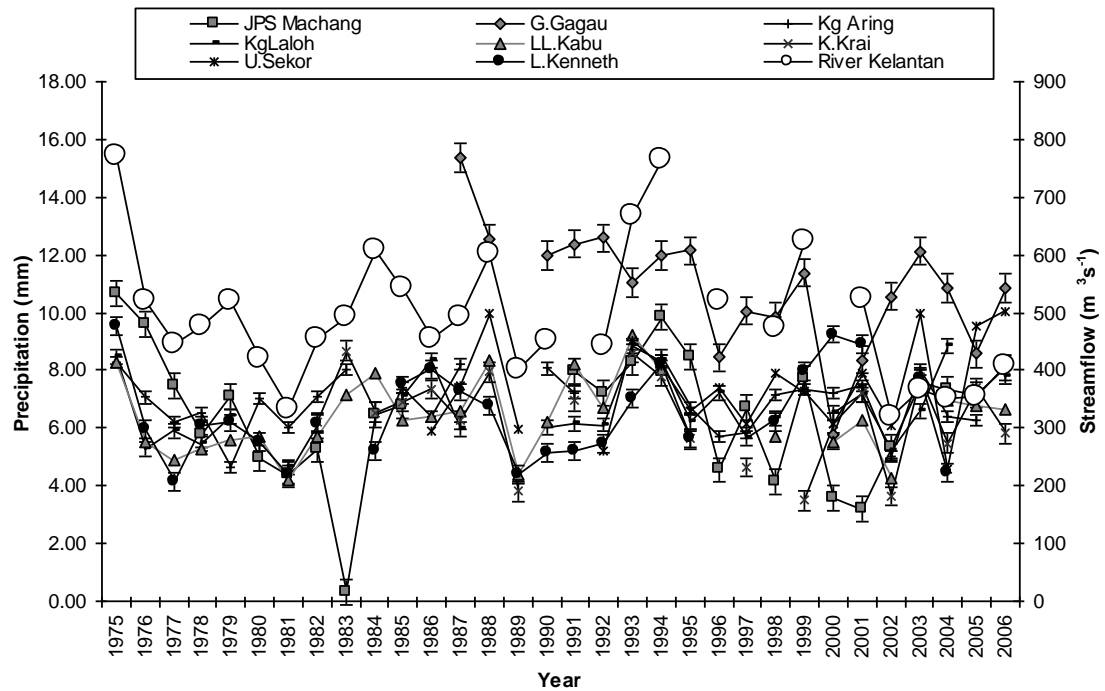
Figure 5-3 Plot of discharge (o) against year for the River Kelantan station
for 1970-2006. The mean precipitation (■) for all rain gauge stations flowing
into the River Kelantan station are shown along with standard error bars.
There is no obvious trend in either series.

5.2.4 Upstream catchment trend analysis (1984 -2006)

The above analysis was repeated for the 22 year period, to maximize the spatial
coverage of the trend analysis. Eight precipitation stations corresponding to the
upstream streamflow station were suitable for the analysis (Table 5-3).

The streamflow of the River Galas indicates that all the variables such as annual,
seasonal and monthly time series showed significant increasing trends. However, the
strength of trend for all variables is lower than for the 31 year period. Furthermore, for
the monthly analysis, December showed no significant trend at the 90% confidence
level.

For the annual analysis, only one station showed a significant (decreasing) trend in
precipitation (i.e. BP Bertam). For the seasonal analysis, three seasons showed apparent
trends, with a decreasing trend (i.e. AMJ and JAS) for the stations of Gua Musang and
BP Bertam in the dry season, and Brook station showing an increasing significant trend

98

for the OND season. The results imply that for the stations with significant trends, less rainfall is being received in the dry seasons which cause drier conditions.

Monthly analysis revealed various trends. All of the stations exhibited increasing or decreasing trends, apart from the Ladang Kuala Balah station. For the Brook station, the monthly analysis is in good agreement with the seasonal analysis. Specific wet months exhibited significant increasing trends (i.e. January, November, December and September). The stations of Gua Musang and BP Bertam also show good agreement between the seasonal and monthly analysis. The month of April exhibits a significant decreasing trend as shown by the seasonal analysis for the season of AMJ (i.e. Gua Musang). Apart from that, the significant decreasing trend for the month of September was in good agreement with the decreasing trend for the JAS season for the BP Bertam station. Furthermore, significant decreasing trends for the month of February were observed for the stations of Blau and Gemala (Figure 5-5) and significant increasing trends for the months of January and December were observed for the Gob and Dabong stations (Table 5-3).

In the upstream sub-catchment, for the shorter 22 year period, streamflow appears to be increasing significantly in all months except December. In contrast, the dry months showed significant decreasing trends in precipitation, whereas, wet months received more rainfall and caused ensuing wetter periods.

5.2.5 Downstream catchment trend analysis (1984 -2006)

The trend analysis of the River Kelantan streamflow for the 22 year period is shown in Table 5-4. Annual analysis revealed a significant decreasing trend at the 90% significance level. Furthermore, seasonal analysis revealed that the early and late dry seasons exhibited significant decreasing trends (i.e. AMJ and JAS). In addition, monthly analysis showed that six significant decreasing trends were detected. The monthly trends coincide with the seasonal analysis results (i.e. March, May, June, July, September and October) with the strongest decreasing trend in September.

Trend analysis of the precipitation stations corresponding to the River Kelantan streamflow station showed that for the annual analysis, only one station exhibited a trend at the 90% significance level (i.e. Gunung Gagau). Seasonal analysis showed that

two seasons exhibited significant increasing and decreasing trends. The late wet season (JFM) showed significant increasing trends for the stations of Kg Aring and Ladang Kenneth. Gunung Gagau showed a decreasing trend for the OND (wet) season. Kg Aring also exhibited a significant decreasing trend for the late dry season of JAS (Table 5-4). The monthly analysis revealed that six from eight precipitation stations have significant trends. Ladang Kenneth station showed the strongest significant increasing trends for the months of January, June, August and December (Figure 5-4).

5.2.6 Summary of trends analysis for the downstream and upstream sub-catchments.

In summary, although there are some inconsistencies, a general pattern has been revealed in which streamflow is increasing in all seasons upstream, but is decreasing in the dry season downstream. The pattern in streamflow downstream is fairly well matched by increases in precipitation in the wet season and decreases in precipitation in the dry season. These changes point to a seasonal shift in the timing (later onset and earlier end) and intensity (more intense) of the monsoon in the Kelantan catchment. In the upstream area, the increases in streamflow are not matched by universal increases in precipitation, but rather by increases in the wet season only and decreases in the dry season, as for the downstream sub-catchment. The increases in streamflow in the dry season are, thus, more difficult to explain. One reasonable explanation may be due to increases in sedimentation in the catchment due to logging activites or conversion of forest to agriculture which may lead to increases in streamflow in the upstream area (Wilk et al., 2001). In the next section, changes in land use in both sub-catchments are examined as a possible contributing factor to the observed changes in streamflow.
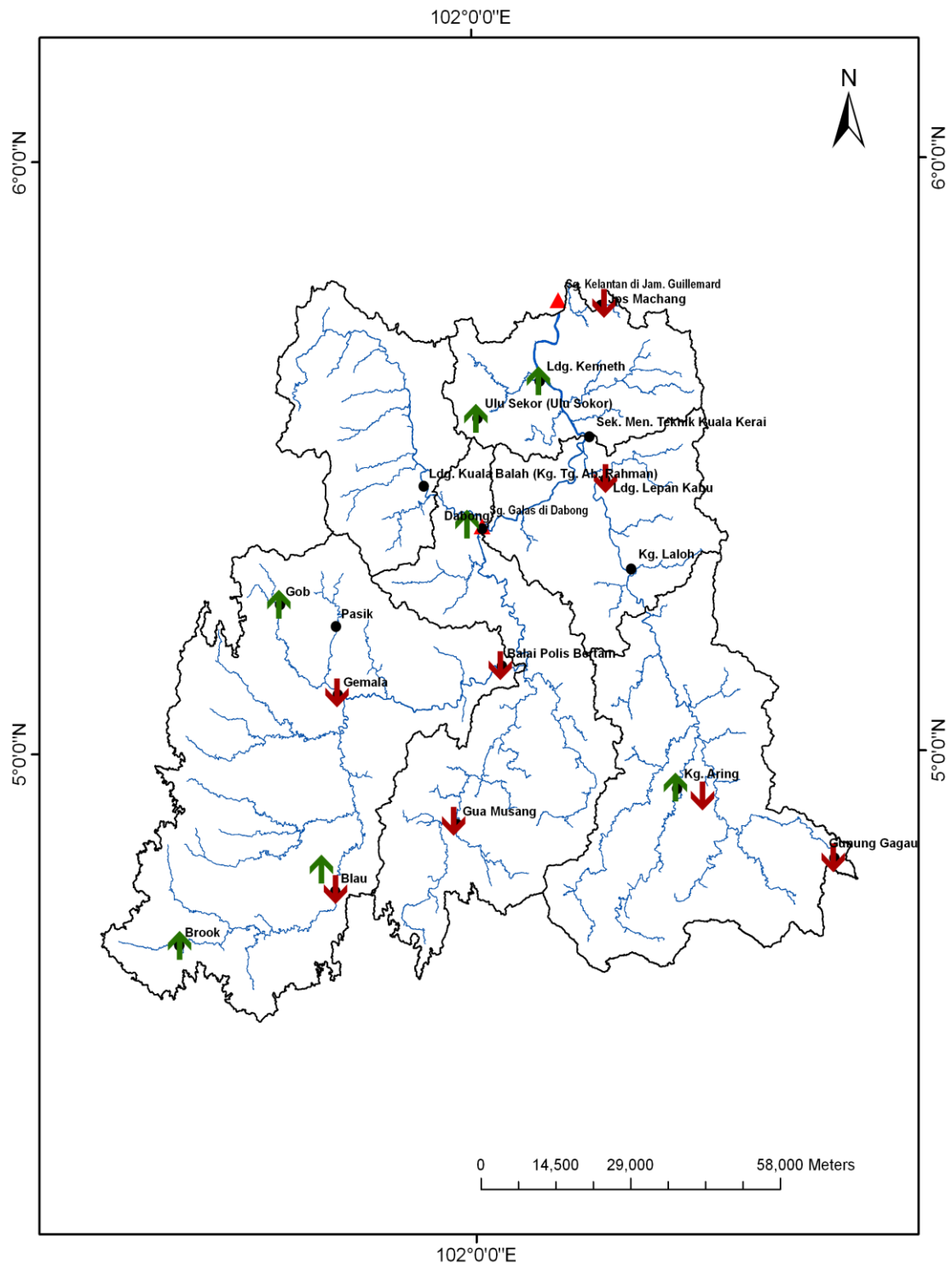
Figure 5-4 Precipitation station map indicating stations with increasing (↑) and decreasing (↓) significant trends for monthly time-series for the Kelantan catchment (1984-2006) and not significant trend (●).

5.3 LAND USE CLASSIFICATION

5.3.1 Image pre-processing result

Atmospheric and geometric corrections were done prior to land use classification. The atmospheric correction was performed using the ATCOR 2 software to eliminate the effects of solar illumination and the atmosphere generally (e.g. water vapour, dust, aerosol particles) such that the images represented, as closely as possible, the true reflectance of the Earth's surface at the time of imaging. The flowchart of atmospheric correction procedure for the Landsat TM image as shown in Figure 5-5 and examples steps involving as shown in Figure 5-6 and Figure 5-7.
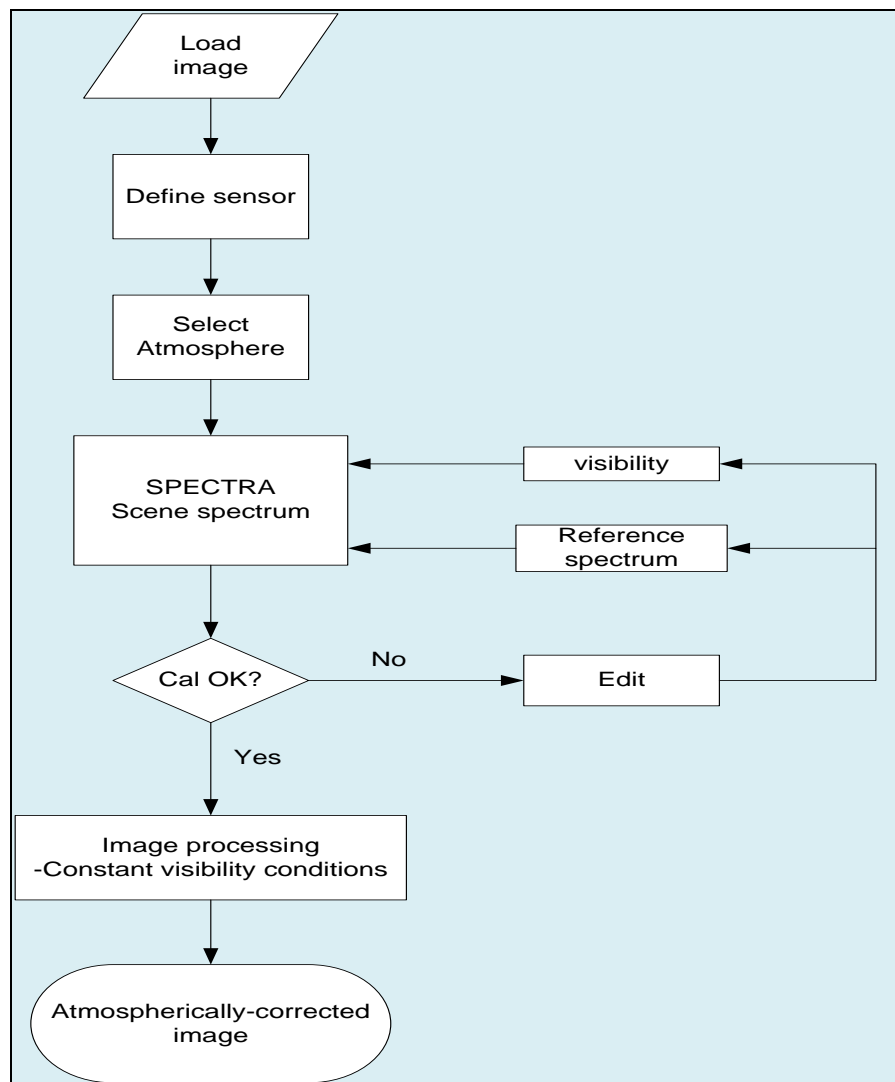
Figure 5-5 Atmospheric correction flowchart using ATCOR2 software.
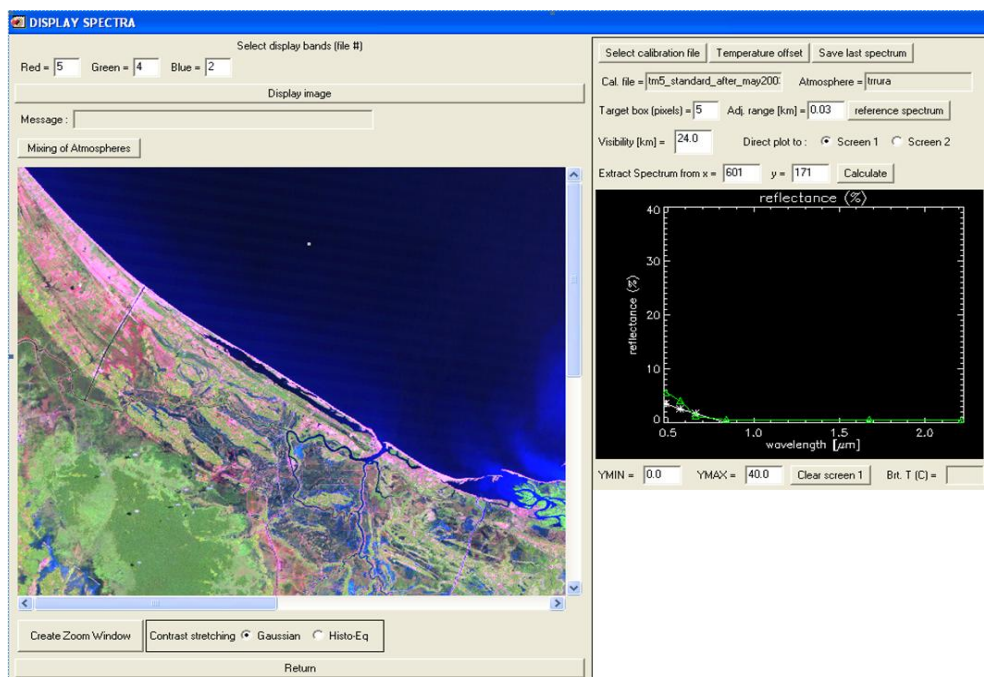
Figure 5-6 The extract of water spectrum from the study area at (left-hand side) column = 601 and row = 171 and (right-hand side) comparison with reference spectrum calibration file in ATCOR2.
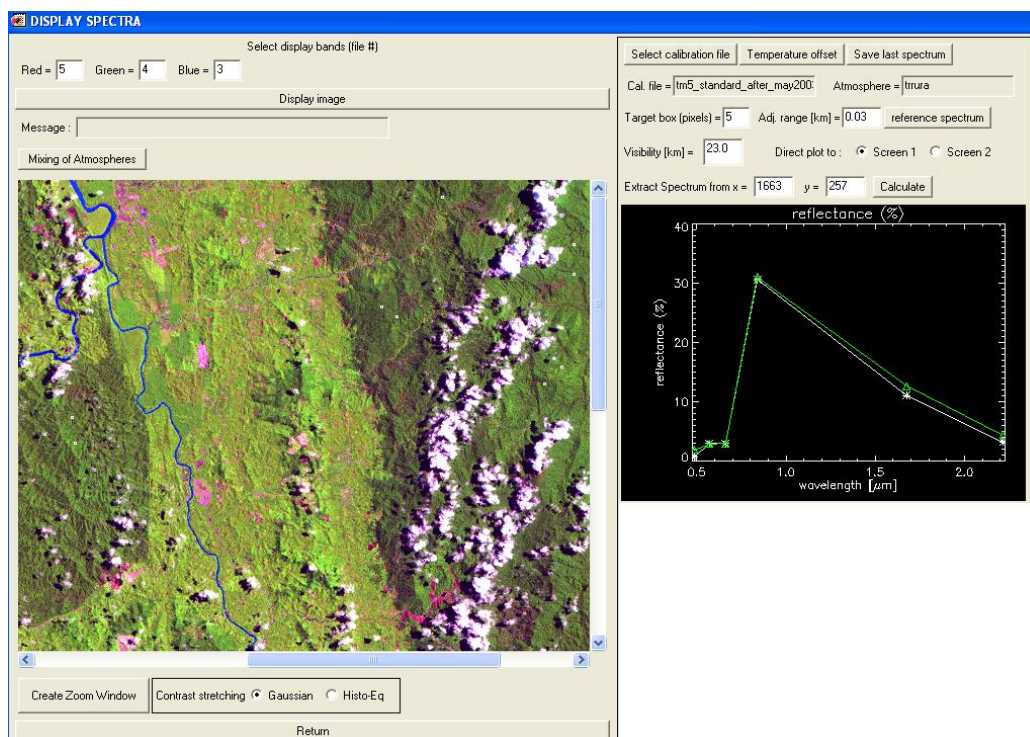
Figure 5-7 The extract of forest spectrum from the study area at (left-hand side) column = 1663 and row = 257 and (right-hand side) comparison with reference spectrum calibration file in ATCOR2.

Subsequently, the 1988 image was corrected for geometric error by first transforming to a Universal Transverse Mercator (UTM) (Zone 47, North) projection. The geometric transformation equation was computed using 50 ground control points. The root mean square error (RMSE) which measured the accuracy of geometric correction result was less than 0.4 pixels (Figure 5-8). It is important to have RMSE as minimum as possible of the multitemporal image in order to avoid misclassification of land use map (Ippoliti-Ramilo et al., 2003; Jiang et al., 2004). The image for the year 2000 was then co-registered to the georeferenced 1988 image. Nearest neighbour resampling which retains the radiometric information on the images (Jensen, 1996a; Lillesan and Kiefer, 2000) was applied with an output pixel size of 30×30 m. The final geometrically-corrected images of the study area for 1988 and 2000 are shown in Figure 5-9 and Figure 5-10.
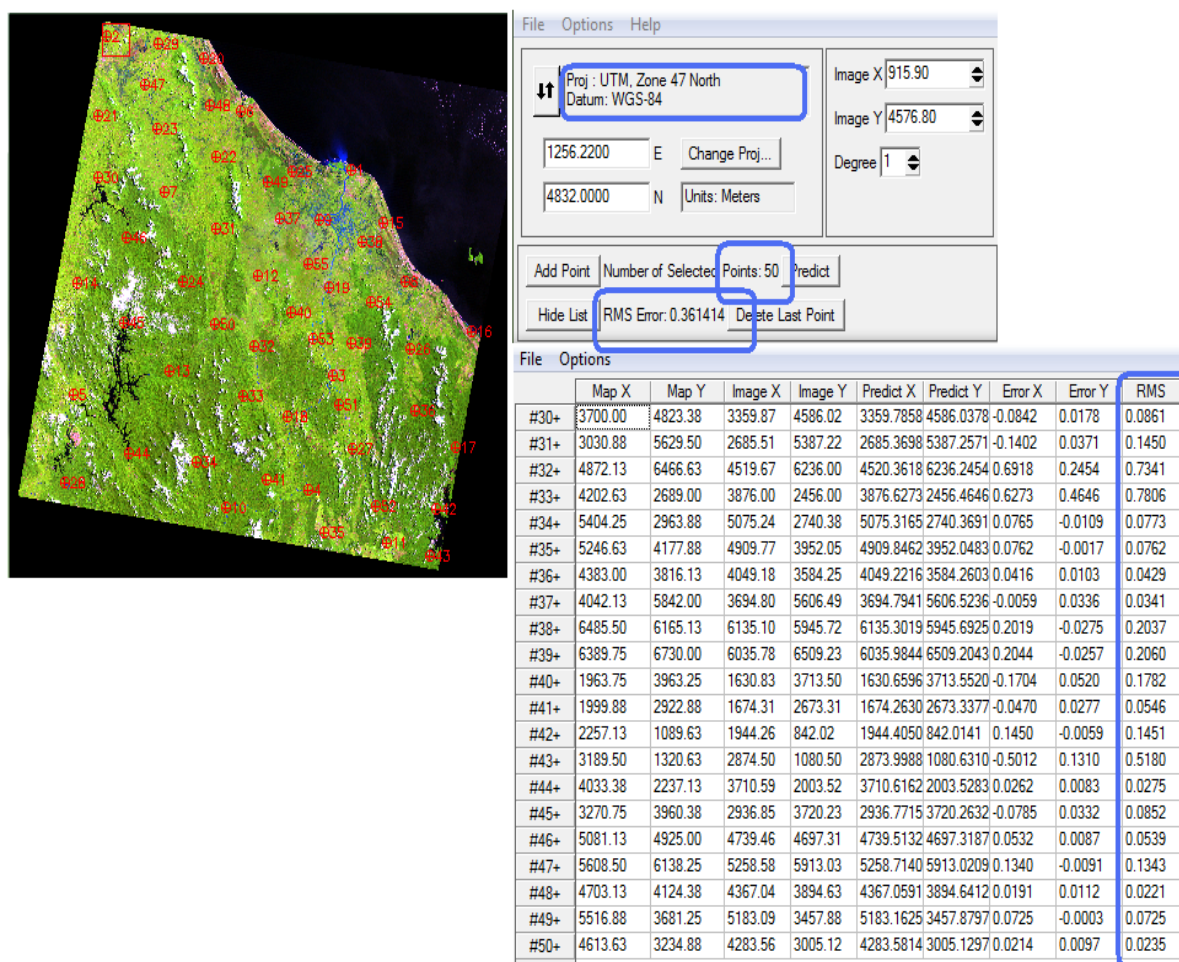
Figure 5-8 Ground controls points selection and RMSE for the 1988 image.
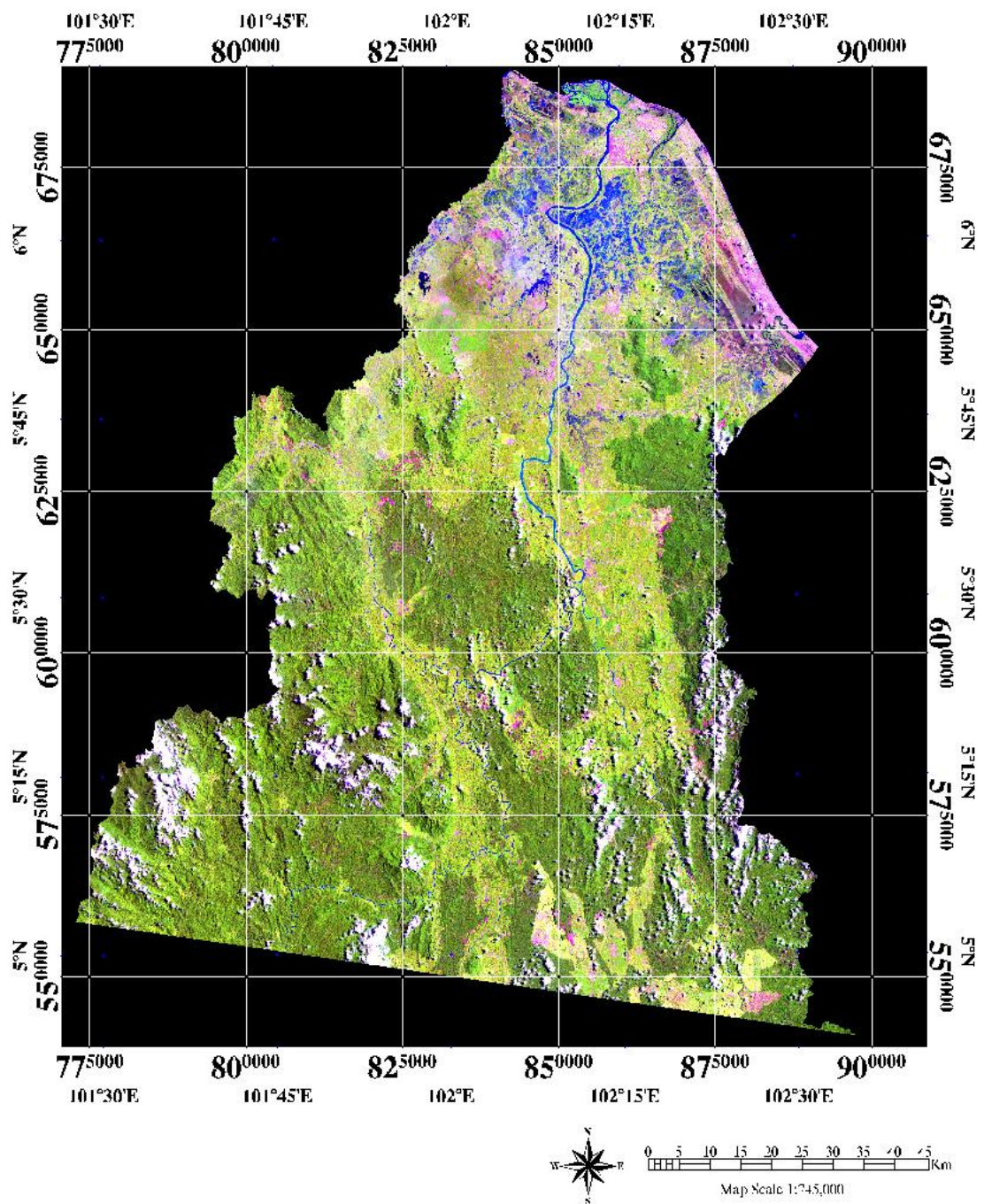
Figure 5-9   The 1988 false color composite geometrically-corrected image of Landsat TM covering the Kelantan area: Red= TM5 (MIR), Green = TM4 (NIR) and Blue = TM3 (Red).
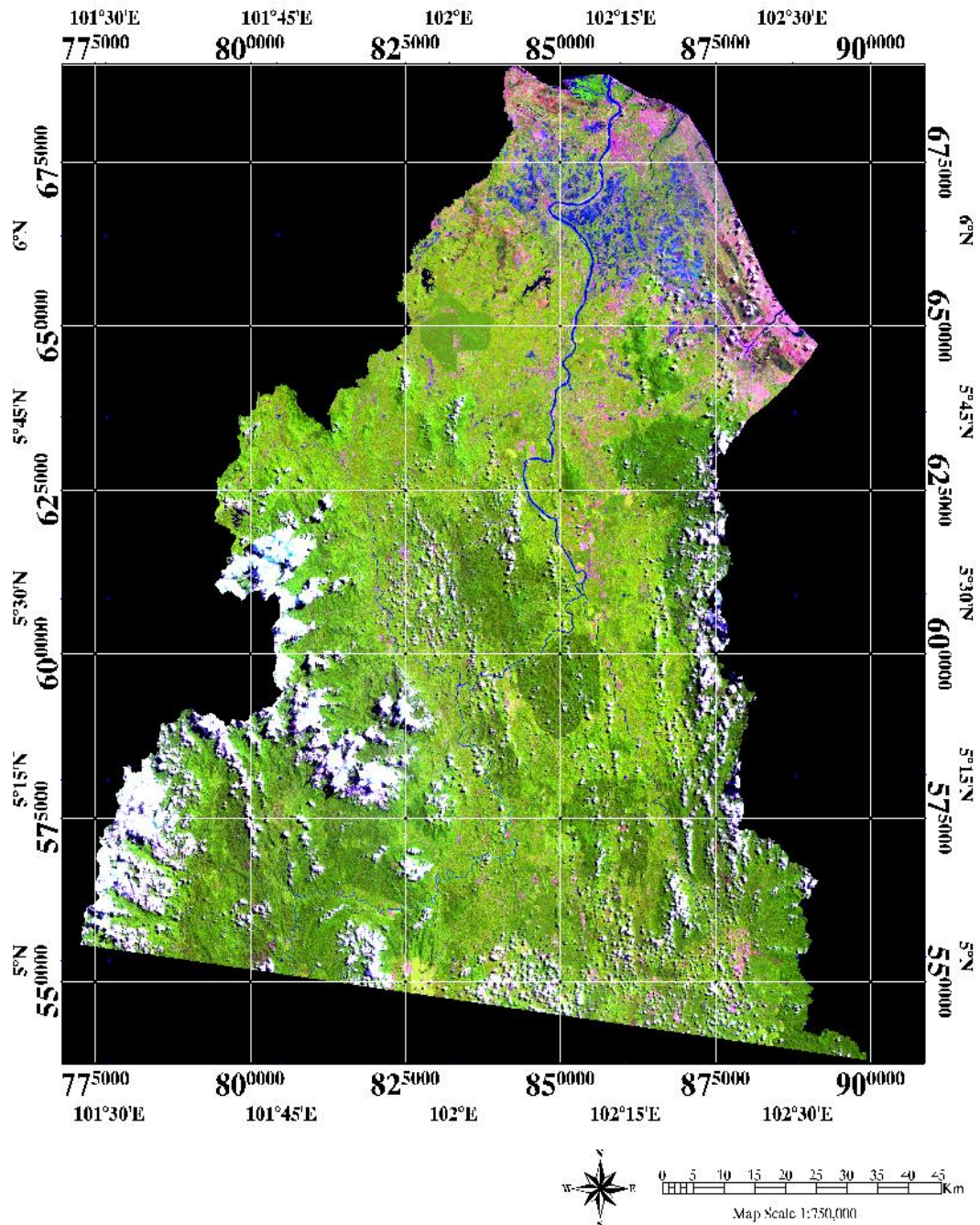
Figure 5-10 The 2000 false color composite geometrically-corrected image
of Landsat TM covering the Kelantan area: Red= TM5 (MIR), Green = TM4
(NIR) and Blue = TM3 (Red).

Prior to land use classification, cloud and shadow pixels in the image were masked out

using band threshold values, particularly, in the near-infrared band (cloud pixels) and

red band (shadow pixels). Masking was important to avoid errors due to cloud cover,

especially for built-up land since the area is associated with relatively brighter

reflectance values compared to other features (i.e. forest, agriculture, water). The

atmospherically and geometrically-corrected images after cloud and shadow mask as shown in Figure 5-11 and Figure 5-12.
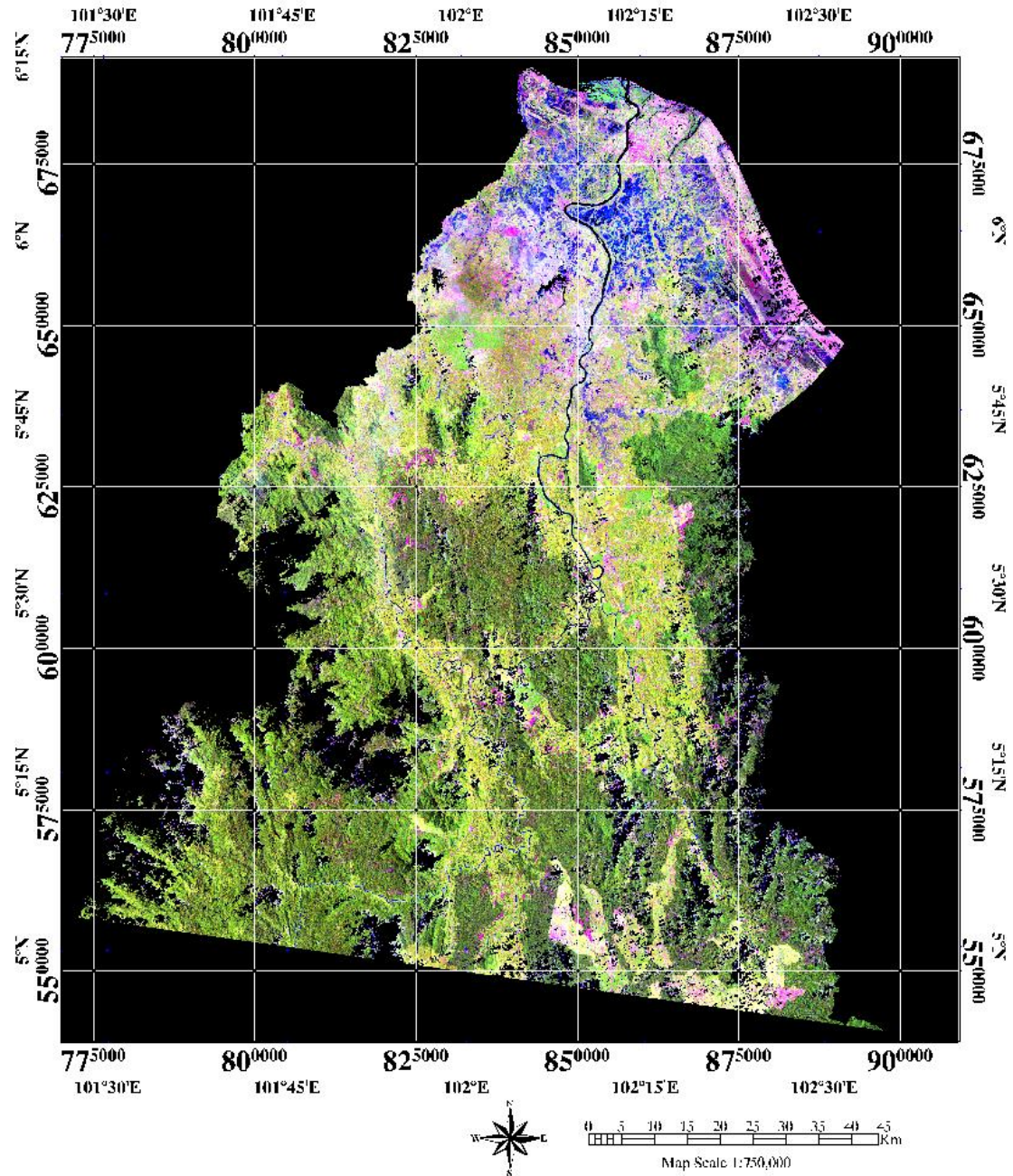
Figure 5-11 The 1988 false color composite cloud-shadow masked image of Landsat TM covering the Kelantan area: Red= TM5 (MIR), Green = TM4 (NIR) and Blue = TM3 (Red).
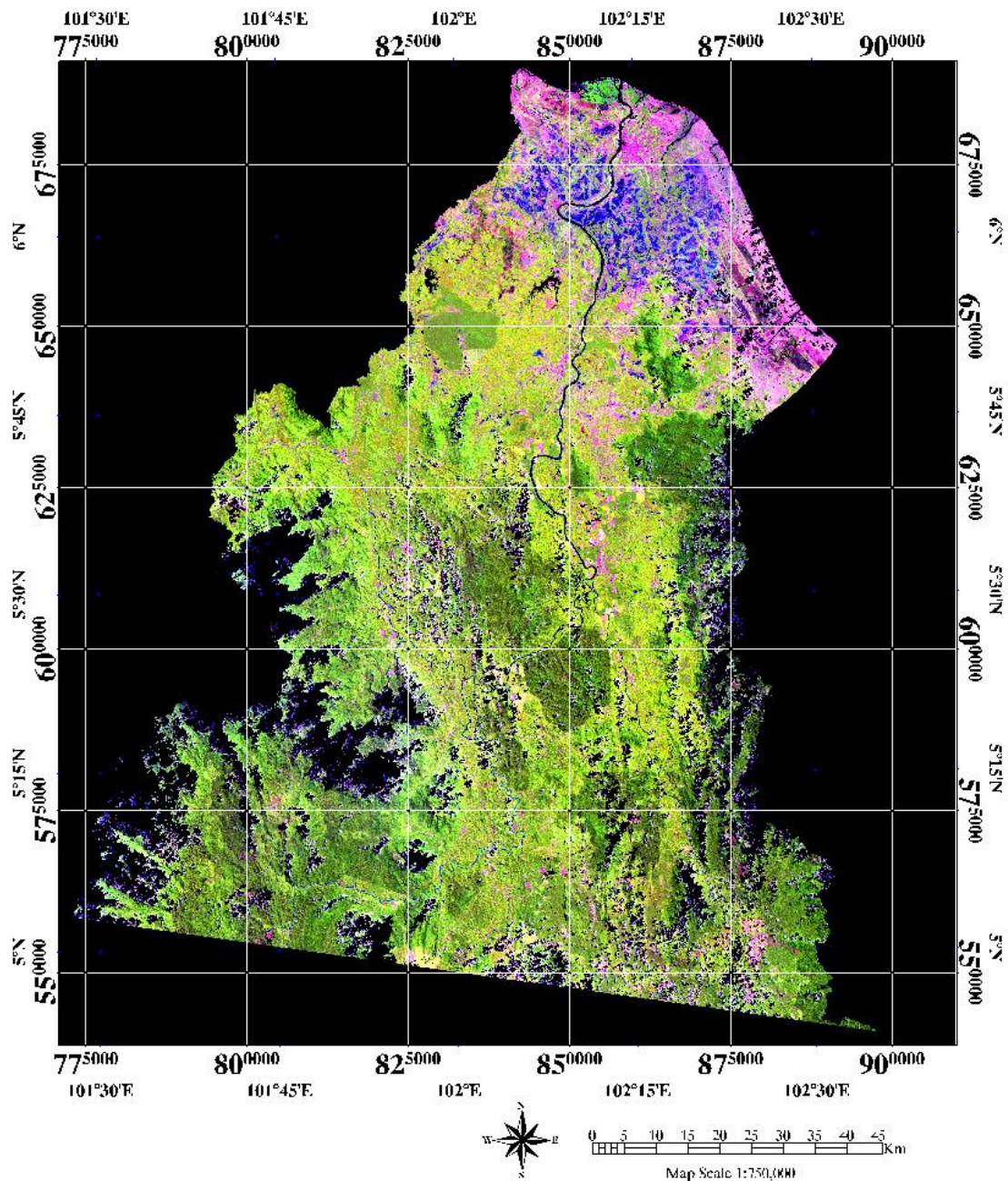
Figure 5-12 The 2000 false color composite cloud-shadow masked image of
Landsat TM covering the Kelantan area: Red= TM5 (MIR), Green = TM4
(NIR) and Blue = TM3 (Red).

5.3.2 Land use classification processes

A land use map was derived using land use classification. The maximum likelihood
algorithm was used to classify land use because the algorithm takes the distributions of
the classes into account via a variance-covariance matrix. Based on the multivariate

Gaussian distribution (which was appropriate in this case) the algorithm estimates the probability that a given pixel belongs to a specific land use class. The processes involved in producing a land use maps for the 1988 and 2000 images is shown in Figure 5-13.
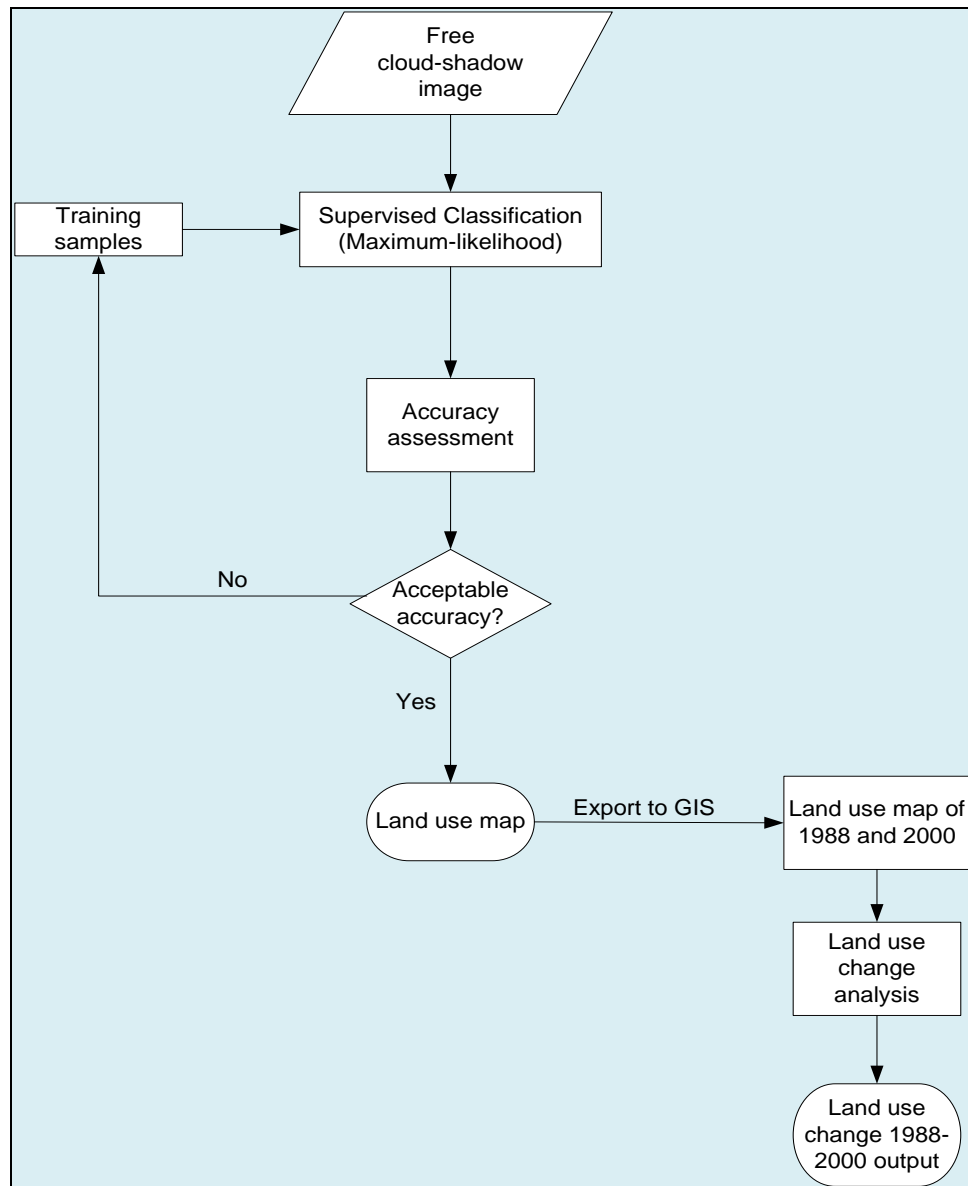
Figure 5-13 Flowchart of land use classification of Landsat TM images of the year 1988 and 2000 using Maximum-Likelihood algorithm.

A stratified random spatial sample of training pixels was used for supervised classification of the image into nine land use categories (i.e. forest, built-up, bare soil, paddy, mangrove, oil palm, rubber, mixed-agriculture and water) (Figure 5-14).

Accuracy assessment was undertaken for 100 randomly selected points. Accuracy assessment revealed that the accuracy of classification for 1988 was 89.5% with a Kappa coefficient of 0.81. Meanwhile, for the year 2000, the accuracy was 96.9% with a Kappa coefficient of 0.96. Both accuracy results met the minimum standard of 85% stipulated by the United States Geological Survey (USGS) classification system (Anderson et al., 1976). The results suggest that the land use map created using the maximum likelihood algorithm is a sufficiently reliable representation of the real land surface.
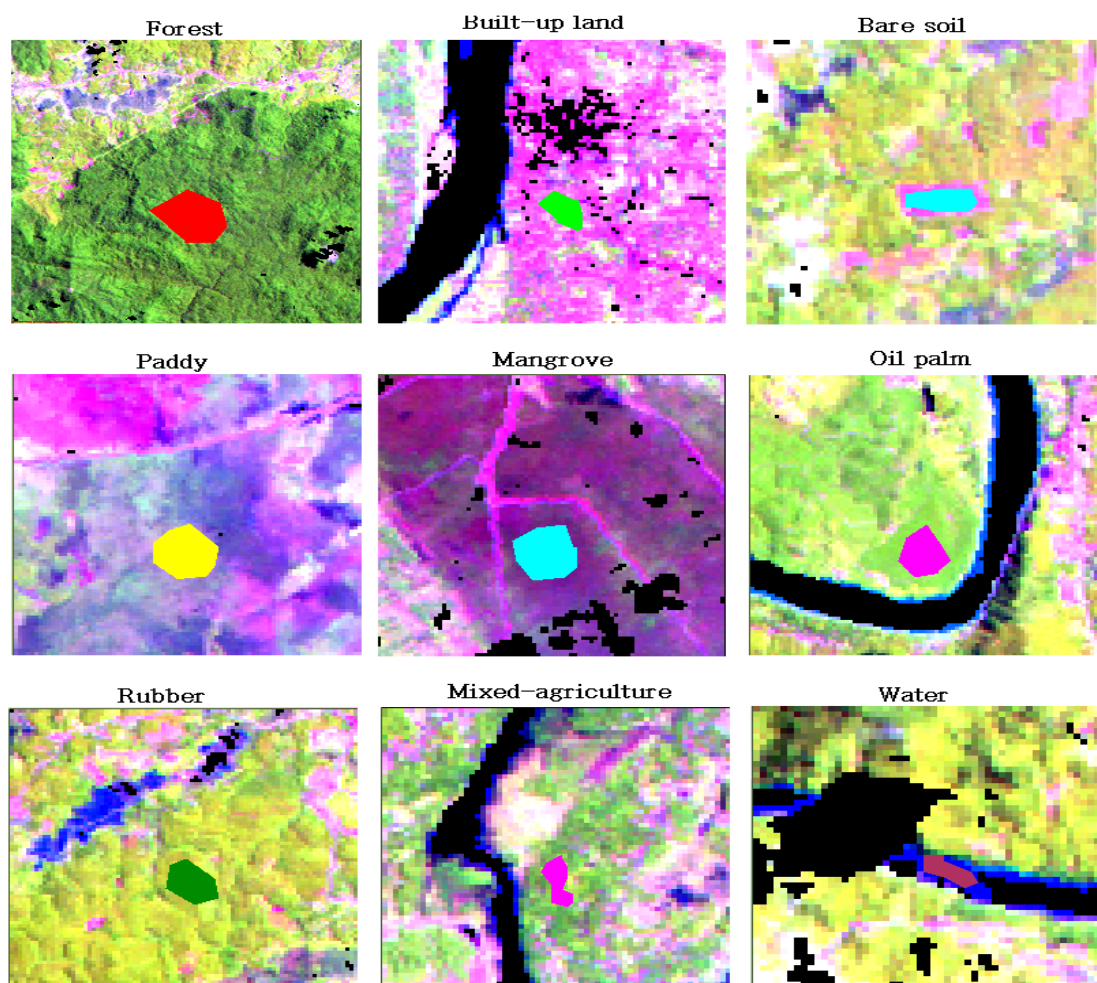
Figure 5-14 Example of training samples of nine land use classes.

Post-classification change detection analysis was applied using the ARCGIS 9.2 software to determine where the land use has changed and the specific class of land use conversion. The land use change map was created using the following formula: *LUC* =

Land use map (1988) x 10 +Land use map (2000). The land use change class was represented using a 2-digit class code number. The first digit represents the land use class code number in 1988 and the second number represents the land use class code in 2000. The land use code number represents forest (1), water (2), mixed agriculture (3), bare soil (4),built-up land (5), mangrove (6), oil palm (7), rubber (8) and paddy (9) for the River Galas and River Kelantan sub-catchments area. For example, class 13 means that the land use in 1988 was forest and was converted to mixed agriculture in 2000. No change is represented with the code number zero.

5.4   Land use change analysis

The land use in the study area is mainly forest and mixed agriculture. Land use change analysis was carried out using two Landsat TM satellite sensor images for the years of 1988 and 2000, as described in Chapter 3 (Chapter Methods). Land use change analysis was undertaken for two sub-catchment areas, which correspond to the stream flow stations River Galas (representing upstream) and River Kelantan (representing downstream). Figure 5-15 and Figure 5-16 depict the land use maps for these sub-catchment areas. Land use was represented by nine classes; forest, water, mixed-agriculture, , bare soil, built-up, , mangrove, oil palm, rubber, and paddy.

In the study area, the forest class represents rainforest or tropical forest which is characterized by high rainfall (i.e. annual rainfall between 1750-2000 mm) as experienced in the study area. More than 50% of the study area is still covered by forest (Dahlan and Abdullah, 2006). According to the Kelantan state Forest Management Unit (FMU), the forest area is divided into three categories which are Permanent Forest Estate (PFE), National Park/Wildlife Reserves and Stateland Forest. The built up land class comprises residential, transportation networks and industrial areas. Mixed-agriculture comprises orchards, horticulture, vegetables and spices plantations. Meanwhile, water comprises rivers, lakes and marshland.
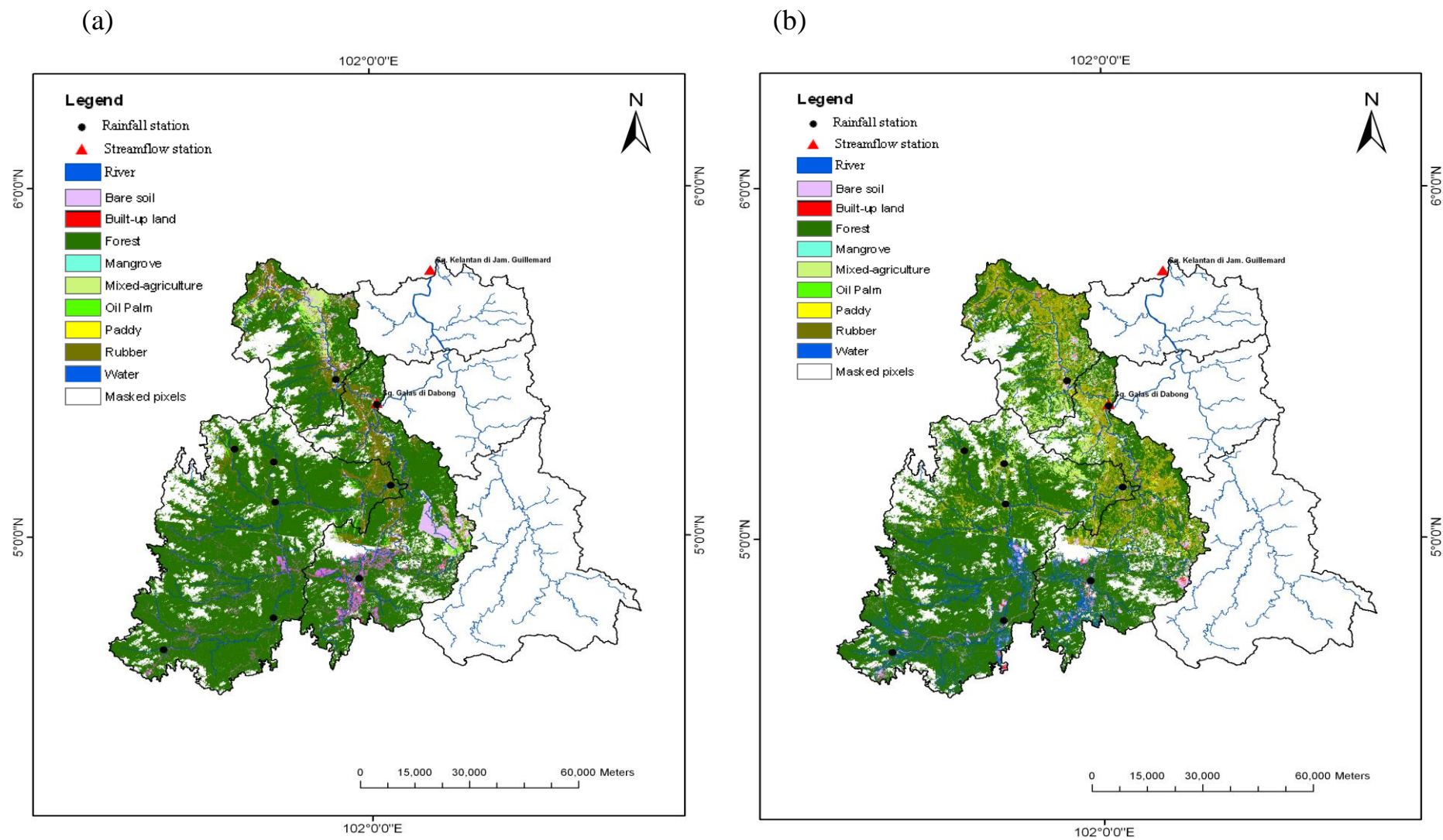
Figure 5-15 Land use maps of upstream sub-image obtained using the ML algorithm for the years (a) 1988 and (b) 2000.
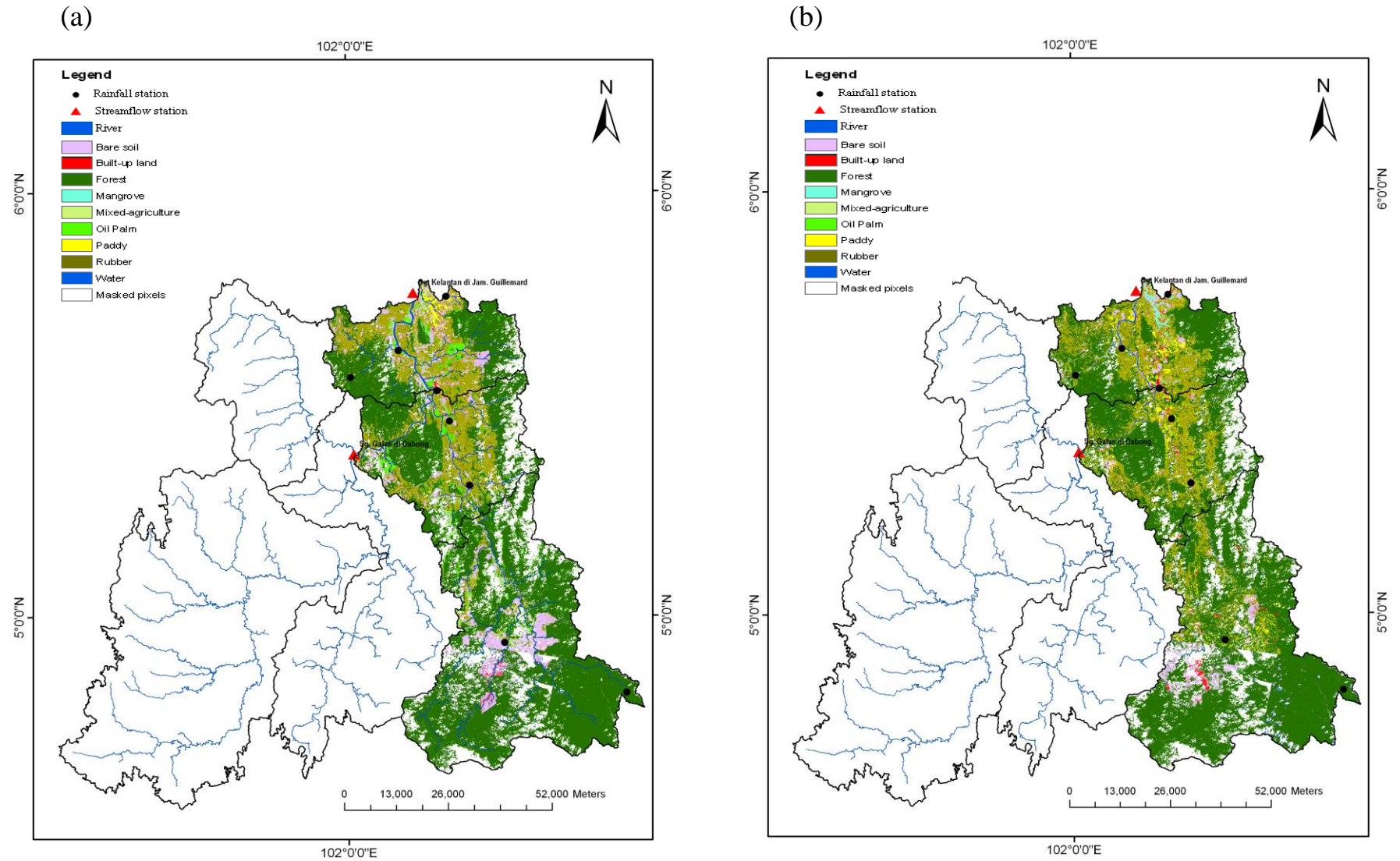
Figure 5-16 Land use maps of the "downstream" sub-image obtained using the ML algorithm for the years (a) 1988 and (b) 2000.

A land use map depicting change from forest to agricultural land (i.e. paddy, oil palm, rubber and mixed-agriculture) for the River Galas and River Kelantan sub-catchments is shown in Figure 5-17. For the River Galas sub-catchment, the largest total increasing land use was agricultural land with a large increase of 66.2% (Table 5-5). The increase in agricultural land occurred mostly in the Gua Musang district. The second largest increase in area was for built-up land (14.8%). Meanwhile, land use classes decreasing in area were forest (a decrease of -11.8%), bare soil (-37.8%), mangrove (-24.2%) and water (-7.7%).

For the River Kelantan sub-catchment three land use classes increased in area: agricultural land (oil palm and rubber) (22.4%), forest (3.2%) and built-up land (2.4%). The increase in forest area is similar to that reported by Global Forest Resource Assessment (FAO, 2005) which stated that up to the year 2000 forest plantation area was about 1659 hectares which involved forest production and protections programme. In addition, a report from the Kelantan Forest Department (2006), stated that forest replantation programme of about 8784 hectare involved bamboo and rattan plantation from 1989 to 2002. Land use classes decreasing in area were bare soil (-52.7%), mangrove (-52.8 %), as well as mixed-agriculture (-30.4%), paddy (-7.7%) and water (-6.4%). The results are summarized in Table 5-5.

Of particular importance is to evaluate the land conversion from forest to agricultural land. These two classes are the dominant land use classes in the study area. In addition, these two classes can have a significant impact on the hydrological response. Analysis of the River Galas sub-catchment showed that most land use conversion was from forest to agricultural land (rubber and mixed-agriculture) (9.3%). The equivalent figure for downstream River Kelantan was only 4.5%. The second most common conversion was from mixed-agriculture to forest with 3.3% (River Galas) and 6.5% (River Kelantan). The third most common conversion was from bare soil to agricultural land with 1.7% (River Galas) and 3.7% (River Kelantan). The remaining percentages for land use conversion were less than 0.5%.
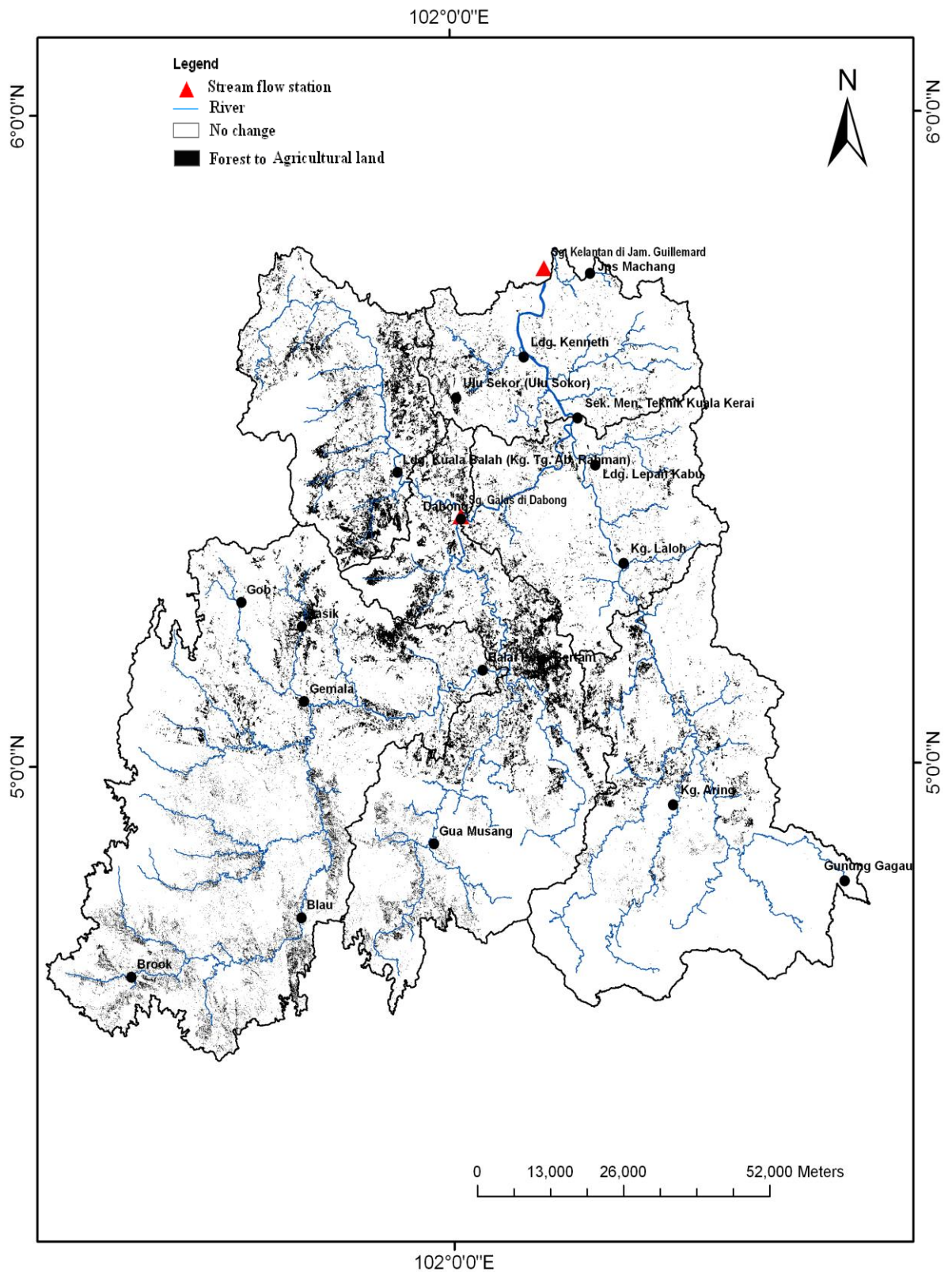
Figure 5-17 Map of land use change from 1988 to 2000 for conversion from forest to agricultural land as predicted using the ML algorithm for the Kelantan catchment.

Table 5-5 Land use change result for River Galas (upstream) sub-catchment streamflow. Classification was undertaken for both years using maximum likelihood classification.

River Galas (Upstream)					
	1988		2000		2000-1988
Land use class	Pixels count	%	Pixels count	%	% change
Forest	4927928	74.27	4347143	65.52	-11.8
Built-up	63572	0.96	73009	1.1	+14.8
Bare soil	453759	6.84	282016	4.25	-37.8
Paddy	27481	0.41	40850	0.62	+48.6
Mangrove	35143	0.53	26624	0.4	-24.2
Oil palm	238126	3.59	599055	9.03	+151.6
Rubber	692366	10.43	786903	11.86	+13.7
Mixed-agriculture	179007	2.7	463156	6.98	+158.7
Water	17934	0.27	16560	0.25	-7.7
Total	**6635316**	**100**	**6635316**	**100**	

River Kelantan (Downstream)					
	1988		2000		2000-1988
Land use class	Pixels count	%	Pixels count	%	% change
Forest	2674805	60.83	2760395	62.77	+3.2
Built-up	69375	1.58	71004	1.61	+2.35
Bare soil	407369	9.26	192869	4.39	-52.65
Paddy	50321	1.14	46438	1.06	-7.72
Mangrove	39813	0.91	18805	0.43	-52.77
Oil palm	241577	5.49	432812	9.84	+79.16
Rubber	705600	16.05	726177	16.51	+2.92
Mixed-agriculture	193229	4.39	134571	3.06	-30.36
Water	15249	0.35	14267	0.32	-6.44
Total	**4397338**	**100**	**4397338**	**100**	

5.5 SYNTHESIS

The analysis of streamflow change in comparison to both precipitation and land use changes revealed some interesting results. The River Kelantan representing the downstream catchment exhibited decreasing trends in streamflow predominantly in the dry season. The trends in precipitation time series were in agreement with the streamflow trends. The results imply that the decreasing trends observed in streamflow for the downstream catchment may be due primarily to the decreasing trends in precipitation. Meanwhile, the River Galas representing the upstream sub-catchment

revealed significant increasing trends in streamflow in all seasons. However, precipitation was observed to increase only in the wet season and decrease in the dry season.

Both sub-catchments showed that wet months or seasons are becoming wetter (i.e. increasing trends in the months of January, November and December or seasons of JFM, OND). The annual flooding report for the Kelantan catchment suggests that intense rainfall was received recently in these particular months (DID 1997, DID 2003, DID 2004). The results also signify that dry months are becoming drier for certain stations. The trend analysis, thus, revealed that a seasonal shift in the monsoon may be occurring (to OND and JFM). According to the Kelantan flooding report in the years of 2006 and 2007, the Kelantan basin experienced flooding twice per year (i.e. in the year 2006 flooding occurred on 12 February and 19 December; flooding in 2007 occurred on 08 January and 13 December). The report supports the present findings that there may be a seasonal shift in intense monsoonal rainfall in the Kelantan catchment.

The land use change analysis suggested that the upstream area experienced most land use change (Table 5-5). Most land use conversion occurred from forest to mixed-agriculture in the upstream area, but some conversion to built land was also evident. This accords with local knowledge. Since the introduction of the Malaysia diversification plantation programme in the late 1970s, the Malaysia government has provided incentives to farmers to cultivate oil palm and rubber plantation. Most of the oil palm and rubber estates were established upstream over an area of 20540.6 hectares (PPLRNK, 2007).

Deforestation for agriculture can alter the hydrological response of the land such that the observed increased flows, particularly in the dry season, in the upstream area might be partially a function of change in land use from forest to mixed-agriculture. The intensive use of machines and alteration of soil structure during early stages of the plantation process may contribute to a change in infiltration capability, reduce evapotranspiration rate and subsequently lead to increases in runoff volume (Moussa et al., 2002; White and Howe, 2004). Nik (1988) found that conversion of forest to agricultural land in Malaysia led to substantial increases in annual water yield of 1100 mm (117%) and 706 mm (157%) in the first and second years after logging.

In the upstream area, the increase in agricultural land was large (66.2%) with most of this change coming directly from deforestation (9.3%). In these circumstances, land use change could be a significant factor in addition to precipitation change in explaining the observed changes in streamflow in the area. While this argument is compelling, increased magnitude and intensity of precipitation over short periods might also lead to an increase in streamflow, where there is no increase in precipitation mean. Thus, some uncertainty remains.

Others factors may be appropriate to explain the trends detected in streamflow such as temperature changes, evapotranspiration (ET), potential ET and water abstraction. However, this information was not included in the time series analysis due to the non availablitity of the data record and also due to severely missing data for the chosen period. The omission of change in variables such as temperature, evapotranspiration and water extraction should not undermine greatly the validity of the results in general terms in relation to trend detection, although some caution is warranted especially to explain the trend detected in seasonal hydrological variables. It is widely acknowledged that the transformation of precipitation into streamflow (and potentially flooding) in a catchment involves a highly complex and nonlinear system (Bronstert, 2003; Segond et al., 2007). The interaction of many variables such as topography, climate conditions, soil characteristics and base-flow water conditions, as well as channel and drainage density, may cause large uncertainties in trend detection studies (Bronstert, 2003). Thus, further investigation incorporating more detailed data on hydrological conditions and hydraulic characteristics over the historical period is needed to provide more accurate trend detection in time-series hydrological data.

5.6 SUMMARY

The Mann-Kendall test was employed to detect monthly, seasonal and annual trends in a monsoon catchment area. Significant increasing and decreasing trends of streamflow and precipitation were observed. Importantly, a seasonal shift in monsoon precipitation to OND and JFM was detected.

Land use changes may also play a role in determining the observed changes in streamflow. In particular, expansion of built-up areas in the north of the study area

(downstream) and deforestation in the south and southwest (upstream) provide plausible contributory factors that may affect hydrological processes and subsequently increase streamflow and the risk of flooding. The large amount of agricultural conversion (almost 70%) in the Kelantan catchment revealed by the land use change analysis provides an important factor that may have contributed to the observed increases in streamflow.

In the next analysis as described in the Chapter 6, the HEC-HMS hydrological model was used to quantify the relationship between streamflow, precipitation and land use changes in the Kelantan basin. An investigation of the hydrological impact of precipitation and land use changes on stream flow and flooding in the Kelantan catchment were presented.

Chapter 6

Hydrological Modelling: Past and Current Runoff Simulations

6.1   INTRODUCTION

This chapter deals with the application of the HMS hydrologic model to the River Kelantan catchment. Firstly, details of the sequence of steps required to derive the hydrological model using HEC-GeoHMS and later HEC HMS are described in this chapter. This chapter explains the runoff model for two periods which are (i) a past event using 1988 and 1995 for calibration and validation, respectively, and for (ii) a "current" event using 2004 and 2006 for calibration and validation using 15 minutes time interval. However, due to missing data for the observed discharge for 1988 and 1990, the runoff simulation for 2004 is presented first. The model parameter calibrations and validations for each period are also explained. In addition, sensitivity analysis is carried out to evaluate which parameters have the most effect on hydrological response in the River Kelantan catchment. The last part of the analysis tries to quantify how much observed changes in land use and climate affect runoff volume in the Kelantan catchment.

6.2 HEC-GeoHMS SUB-BASIN DELINEATION FOR RIVER KELANTAN

HEC GeoHMS is an embedded tool built in ARCGIS. The main purpose of the tool is to help in sub-basin delineation and to extract physical characteristics from a DEM. The output from HEC GeoHMS processing later was used in the HEC HMS hydrological software. The main data for this sub-basin are from a DEM.

6.2.1 DEM data analysis

Shuttle Radar Topography Mission (SRTM) digital elevation model (DEM) data were provided by the Consultative Group for International Agriculture Research–Consortium for Spatial Information (CGIAR-CSI) (http://srtm.csi.cgiar.org/). The data have a horizontal resolution of 30 m and vertical resolution of 90 m. The data were used to delineate sub-basins in the study area. The data were subjected to error correction by filling in sinks using the Arc Hydro tool in the ARCGIS software Figure 6-1. The steps were done to allow for the smooth water flow from upstream to downstream (i.e. by modifying a cell surrounded by higher elevation cells which cause the water to not flow to the lower elevations or to the downstream area). Further datasets used in sub-basin delineation included river network and soil type data layers obtained from the Malaysia Department of Irrigation (DID). In addition, land use data were provided by the Department of Town and Country Planning Malaysia (TCPD).

6.2.2 Preparation of hydrology networks

HEC GeoHMS was utilized to derive physical characteristics in the HEC-HMS model. The program is an add-in tool built in the ArcGIS software developed by USACE. The preprocessing is divided into three main stages; a) terrain preprocessing, b) basin processing and, c) HMS project set-up as shown in Figure 6-2.
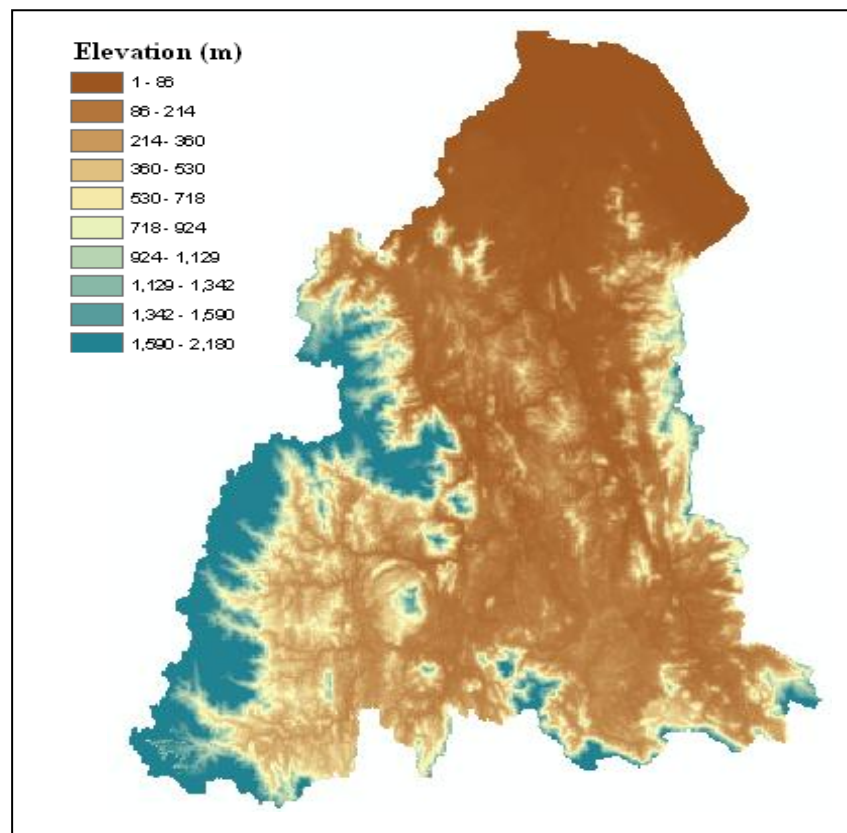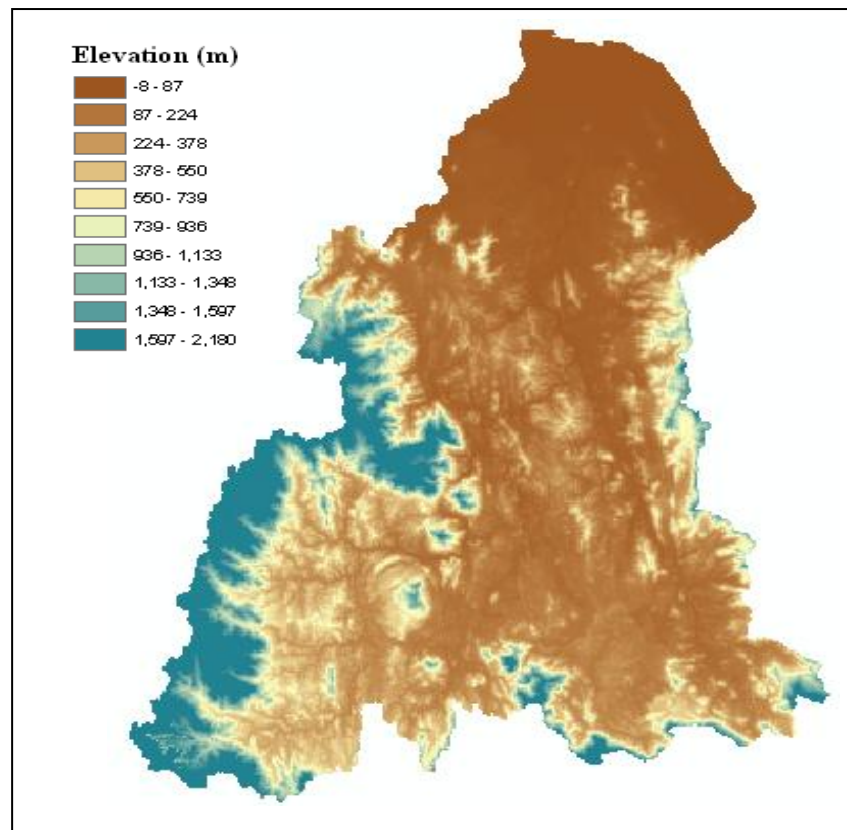
Figure 6-1 The DEM data (top) before and (bottom) after filling of DEM sinks using HEC GeoHMS.
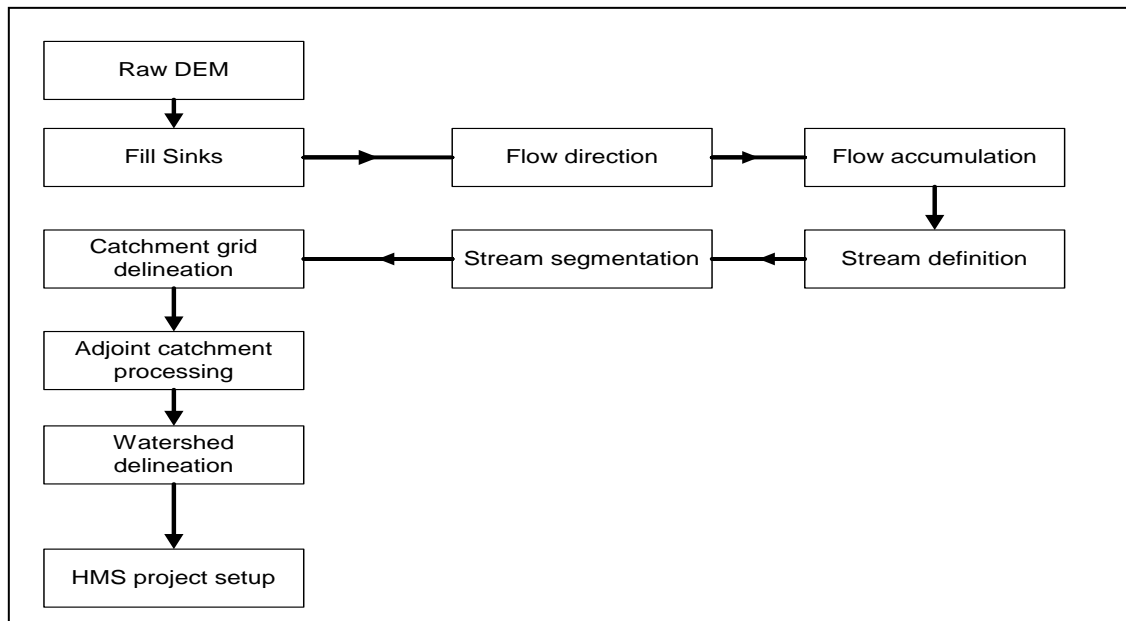
Figure 6-2 HEC GeoHMS processing including terrain preprocessing, basin processing and HMS project setup.

6.2.2.1 Terrain pre-processing

Terrain processing is a powerful tool because it provides several functions to prepare a geospatial network of a catchment in grid and vector formats. The function provides outputs in grid and vector formats. The function flow direction calculates the direction of flow of the steepest descent from the grid cells in the filled sinks DEM data. The process uses the eight-point pour algorithm (which are east, southeast, south, southwest, west, northwest, north and northeast) (Figure 6-3). Flow accumulation is calculated from flow direction by accumulating the number of cells upstream of a given cell. Subsequently, stream definition was computed using the threshold value of 1% of the maximum flow accumulation (139583 cells or 125.625 km^2).

Stream segmentation creates a stream segment in grid format that has a unique grid code that is specific to that segment (either a segment is a head segment or a segment exists between two segment junctions). Catchment grid delineation was then performed that creates a grid in which each grid carries a grid code indicating to which catchment the grid belongs. Subsequently, catchment polygon processing was performed to convert the catchment grid into a vector or polygon feature (Figure 6-3).
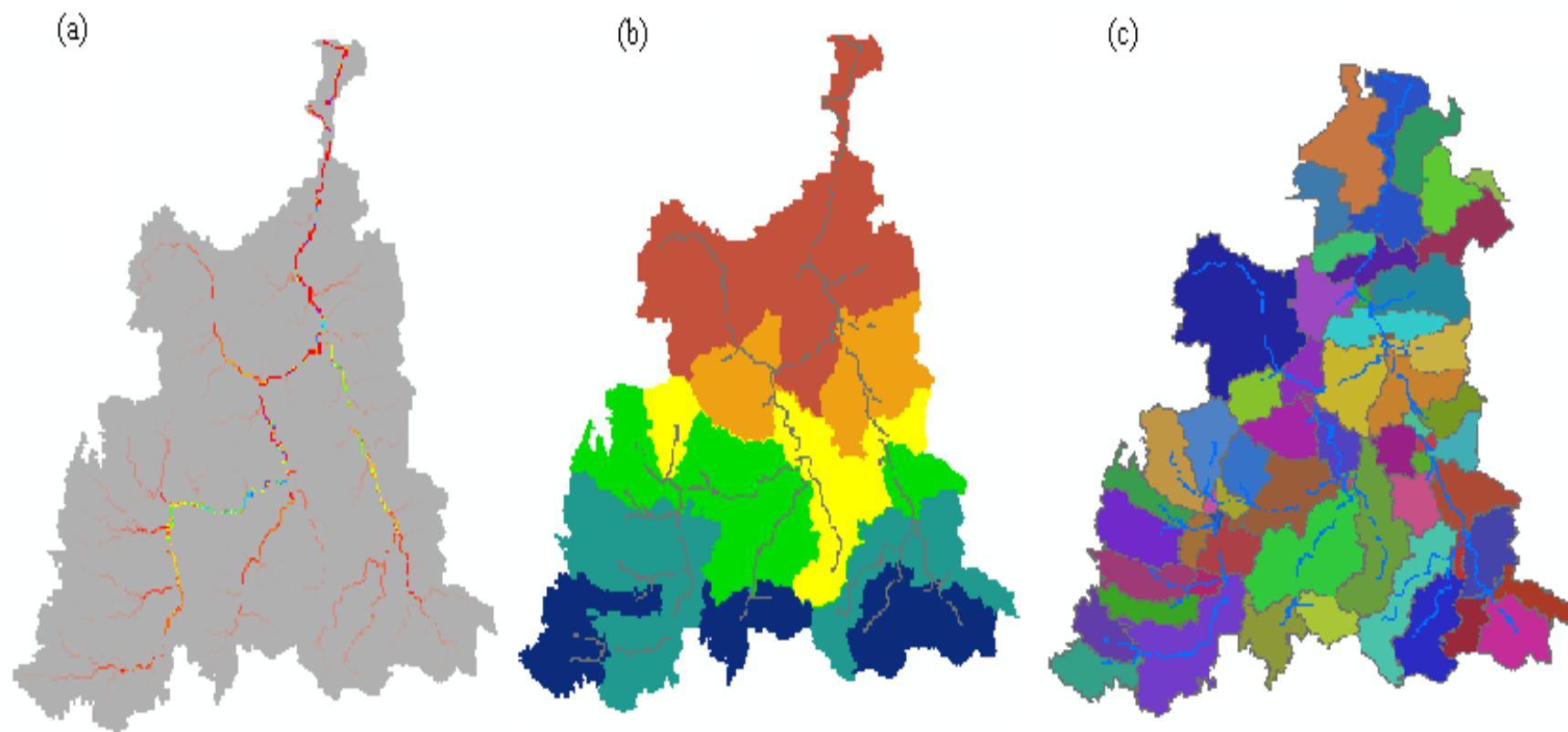
Figure 6-3 (a) Flow direction, (b) catchment grid (raster) and (c) catchment polygon (vector) derived from terrain pre-processing function flow.

6.2.2.2 **Basin processing**

Basin processing was performed after the terrain preprocessing was completed. The process was used to revise the catchment delineation. The processes involved in the basin processing were basin merge, basin subdivision, river merge, river profile, split basin at confluences and batch sub-basin delineation. The catchments later known as sub-basins, were then merged according to land use and soil type groups. The final six sub-basin polygons were derived as presented in Figure 6-4.
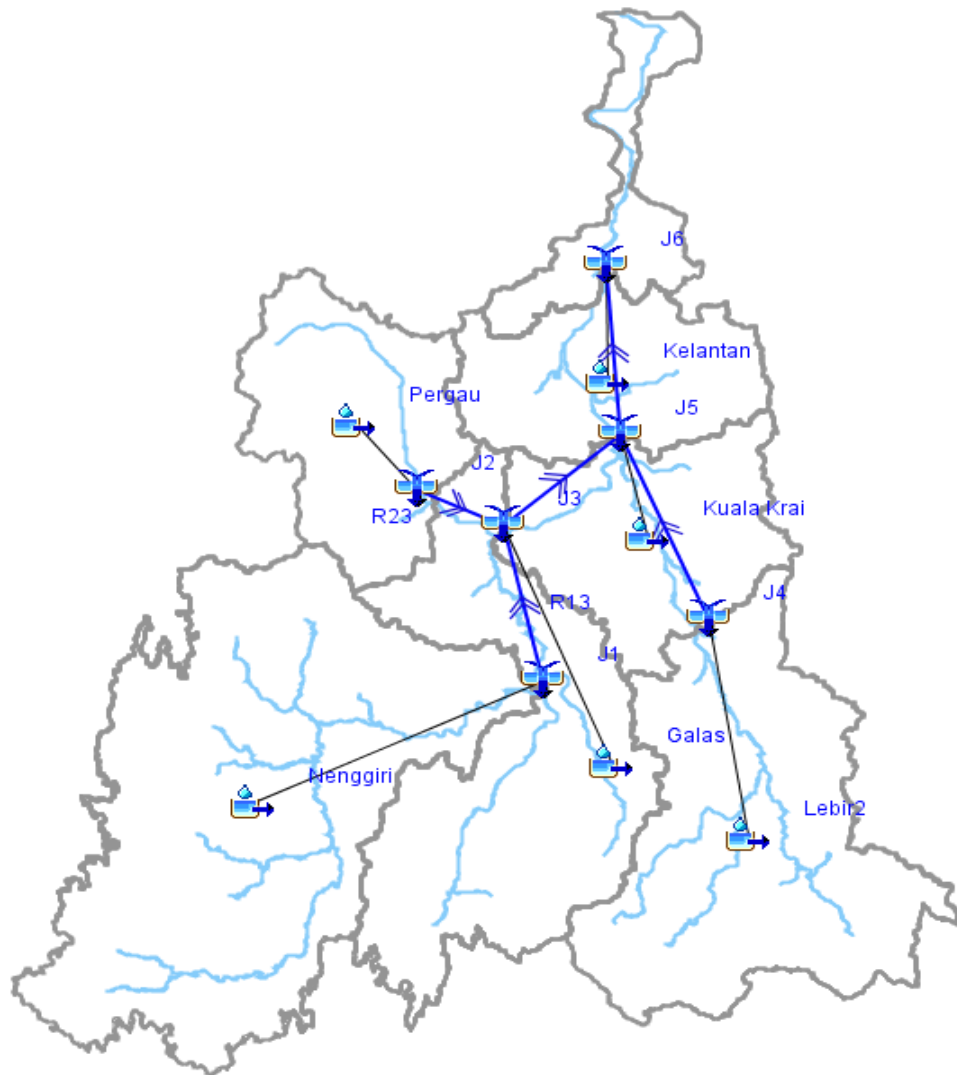
Figure 6-4 The six sub-basins (i.e. Nenggiri, Galas, Pergau, Lebir, Kuala Krai and Guillemard Bridge) as derived from the HEC-GeoHMS tool processing.

6.2.2.3 **Parameter estimation**

Parameters in a hydrological model are based on measured or inferred parameters (Yu et al., 2001). Measured parameters may be obtained for example through observation of catchment characteristics in the field or through GIS measurement. These measured parameters may include sub-basin area (km^2), slope, flow length (km) and percentage of impervious surface. Inferred parameters which are impossible to measure or be derived through observation in the field are estimated using a mathematical model. Such inferred parameters are used within the loss model (i.e. initial abstraction, SCS CN, % of impervious surface), transform model (i.e. lag time) and routing method (i.e. lag time) as described in Chapter 3 (i.e. Chapter Methods). These inferred or estimated parameters are subjected to sensitivity analysis and calibration processes.

6.3   HYDROLOGIC MODELLING USING HEC-HMS

The rainfall-runoff model was performed to quantify precipitation and land use change factors influencing the hydrological response. Although in Chapter 5 analysis was performed on an annual, seasonal and monthly basis, due to incomplete data to run a continuous-based runoff model, an event-based model was used. Therefore, an event-based model was deemed suitable since the goal of the analysis was not solely to forecast changes in streamflow, but rather to evaluate the effects of two variables on hydrological response

The event-based runoff model was applied using two periods to replicate *past* and *current* storm events. The past event was using the year 1988 due to this year being the year for which a cloud-free remotely-sensed image (i.e. Landsat TM) existed and to derive model parameters (i.e SCS CN and percentage of impervious surface). The year of 2004 was chosen because it was the year for which the latest precipitation and stream flow data records were completed and suitable for use when this study was carried out. Furthermore, the 1988 event represents conditions prior to, and the 2004 event represents conditions after, significant deforestation, afforestation and expansion of agricultural land. Both models were calibrated and validated to represent the specific characteristics of the hydrologic response during each period. However, the 2004 event was used as a baseline, and conditions for 1988 simulated using observed data for

precipitation and land use during 1988. Use of a hydrological model was advantageous because it allowed conversion of all units to discharge (i.e., m³s⁻¹) facilitating direct comparison of precipitation and land use effects. The effects of precipitation and land use changes on peak flow and runoff volume were investigated both singly and in combination

The past runoff model used 1988 for calibration and 1995 for validation. Meanwhile, for the current event, 2004 and 2006 were chosen for calibration and validation respectively. Figure 6-5 represents the rainfall-runoff processes included in the storm event model in the study area.
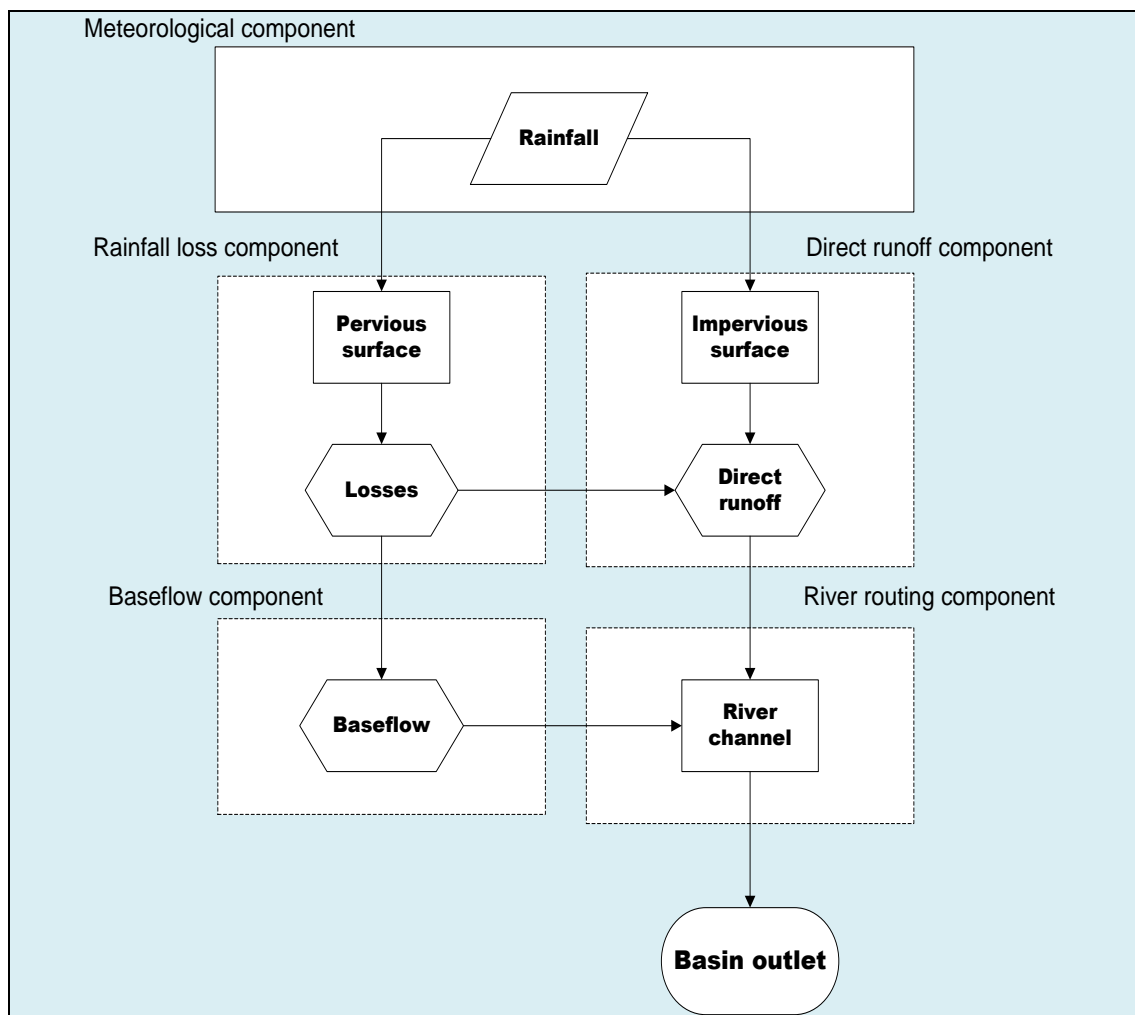
Figure 6-5   The rainfall-runoff processes used in the HEC-HMS model for the storm event.

6.3.1 Basin model

The basin model performed using the HEC GeoHMS delineated six sub-basins as shown in Figure 6-4 for past and current storm events. From these sub-basins, the sub-model measured and inferred parameters of each sub-basin are shown in Table 6-1. The sub-models used consisted of loss, transform and baseflow. For the routing model initial parameter values were used as derived from multiple sources. The sub-model and parameter values for the year of 1988 are showed in Table 6-2 and for the year of 2004 in Table 6-3.

Table 6-1 Sub-basin model parameters used to run runoff model simulation for the year of 2004 storm event. DID is Department of Irrigation and Drainage.

Sub Model	Parameter	Symbol	Units	Source
Loss	Initial abstraction	I_a	mm	DID
	Curve number	CN	-	GIS
	Impervious	I_{mp}	%	GIS
	Area	A	km^2	GIS
Transform	Lag time	L_t	min	GIS
Baseflow	Constant monthly	C_m	m^{3}s^{-1}	DID
Routing	Lag	L_g	min	DID

Table 6-2 Initial values (uncalibrated) for each sub-basin model parameter for the loss, transform, baseflow and routing models used in HEC-HMS for the year 1988.

Sub-basin	A	I_a	CN	I_{mp}	L_t	L_g
Nenggiri	3708.7	10	30	0.15	1000	20
Pergau	1243.1	10	35	0.48	750	60
Galas	2261.1	10	65	0.59	1400	1200
Lebir	2392.0	10	40	0.34	1700	120
Kuala Krai	1244.1	10	64	0.31	1700	120
Guillemard Bridge	1079.6	10	50	0.60	1600	500

Table 6-3 Initial values (uncalibrated) for each sub-basin model parameter for the loss, transform, baseflow and routing models used in HEC-HMS for the year 2004.

Sub-basin	A	I_a	CN	I_{mp}	L_t	C_m	L_g
Nenggiri	3708.7	10	38	0.31	1000	101.0	20
Pergau	1243.1	10	53	0.88	750	217.2	60
Galas	2261.1	10	75	0.80	1400	772.4	1200
Lebir	2392.0	10	50	0.72	1700	147.1	120
Kuala Krai	1244.1	10	85	0.81	1700	147.1	120
Guillemard Bridge	1079.6	10	65	1.44	1600	248.6	500

6.4 METEOROLOGICAL MODEL

The meteorological model in HEC-HMS includes precipitation and evapotranspiration (ET) for continuous runoff modeling and evapotranspiration is negligible for the event model due to the intensity of the storm being modeled, continuous saturation of the air and because ET volume is negligible compared to runoff volume (Knebl et al., 2005; Cunderlik and Simonovic 2007; McColl and Aggett, 2007). Therefore, no information of evapotranspiration included in the model. Depth of rainfall was calculated using the Thiessen polygon gauge weight method and time weight as described earlier (i.e. Chapter Methods). Details of depth weight and time weight for past and current runoff model are shown in Table 6-4.

Table 6-4 Depth and time weight for each sub-basin used in the HEC-HMS model.

Depth weight and time weight							
Sub-basin	Blau	Gemala	Gua Musang	JPS Machang	Kg Aring	Kg Laloh	Ulu Sekor
Nenggiri	0.51	0.49	-	-	-	-	-
	0.7	0.3					
Pergau	-	-	-	-	-	-	1.0
							1.0
Galas	-	-	1.0	-	-	-	-
			1.0				
Lebir	-	-	-	-	0.56	-	-
					0.8		
Kuala Krai	-	-	-	-	-	1.0	-
						1.0	
Guillemard Bridge	-	-	-	1.0	-	-	-
				1.0			

6.5 CONTROL SPECIFICATION

To run the runoff simulation different dates were chosen to match the time series trend analysis and for the future runoff simulation analysis. Historical dates were used for calibration and validation. A storm event was chosen based on monsoon rainfall which is between the months of November to January. The runoff calibration used rainfall and discharge data of December for the years of 1988 and 2004. For validation the same months were used (i.e. December) for the years of 1990 and 2006. Both data of precipitation and discharge used a time interval of every 15 minutes to give a good representation of rainfall and flow characteristics within the sub-basin of the study area.

6.6   HYDROLOGIC MODEL RESULTS FOR THE RIVER KELANTAN

The following paragraphs present the results of rainfall-runoff model simulation, calibration and validation. Firstly, the 2004 runoff is presented followed by the runoff in 1988.

6.6.1 Pre-calibrated hydrograph simulation results for the year 2004

From the pre-calibration result, an acceptable shape of hydrograph was achieved. The rising and receeding limbs showed acceptable agreement between observed and simulated hydrographs. As described in the chapter methodology, five goodness-of-fit measurements were used which are the mean absolute error (MAE), root mean square error (RMSE), coefficient of determination (R_2), Nash-Sutcliffe efficiency index (E_f) and percentage of bias (%BIAS).

From the six sub-basins modelled, the goodness-of-fit between observed and simulated data were acceptable with moderate accuracy of E_f for Nenggiri (0.51), Lebir (0.52), Kuala Krai (0.66) and Kelantan (0.66). Flow comparison between observed and simulated data for Pergau and Galas was unsatisfactory, for example, Galas with an E_f of only 0.10 (Table 6-5 and Table 6-6). To improve the predictive power of the model, parameter sensitivity analysis was carried out before the calibration process was performed. The sensitivity analysis was done to assist the calibration process by optimizing only the parameters which showed high sensitivity.

Table 6-5 Observed, calibrated and validated statistics and goodness-of-fit for the years of 2004 (calibrated) and 2006 (validated). SD; Standard deviation, MAE; Mean absolute error, RMSE; Root mean square error, R_2; Coefficient of determination, E_f: Nash Suctcliffe efficiency index, %BIAS; Percentage of bias, Peak Q; Peak discharge; PEPQ; Percentage error of peak discharge, PERV; Percentage error of runoff volume.

	Observed 2004	Calibrated 2004	Observed 2006	Validation 2006
	Nenggiri			
Mean	396.59	479.65	251.36	203.35
SD	408.01	610.32	222.66	115.95
MAE	-	158.88	-	97.08
RMSE	-	255.58	-	151.82
R_2	-	0.931	-	0.67
E_f	-	0.608	-	0.54
%BIAS	-	-20.94	-	19.1
Peak Q	1643.2	2055	1080.1	545.1
Volume	120.17	145.36	61.86	53.78
PEPQ(%)	-	25.06	**-**	-49.53
PERV(%)	-	20.96	-	-13.06
	Pergau			
Mean	518.21	428.51	-	-
SD	183.72	193.19	-	-
MAE	-	113.34	-	-
RMSE	-	151.77	-	-
R^2	-	0.62	-	-
E_f	-	0.25	-	-
%BIAS	-	17.3	-	-
Peak Q	787.52	863.7	-	-
Volume	468.41	359.44	**-**	**-**
PEPQ(%)	**-**	9.67	-	-
PERV(%)	**-**	-23.3	-	-
	Galas			
Mean	1435.63	1166.64	1222.47	1128.94
SD	772.17	605.86	468.51	409.7
MAE	-	290.21	-	126.87
RMSE	-	415.42	-	212.91
R_2	-	0.85	-	0.84
E_f	-	0.75	-	0.79
%BIAS	-	18.74	-	7.65
Peak Q	3158.5	3010.2	2378	2439
Volume	713.38	595.85	497.47	469.79
PEPQ(%)	-	-4.7	-	2.57
PERV(%)	-	-16.48	-	-5.56

Table 6-6 Observed, calibrated and validated statistics and goodness-of-fit for the years of 2004 (calibrated) and 2006 (validated). SD; Standard deviation, MAE; Mean absolute error, RMSE; Root mean square error, R_2; Coefficient of determination, E_f; Nash Suctcliffe efficiency index, %BIAS; Percentage of bias, Peak Q; Peak discharge; PEPQ; Percentage error of peak discharge, PERV; Percentage error of runoff volume.

	Observed 2004	Calibrated 2004	Observed 2006	Validation 2006
		Lebir		
Mean	571.38	539.47	355.36	325.65
SD	476.92	498.45	399.97	308.26
MAE	-	75.64	-	117.44
RMSE	-	100.80	-	161.38
R_2	-	0.96	-	0.87
E_f	-	0.96	-	0.84
%BIAS	-	5.58	-	8.36
Peak Q	1647.70	1665.60	1471.50	1256.80
Volume	268.45	253.46	142.50	136.97
PEPQ(%)		1.09		-14.59
PERV(%)		-5.58		-3.88
		Kuala Krai		
Mean	571.38	547.68	355.36	318.50
SD	476.92	372.71	399.97	305.59
MAE	-	110.49	-	110.19
RMSE	-	167.21	-	155.63
R_2	-	0.91	-	0.89
E_f	-	0.88	-	0.85
%BIAS	-	4.15	-	10.37
Peak Q	1647.70	1336.00	1471.50	1224.70
Volume	516.14	494.68	273.98	255.71
PEPQ(%)		-18.92		-16.77
PERV(%)		-4.16		-6.67
		Guillemard Bridge		
Mean	3190.370	3285.687	1133.990	1216.743
SD	476.920	3981.705	1072.170	1103.063
MAE	-	219.816	-	392.500
RMSE	-	267.482	-	521.920
R_2	-	0.997	-	0.789
E_f	-	0.996	-	0.763
%BIAS	-	-2.988	-	-7.297
Peak Q	12117.000	12586.200	3802.200	4265.900
Volume	3321.630	3420.710	1061.660	1204.990
PEPQ(%)		3.87		12.20
PERV(%)		2.98		13.50

6.6.2 Sensitivity analysis

Sensitivity analysis is a method to determine which parameters of the model have the greatest impact on the runoff hydrograph results. The analysis ranks the parameters based on highest to lowest error the parameters contribute to the model. Nevertheless, sensitivity analysis also acts as pre-assessment for the model calibration and reduction of uncertainty (Hamby, 1994). The absolute sensitivity index was used to rank the parameters used (Al- Abed and Whitley 2002; Abed et al., 2004).

As described earlier in Chapter 3, local sensitivity analysis was used. This method is deemed to be suitable in this study since the ultimate aim of sensitivity analysis was to identify which parameters the model output is sensitive to and, hence provide good performance to model calibration to achieve acceptable agreement between observed and simulated hydrographs. It is not to analyze the interactions among parameters as demonstrated by global sensitivity analysis (Saltelli et al., 2004).

The sensitivity analysis was applied to four parameters which are I_a, CN, L_t and $I_{mp.}$ To rank the parameter's sensitivities, five runoff characteristics were examined which are peak discharge (PF), runoff volume (RV), total direct runoff (TDR), total baseflow (TBF) and total loss (TL). Finally, all the absolute sensitivity values were averaged as in average absolute sensitivity (AAS) in order to rank them. The results of the percentage parameter change versus percentage error in peak discharge and runoff volume are shown in Figures 6-6 and 6-7. Thus, the rank of model parameters showed in Table 6-7 to Table 6-10 for all sub-basins representing upstream (i.e. Nenggiri, Pergau and Galas) and downstream (i.e. Lebir, Kuala Krai and Guillemard Bridge).

The absolute sensitivity index analysis revealed that the initial abstraction (I_a) and percentage of impervious surface (I_{mp}) of the loss model parameter have a small impact on variation in the runoff model output for all sub-basins and is, thus, considered as not important to determine the model output. All of the sub-basins depicted that curve number (CN) and lag time (L_t) have the greatest impact on peak discharge and runoff volume. Curve number relates to the capability for soil infiltration and soil storage (Cunderlik and Simonovic, 2007; Wang et al., 2008).
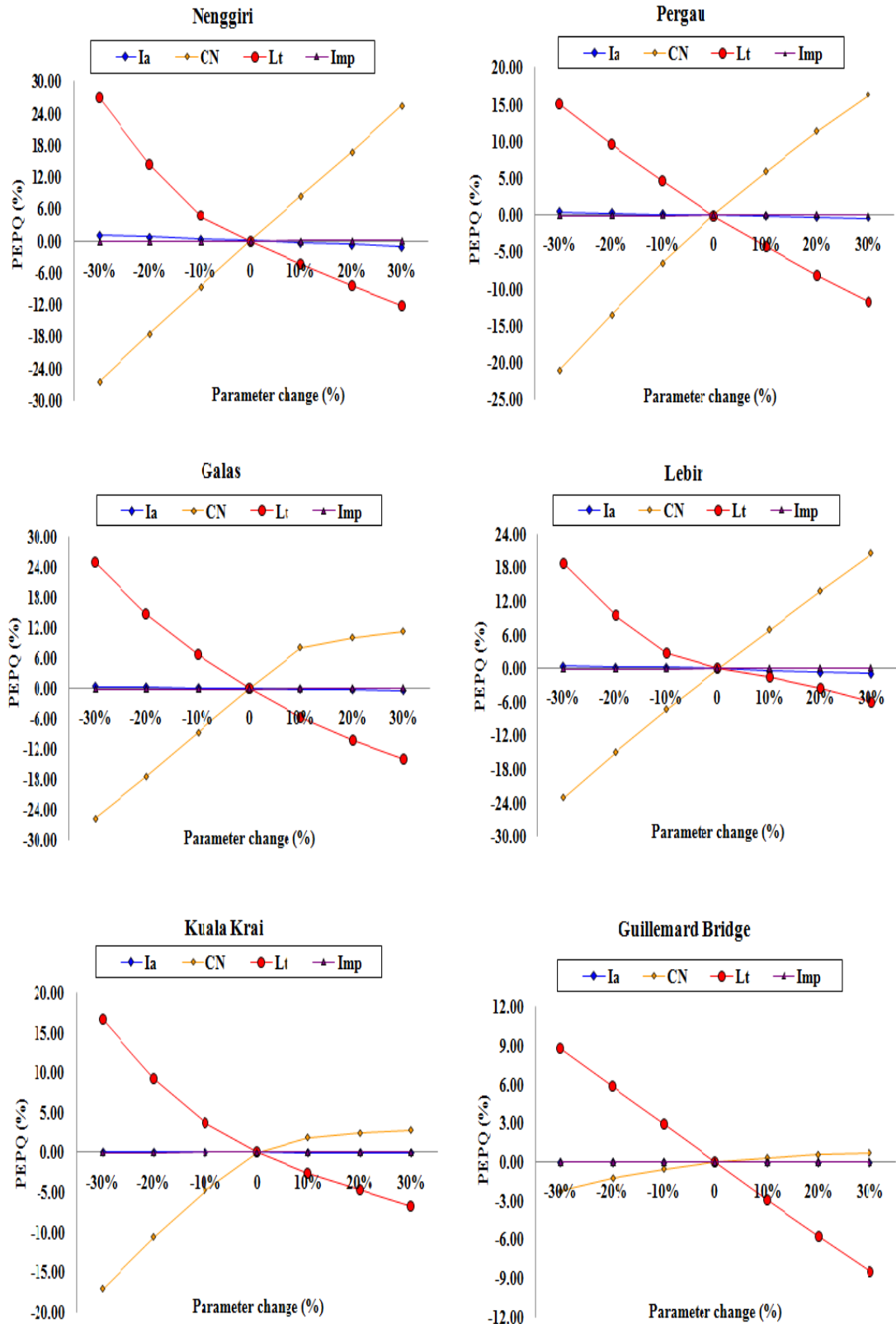
Figure 6-6 Sensitivity plot of percentage error peak discharge (PEPQ) using absolute sensitivity index for six gauge station in the River Kelantan.
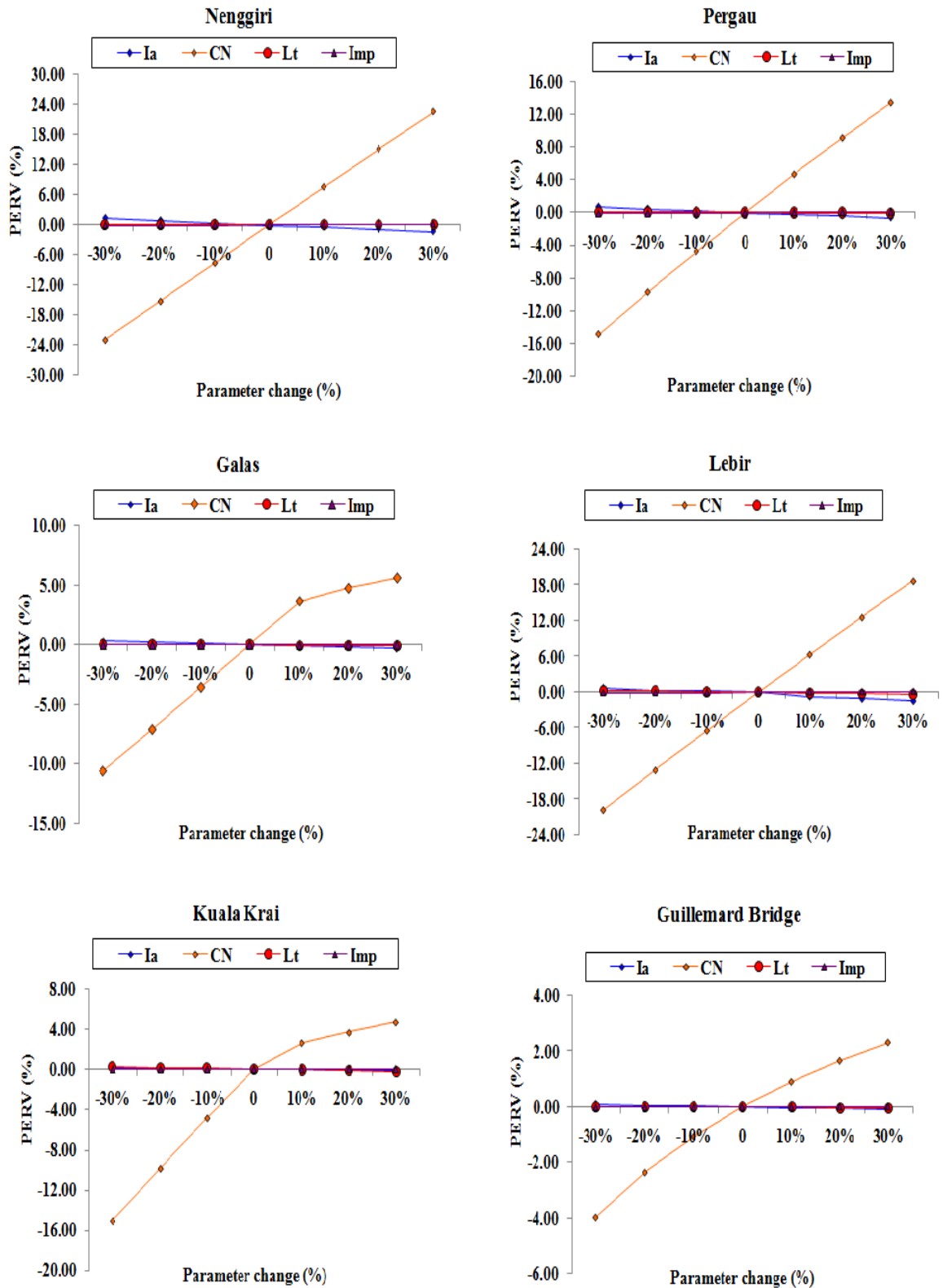
Figure 6-7 Sensitivity plot of percentage error runoff volume (PERV) using absolute sensitivity index for six gauge station in the River Kelantan.

Table 6-7 Parameter ranks using absolute sensitivity index analysis for the Nenggiri sub-basin.

Parameter	Peak flow (EPF)	Runoff volume (ERV)	Total direct runoff (ETD)	Total baseflow (ETBF)	Total loss (ETL)	Average Sensitivity index	Absolute Sensitivity index	Rank Order
Ia	-0.0379	-0.0453	-0.0574	0.0000	0.0391	**-0.020**	**0.020**	3
CN	0.8723	0.7618	0.9654	0.0000	-0.6542	**0.389**	**0.389**	1
Is	0.0030	0.0034	0.0044	0.0000	-0.0031	**0.002**	**0.002**	4
Lt	-0.6106	-0.0003	-0.0006	0.0000	0.0000	**-0.122**	**0.122**	2

Table 6-8 Parameter ranks using absolute sensitivity index analysis for the Galas sub-basin.

Parameter	Peak flow (EPF)	Runoff volume (ERV)	Total direct runoff (ETD	Total baseflow (ETBF)	Total loss (ETL)	Average Sensitivity index	Absolute Sensitivity index	Rank Order
Ia	-0.014	-0.010	-0.030	0.000	0.134	**0.016**	**0.016**	3
CN	0.817	0.338	1.053	0.000	-3.313	**-0.221**	**0.221**	1
Is	0.001	0.001	0.002	0.0000	-0.008	**-0.001**	**0.001**	4
Lt	-0.613	-0.002	-0.005	0.000	0.000	**-0.124**	**0.124**	2

Table 6-9 Parameter ranks using absolute sensitivity index analysis for the Lebir sub-basin.

Parameter	Peak flow (EPF)	Runoff volume (ERV)	Total direct runoff (ETD	Total baseflow (ETBF)	Total loss (ETL)	Average Sensitivity index	Absolute Sensitivity index	Rank Order
Ia	-0.022	-0.036	-0.050	0.000	0.068	**-0.008**	**0.008**	3
CN	0.738	0.646	0.896	0.000	-1.205	**0.215**	**0.215**	1
Is	0.003	0.004	0.005	0.000	-0.007	**0.001**	**0.001**	4
Lt	-0.390	-0.012	-0.017	0.000	0.000	**-0.084**	**0.084**	2

Table 6-10 Parameter ranks using absolute sensitivity index analysis for the Guillemard Bridge sub-basin.

Parameter	Peak flow (EPF)	Runoff volume (ERV)	Total direct runoff (ETD	Total baseflow (ETBF)	Total loss (ETL)	Average Sensitivity index	Absolute Sensitivity index	Rank Order
Ia	0.000	-0.003	-0.003	0.000	0.087	**0.016**	**0.016**	3
CN	0.049	0.106	0.125	0.000	-2.525	**-0.449**	**0.449**	1
Is	0.000	0.000	0.001	0.000	-0.015	**-0.003**	**0.003**	4
Lt	-0.289	-0.0007	-0.0008	0.0000	0.0000	**-0.058**	**0.058**	2

6.6.3 Calibration runoff model for 2004

Model calibration is a systemic approach of adjusting model parameters values to derive acceptable hydrographs between the simulated and observed events. According to Madsen (2000) the objective of model calibration is to appropriately select model parameters so that the model simulates the hydrological behaviour of the catchment as closely as possible. In the HEC-HMS model, an objective function is used to measure quantitatively the match between these two hydrographs. The function measures the degree of difference between simulated and observed hydrographs. The process tries to find the optimum values of parameters which are impossible to be estimated in the field through observation or measurement. Automated calibration was used in the HEC-HMS model by iteratively adjusting the parameter values until the smallest values of the selected objective function were achieved. The objective functions chosen in this analysis are described in Chapter 3 which are the sum of squared residuals (SSR) and peak-weighted RMS error (PWRMSE). The best estimated parameter from one of the objective functions was used.

Three parameters were suitable for model calibration which are initial abstraction (I_a), Curve number (CN) and lag time (L_t). The results for past and current storm events chosen are shown in Table 6-11.

Table 6-11 Calibration parameter results with two objective functions for the storm events in 1988 and 2004 of the Galas sub-basin.

	Dec 2004	Dec 2004	Dec 1988	Dec 1988
	Sum squared residuals (SSR)	Peak-weighted RMS error (PWRMSE)	Sum squared residuals (SSR)	Peak-weighted RMS error (PWRMSE)
Initial abstraction (mm)	2	9.2	2	10
Curve number	80	76	76.4	74
Lag time (hr)	1600	1425	1800	1427
E_f	0.75	0.63	0.95	0.86

The results show that the SSR objective function provides better calibration result rather than PWRMSE between simulated and observed hydrographs. The model performance was assessed using the method described in Chapter 3 (i.e. Nash Sutcliffe efficiency index (E_f), MAE, RMSE, and %BIAS) (Table 6-5 and Table 6-6). The SSR

objective function was used since it provided the largest E_f of 0.75 in 2004 and 0.95 in 1988 (Table 6-11).

The calibrated parameter and hydrograph results for the six sub-basins were acceptable: The main aim of the study was to establish a repeatable procedure to simulate land use and climate change effects and not to replicate perfectly the observed hydrograph (Table 6-12)(McColl and Aggett, 2007). Figure 6-8 to Figure 6-13 show the calibrated hydrographs between simulated and observed for the chosen years at the Nenggiri, Pergau, Galas, Lebir, Kuala Krai and Jambatan Guillemard discharge stations.

The mean and SD values revealed that the calibrated values are little different to the observed values for 2004. The model performance statistics showed that all of the stations have increased accuracy in term of E_f, MAE, RMSE, %BIAS. The higher accuracy of E_f was depicted by the Galas, Lebir, Kuala Krai and Guillemard Bridge stations with an E_f between 0.75 to 0.996. However, moderate and low E_f values were exhibited by the Nenggiri and Pergau stations with an Ef of 0.608 and 0.25. The % of BIAS also showed a large reduction in errors for all sites. Meaanwhile, the coefficient of determination (R_2) showed the highest agreement between simulated and observed hydrograph with all of the sub-basins with values above 0.80 except for the Pergau station of 0.62. The PEPQ and PERV also showed satisfactory agreement between the simulated and observed values with PEPQ for all sites being less than $\pm 25\%$, and PEV results of $\pm 23\%$ (Table 6-5). The lowest error was represented by the Guillemard Bridge station of 3.87% for PEPQ and 2.98% for PERV. According to Moriasi et al. (2007) any simulated runoff model is recommended as satisfactory if the E_f is more *then* 0.50 and %BIAS is within $\pm 25\%$. In addition, Cheng (2006) stated that a runoff model is considered good if the PEPQ is less than 20% according to the national criteria for flood forecasting in China. The result from the study with $\pm 25\%$ was deemed satisfactory which suggests that these hydrograph characteristics can be estimated appropriately using the calibrated input parameters. However, the inability of the simulated hydrograph to properly match the shape of the peak discharge, rising and recession limbs may due to the semi-distributed nature of the input parameters used or it is an indication that additional inputs parameters may be required (Ahmad and Simonovic, 2005).

In summary, the calibration results clearly showed enhancement in the model performance. Subsequently, to test the reliability of the calibrated model parameters a validation procedure was carried out to confirm the parameters chosen from calibration procedure using a runoff event in December 2006.

Table 6-12 Calibrated parameter values for each sub-basin and for model parameters for loss, transform, baseflow and routing models used in the HEC-HMS for the year of 2004.

Sub-basin	A	I_a	CN	I_{mp}	L_t	L_g
Nenggiri	3708.7	10	40	0.38	900	10
Pergau	1243.1	10	55.7	1.10	700	50
Galas	2261.1	2	80	0.97	1600	1550
Lebir	2392.0	11	55.7	0.91	1822	98
Kuala Krai	1244.1	2	77.5	0.97	1950	98
Guillemard Bridge	1079.6	10	74.2	1.57	1750	300

(a)
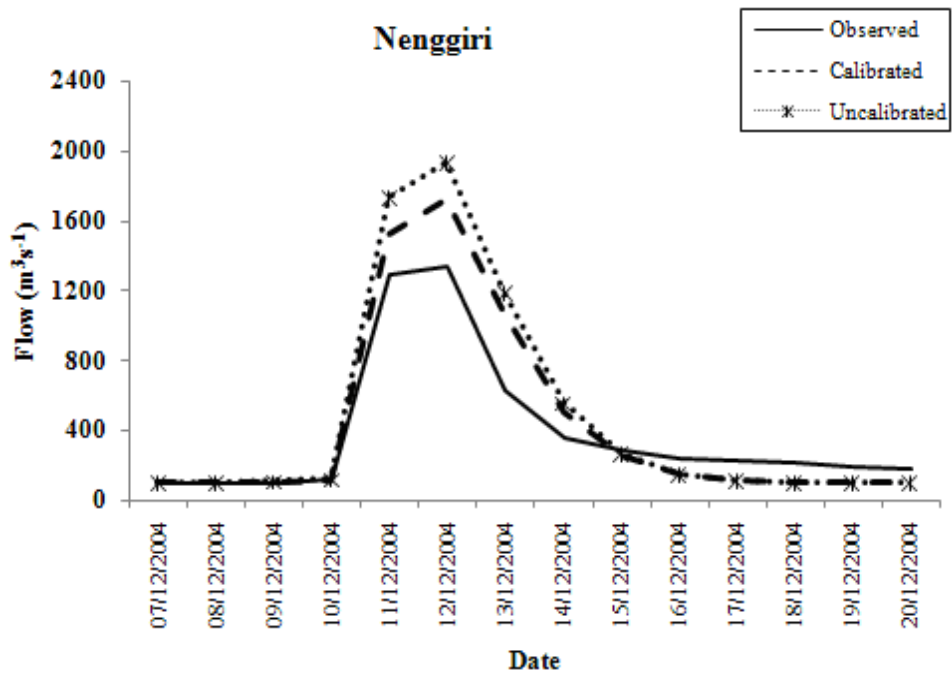
(b)
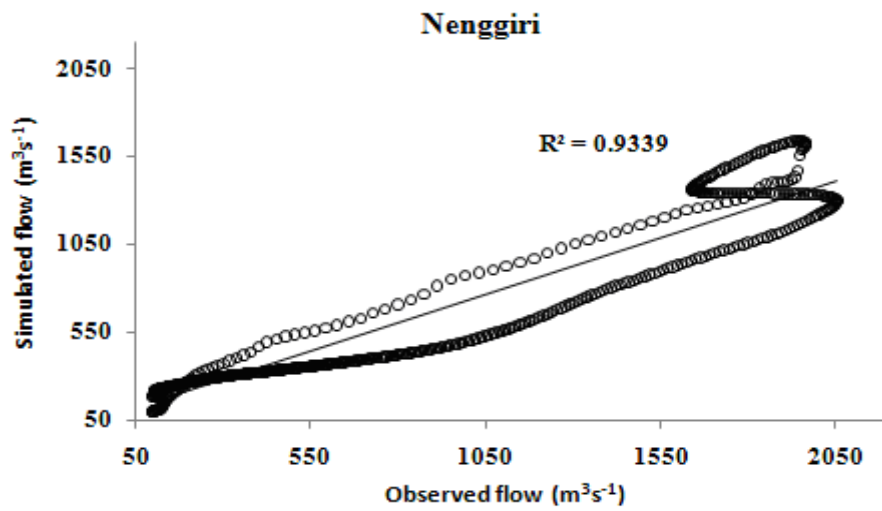
Figure 6-8 (a) Hydrographs (observed, uncalibrated, calibrated) and (b) scatterplot (calibrated) of Nenggiri station.

(a)

(b)
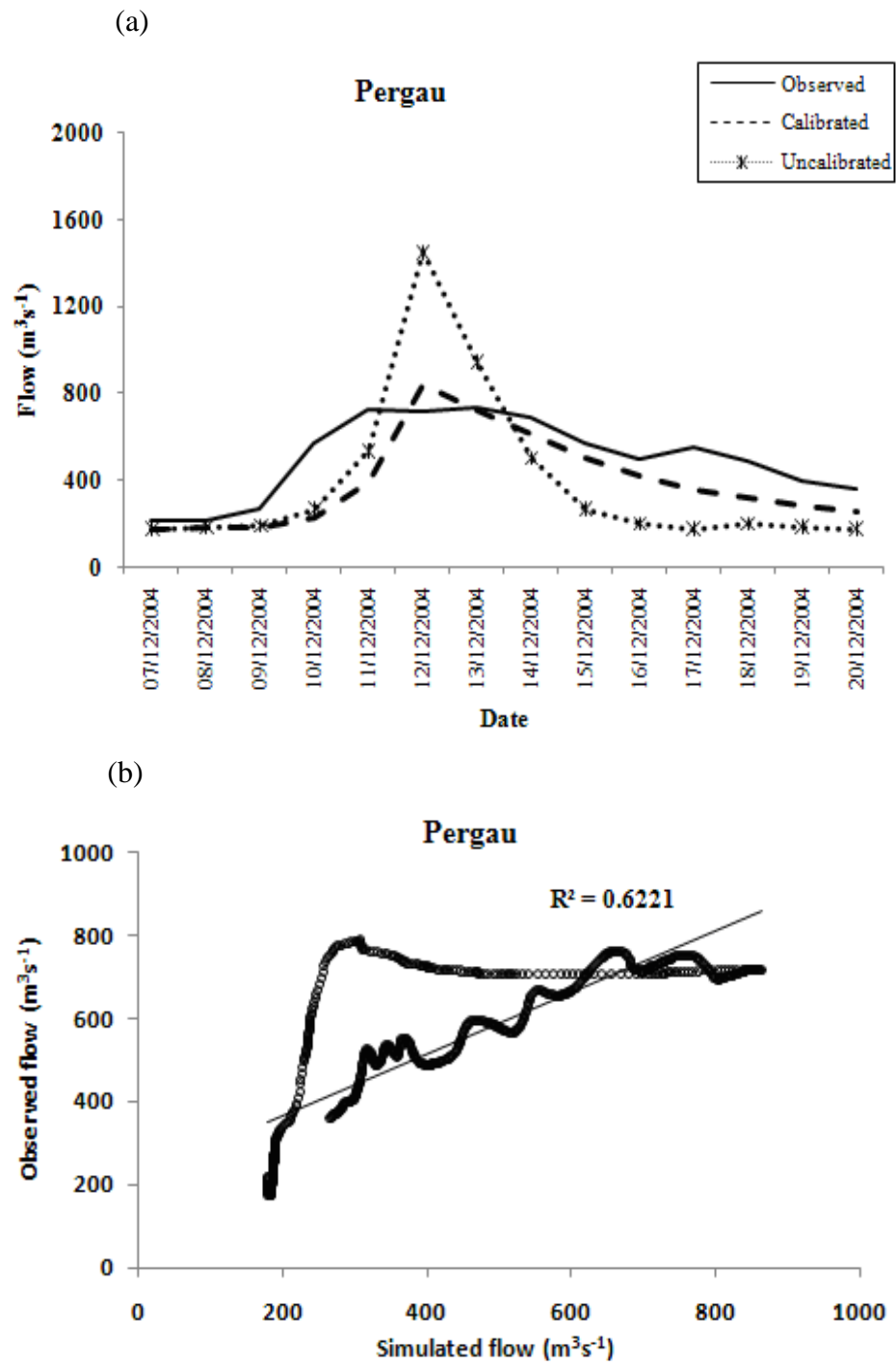
Figure 6-9 (a) Hydrographs (observed, uncalibrated, calibrated) and (b) scatterplot (calibrated) of Pergau station.
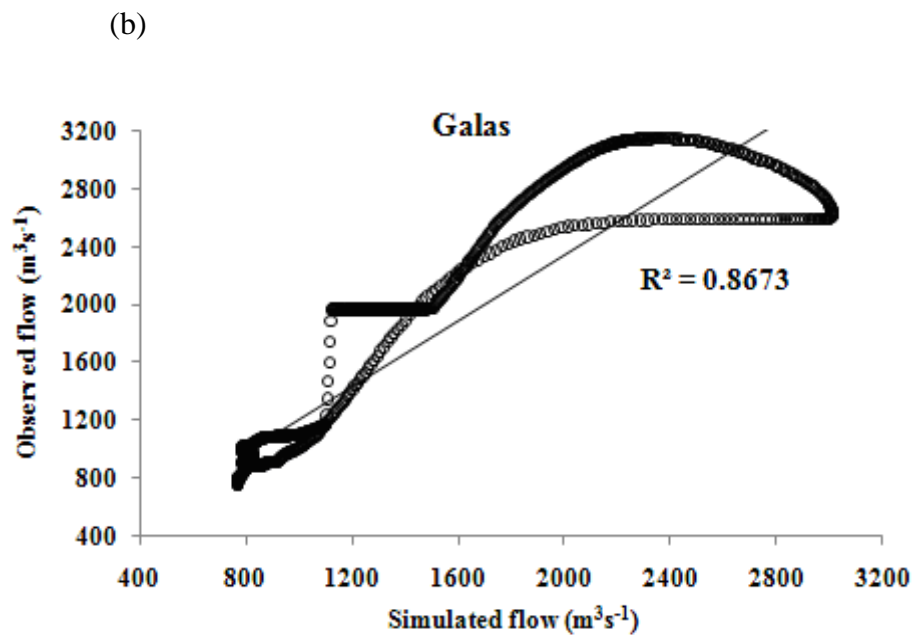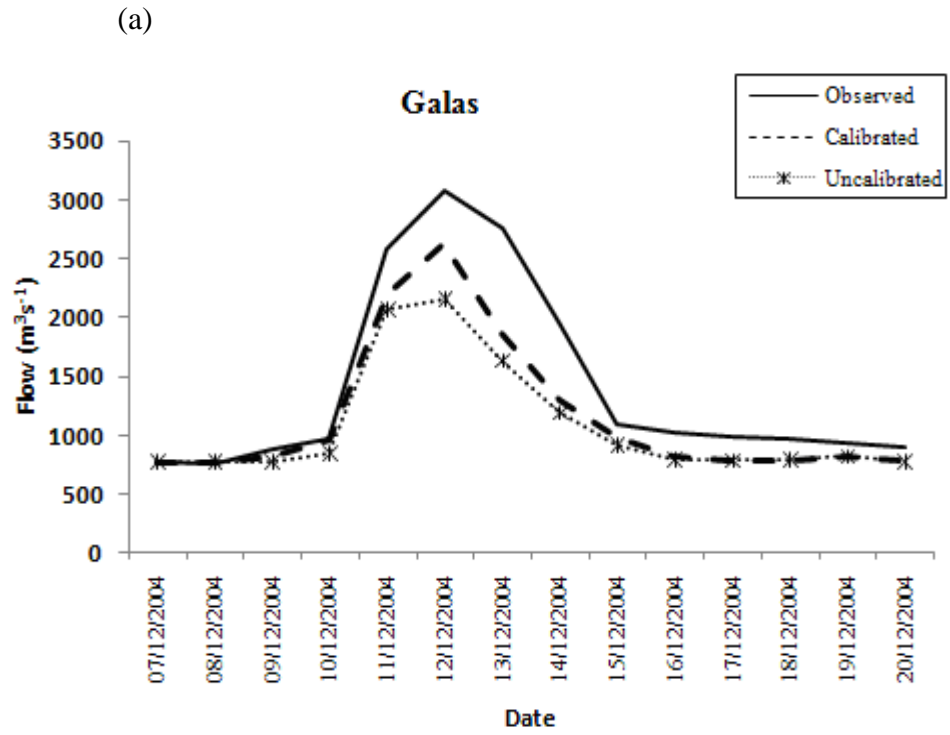
Figure 6-10 (a) Hydrographs (observed, uncalibrated, calibrated) and (b) scatterplot (calibrated) of Galas station.

(a)

(b)
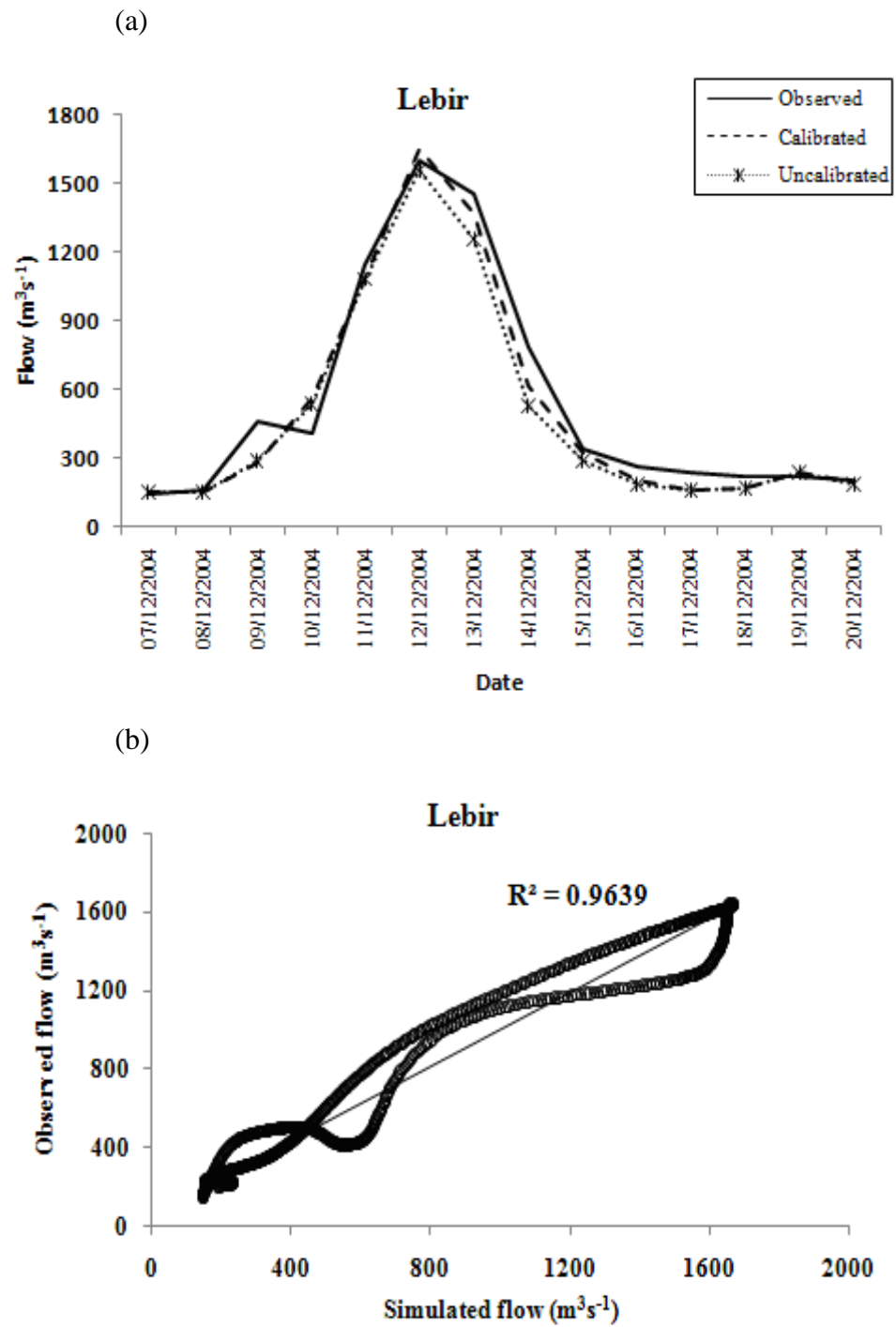
Figure 6-11 (a) Hydrographs (observed, uncalibrated, calibrated) and (b) scatterplot (calibrated) of Lebir station.

(a)

(b)
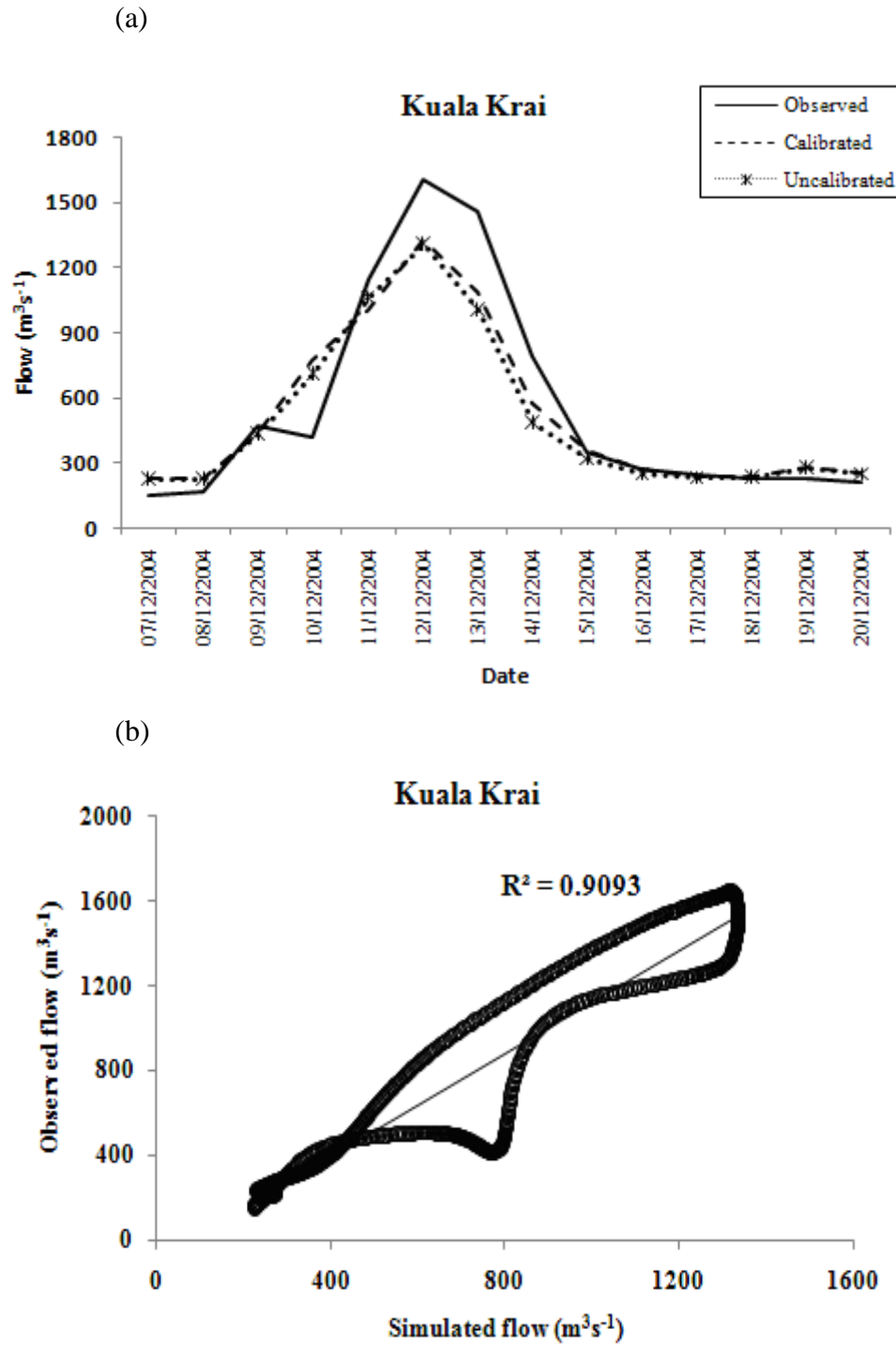
Figure 6-12 (a) Hydrographs (observed, uncalibrated, calibrated) and (b) scatterplot (calibrated) of Kuala Krai station.

(a)

(b)
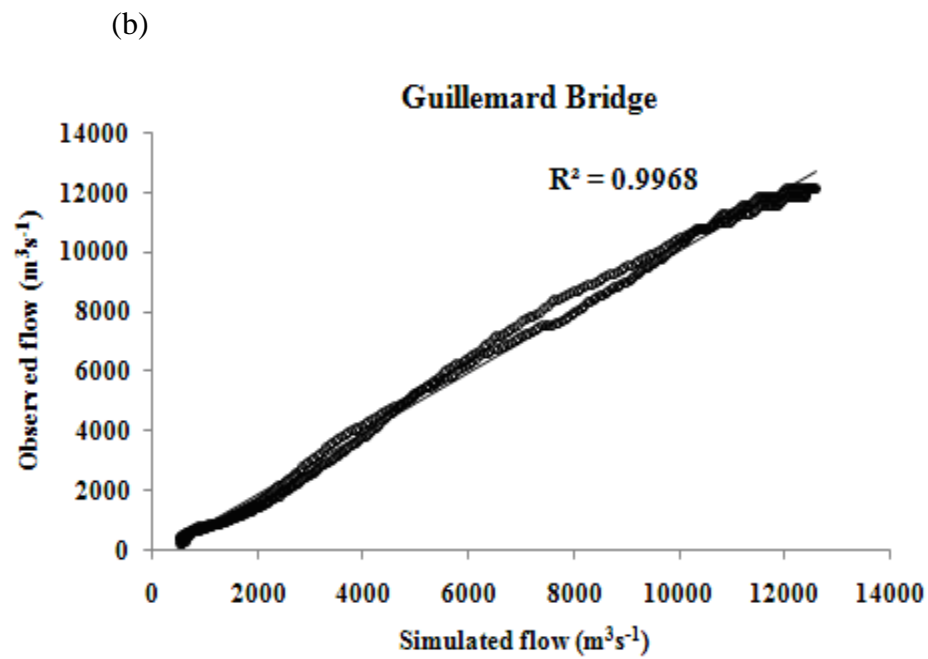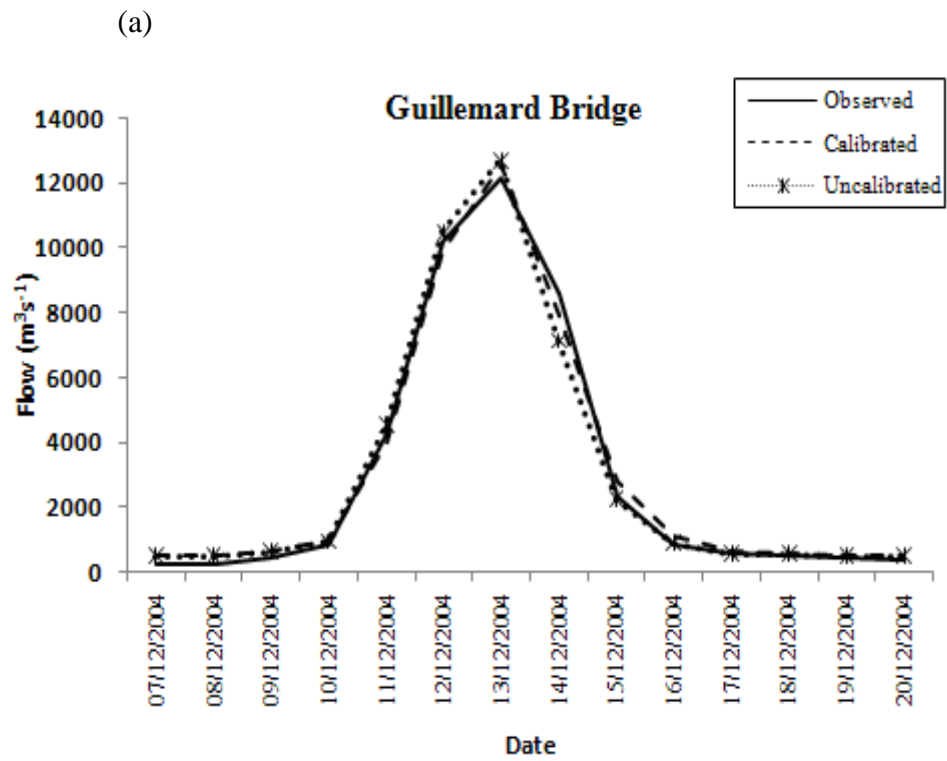
Figure 6-13 (a) Hydrographs (observed, uncalibrated, calibrated) and (b) scatterplot (calibrated) of Guillemard Bridge station.

6.6.4 Validation using the 2004 storm event

For validation, an event in December 2006 was used because it is closely resembled the runoff event in December 2004 which was captured during flooding. In the validation procedure all of the parameters were held constant. The parameter values in Table 6-12 were used for model validation purposes. The validation results for the 2006 validation period are presented in Table 6-5.

Validation results showed that there was acceptable agreement between simulated and observed hydrographs with E_f between 0.54 to 0.85. The highest accuracy was exhibited by the Kuala Krai station with acceptable E_f and lowest MAE, RMSE, and %BIAS. The Nenggiri, Galas, Lebir and Guillemard Bridge indicated acceptable validation accuracy. However, the Pergau has no observed record of streamflow for 2006. Thus, no validation was performed for this station.

The percentage errors in peak discharge (PEPQ) and runoff volume (PERV) for 2006 are also presented in Table 6-5. The results indicated that overall, the errors between observed and simulated hydrographs were small with less than ± 17% in PEPQ except for the Nenggiri station of ± 49%. The PERV was less than ± 14% for all stations.

6.6.5 Runoff simulation results for the year 1988

The runoff simulation for 1988 was applied only to the Galas sub-basin because there was no observed discharge for the other five sub-basins. The Galas sub-basin is the most upstream stream flow gauge. There is no recorded data for the other two upstream discharge station (i.e Nenggiri and Pergau) for every 15 minute time interval. The only available complete recorded data for these two stations were only available from 2002 onward (for short time interval) and also due to severely missing data before this period. Hence, to make an association with the land use change analysis as presented earlier in Chapter 5, the year 1988 runoff model was simulated and discussed.This time interval was chosen because to give a good representation of rainfall and flow characteristics within the sub-basin of the study area. Due to that, only the result from the Galas sub-basin is presented here.

6.6.6 Pre-calibration results for the year 1988

Pre-calibration results showed acceptable agreement in shape between the simulated and observed hydrographs. The rising and receeding limbs of the simulated and observed hydrographs were also in acceptable agreement (Figure 6-14). Subsequently, model calibration was performed for three parameters (i.e. initial abstraction, CN and lag time) as indicated from the sensitivity analysis applied in the 2004 runoff model. The same objective function was used which is the sum of squared residuals.

The uncalibrated results showed that Ef and R_2 were in good agreement with values of 0.85 and 0.86. The %BIAS, PEPQ and PERV showed small error values of 7.91%, -5.8% and -7.9% respectively (Table 6-13).

Table 6-13 The Galas uncalibrated, calibrated and validated statistics and goodness-of-fit for the runoff events in 1988 (calibration) and 1990 (validation).

	Observed 1988	Calibrated 1988	Observed 1990	Validation 1990
		Galas		
Mean	1345.87	1287.79	1184.85	1145.47
SD	1099.04	959.98	546.4559	611.74
MAE	-	176.32	-	245.11
RMSE	-	253.56	-	324.15
R^2	-	0.96	-	0.73
E_f	-	0.95	-	0.79
%BIAS	-	4.32	-	3.32
Peak Q	3823.1	3518.3	2764	2595.2
Volume	668.87	639.97	634.06	613.02
PEPQ(%)		-8.0		-6.11
PERV(%)		-4.3		-3.32

6.6.7 Calibrated results for the year 1988

The calibrated model for 1988 showed greater accuracy than the uncalibrated model. The MAE and RMSE showed reduced errors compared to the uncalibrated model. The R_2 also showed a large improvement of 0.96 compared to the un-calibrated value of 0.86. The E_f increased to 0.95 and %BIAS reduced to 4.3% from 7.9% previously (Table 6-13). The PEPQ showed a slight decrease to -8.0% as compared to the un-

calibrated value of -5.8%. However, the calibrated PERV showed a reduced error of -4.3% as compared to the uncalibrated error of -7.9%. Overall, the calibration result using SSR represented greater goodness-of-fit between the simulated and observed hydrographs.

(a)

(b)
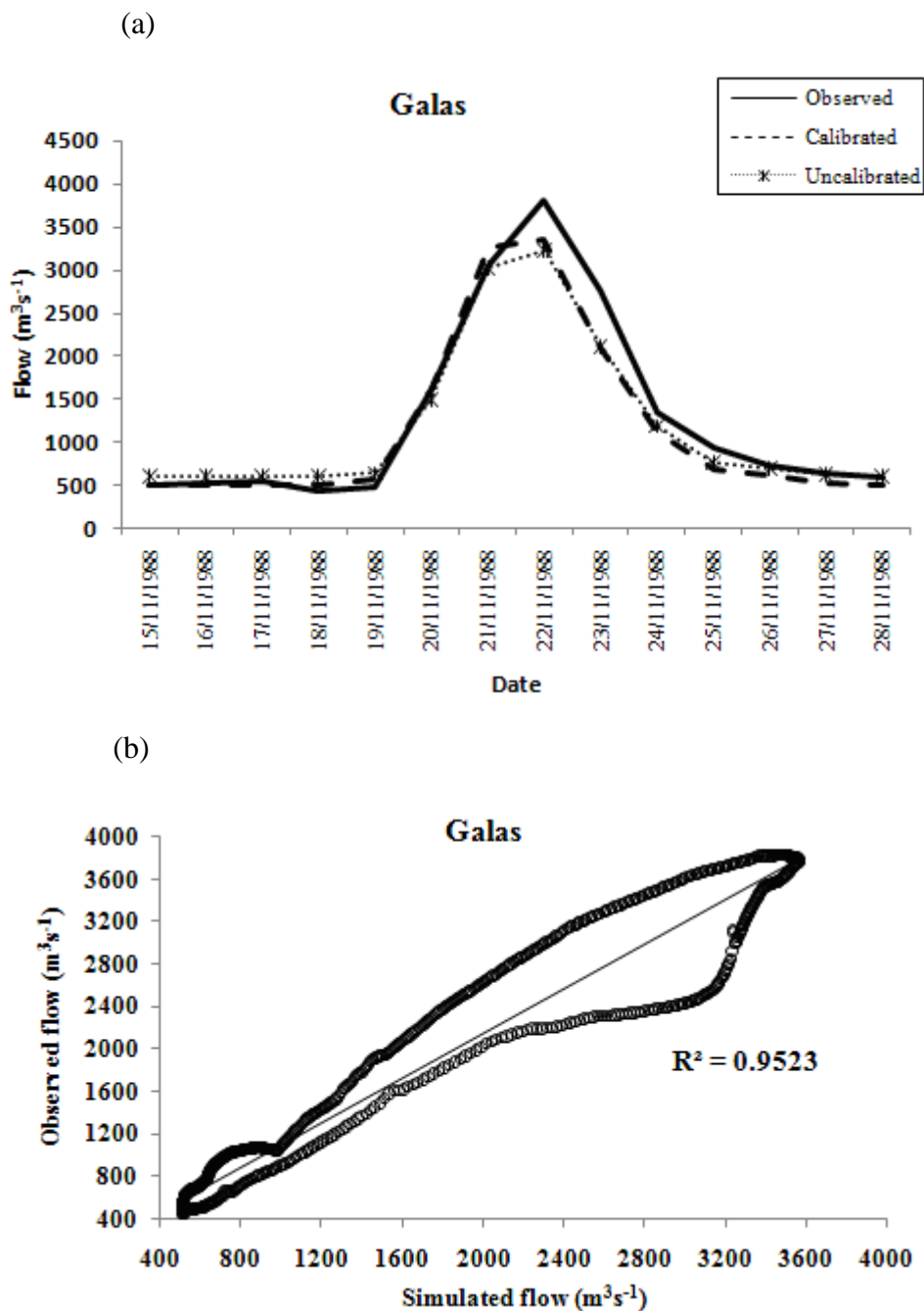
Figure 6-14 (a) Hydrographs (observed, uncalibrated, calibrated) and (b) scatterplot (calibrated) of Galas station.

6.6.8 Validation of runoff model in 1988

Validation for the 1988 runoff model was performed using a 1990 storm event with similar conditions as in 1988, which is during the monsoon season with high rainfall volume. As described earlier in section 6.6.4 (i.e. 2004 runoff model validation), all the parameters for validation were held constant. The results showed that acceptable agreement between simulated and observed hydrographs for the 1990 storm event was achieved using parameters derived in 1988. Overall, the coefficient of determination between simulated and observed was 0.73, the E_f was 0.79 and the % BIAS was 3.32% (Table 6-13).

6.7 RUNOFF SIMULATION USING HISTORICAL DATA

To understand and quantify changes in the hydrological system and runoff generation over the last three decades, land use and precipitation inputs were varied, both separately and in combination. The model calibrated to the 2004 runoff event was used to provide a baseline scenario. To simulate runoff change due to land use and precipitation changes attention was given to differences in peak discharge and runoff volume resulting from the replacement of land use and precipitation data for 2004 with the equivalent data for 1988. Any observed changes in outputs are attributable to these two inputs only; the other parameters were held constant. Three scenarios were simulated: land use change, climate (precipitation) change and a combination of both.

6.7.1 Land use change scenario

Two land use maps were derived by classifying Landsat TM images as described in section 3.2. The percentages of each land use type for each sub-basin are shown in Table 6-14. Overall, forest was dominant in these six sub-basins, followed by agricultural land (i.e. rubber, oil palm and mixed-agriculture) built-up land and bare soil. Other land uses such as paddy, mangrove and water contributed moderate and small percentages, respectively (Table 6-14). For three upstream sub-basins (i.e. Nenggiri, Pergau and Galas) deforestation and an increase in agricultural land were observed. Meanwhile, in the downstream area, represented by the Lebir, Kuala Krai and Guillemard Bridge sub-basins, a small increase in forest was observed (e.g., an

increase from 1988 to 2000 of 53.9% to 63.4% in Kuala Krai and 45.9% to 52.2% in
Guillemard Bridge).

Table 6-14 Land use (%) in 1988 and 2000 using maximum likelihood classified
Landsat TM images.

	Upstream					
	1988 (%)			2000 (%)		
Land use class	Nenggiri	Pergau	Galas	Nenggiri	Pergau	Galas
Forest	90.17	61.61	71.76	82.49	51.91	65.98
Built-up land	*0.19*	*0.59*	*0.71*	*0.38*	*1.1*	*0.97*
Bare soil	3.01	7.64	12.24	3.26	2.69	5.66
Paddy	0	0.57	0.06	0.82	1.9	2.62
Mangrove	0	0.2	0.15	0.07	1.11	0.26
Oil Palm	0.55	2.02	1.2	0.04	0.11	0.12
Rubber	5.45	18.18	12.16	9.17	27.27	19.13
Mixed-agriculture	0.32	9.14	1.32	3.38	13.9	5.02
Water	0.31	0.05	0.42	0.39	0	0.24
	Downstream					
	1988 (%)			2000 (%)		
Land use class	Lebir	Kuala Krai	Guillemard Bg.	Lebir	Kuala Krai	Guillemard Bg.
Forest	83.37	53.92	45.93	83.54	63.37	52.17
Built-up land	*0.43*	*0.37*	*0.67*	*0.91*	*0.97*	*1.57*
Bare soil	9.16	8.29	12.25	5.18	2.08	4.71
Paddy	0.07	0.19	2.3	0.13	0.21	2.11
Mangrove	0.09	0.05	0.17	0.07	0.05	0.09
Oil Palm	1.32	3.9	3.81	2.16	5.97	5.76
Rubber	3.01	30.63	32.46	7.03	26.16	31.45
Mixed-agriculture	2.13	2.5	2.3	0.54	1.16	2.11
Water	0.41	0.15	0.11	0.45	0.02	0.04

It should be noted that the increase in forest area for the downstream area was
dominated by increases in bamboo and rattan plantations as reported by the Kelantan
Forestry Department (KFD) (2006). In addition, according to the National Forest
Inventories III (NFI3) report about 37,000 hectares for the whole of Kelantan was
subjected to slash and burn agriculture activities by native people which may have
caused thick bamboo forest to replace forest areas (KFD, 2006). An increase in shrub
vegetation was also observed (Jusoff and Senthavy, 2003).

Using the SCS loss model in HEC-HMS, land use changes were represented by the CN and percentage of impervious surface. Determination of CN depends on the watershed's soil, antecedent moisture content (AMC) and land use/cover conditions. In the study area, nine land use types were derived consisting of forest, built-up land, bare soil, paddy, mangrove, rubber, oil palm, mixed-agriculture and water. The AMC type two (AMC II) was used, which represents average soil wetness, and most of the Kelantan's soil falls in hydrologic soil group B (i.e. moderately low runoff potential). The CN values published in Technical Report 55 (TR 55) by USDA (1986) were used as a reference to infer the CN values. Percentage of impervious surface was estimated from the percentage of built-up land derived from the land use classification (USDA, 1986). The CN values and percentage of impervious surface for all sub-basins are shown in Table 6-15.

Table 6-15 Changes in CN and impervious surface (%) (i.e. from built-up land area) representing land use changes from 1988 to 2004 observed from the classified Landsat TM images.

Sub-basin	CN 1988	Impervious surface in 1988 (%)	CN 2004	Impervious surface in 2004 (%)
Nenggiri	36	0.19	40	0.38
Pergau	51.4	0.59	55.7	1.1
Galas	76.4	0.71	80	0.97
Lebir	58.3	0.43	57.7	0.91
Kuala Krai	78.1	0.37	77.5	0.97
Guillemard Bridge	75.3	0.67	74.2	1.57

The baseline calibrated runoff result for 2004, in terms of peak discharge and runoff volume, is shown by scenario A in Table 6-16. Different peak discharge and runoff volume values were observed by holding the precipitation constant (i.e., for 2004), but using the land use scenario observed for 1988 (scenario B). Under scenario A, all upstream gauges (i.e. Nenggiri, Pergau and Galas) exhibited an increase in peak discharge and runoff volume compared to scenario B. The result predicts that peak discharge and runoff volume increased between 1988 and 2004 as a function of land use changes. The largest differences between scenario A and scenario B were observed for the Nenggiri gauge with predicted differences of 9.6% in peak discharge and 8.4% in runoff volume. The smallest predicted difference in runoff due to land use change

was observed for the Pergau gauge with differences of 3.3% and 1.5% for peak discharge and runoff volume, respectively (Table 6-16).

Interestingly, for the downstream gauges (i.e. Lebir, Kuala Krai and Guillemard Bridge) a small decrease in peak discharge and runoff volume was predicted (in 2004) compared to scenario B (land use from 1988). The differences between these two scenarios were very small (between -0.6% to -0.04% in peak discharge and between -0.4% to -0.1% in runoff volume). The result suggests that peak discharge and runoff volume may have decreased between 1988 and 2004 as a function of land use changes, but by only a small percentage compared to the increases for the upstream gauges. The predicted decrease is due to the small increase in afforestation observed in the sub-basins where these three gauges are located (Table 6-16).

Scenario B shows that, holding the rainfall input constant (i.e., using the 2004 event), runoff is expected to have increased as a function of deforestation, agricultural conversion and urbanization for the upstream gauges in the study area. The land use change analysis from 1988 to 2000 for the upstream area (i.e. in the River Galas sub-basin) revealed a large percentage of total agricultural conversion (i.e. mixed-agriculture of 158.7%, oil palm of 151.6% and rubber of 13.7%) and increase in built-up land by 14.8% (Adnan and Atkinson, 2010). The change analysis presented here implies that these land use changes may be significant contributors to increases in peak discharge and runoff volume in the upstream area.

Table 6-16 Runoff simulation in 2004 using historical land use and precipitation data in 1988 for six sub-basins in the River Kelantan catchment. A; Calibrated runoff model in 2004, B; runoff in 2004 using land use in 1988, C; runoff in 2004 using precipitation in 1988, D; runoff in 2004 using land use and precipitation in 1988.

	SA	SB	SA-SB		SC	SA-SC		SD	SA-SD	
			AB_{diff}	% Diff		AC_{diff}	% Diff		AD_{diff}	% Diff
Nenggiri										
Peak discharge	2055	1875.8	**179.2**	**9.6**	1613	**442**	**27.4**	1461.9	**593.1**	**40.6**
Runoff volume	145.36	134.1	**11.26**	**8.4**	118.66	**26.7**	**22.5**	109.35	**36.01**	**32.9**
Pergau										
Peak discharge	863.7	819.1	**44.6**	**5.4**	727.9	**135.8**	**18.7**	688.3	**175.4**	**25.5**
Runoff volume	359.4	345.84	**13.56**	**3.9**	319.7	**39.75**	**12.4**	307.73	**51.67**	**16.8**
Galas										
Peak discharge	3010.5	2913.3	**97.2**	**3.3**	2643.2	**367.3**	**13.9**	2547.2	**463.3**	**18.2**
Runoff volume	595.9	586.9	**9.0**	**1.5**	561	**34.94**	**6.2**	552.34	**43.56**	**7.9**
Lebir										
Peak discharge	1724.2	1734.1	**-9.9**	**-0.6**	1358	**366.2**	**27**	1366.5	**357.7**	**26.2**
Runoff volume	261.64	262.8	**-1.15**	**-0.4**	215.1	**46.56**	**21.6**	216.01	**45.63**	**21.1**
Kuala Krai										
Peak discharge	1243.7	1248.1	**-4.4**	**-0.4**	1039.7	**204**	**19.6**	1043.9	**199.8**	**19.1**
Runoff volume	461.21	462.5	**-1.29**	**-0.3**	408.15	**53.06**	**13**	409.32	**51.89**	**12.7**
Guillemard Bg.										
Peak discharge	12615.2	12620.4	**-5.2**	**-0.04**	10474.8	**2140.4**	**20.43**	10481.2	**2134**	**20.4**
Runoff volume	3440.23	3443.64	**-3.41**	**-0.1**	2915.09	**525.14**	**18.01**	2918.87	**521.36**	**17.9**

AB_{diff} is the absolute difference; % Diff is the percentage difference.

6.7.2 Precipitation change scenario

To represent changes in precipitation between 1988 and 2004 one might consider substituting the 2004 event by the 1988 event. However, this is not a suitable strategy because the precipitation in 1988 was different to that in 2004 in terms of both intensity and duration. Rather, the general trend in terms of precipitation change is of interest. Precipitation stations corresponding to the upstream and downstream discharge stations were used. More specifically, the monthly mean daily precipitation averaged over eight stations (i.e. BP Bertam, Blau, Gemala, Brook, Gob, Gua Musang, Dabong, Ladang Kuala Balah) in the upstream area and seven stations (Gunung Gagau, Kg Aring, Kg Laloh, Ladang Lepan Kabu, Kuala Krai, Ulu Sekor, Ladang Kenneth and JPS Machang) in the downstream area were used (Figure 6-15) (Adnan and Atkinson, 2010).

Regression models were fitted to the December mean daily precipitation against time (in years) for the upstream and downstream areas separately, and temporal trends were obtained. December was chosen amongst all months because it corresponded to the month of the modeled event and it represents the monsoonal season of most interest. The upstream and downstream trend equations were $y = 0.0746x + 7.8809$ and $y = 0.1619x + 12.717$, respectively, where y is predicted December mean daily precipitation and x is time (in years, where 1975 is 1, 1976 is 2, etc). From the regression models, December mean daily precipitation was predicted for the years of interest, 1988 and 2004, and the percentage difference between 2004 and 1988 was calculated. Subsequently, the observed precipitation event in 2004 was scaled by the percentage difference to represent the precipitation event *as if in 1988* and this was input to the runoff model calibrated to the 2004 event. The precipitation plot is shown in Figure 6-16 and the percentage difference calculation for precipitation is shown in Table 6-17.
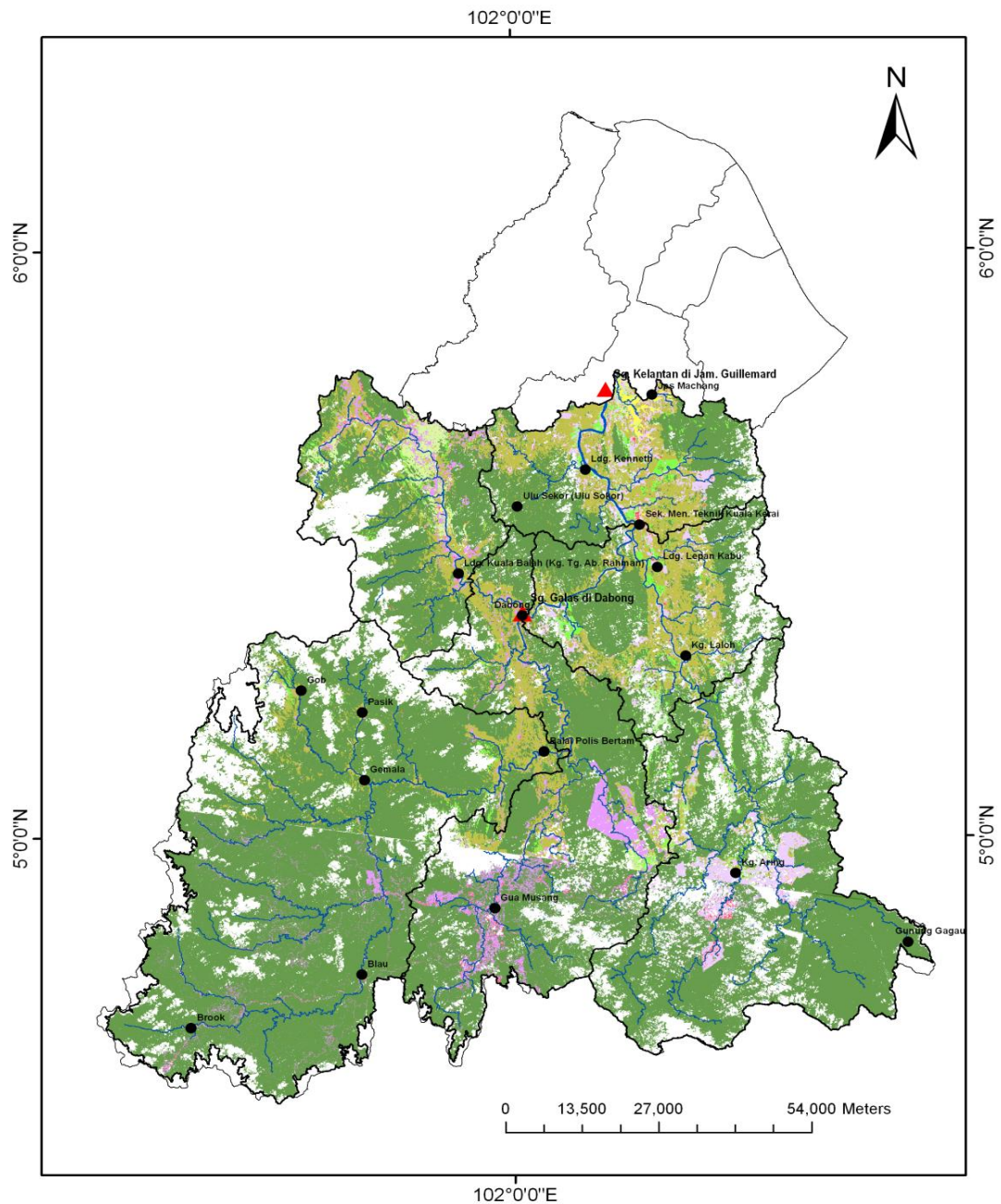
Figure 6-15 Map of the Kelantan catchment showing streamflow stations (▲) and precipitation stations (●) with Landsat TM satellite sensor images overlaid corresponding to the upstream and downstream catchments.

(a) Upstream catchment
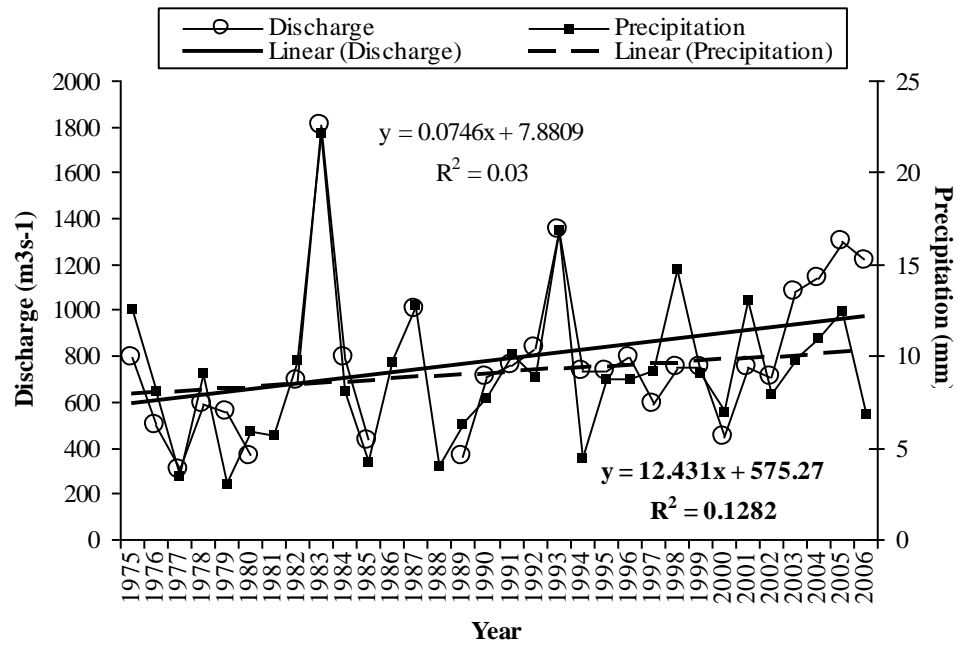
(b) Downstream catchment
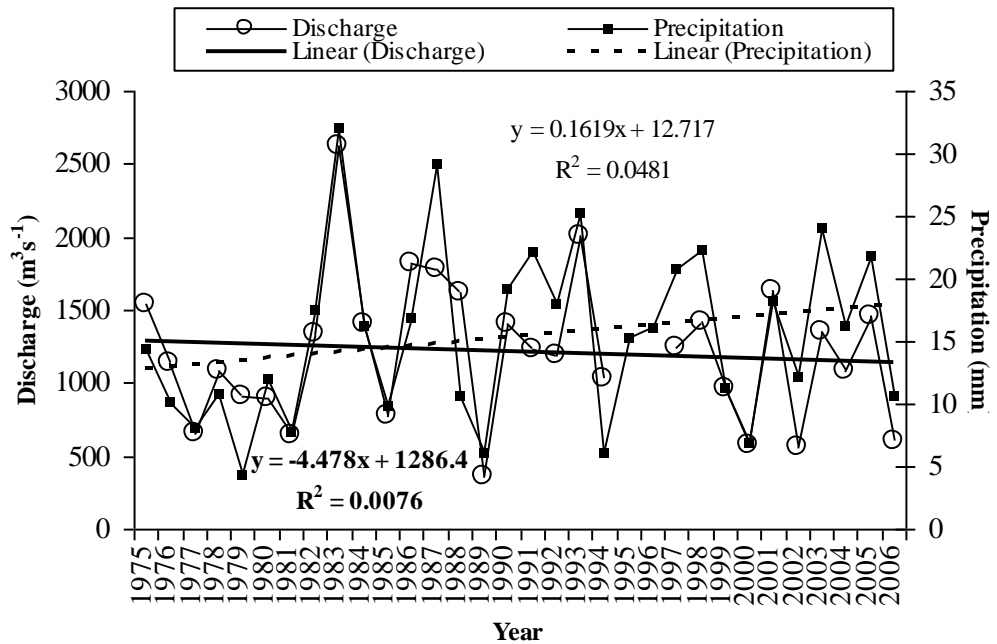
Figure 6-16 Regression plots for the (a) upstream and (b) downstream area in the River Kelantan.

Table 6-17 Precipitation percentage change calculated from the regression models in Figure 10.

Upstream			
	Rainfall		**% Difference (2004-1988)**
	1988	**2004**	
	8.85	10.04	13.5
Downstream			
	Rainfall		**% Difference (2004-1988)**
	1988	**2004**	
	14.82	17.41	17.5

Scenario C used as inputs the land use for 2004 and precipitation adjusted to represent 1988, as calculated from Table 6-17. Scenario A, representing the 2004 rainfall scenario, produced increases of 13.5% in runoff volume compared to scenario C (1988) for the upstream area and 17.5% for the downstream area. Large predicted differences were observed for all gauge stations within both the upstream and downstream areas. For example, in the upstream area the Nenggiri, Pergau and Galas gauges exhibited increases of 27.4%, 18.7%, 13.9% in peak discharge and 22.5%, 12.4% and 6.2% and runoff volume, respectively. The downstream sub-basins of Lebir, Kuala Krai and Guillemard Bridge, exhibited larger increases of 27%, 19.6% and 20.43% in peak discharge and 21.6%,13.0% and 18.01% in runoff volume, respectively (Table 6-16).

Scenario C demonstrated that trends in precipitation over the period 1988 to 2004 led to relatively moderate increases in hydrological response (peak discharge and runoff volume) in the upstream area, as represented by the Galas gauge. Meanwhile, trends in precipitation over the same period for the downstream area led to large increases in hydrological response as shown by the Lebir and Guillemard Bridge gauges. The results suggest that observed increases in precipitation are predicted to affect the whole of the River Kelantan catchment, but particularly the downstream area.

6.7.3 Combination of land use and precipitation change scenarios

In scenario D, both precipitation and land use scenarios from 1988 were used as inputs to the runoff model calibrated to the 2004 event. The combination resulted in the largest differences with the baseline scenario for all gauges. Again, the Nenggiri gauge

exhibited the largest differences amongst the set of gauges with a 40.6% increase in peak discharge and 32.9% increase in runoff volume. The Lebir gauge provided the second largest differences with increases of 26.2% in peak discharge and 21.1% in runoff volume (Table 6-16) followed by Pergau with increases of 25.5% in peak discharge and 16.8% in runoff volume. This is in agreement with the results from scenarios B and C in which Nenggiri produced the largest differences due to changes in land use and precipitation, and scenario C in which Lebir produced the largest differences due to changes in precipitation. The other gauges for each sub-basin exhibited differences in peak discharge and runoff volume in the range 7.9% to 20.4%.

The above results demonstrate that for the upstream area (i.e. Nenggiri) increases in precipitation and land use changes led to the greatest increases in peak discharge and runoff volume. The results imply that in the 16 year period from 1988 to 2004 precipitation changes of 13.5% in December and land use conversion from forest to agricultural land, as well as urbanization, are likely causes of significant increases in runoff generation in the upstream area. The results also suggest that precipitation trends from 1988 to 2004 may have led to significant increases in runoff generation in the downstream area, as demonstrated by the Lebir and Guillemard Bridge gauges.

6.8   DISCUSSION

6.8.1 Changes in hydrological response due to changes in precipitation and land use

The effect of land use (i.e. scenario B) on peak discharge and runoff volume varied between the upstream and downstream areas. In the upstream area, both precipitation and land use change from 1988 to 2004 resulted in an increase in peak discharge and runoff volume. Such increases in peak discharge and runoff volume are probably due to more intense rainfall as well as deforestation and conversion to agricultural land (i.e. rubber, oil palm and mixed-agriculture). The early stages of plantation may lead to soil compaction, crusting and sealing which might lead to infiltration excesses, especially during high rainfall intensity events (Bronstert et al., 2002; Connell et al., 2007). Hence, plantation development may cause excess runoff as a result of the formation of a surface crust with low moisture storage capacity and hydraulic conductivity. For the

downstream area, afforestation was observed between the two land use classifications. This afforestation was relatively limited in extent from 1988 to 2004 which led to small changes in the CN value, for example, from 75.3 in 1988 to 74.2 in 2004 for the Guillemard Bridge sub-basin.

Sensitivity analysis demonstrated that land use change, modelled through changes in the SCS CN, can have an important impact on peak discharge and runoff volume (Hernandez et al., 2000). However, peak discharge is more sensitive to land use (and precipitation) changes compared to runoff volume (Saghafian et al., 2008). The larger the CN and percentage of impervious surfaces the higher the peak discharge and runoff volume. Thus, land use conversion from forest to agricultural land and urbanization may have important effects on peak discharge. For example, convective storm events producing intense rainfall within a short period of time can cause higher peak discharge especially when combined with large areas of impervious surfaces associated with built-up areas. Similarly, Nearing et al. (2005) suggested that changes in land use and surface cover such as deforestation due to slash and burn activities or alterations in surface slope due to farming may have large impacts on peak discharge and runoff susceptibility.

Precipitation changes (i.e. scenario C) led to large increases in peak discharge and runoff volume in both the upstream and downstream areas. For all sub-basins, peak discharge and runoff volume were greater in 2004 compared to 1988, although the percentage change in precipitation for the upstream area was smaller (i.e., 13.5%) than for downstream (i.e., 17.5%), as shown in Table 6-17. Importantly, in the upstream area the magnitude of the increases in hydrological response (i.e., peak discharge and runoff volume) due to observed increases in precipitation were about three to four times greater than those due to observed land use changes. This supports the view that climate-related changes are the principle cause of increases in hydrological response and, thus, also increases in flooding. In the downstream area precipitation changes led to large increases in hydrological response, where land use changes had little effect, again supporting the view of precipitation change as the major driver of hydrological response.

Scenario D, which combines land use and precipitation changes from 1988 to 2004, led to the largest hydrological response in 2004. The total increases in peak discharge and

runoff volume were larger compared to the changes arising from scenarios B or C alone. It is plausible that the combination of land use and precipitation changes should lead to the largest increases in peak discharge and runoff volume, particularly in the upstream area. The result of combining both factors is also in fair agreement with the summation of the results of the land use and precipitation scenarios, suggesting a degree of independence.

In summary, in the upstream area the observed precipitation and land use changes contributed large increases in peak discharge and runoff volume, with observed precipitation causing increases about three-to-four times larger than observed land use changes. In contrast, in the downstream area, the large observed precipitation changes shown by the trend analysis were the only cause of increases in the hydrological response, with land use changes leading to a slight decrease in response.

6.8.2 Comparison of predictions from the runoff model and observed changes in discharge volume

In previous research, a time-series trend analysis was undertaken for the River Kelantan catchment (Adnan and Atkinson, 2010). The percentage changes in mean annual streamflow between 1988 and 2004 observed by the fitted trends in that study were 26.9% (upstream, Galas station) and -5.8% (downstream, Guillemard Bridge station). However, in the present study, under scenario D the increases in runoff volume predicted by the hydrological model as a function of observed changes in land use and precipitation between 1988 and 2004 were 7.9% for the Galas station and 17.9% for the Guillemard Bridge station, respectively. Thus, the match between the changes in discharge observed (i.e., predicted by the trends fitted to time-series discharge data) and the changes in discharge predicted using the hydrological model, with land use change and precipitation change as inputs, is relatively poor. While a perfect match is not expected since the goal of the analysis is not to forecast changes in hydrological response, but rather to evaluate the effects of two variables on hydrological response, this mis-match deserves comment.

6.8.2.1 Missing variables

Some variables that may have changed between 1988 and 2004 were not included in the hydrological model when used to calculate the peak discharge and runoff volume for 1988 conditions. In particular, the contributions of changes in temperature, evapotranspiration (i.e., for continuous runoff modeling), irrigation and water extraction, for agricultural purposes as well as for domestic and non-domestic usage, were not included. Temperature and evapotranspiration were held constant within the fitting of the models (e.g., to the 2004 event) because over the limited period of a monsoonal *storm* their effects relative to the huge amounts of precipitation delivered is expected to be minimal. Of course, when comparing two different time periods separated by 16 years, that may not be the case and, thus, temperature and evapotranspiration represent missing variables from the analysis. For this reason, close agreement between the predicted and observed percentage changes in discharge is not expected.

In the River Kelantan catchment, irrigation is required mainly for paddy cultivation which covers a very large area, particularly in the downstream area. Following the introduction of fully-fledged irrigation facilities in the l970s, the Kemubu Irrigation Project (KADA) was implemented in Kelantan to boost rice plantation (Abdullah, 2002). Previously, rice was planted once a year in the main season (i.e. between May and September), but with the KADA two rice cropping seasons were possible (i.e. December and May). In addition, Malaysia's Water Management Association (MWA) estimated that in 2002, about 37.7 million cubic metres of water was extracted from the River Kelantan for agricultural, domestic and non-domestic purposes (MWA, 2004; Mahasim et al., 2005). In Kuala Krai district (i.e. situated adjacent to the Guillemard Bridge streamflow gauge station) about 273 million litres of water per day is extracted from the River Kelantan for drinking water purposes (MWA, 2004). Water consumption per capita is about 144 litres per capita per day and this represents a lower level of consumption compared to other states in Malaysia due to insufficient supply of water.

In comparison to temperature and evapotranspiration, water abstraction for irrigation and drinking purposes are potentially large unmeasured change variables. For the upstream discharge station the discharge is actually much less in 1988 than predicted

(i.e., discharge is increasing through time). Since water abstraction is known to occur mainly downstream, and the amount of abstraction is known to be increasing, abstraction does not represent a plausible explanation for the observed changes in the upstream gauge. However, for the downstream gauge, change in the amount of water abstraction for irrigation and drinking purposes represents a possible explanation for the discrepancy between the observed percentage in discharge (-5.8%, or 3.1%) and that predicted (17.9%). In particular, the rather sudden decrease in discharge from 2001 to 2006 might be explained by this factor.

By comparing the observed trends in discharge with the predicted runoff volume from the HEC-HMS model, it is possible to suggest that alongside the measured variables of precipitation change and land use change, sizeable changes in other influential variables such as the amount of water abstracted for irrigation, are likely to have occurred, particularly in the downstream catchment. Further investigation might concentrate on isolating these missing variables and integrating their effects into the present analysis.

The omission of change in variables such as temperature, evapotranspiration and water extraction should not undermine greatly the validity of the results in general terms in relation to the effects of land use and precipitation change, although some caution is warranted. It is widely acknowledged that the transformation of precipitation into runoff (and potentially flooding) in a catchment is a highly complex and nonlinear system (Bronstert, 2003; Segond et al., 2007). The interaction of many variables such as topography, climate conditions, soil characteristics and base-flow water conditions, as well as channel and drainage density, may cause large uncertainties in runoff generation from hydrologic modelling (Bronstert, 2003). Thus, further investigation incorporating more detailed data on hydrological conditions and hydraulic characteristics over the historical period is needed to provide more accurate modeling of the hydrological response to the measured precipitation and land use change inputs.

6.8.3 Interpretation of observed time-series

The time-series plot of observed precipitation and observed discharge over the period of interest (Figure 6-16) highlights the expected dependence of changes in discharge on changes in precipitation. The pattern of changes in discharge is strikingly similar to the

pattern of changes in precipitation. However, the plot, while informative, does not remove the need for the hydrological model analysis, as presented above. First, it is not surprising that the correlation between changes in discharge and precipitation is so large. The plot represents conditions during the month of December each year, during monsoonal rains. Thus, a very high proportion of the precipitation will turn to runoff and find its way to the river channel.

Second, and most importantly, it is not possible to use the plot to infer the effect of changes in land use. It was suggested above that there may be several missing variables from the change analysis, including water abstraction which may have a significant effect. Where this is the case, a hydrological model is required to quantify the expected effects of precipitation and land use changes. For example, if water abstraction is increasing through time and land use is changing leading to an increase in discharge, these effects may cancel out and not show at all in Figure 6-16. The view taken here is that Figure 6-16 provides supporting evidence for the analysis undertaken using the hydrological model.

6.8.4 Management

Observation and investigation of historical long-term changes in land use and precipitation characteristics can provide insights into the causes of changes in catchment runoff generation. The knowledge gathered from this kind of analysis can lead to improved management policies, especially to mitigate changes in hydrological response and their consequences (Fowler et al., 2003). Based on such information, suitable strategies can be implemented by decision makers, including land use planners, such as controlling rapid urban development, particularly along the river and in floodplain areas, and the implementation of sustainable land use planning involving environmentally-friendly artificial drainage schemes or the development of pervious urban structures. Hence, the risk associated with an increase in the surface runoff hazard can potentially be reduced. This research suggests that future land use planning and development activities should consider the influence of observed and future likely changes in climate (precipitation, temperature and evapotranspiration) on the hydrological response and, thereby, the risk of flooding and plan appropriate mitigation

strategies. In this context of climate change, planners should also consider the impact of land use changes on peak discharge and runoff generation.

6.9   SUMMARY

A simple framework was presented for quantifying the effects of precipitation change and land use change on peak discharge and runoff generation based on limited knowledge of historical and present conditions. Specifically, a hydrological model fitted to a "present day" (2004) storm event was used to recreate conditions as if for a previous time period (1988). The land use input was replaced with land use observed for the previous time period and the precipitation input was adjusted proportionally according to the precipitation amounts predicted for 2004 and 1988 based on a temporal trend fitted to time-series precipitation data.

A hydrological model was used to show that land use change, predominantly deforestation for agricultural purposes, has potentially caused some increases in hydrological response over time (i.e. 16 years) in the upstream area. However, observed precipitation changes of 13.5% over the 16 year period were predicted to have led to a much greater increase in hydrological response in the upstream sub-basins. The predicted effect of precipitation change was about three-to-four times greater than that of land use change in the upstream area. In the downstream area land use change was predicted by the model to have led to a very small (if any) decrease in hydrological response between 1988 and 2004. Conversely, precipitation change of 17.5% over the 16 year period was predicted to have led to a large increase in hydrological response. In summary, observed precipitation trends were predicted to be the major driver of change in hydrological response in the whole Kelantan catchment between 1988 and 2004.

The framework used in this analysis was used to analyse *future* land use and precipitation scenarios, as presented in the next chapter (i.e. Chapter 7).

Chapter 7

Simulating future scenarios

7.1   INTRODUCTION

A runoff model (using 15 minute time period) for the Kelantan catchment was established in the previous chapter using the 1988, 1990, 2004 and 2006 calibration and validation models. This chapter used the runoff model in 2004 as a current model (or baseline model) to run what-if analysis for *future* scenarios. The what-if analysis was used to simulate floods in the future (i.e. in the years 2020s, 2050s and 2080s) and evaluate changes in peak discharge and runoff volume. The future runoff model used the same sub-models and parameter values as in the 2004 storm event: only the data inputs varied (i.e. land use and precipitation) as described in the Chapter 3 (Chapter Methods). All the results together with discussion and conclusions are presented in this chapter.

7.2   WHAT-IF SCENARIOS FOR PRECIPITATION CHANGE

7.2.1 Climate input of River Kelantan of HEC-HMS model

A regional climate-modelling tool used by the Malaysian Meteorological Department is known as Providing Regional Climates for Impact Studies (PRECIS) (Marengo et al., 2009; Marengo and Ambrizzi, 2006).The model developed by the Hadley Centre, United Kingdom known as Providing Regional Climates for Impact Studies (PRECIS) was used as a tool by the Malaysian Meteorological Department (MMD) to study precipitation projections in the future. The model is a RCM derived using dynamical

downscaling approach which uses meteorological boundary conditions from the Hadley Centre HadCM3 AOGCM. The model was developed by the Hadley Centre, United Kingdom. Observational data (i.e. temperature and rainfall) of 60 km resolution from the Climate Research Unit of the University of East Anglia, United Kingdom were used to validate the baseline (1961 – 1990) regional climate simulation at 50 km resolution. The regional simulation for PM used the SRES A1B scenario for the period from 2001 to 2099. The PRECIS results showed that temperature was predicted to increase by 1.1^{O}C, 1.7^{O}C and 2.9^{O}C for the period of 2020-2029, 2050-2059 and 2090-2099 respectively for North-East PM where the River Kelantan catchment is situated.

The projected model simulated a reduction (i.e. in early years of the simulation) and an increase (i.e. in later years of the simulation) in average annual precipitation for eastern Peninsular Malaysia within which the River Kelantan catchment is located. The scenario was based on general projected change in precipitation for Malaysia under the A1B storyline using 1961-1990 as a baseline period. The A1B storyline or medium scenario was used to run precipitation scenarios for the periods of 2020s, 2050s and 2080s since it provides continuous practice of present day standards in regard to socioeconomic activities and fuel type usage. The analysis framework for the future climate change and land use change scenarios is shown in Figure 7-1. The climate change model output, in the form of the percentage of precipitation changes projected to increase and decrease, were used as an input to run future hydrological response projections in the Kelantan catchment (Figure 7-2). This chapter used runoff model that developed in previous Chapter 6 of the River Kelantan HEC-HMS hydrological modeling. Thus, this chapter does not relate to the trend found in the streamflow data as discussed in Chapter 5. The input used for the future precipitation scenarios from the PRECIS HadCM3 model for Malaysia (Chinvanno, 2007; MMD, 2009) is presented in Table 7-1.
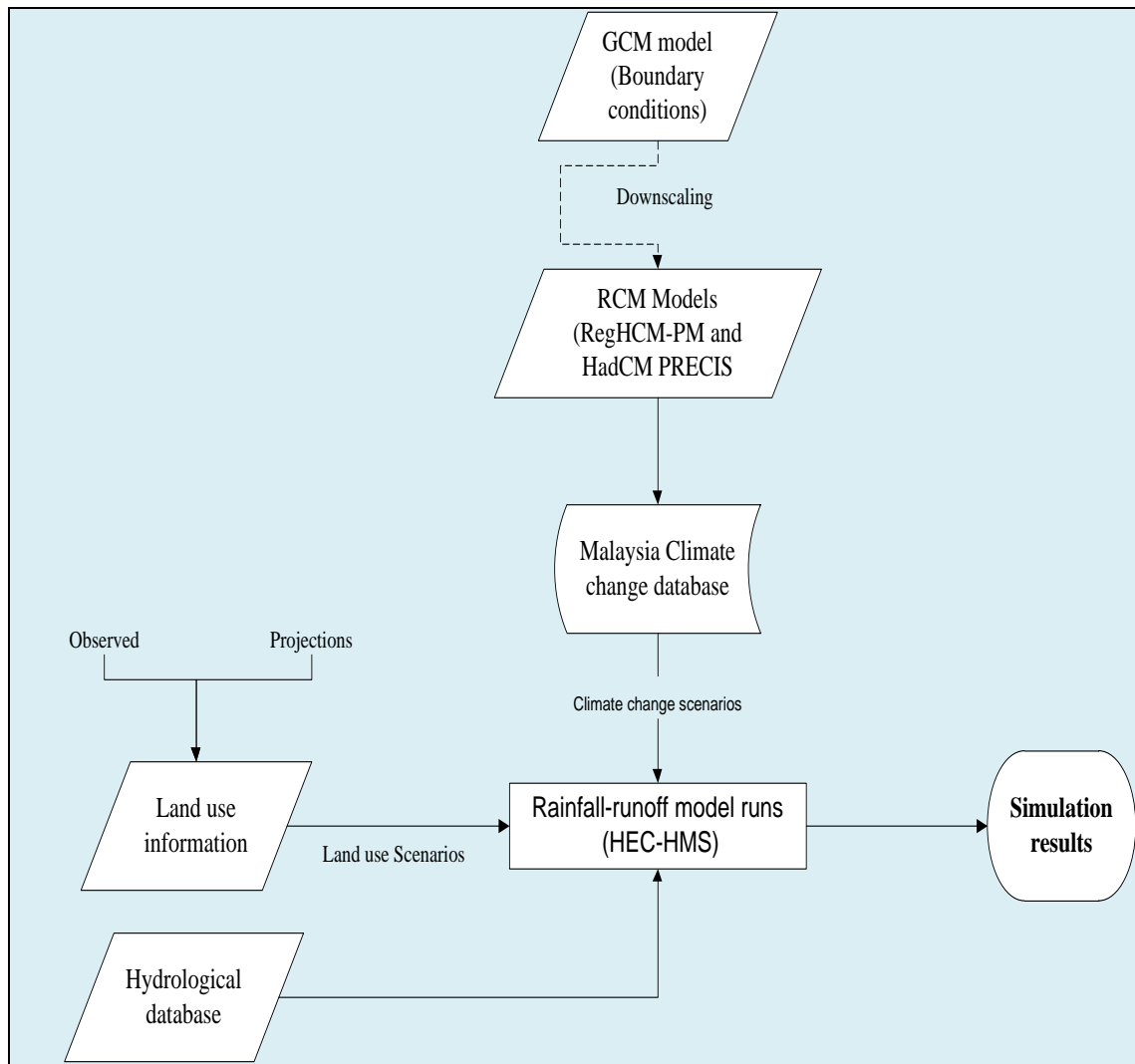
Figure 7-1   Framework for hydrological response and runoff modelling in future scenarios.

Table 7-1 Precipitation input data used for future runoff projection in the Kelantan catchment for 2010-2090 using the 1961-1990 baseline period using the PRECIS HadCM3 model.

	Year		
	2020s (%)	2050s (%)	2080s (%)
Low	-5	-6	4.1
Medium	-10	10	15
High	-18.7	15	25

(a)

(b)

(c)

(d)

(e)
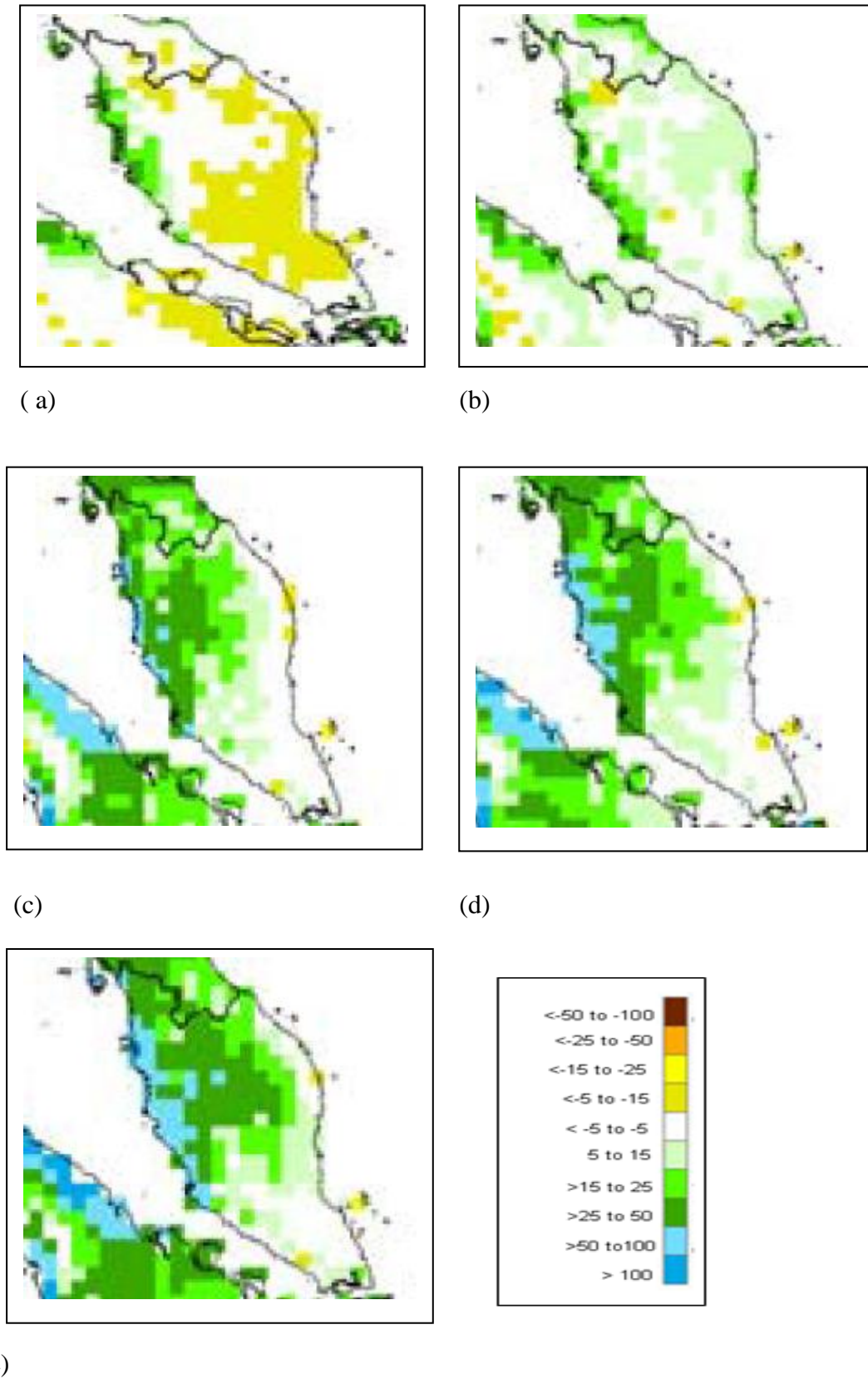
Figure 7-2   Precipitation change scenarios (in percentage) for the periods of (a) 2020,
(b) 2030, (c) 2070, (d) 2080 and (d) 2090 in the Kelantan area using the PRECIS
HadCM3 model.

7.2.2 Run-off results for River Kelantan due to precipitation change projection from A1B scenarios.

The result of applying the precipitation change scenarios using the A1B storyline for the periods of 2020s, 2050s and 2080s are presented in Table 7-2 to Table 7-4. These results were produced by running the HEC-HMS model to obtain forecast of peak discharge and runoff volume. The results were compared to the 2004 baseline peak discharge and runoff volume results. The 2020s precipitation input from the PRECIS HadCM3 model projected decreased precipitation (low percentage of -5%, medium percentage of -10% and high percentage of -18.7%) (Table 7-1). Overall, the result for 2020s showed a decreased peak discharge and runoff volume, both in absolute difference and percentage difference values, for six streamflow gauge stations in the study area (Table 7-2). The decreased percentages differences in peak discharge and runoff volume for all stations were in the range -4.1% to -26.9% and -2.0% to -23.0%, respectively. The Nenggiri station exhibited the largest differences in peak discharge and runoff volume compared to the other five gauge stations. The absolute difference was calculated to estimate the actual differences in forecast runoff in the 2020s as compared to runoff in 2004. The peak discharge difference is in the range of -44.7 m^3s^{-1} to -2287.3 m^3s^{-1}, whereas for the runoff volume difference is in the range -9.2 m^3s^{-1} to -561.2 m^3s^{-1}. The absolute difference revealed that the Guillemard Bridge exhibited the largest differences in peak discharge and runoff volume from the 2004 values (Table 7-2).

The second period (2050s) precipitation change scenario using the A1B storyline from the HadCM3 scenario showed different projection values. The low climate change percentage of change is -6%, medium with positive percentage difference of 10% and high of 15% (Table 7-1). The precipitation scenario exhibited greater differences in peak discharge and runoff volume as compared to the 2020s simulations. The percentage difference in peak discharge and runoff volume for 2050s were between -8.8% to 23.2% and -7.6% to 20.1% respectively (Table 7-3).

Table 7-2 Absolute difference and percentage difference in peak discharge and runoff volume for 2020s simulations using the PRECIS HadCM3 model. Precipitation change scenarios of low using percentage of -5%, medium of -10% and high of -18.7%.

Station	Abs_{diff} (m^3s^{-1})			Diff (%)		
	Low	Medium	High	Low	Medium	High
Nenggiri						
Peak discharge	-151.5	-301.3	-553.8	-7.4	-14.7	-26.9
Runoff volume	-9.16	-18.2	-33.4	-6.3	-12.5	-23.0
Pergau						
Peak discharge	-44.7	-91.4	-171.4	-5.2	-10.6	-19.8
Runoff volume	-13.06	-26.8	-50.2	-3.6	-7.4	-14.0
Galas						
Peak discharge	-124.0	-248.1	-464.1	-4.1	-8.2	-15.4
Runoff volume	-11.82	-23.6	-44.1	-2.0	-4.0	-7.4
Lebir						
Peak discharge	-105.7	-210.6	-390.9	-6.1	-12.2	-22.7
Runoff volume	-13.52	-26.9	-49.7	-5.2	-10.3	-19.0
Kuala Krai						
Peak discharge	-58.3	-116.7	-218.0	-4.7	-9.4	-17.5
Runoff volume	-15.23	-30.4	-56.7	-3.3	-6.6	-12.3
Guillemard Bridge						
Peak discharge	-611.7	-1223.1	-2287.3	-4.8	-9.7	-18.1
Runoff volume	-150.46	-300.4	-561.2	-4.4	-8.7	-16.3

Ab_{diff} is the absolute difference; % Diff is the percentage difference.

The third period of precipitation change projection is the 2080s with all positive percentage of changes in precipitation. The low scenario change is 4.1%, medium is 15% and high is 25% (Table 7-1). The percentages differences in peak discharge and runoff volume for all stations were in the range of 3.4% to 39.2% in peak discharge and 1.6% to 34.0% in runoff volume (Table 7-4).

Table 7-3 Absolute difference and percentage difference in peak discharge and runoff volume for 2050s simulations using the PRECIS HadCM3 model. Precipitation change scenarios of low using percentage of -6%, medium of 10% and high of 15%.

Station	Abs $_{diff}$ (m^3s^{-1})			Diff (%)		
	Low	Medium	High	Low	Medium	High
Nenggiri						
Peak discharge	-181.7	315.9	477.1	-8.8	15.4	23.2
Runoff volume	-10.99	19.3	29.2	-7.6	13.3	20.1
Pergau						
Peak discharge	-54.1	98.0	146.2	-6.3	11.3	16.9
Runoff volume	-15.81	29.0	43.3	-4.4	8.1	12.0
Galas						
Peak discharge	-148.8	248.0	371.9	-4.9	8.2	12.4
Runoff volume	-14.18	23.7	35.5	-2.4	4.0	6.0
Lebir						
Peak discharge	-126.7	213.4	320.8	-7.3	12.4	18.6
Runoff volume	-7.2	27.5	41.4	-2.8	10.5	15.8
Kuala Krai						
Peak discharge	-70.0	116.8	175.2	-5.6	9.4	14.1
Runoff volume	-18.27	30.6	46.0	-4.0	6.6	10.0
Guillemard Bridge						
Peak discharge	-734	1221.1	1831.8	-5.8	9.7	14.5
Runoff volume	-180.44	299.4	449.4	-5.2	8.7	13.1

Ab$_{diff}$ is the absolute difference; % Diff is the percentage difference.

Overall, the results showed an increase in all scenarios from "low" to "high" scenarios. The 2080s resulted in the largest percentage changes and absolute differences in peak discharge and runoff volume compared to the periods of 2020s and 2050s. All periods showed that the Nenggiri station has the highest percentage differences and the Guillemard Bridge showed the largest absolute differences.

Table 7-4 Absolute difference and percentage difference in peak discharge and runoff volume for 2080s simulations using the PRECIS HadCM3 model. Precipitation change scenarios of low using percentage of 4.5%, medium of 15% and high of 25%.

	Abs $_{diff}$ (m^{3}s^{-1})			Diff (%)		
	Low	Medium	High	Low	Medium	High
Nenggiri						
Peak discharge	129.1	360.4	806.3	6.3	17.5	39.2
Runoff volume	7.88	21.7	49.4	5.4	14.9	34.0
Pergau						
Peak discharge	41.4	138.3	243.6	4.8	16.0	28.2
Runoff volume	12.3	40.9	72.1	3.4	11.4	20.1
Galas						
Peak discharge	101.7	371.9	619.4	3.4	12.4	20.6
Runoff volume	9.7	35.5	59.3	1.6	6.0	9.9
Lebir						
Peak discharge	87.2	320.8	540.0	5.1	18.6	31.3
Runoff volume	11.19	41.4	69.5	4.3	15.8	26.6
Kuala Krai						
Peak discharge	47.9	175.2	292.1	3.9	14.1	23.5
Runoff volume	12.53	46.0	76.8	2.7	10.0	16.6
Guillemard Bridge						
Peak discharge	500.4	1831.8	3052.9	4.0	14.5	24.2
Runoff volume	122.44	449.4	749.3	3.6	13.1	21.8

Ab$_{diff}$ is the absolute difference; % Diff is the percentage difference.

Table 7-5 Summary percentage differences in peak discharge and runoff volume for the 2020s, 2050s and 2080s using the PRECIS HadCM3 model.

	2020s (%)	2050s (%)	2080s (%)
Peak discharge			
Nenggiri	-26.9 to -7.4	-8.8 to 23.2	6.3 to 39.2
Pergau	-19.8 to -5.2	-6.3 to 16.9	4.8 to 28.2
Galas	-15.4 to -4.1	-4.9 to 12.4	3.4 to 20.6
Lebir	-22.7 to -6.1	-7.3 to 18.6	5.1 to 31.3
Kuala Krai	-17.5 to -4.7	-5.6 to 14.1	3.9 to 23.5
Guillemard Bg.	-18.1 to -4.8	-5.8 to 14.5	4.0 to 24.2
Runoff volume			
Nenggiri	-23.0 to -6.3	-7.6 to 20.1	5.4 to 34.0
Pergau	-14.0 to -3.6	-4.4 to 12.0	3.4 to 20.1
Galas	-7.4 to -2.0	-2.4 to 6.0	1.6 to 9.9
Lebir	-19.0 to -5.2	-2.8 to 15.8	4.3 to 26.6
Kuala Krai	-12.3 to -3.3	-4.0 to 10.0	2.7 to 16.6
Guillemard Bg.	-16.3 to -4.4	-5.2 to 13.1	3.6 to 21.8

In summary, precipitation change analysis using the rainfall-runoff model revealed two patterns of changes in peak discharge and runoff volume (Table 7-5). The first period represented by the 2020s showed that discharge, and potentially flooding, in the future as represented by peak discharge and runoff volume decreased compared to the baseline year of 2004. The reasonable explanation for this result is that according to the IPCC (2007), the temperature is projected to increase continuously with several projected La-Nina events in the 2020s for the Malaysia region as presented in Chapter 2 under Malaysia climate change projections. Thus, dry conditions are expected to occur for the period of 2020s and may even cause drought to occur in the study area for this period.

However, in the second period of the 2050s climate scenario a negative percentage change was exhibited for the low and medium scenarios and a high percentage change exhibited for the high scenario with positive differences. More rainfall is expected to occur in this period as compared to the 2020s period. The absolute and percentage differences also revealed greater change compared to 2020s. The temperature trend for the same period is projected to decrease slightly and due to that precipitation is expected to increase.

The third period represented by 2080s positive percentage change was projected for the low, medium and high scenarios. This period also suggests that in the future flooding may increase due to the largest increases in peak discharge and runoff volume. The temperature exhibited the highest increase as compared to the periods of 2020s and 2050s accompanied by the El-Nino events projected for the periods such as 2084 and 2091. Thus, this may also cause expected increases in precipitation for this modeled period.

The future precipitation change scenario for the periods 2020s to 2080s clearly revealed that in the future precipitation is expected to increase and subsequently may cause more frequent and more intensive flooding to occur for the Kelantan area. In the future, land use change is also predicted to happen. Many researchers suggested that apart from climate change, land use change is also predicted to have a huge impact on runoff and flooding for a catchment (Dalzell et al., 2005; Lopez-Moreno et al., 2006; Bahar et al., 2008; Cuo et al., 2009). The next section simulates how expected land use changes may impact on runoff and flooding in the study area in the future.

7.3   SCENARIOS FOR LAND USE CHANGE

Two hypothetical scenarios for land use were adopted; the first one using an arbitrary land use change scenario and the second using land use projections as estimated from various sources. The first land use scenario, also known as *the land use sensitivity scenario* was simulated to quantify land use type effects on hydrological response in the River Kelantan catchment. The second land use scenario also known as *likely projected scenario* was used to provide likely changes to land use in the future. There are several justifications for the latter land use change scenario. Observed previous land use change (i.e. in the year 1988 to 2000), future agricultural projections (i.e. oil palm and rubber plantations), availability of suitable land for agriculture and population growth rate are some factors taken into consideration.

7.3.1 Land use sensitivity scenario

The land use sensitivity scenario was performed to study sensitivity of each land use types and also to know what types of land use change significantly affect peak discharge and runoff volume. This analysis was carried out also to provide plausible causes and effects if such developments were observed in the future in the study area. The key factor of land use change involved in the land use sensitivity scenario was degradation of forest area since it is observed to be happening in the study area. Decreases in forest area are assumed to cause increases in agricultural and built-up land with possible proportions as portrayed in Table 7-6. Six land use change scenarios were used which are named low, medium, high, extreme 1 (equal proportion i.e. 50% each changes to agricultural and built-up lands), extreme 2 (all i.e. 100% forest area is converted to agricultural land), and extreme 3 (i.e. 100% forest area is converted to built-up land). These changes in land use were applied to study the effect of increases in each type and in combinations land use types (i.e. agricultural and built-up land) on hydrological response in the River Kelantan catchment. The difference from the baseline runoff model was calculated and the results were presented.

Table 7-6 Land use sensitivity scenario.

	Sensitivity scenario					
	Low	Medium	High	Extreme 1	Extreme 2	Extreme 3
Forest	-20	-40	-60	-100	-100	-100
Agricultural land	+20	+30	+40	+50	+100	
Built-up land	0	+10	+20	+50		+100

7.3.1.1 SCS CN Calculation

Based on the above land use changes as presented in Table 7-6 the SCS CN was calculated. The 2004 land use was used as a baseline and all the land use types were kept constant except for three land use types which are forest, agricultural (i.e. rubber, oil palm and mixed-agriculture) and built-up land. The new SCS CN resulted from the sensitivity land use changes scenario presented in Table 7-7 and Figure 7-3.

Table 7-7 SCS CN for land use sensitivity scenario.

	Baseline CN	What-if CN					
	Current	Low	Medium	High	Extreme 1	Extreme 2	Extreme 3
Nenggiri	40	46.2	50.6	61.3	77.9	70.2	85.6
Pergau	55.8	59.2	63.5	67.8	77.5	72	83
Galas	80.9	82.5	84.3	86.1	89.9	89	90.8
Lebir	57.7	59.8	63.7	67.6	77.1	68.2	86.1
Kuala Krai	77.4	77.8	78.9	80.1	83.1	79.3	86.9
Guillemard Bg.	74.2	75.3	76.9	78.6	82.6	79.4	85.7
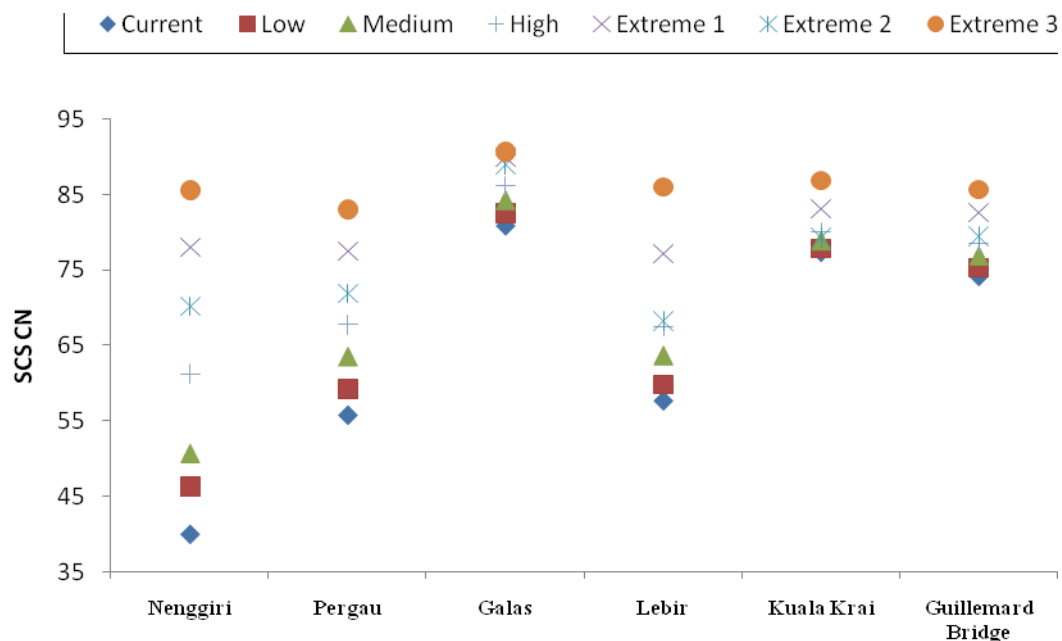
Figure 7-3   SCS CN of baseline and land use sensitivity scenarios.

The SCS CN of the land use sensitivity scenarios showed that for all sub-basins the CN was higher for the extreme 1 scenario than extreme 2. This suggests that conversion of forest to a combination of agricultural and built-up lands resulted in a higher CN as compared to only forest conversion to agricultural land. The extreme 3 scenario showed the largest CN for all sub-basins. This suggests that built-up land gives the largest CN as compared to agricultural land and the combination of agricultural and built-up lands.

7.3.1.2 **Land use sensitivity scenario runoff results**

Using the new calculated CN as presented in Table 7-7 differences in peak discharge and runoff volume were calculated from the observed baseline. The result showed that land use sensitivity scenario extreme 3 has the highest increases in peak discharge absolute difference compared to the others scenarios (Figure 7-4 (a)). This suggests that conversion from forest to built-up land (i.e. 100%) was the largest contribution to increases in peak discharge for all streamflow gauges in the River Kelantan catchment. More interestingly, the extreme 1 land use scenario leads to greater increases (i.e. in peak discharge and runoff volume) compared to the extreme 2 scenario. The extreme 1 scenario models a decrease in 100% of forest to 50% increase in agricultural and 50%

176

increase in built-up land. Meanwhile, the extreme2 scenario represents decreases of 100% in forest to agricultural land. The result suggests that built-up land plays a significant role in increasing peak discharge. The combination of agricultural and built-up land was the second greatest contributor to differences in peak discharge. Agricultural land was the third highest contribution to increases in hydrologic change in the study area.

Amongst the individual flow gauges stations the Nenggiri station which is located in the most upstream part of the study area exhibited the largest increases in peak discharge compared to the other five flow gauges (i.e. 12.8% to 149.2%). For the downstream area, the Lebir station showed the largest increases compared to the other two gauges (which are Kuala Krai and Guillemard Bridge) (i.e. 2.2% to 40.0%). This result is well understood since these two stations are located in the sub-basin which has the highest deforestation that has already occurred. Moreover, the Guillemard Bridge showed the smallest increases in peak discharge with only 0.04% (i.e. low scenario) to 0.6% (i.e. extreme 3 scenario). The result may imply that deforestation that happened in the upstream area as well as in the Lebir sub-basin may contribute to increases in peak discharge.

The percentage difference in peak discharge is also presented in Figure 7-4 (b). The results showed a similar pattern to absolute difference in peak discharge. The extreme 3 scenario showed the largest increases followed by the extreme 1 and extreme 2 scenarios. Again, the Nenggiri exhibited the largest increases in peak discharge and runoff volume compared to the other five gauges in the River Kelantan catchment. However, the results showed that runoff volume was less sensitive compared to the peak discharge with increases in peak discharge being higher than the increases in runoff volume (Table 7-8). To understand why this sub-basin has the largest increases, it is necessary to consider the size of sub-basin. The Nenggiri sub-basin covers approximately 31% of the total catchment followed by the Lebir sub-basin of 20% and third by the Galas of 18.9%. Additionally, these three sub-basins have a high conversion from forest to agricultural land, especially for oil palm and rubber plantation

Table 7-8 Absolute difference and percentage difference in peak discharge and runoff volume arising from land use sensitivity scenarios low, medium, high, extreme 1, extreme 2 and extreme 3.

	Low		Medium		High		Extreme 1		Extreme 2		Extreme 3	
	Abs_{diff} (m^3s^{-1})	% Diff	Abs_{diff} (m^3s^{-1})	% Diff	Abs_{diff} (m^3s^{-1})	% Diff	Abs_{diff} (m^3s^{-1})	% Diff	Abs_{diff} (m^3s^{-1})	% Diff	Abs_{diff} (m^3s^{-1})	% Diff
Peak Discharge												
Nenggiri	263.0	12.8	703.5	34.2	1422.7	69.2	2502.0	121.8	1507.2	73.3	3066.5	149.2
Pergau	32.7	3.8	100.0	11.6	157.9	18.3	267.6	31.0	147.9	17.1	342.5	39.7
Galas	61.1	2.0	111.0	3.7	148.6	4.9	183.7	6.1	180.5	6.0	186.9	6.2
Lebir	38.7	2.2	172.7	10.0	295.6	17.1	539.1	31.3	214.9	12.5	689.9	40.0
Kuala Krai	1.4	0.1	22.1	1.8	42.2	3.4	87.8	7.1	14.0	1.1	131.7	10.6
Guillemard Bg.	4.8	0.04	19.3	0.2	32.0	0.3	55.4	0.4	25.9	0.2	71.6	0.6
Runoff volume												
Nenggiri	16.6	11.4	42.6	29.3	79.8	54.9	135.2	93.0	81.3	56.0	168.7	116.0
Pergau	9.8	2.7	33.0	9.2	53.5	14.9	95.2	26.5	46.3	12.9	129.1	35.9
Galas	6.0	1.0	12.2	2.0	17.5	2.9	24.7	4.1	22.4	3.8	27.0	4.5
Lebir	5.0	1.9	27.3	10.4	47.1	18.0	89.8	34.3	29.2	11.2	125.6	48.0
Kuala Krai	0.2	0.1	9.1	2.0	17.5	3.8	38.0	8.2	4.4	1.0	61.2	13.3
Guillemard Bg.	2.7	0.1	17.8	0.5	31.7	0.9	62.5	1.8	19.3	0.6	93.8	2.7

Ab_{diff} is the absolute difference; % Diff is the percentage difference.

(a)
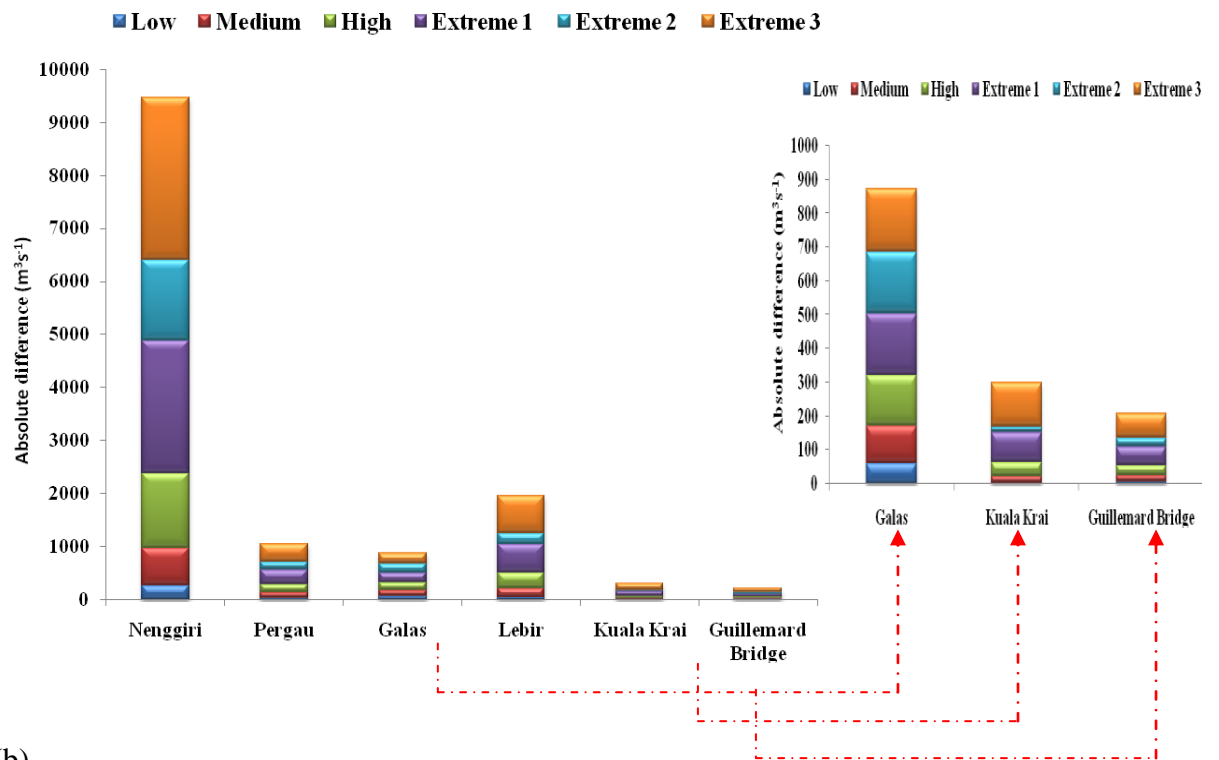
(b)
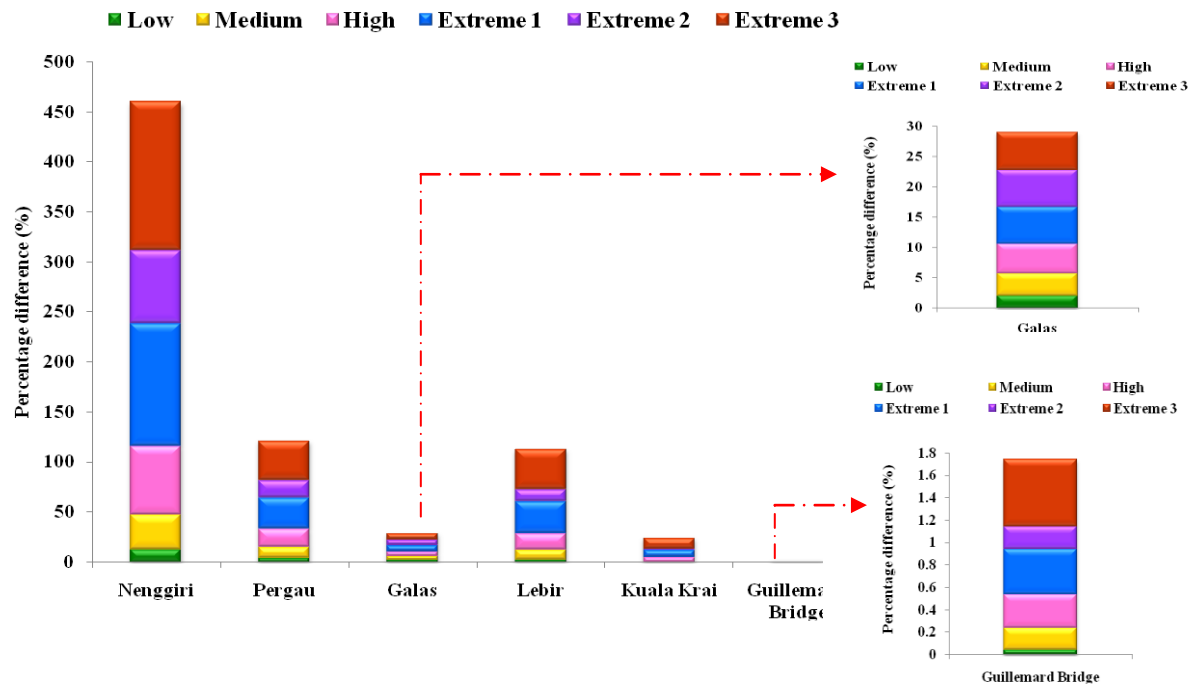
Figure 7-4   Peak discharge (a) absolute difference (b) percentage difference using land use sensitivity scenarios low, medium, high, extreme 1, extreme 2 and extreme 3

7.3.2 Likely future projections of land use

The second hypothetical future land use change scenario examined is based on likely projections. There are several justifications for this scenario. The first justification is the types of land use changes that have been observed in the past. According to the land use change map analysis presented in Chapter 5, most land use conversion was from forest to agricultural land (i.e. rubber, oil palm and mixed-agriculture) and an increase in built-up land was also observed. Agricultural plantation increased significantly (i.e. almost 70%) over the 12 year period of the Landsat TM image classification analysis. The increase in agricultural area, particularly in oil palm, was also evidenced in several reports. For example, Hai (2000) reported that for the Kelantan area, an increase in oil palm area from 18,238 hectares in 1980 to 80,407 hectares in 1999 has led to increased production of crude palm oil from 27,034 tonnes in 1980 to 215,723 tonnes in 1999. Additionally, Abdullah (2003) stated that there have been tremendous increases in oil palm plantation from 1980 of 1.48 million hectares to 3.38 million hectares in 2000 for Peninsular Malaysia where the study area is located. Increases in other agricultural plantations such as cocoa of 9,831 hectares from 1980 to 1998 was also reported by Hai (2000). The ADB (2009) also reported that increases in land conversion, especially from non-agricultural areas (i.e. forestland) to cropland such as oil palm, natural rubber, rice paddy and coffee occurred in Southeast Asian countries. The land conversion into agricultural areas has caused a reduction in primary forest for Southeast Asian countries of about -27% between 1990 to 2005. It is clear that agricultural land is a major land use and is expected to increase continuously in the future through reductions in forest area.

Secondly, consideration was also given to the kinds of land use changes that can be expected in the future. According to ADB (2009), Southeast Asian countries are one of the world's largest producers of palm oil and natural rubber with an increase in average annual production of palm oil from 86 million tonnes during 1996-2001 to 139 million tons in 2002-2007 periods. In addition, the same report also stated that Malaysia, Indonesia and Thailand alone contribute about 75% of the world's total natural rubber plantation. Therefore, in the future increases in agriculture are expected to occur in Malaysia as projected by The Third National Agricultural Policy (NAP3) of 4.92 million hectares in the year 2020 for East Malaysia (Abdullah, 2003) due largely to an

export-oriented demand. However, over a longer period suitable land for new oil palm is limited with competing demands for industrialization and urbanization due to population growth. Current projections suggest that the population of Malaysia will increase to 40.6 million in 2020 from 22.3 million in 2000 (Malaysia Department of Statistics, 2000). The increases in population over time involve land area transformation because of increased pressure on land for housing and related infrastructure. A study by Atan (2005) stated that in 2001 built-up area was approximately 3.3% and was expected to increase to 5.8% in 2020. Therefore, to study runoff changes in the future the changes to these three land uses (i.e. forest, agricultural land and built-up area) were simulated, while the other land uses were kept constant.

To ensure that the land use scenarios reflected plausible and acceptable land conversions, land suitability for agriculture was studied and calculated. Reasonable land conversion from forest area to agriculture and built-up land was taken into account. The basic criterion for land suitable for agriculture was estimated from current forest land with slope of less than 20%. Detailed explanation is given in the next section to simulate peak discharge and runoff volume using likely projected land use change scenario for future.

As mentioned earlier, the likely projected land use scenario used three land use types which are forest, agricultural land and built-up land. Due to limited information on land use projections (i.e. area projection and spatial map) for the River Kelantan catchment, the information on projection of land use types for the future was based on observation of the past and current land use situations and rational assumptions as described earlier.

Forest is expected to decrease for all periods (i.e. 2020s to 2080s). However, contrary to the forest scenario for the said periods, agricultural land is expected to increase rapidly for the first two periods and expected to increase in the third period, but with reduced percentage compared to the first two periods due to expectation of limited available land for further agricultural development. Furthermore, built-up land is expected to increase due to continuously increasing population growth and may cause increases in the rate of urbanization and industrialization in future scenarios. For the built-up land scenarios, an increase of 5.8% for 2020s as reported by Atan (2005) was

used and further reasonable increases of 10% in 2050s and 20% in 2080s were used for future scenarios.

Future land use estimation also was based on currently suitable land potential to be converted to agricultural land. As suggested above, the suitable area was considered as forest land with slope less than 20^0.

7.3.3 Forest to agricultural land suitability area

Analysis of suitable area for conversion from forest to agricultural land was undertaken using spatial criteria analysis. Areas that are suitable to be converted to agricultural land (i.e. rubber, oil palm and mixed agriculture) were derived using GIS spatial analysis calculations. The current land use map in 2000 derived from supervised classification was used as a baseline map.

Projected land suitable for agriculture was derived using GIS data manipulation. Criteria of forested area with less than 20^0 slopes which receive high rainfall (i.e. 1700 to 3000 mm yr^{-1}) were used to identify suitable sites for agricultural area (Goh, 2000; Paramanathan, 2000). Since the whole Kelantan catchment receives high rainfall, only forest land use with slope less than 20^0 was selected using spatial analyst in the ArcGIS software. Suitable areas for conversion from forest to agricultural land for each sub-basin using GIS analysis are shown in Figure 7-5.

(a) Nenggiri
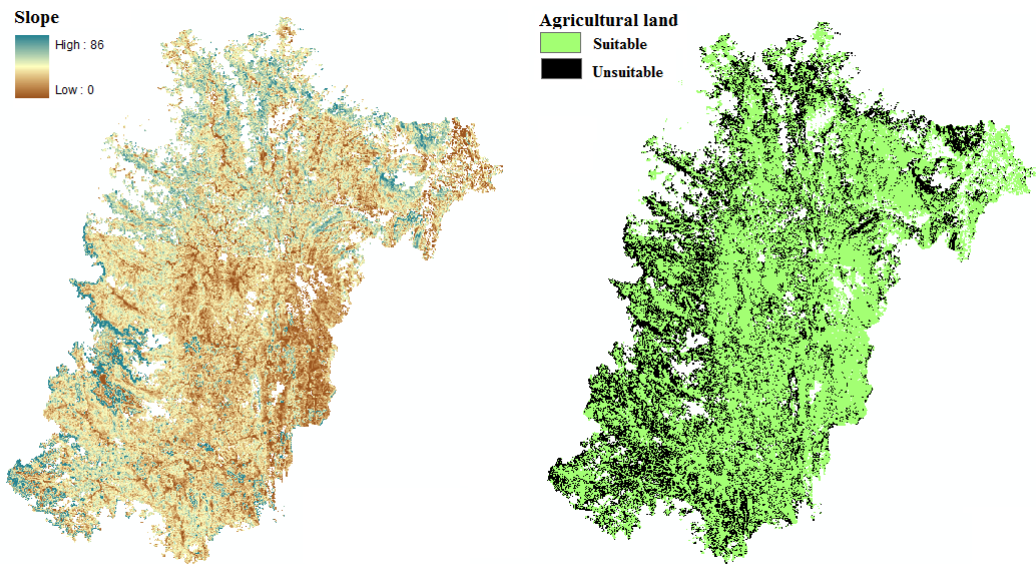
(b) Kelantan
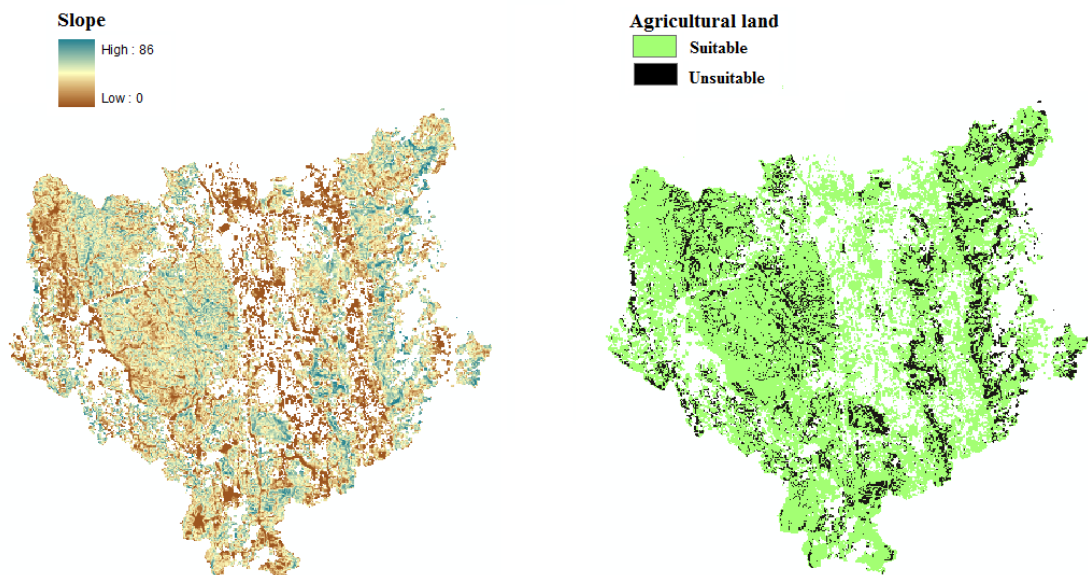
Figure 7-5   GIS analysis of forest area overlaid with slope map (left-hand side) and suitable area (right-hand side) using criteria of forest with slope less than 20^0 for (a) Nenggiri sub-basin and (b) Kelantan sub-basin.

In summary, land suitability for agriculture calculated using GIS spatial analysis revealed that minimally, the suitable land to be converted from forest to agricultural land is 58% of the total area in Kelantan (Table 7-9). From this minimal value, a value of maximum 60% increase in agricultural land was used for the likely future land use scenario for all sub-basins.

Table 7-9 Agriculture land use scenario for each sub-basin.

Sub-basin	Total area	Agriculture Current area		Agriculture Potential area		Agriculture Future area	
	km^2	km^2	%	km^2	%	km^2	%
Nenggiri	3035.07	382.14	12.6	1373.48	45.3	1755.62	57.8
Pergau	1000.44	413.07	41.3	508.77	50.9	921.84	92.1
Galas	1872.09	454.36	24.3	901.86	48.2	1356.22	72.4
Lebir	1866.99	181.62	9.7	1142.45	61.2	1324.07	70.9
Kuala Krai	1041.08	346.57	33.3	444.62	42.7	791.19	76.0
Guillemard Bridge	989.90	389.16	39.3	373.46	37.7	762.62	77.0

7.3.4 Likely future projection land use scenario

From these three land use changes (i.e. forest, agricultural and built-up land), three likely scenarios were created to simulate runoff changes due to land use changes for the 2020s, 2050s and 2080s as presented in Table 7-10.

Table 7-10 Likely projected land use change scenarios for 2020s, 2050s and 2080s.

Land use	2020s (%)	2050s (%)	2080s (%)
Forest	-15	-40	-60
Agricultural land	+9.2	+30	+40
Built-up	+5.8	+10	+20

Scenarios for the first to the second periods (i.e. 2020s to 2050s) simulate a rapid rate of decrease in forest, an increase in agricultural land and a smaller rate of increase in built-up land. This is due to observed land use conversion from 1988 to 2000 apart from projected increases in agriculture plantation and urbanization as reported in several studies (Atan, 2005; Samat, 2006) which clearly showed this kind of trend. The

rapid rate expected to occur since these two periods may involve the highest rate of population growth and high conversion of suitable land for agriculture (Hai, 2000). Furthermore, the scenario for the 2080s was developed according to the report by ADB (2009) which suggested that forest and agricultural land may decrease and increase, respectively, with a smaller rate compared to the first two periods. In contrast, a higher increasing rate of built-up land due to population growth was used.

7.3.5 CN calculations and input in runoff model

Using the likely projected land use scenario, the SCS CN was calculated as described in Chapter 3. The scenario of decreased forest and increased agricultural land and built-up area were used for all three time periods. The CN range for the 2020s scenario was between 45.6 to 82.2 with an increased percentage of 14% for minimum CN and maximum CN of 2.3% from baseline CN values. The 2050s scenario used a similar land use change scenario, however, with a higher value of decreased forest and increased agricultural and built-up land. The range of CN for the scenario 2 was between 53.8 to 84.3 which relates to an increase of 34.5% in the minimum and 5.4% in the maximum CN values. The CN for the 2080s scenario depicted the largest values with a range of 61.3 to 86.1 (Table 7-11). These CN values were used in the HEC-HMS model together with the percentage of impervious surface as presented in Table 7-11.

Table 7-11 SCS CN for future likely projected land use scenarios.

Sub-basin	CN 2020s	Built-up (%)	CN 2050s	Built-up (%)	CN 2080s	Built-up (%)
Nenggiri	45.6	5.8	53.8	10.0	61.3	20
Pergau	58.0	5.8	61.9	10.0	64.8	20
Galas	82.2	5.8	84.3	10.0	86.1	20
Lebir	60.3	5.8	63.7	10.0	67.6	20
Kuala Krai	78.1	5.8	78.9	10.0	80.1	20
Guillemard Bg.	75.4	5.8	76.9	10.0	78.6	20

Amongst the individual sub-basins the CN for the Galas sub-basin was the highest with a projected CN of 86.1 in the 2080s scenario. The 2080s CN values depicted that although agriculture was predicted to increase with a smaller rate compared to the

2020s and 2050s periods, with the continuous increased rate in built-up land, the 2080s CN was the highest compared to previous periods (Figure 7-6). This suggests that increases in built-up land area may cause significant changes to the loss model calculations in the HEC-HMS. In addition, decreases in forest may also caused higher CN values which later may be attributed to the possibility of higher runoff occurring.
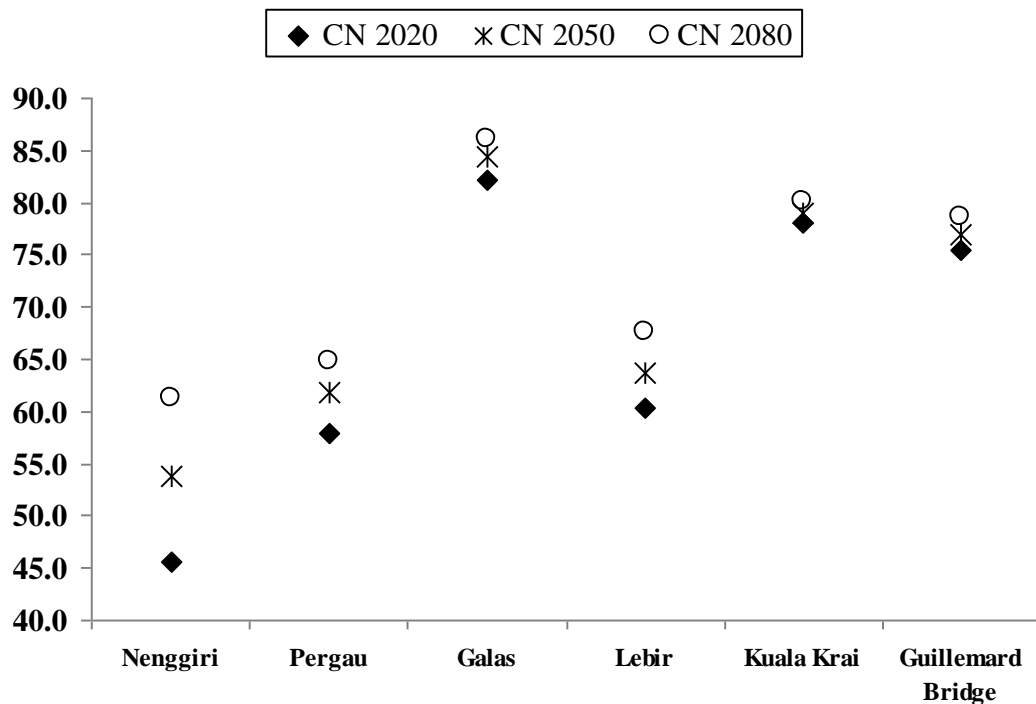
Figure 7-6   The SCS CN of future likely projected land use scenarios (i.e. 2020s, 2050s and 2080s) for all six sub-basins in the River Kelantan catchment.

7.3.6 Run-off results for likely future projections land use scenario

Differences in peak discharge and runoff volume were calculated and compared to the baseline runoff model (i.e. in 2004). The main differences between the 2020s and 2050s scenarios are that the land use scenario in the 2050s is projected to include a rapid increase in agricultural land (from 9.2% to 30%) and gradual increase in built-up land (from 5.8% to 10%). The scenario projects that forest continues to decrease, but there is an expected increase in agricultural land with a lower rate (i.e. 30% to 40%) and an increase in built-up land with a higher rate (i.e. 10% to 20%). Results showed that all scenarios led to increases over time with larger increases in peak discharge and runoff volume projected in the 2080s scenario compared to the 2020s scenario.

The Nenggiri gauge station exhibited the largest differences with increases in peak discharge of 2404.6, 2910.4 and 3477.0 m^3s^{-1} for the periods of 2020s, 2050s and 2080s respectively (Figure 7-7). The estimated percentage differences in peak discharge compared to the 2004 runoff model for the Nenggiri sub-basin were 17.0%, 41.6% and 69.2% for the 2020s, 2050s and 2080s, respectively (Table 7-12). The difference in runoff volume for this station is in the range 16.4% to 54.9%.

The other five streamflow gauge stations exhibit smaller percentage differences (i.e. increase) in hydrologic response as compared to the Nenggiri station. A similar pattern of increases in peak discharge and runoff volume were projected, with the scenario in 2080s the highest as compared to the 2020s and 2050s scenarios respectively. The Lebir and Pergau stations exhibited the second and the third largest percentage increases in peak discharge and runoff volume after Nenggiri. The increases in percentage in peak discharge for the other five gauges were in a range of 0.1% (i.e. Guillemard Bridge) to 17.1% (i.e. Lebir) and for runoff volume of 0.2% to 18.0%.

The projection of absolute difference and percentage difference in peak discharge and runoff volume for each station for three time periods (i.e. 2020s, 2050s and 2080s) revealed that the Nenggiri station clearly showed the largest differences (Figure 7-7 and Figure 7-8). To understand why this sub-basin has the largest increases, it is necessary to consider the size of sub-basin. The Nenggiri sub-basin covers approximately 31% of the total catchment followed by the Lebir sub-basin of 20% and third by the Galas of 18.9%. Additionally, these three sub-basins have a high conversion from forest to agricultural land, especially for oil palm and rubber plantation. Many researchers have suggested that deforestation causes less water absorption and evapotranspiration due to reductions in tree stem and leaves to hold the rainfall. In addition, transformation of forest to agricultural land causes destruction to soil infiltration capability due to changes of soil structure such as soil crusting and soil compaction caused by agricultural practices. These may lead to infiltration excess and overland flow if combined with high rainfall intensities (Bronstert et al., 2002). In this case, the study area experiences high intensities of rainfall with prolonged duration, sometimes extended to two weeks, and at the same time intensified agricultural activities are also dominant in the upstream area.

In summary, the results suggest that decreases in forest and increases in built-up land have significant impacts on flood runoff, followed by increases in agricultural land. For example, for all of three scenarios, the periods of 2020s and 2050s are estimated to have a rapid rate of land use change (i.e. decrease in forest, increase in agricultural land and built-up land) and in the period of 2080s, forest and agricultural land were expected to have a lower increase rate, while built-up land continues to increase. However, agricultural land is expected to have a lower increase rate in the 2080s, so that the peak discharge and runoff volume were much higher compared to the other two periods. This result may imply that future built-up development in the Kelantan catchment needs to be considered carefully by policy makers in order to minimize increases in discharge and flooding potential due to land use conversion.

Table 7-12 Absolute difference and percentage difference in peak discharge and runoff volume for the 2020s, 2050s and 2080s using likely projected land use change scenarios.

		2020s			2050s			2080s		
	2004 Baseline		**Abs$_{diff}$**	**% Diff**		**Abs$_{diff}$**	**%Diff**		**Abs$_{diff}$**	**%Diff**
Peak discharge			(m^3s^{-1})	(%)		(m^3s^{-1})	(%)		(m^3s^{-1})	(%)
Nenggiri	2055.0	2404.6	350	17.0	2910.4	855	41.6	3477.0	1422	69.2
Pergau	863.7	903.5	40	4.6	950.3	87	10.0	1000.1	136	15.8
Galas	3010.5	3072.0	62	2.0	3121.5	111	3.7	3159.1	149	4.9
Lebir	1724.2	1803.0	79	4.6	1896.9	173	10.0	2019.8	296	17.1
Kuala Krai	1243.7	1254.6	11	0.9	1265.8	22	1.8	1285.9	42	3.4
Guillemard Bridge	12615.2	12624.3	9	0.1	12634.5	19	0.2	12647.2	32	0.3
Runoff volume			(mm)	(%)		(mm)	(%)		(mm)	(%)
Nenggiri	145.3	169.2	23.8	16.4	195.8	50.5	34.7	225.2	79.8	54.9
Pergau	359.4	372.8	13.4	3.7	388.2	28.8	8.0	406.1	46.7	13.0
Galas	595.9	602.4	6.5	1.1	608.1	12.2	2.0	613.4	17.5	2.9
Lebir	261.6	275.0	13.4	5.1	288.9	27.3	10.4	308.8	47.1	18.0
Kuala Krai	461.2	465.8	4.6	1.0	470.3	9.1	2.0	478.7	17.5	3.8
Guillemard Bridge	3440.2	3448.6	8.4	0.2	3458.0	17.8	0.5	3471.9	31.7	0.9

Ab$_{diff}$ is the absolute difference; % Diff is the percentage difference

. (a) Peak discharge
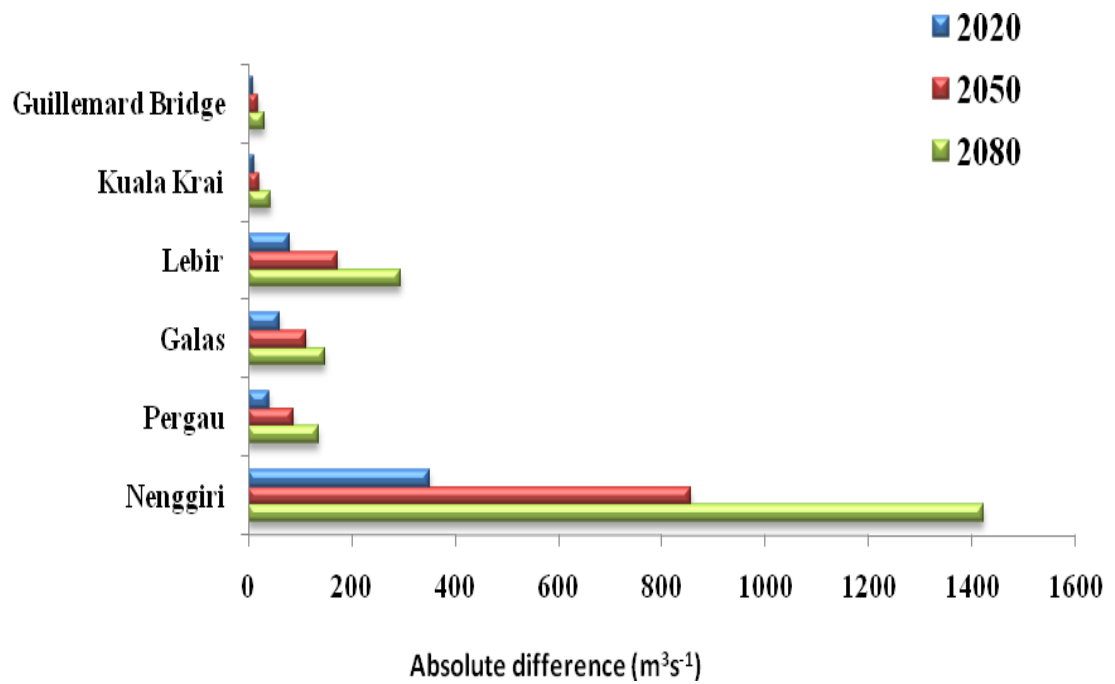
(b) Runoff volume
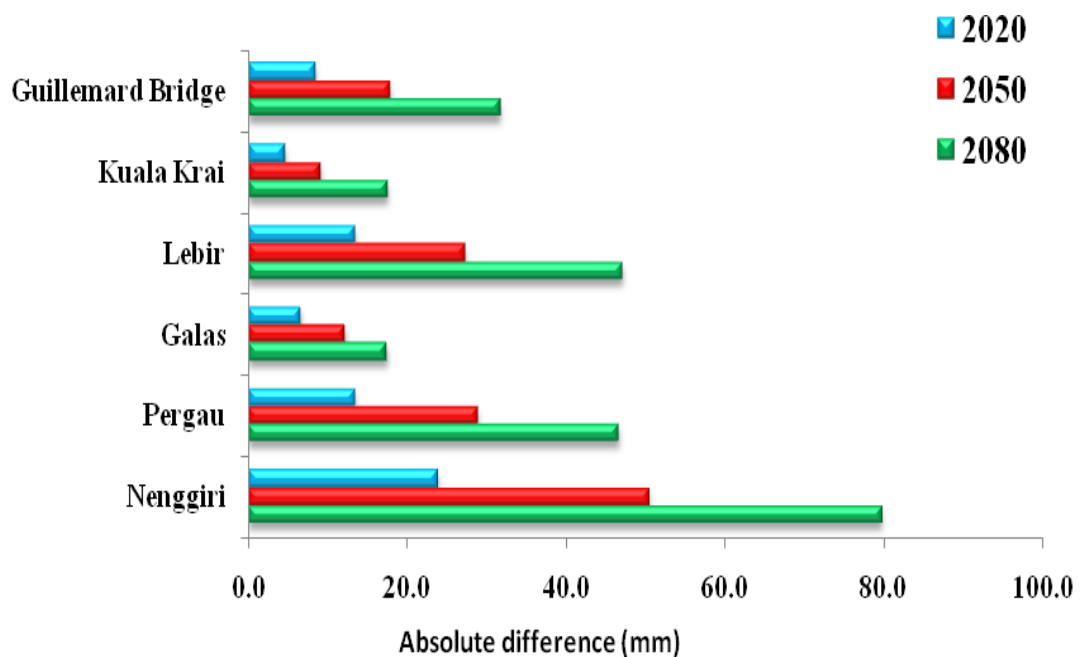
Figure 7-7   The absolute differences in (a) peak discharge and (b) runoff
volume for the 2020s, 2050s and 2080s using the likely projected land use
change for the six gauge stations in the River Kelantan catchment.

(a)   Peak discharge
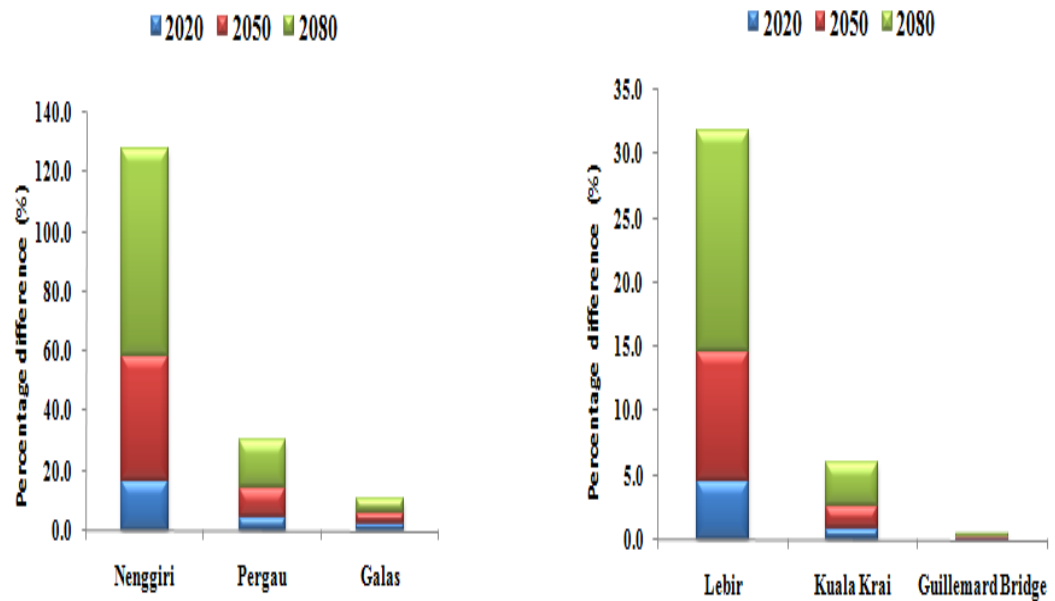
(b)   Runoff volume
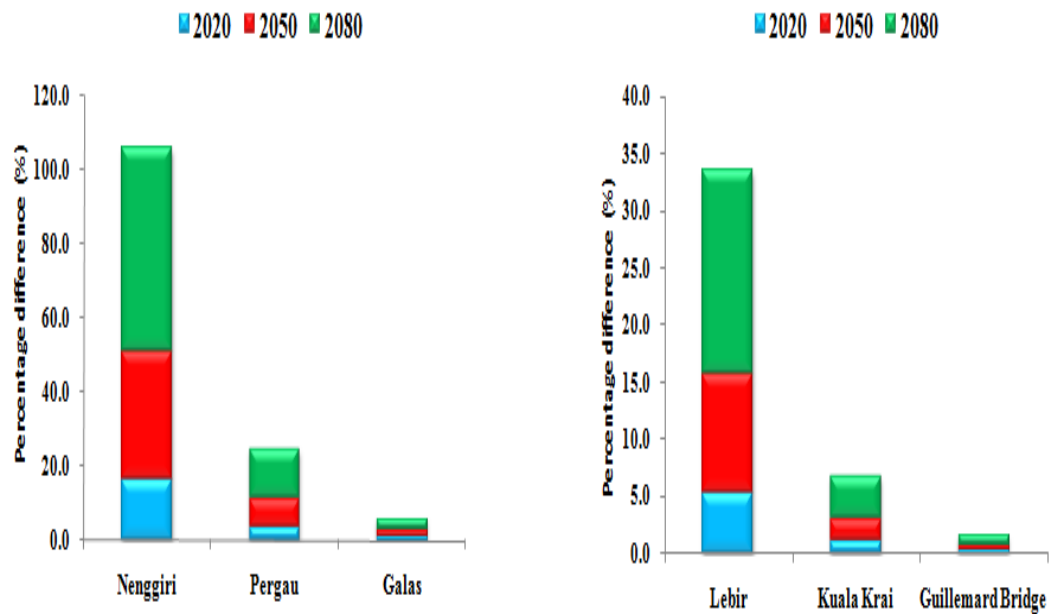
Figure 7-8   The percentage differences in (a) peak flow and (b) runoff
volume for the 2020s, 2050s and 2080s using the likely projected land use
change for the six gauge stations in the River Kelantan catchment.

7.4 Combination of projected climate change and land use

In addition to individual analysis of climate change and land use change effects on runoff response, these two scenarios were combined to quantify the hydrological response in the River Kelantan catchment. This analysis tries to quantify both effects on runoff generation since in reality these two conditions must happen at the same time. The low, medium and high precipitation scenarios were coupled with the likely future projected land use for the periods of 2020s, 2050s and 2080s. The summary of these combinations are presented in Table 7-13 below.

Table 7-13 Combined climate change and land use scenario for future estimation of runoff generation.

| | Time slice | | |
Scenario	2020s	2050s	2080s
Climate change			
Low	-5	-6	+4.1
Medium	-10	+10	+15
High	-18.7	+15	+25
Land use change			
Forest	-15	-40	-60
Agricultural land	+9.2	+30	+40
Built-up land	+5.8	+10	+20

7.4.1 Result of combined scenario

For the 2020s precipitation was predicted to decrease from a low simulation value of -5% to the highest simulation value of -18.7%. This was coupled with decreases in forest and increases in agricultural and built-up lands. The peak discharge showed differences in percentage terms for six gauges with a range of -18.5% to 8.5%. Meanwhile, for the runoff volume the percentage difference lies between -16.1% to 9.3%. All gauges showed decreasing peak discharge and runoff volume with the decreasing in precipitation in low to high simulation combinations except for the Nenggiri station. Interestingly, the Nenggiri station showed that for the low and medium climate change scenarios an increasing trend resulted although precipitation was predicted to decrease. The results may imply that for the upstream station

represented by Nenggiri, land use changes may have a significant effect causing increases in runoff generation compared to the other five gauge station (Table 7-14). In addition, the Nenggiri station demonstrated that with a decrease in precipitation from -5% to -10% together with increases in agricultural land of 9.2% and built up land of 5.8%, peak discharge and runoff volume increased between 0.4% to 9.3%. The high climate change scenario for the Nenggiri sub-basin showed a decreasing trend when precipitation was estimated to decrease by almost -19% (Table 7-14). The other five sub-basins clearly exhibited decreases in trend with the decrease in precipitation rate, which implies that precipitation was a significant factor as compared to land use change. The 2020s absolute differences in peak discharge and runoff volume for six gauge stations in the River Kelantan are shown in Figure 7-9 and Figure 7-10.

The 2050s scenario consists of decreases in precipitation (i.e. -6%) for the low climate change scenario and for the medium and high climate change scenario, increases in precipitation (i.e. 10% to 15%). In this period forest is expected to decrease significantly from -15% (in 2020s) to -40%. The results demonstrate that for the low scenario peak discharge and runoff volume decreased for only three gauges (i.e. Galas, Kuala Krai and Guillemard Bridge). The Nenggiri station once again demonstrated that although precipitation was expected to decrease by the period of the 2050s, peak discharge and runoff volume were estimated to increase by 29.6% and 25.2% respectively for the low climate change scenario. The difference predicted is greater than for the period of the 2020s for the same gauge station (Table 7-14). The increases in runoff volume demonstrated that land use change was a significant factor similar to the 2020s runoff analysis. The historical temporal land use change analysis as discussed in Chapter 5 and simulated future land use projection revealed that the largest forest conversion was to agricultural land with a smaller conversion to built-up land. The other five gauge stations, however, showed a positive relationship with precipitation changes (i.e. increases in precipitation of 10% to 15% together with the land use change scenario, led to increase in runoff generation). The largest increases were demonstrated by the high climate change scenario for which the change in peak discharge was 72.5% (i.e. for Nenggiri). The 2050s absolute differences in peak discharge and runoff volume for six gauge stations in the River Kelantan shown in Figure 7-9 and Figure 7-10.

The 2080s scenario estimates that precipitation increases from 4.1% for the low climate change scenario up to 25% for the high scenario. However, contrary to the periods of the 2020s and 2050s, agricultural land is predicted to increase at a smaller rate compared to the period 2020 to 2050, due to the limited availability of land as explained before. The analysis showed that increases in precipitation together with built-up land and decreases in forested land caused peak discharge and runoff volume continuously to increase from low to high climate change scenario (i.e. 4.2% to 125.8%). In addition, compared to the 2050s analysis, the 2080s analysis exhibited higher increases (i.e. 125.8% in 2080s and 72.5% in 2050s in high scenario) in peak discharge in the Nenggiri station with increases in precipitation from 15% to 25% and built-up land of 30% to 40%. This analysis demonstrated that a reduction in forest area and increases in built-up land can accentuate increases in hydrological response that occur with increases in precipitation (Table 7-14). The 2080s scenario also showed the highest increasing rate in peak discharge and runoff as opposed to the periods of 2020s and 2050s. The effects of land use and precipitation changes on the upstream and downstream areas are summarized in Table 7-15. The overall summary of percentage changes due to land use and precipitation changes to all gauge stations are shown in Table 7-16. The 2080s absolute differences in peak discharge and runoff volume for six gauge stations in the River Kelantan are shown in Figure 7-9 and Figure 7-10.

Table 7-14 Percentage differences in peak discharge and runoff volume for the 2020s, 2050s and 2080s using a combination of climate change and land use change scenarios.

| | Scenario1 | | | Scenario 2 | | | Scenario 3 | | |
| | Low (%) | | | Medium (%) | | | High (%) | | |
	2020s	2050s	2080s	2020s	2050s	2080s	2020s	2050s	2080s
Peak discharge									
Nenggiri	8.5	29.6	78.3	0.4	62.1	102.9	-13.2	72.5	125.8
Pergau	-1.0	3.2	20.6	-6.5	21.5	33.3	-16.0	27.3	45.0
Galas	-2.1	-1.2	8.3	-6.2	11.9	17.1	-13.3	15.9	25.2
Lebir	-1.6	2.2	22.6	-7.8	23.1	37.1	-18.5	29.6	50.4
Kuala Krai	-3.8	-3.8	7.2	-8.5	11.2	17.5	-16.6	15.9	26.9
Guillemard Bridge	-4.8	-5.7	4.2	-9.6	9.8	14.8	-18.0	14.7	24.4
Runoff volume									
Nenggiri	9.3	25.2	62.0	2.2	50.9	81.2	-9.6	59.2	99.1
Pergau	-0.2	3.1	16.4	-4.2	16.3	25.7	-10.9	20.5	34.3
Galas	-0.9	-0.4	4.6	-2.9	6.0	8.9	-6.4	8.0	13.0
Lebir	-0.2	3.9	22.7	-5.5	21.5	35.1	-14.5	27.1	46.6
Kuala Krai	-2.3	-2.0	6.5	-5.6	8.6	13.9	-11.4	12.0	20.6
Guillemard Bridge	-4.1	-4.7	4.5	-8.5	9.2	14.0	-16.1	13.6	22.7

Table 7-15 Differences between upstream and downstream percentage differences in future runoff estimation using climate change and land use change scenarios.

	Scenario 1			Scenario 2			Scenario 3		
	Low			Medium			High		
	2020s	2050s	2080s	2020s	2050s	2080s	2020s	2050s	2080s
Precipitation (%)	-5	-6	4.1	-10	10	15	-18.7	15	25
Forest (%)	-15	-40	-60	-15	-40	-60	-15	-40	-60
Agricultural (%)	9.2	30	40	9.2	30	40	9.2	30	40
Built-up (%)	5.8	10	20	5.8	10	20	5.8	10	20
Upstream: Nenggiri									
Peak discharge (%)	8.5	29.6	78.3	0.4	62.1	102.9	-13.2	72.5	125.8
Runoff volume (%)	9.3	25.2	62	2.2	50.9	81.2	-9.6	59.2	99.1
Downstream: Guillemard Bridge									
Peak discharge (%)	-4.8	-5.7	4.2	-9.6	9.8	14.8	-18	14.7	24.4
Runoff volume (%)	-4.1	-4.7	4.5	-8.5	9.2	14	-16.1	13.6	22.7
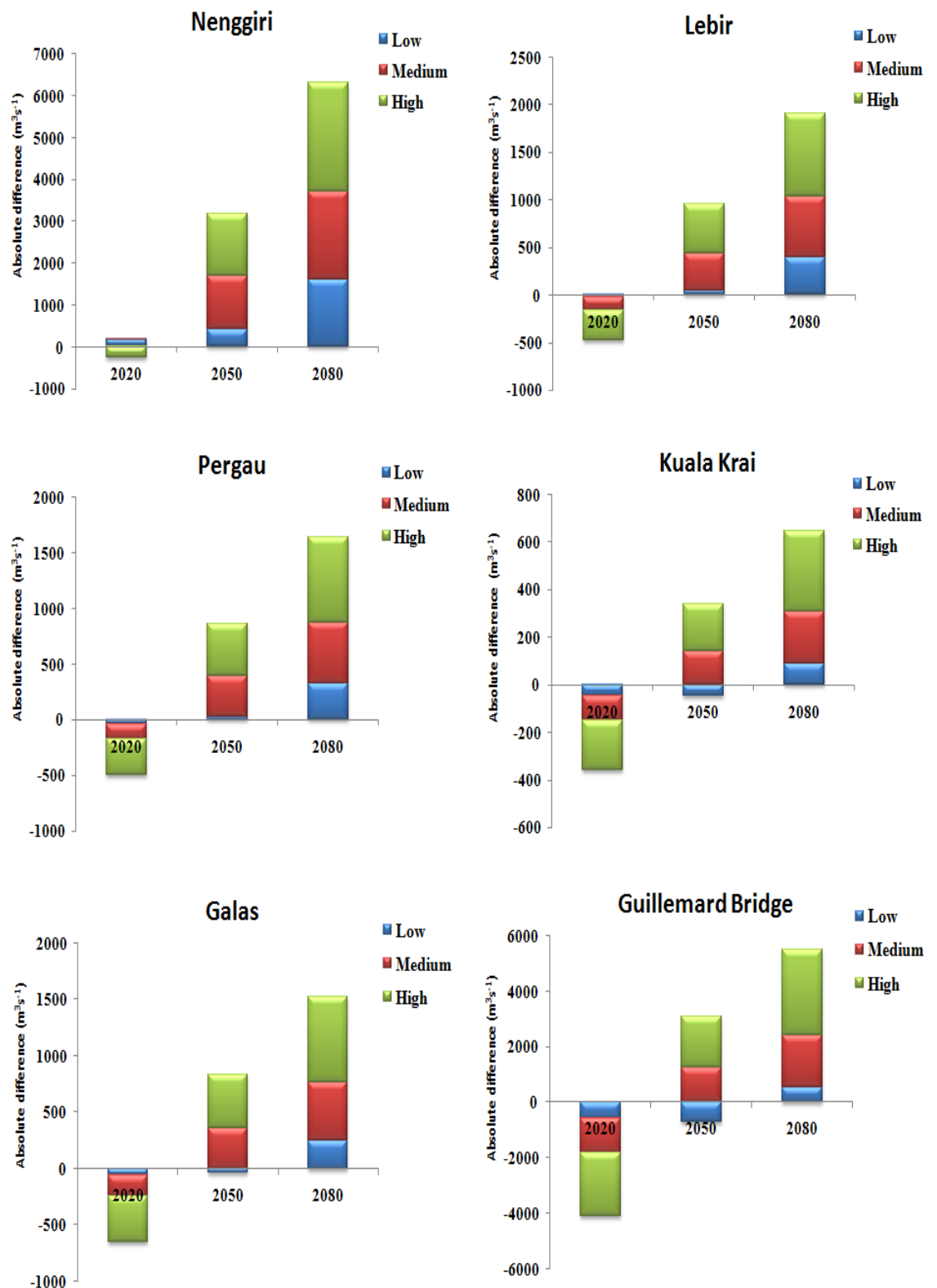
Figure 7-9   Absolute difference in peak discharge for the 2020s, 2050s and 2080s using a combination of climate change and land use change scenarios for the six gauge stations in the River Kelantan catchment.
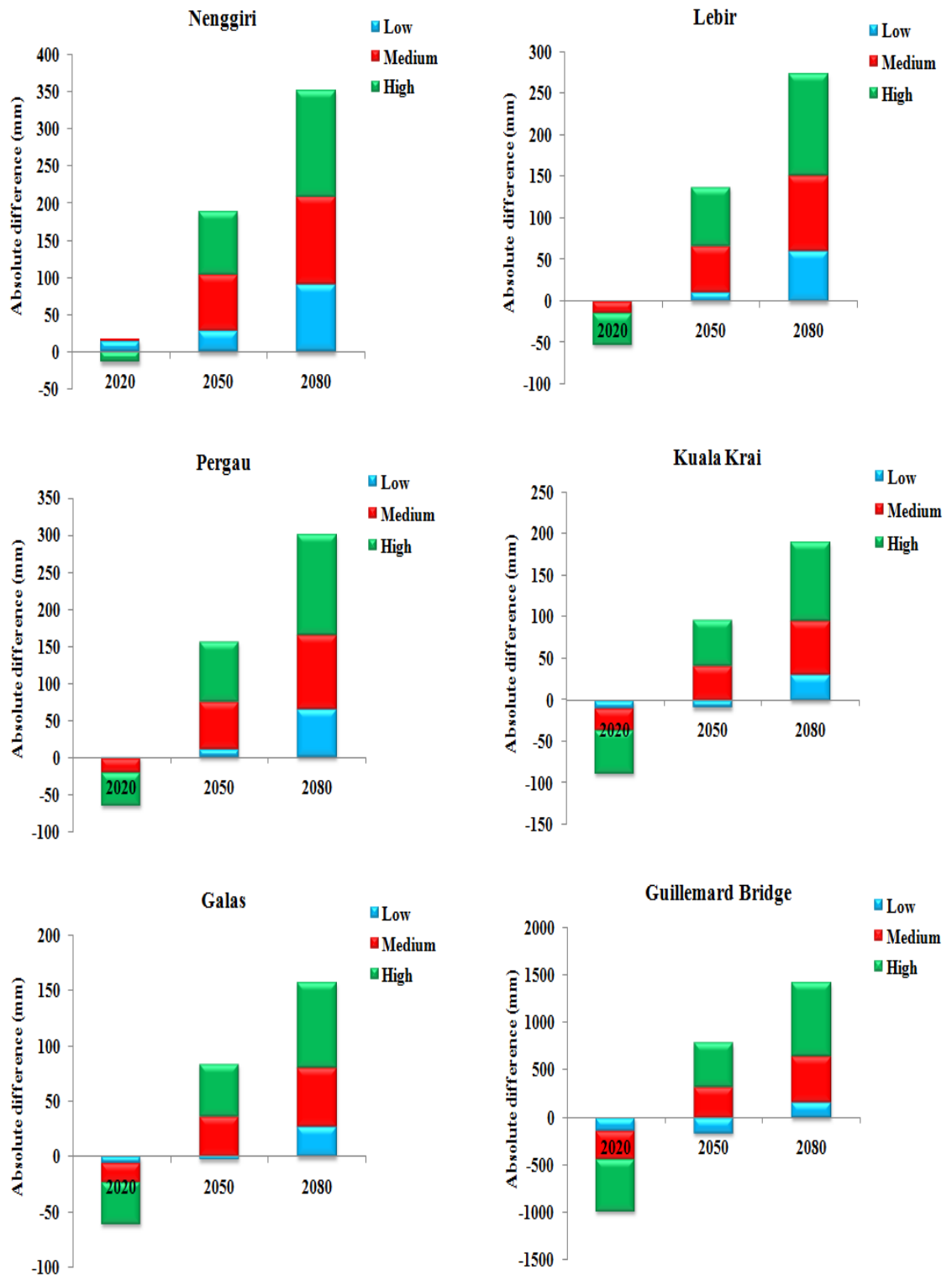
Figure 7-10   Absolute difference in runoff volume for the 2020s, 2050s and 2080s using a combination of climate change and land use change scenarios for the six gauge stations in the River Kelantan catchment.

Table 7-16 Summary percentage differences in peak discharge and runoff volume using a combination of land use and precipitation change scenarios for the 2020s, 2050s and 2080s.

	2020s (%)	2050s (%)	2080s (%)
Peak discharge			
Nenggiri	-13.2 to 8.5	29.6 to 72.5	78.3 to 125.8
Pergau	-16.0 to 1.0	3.2 to 27.3	20.6 to 45.0
Galas	-13.3 to -2.1	-1.2 to 15.9	8.3 to 25.2
Lebir	-18.5 to -1.6	2.2 to 29.6	22.6 to 50.4
Kuala Krai	-16.6 to -3.8	-3.8 to 15.9	7.2 to 26.9
Guillemard Bg.	-18.0 to -4.8	-5.7 to 14.7	4.2 to 24.4
Runoff volume			
Nenggiri	-9.6 to 9.3	25.2 to 59.2	62.0 to 99.1
Pergau	-10.9 to -0.2	3.1 to 20.5	16.4 to 34.3
Galas	-6.4 to -0.9	-0.4 to 8.0	4.6 to 13.0
Lebir	-14.5 to -0.2	3.9 to 27.1	22.7 to 46.6
Kuala Krai	-11.4 to -2.3	-2.0 to 12.0	6.5 to 20.6
Guillemard Bg.	-16.1 to -4.4	-4.7 to 13.6	4.5 to 22.7

7.5   DISCUSSION

The analysis of climate change (i.e. precipitation), land use change and the combination of both scenarios toward runoff generation revealed some interesting outcomes. Using the precipitation scenario for the time periods of 2020s, 2050s and 2080s demonstrated that peak discharge and runoff volume have a positive relationship with the percentage difference in precipitation (i.e. decreases in precipitation caused decreases in runoff generation). Overall, the peak discharge increased up to 39.2% and runoff increased up to 34.0% as presented in the high climate change scenario of 2080s. For the 2020s precipitation simulations, IPCC (2007) stated that water stress was predicted to occur due to precipitation simulated to decrease. In addition, the MMD (2009) predicted that in the Malaysia region less precipitation in the 2020s will also be associated with increases in temperature (i.e. 1.3^{o} C) and also several El-Nino events were also predicted to accompany this period. The study area was simulated to have a reduction in precipitation maximally of about -26.9%. This result may also give implications to the agricultural sector, particularly due to paddy cultivation which is highly dependent on water resources.

Secondly, the land use scenarios that were simulated using two approaches (i.e. land use sensitivity scenario and likely projected change scenario) also revealed some interesting results. The land use sensitivity scenario was used to quantify which land use types have the greatest effect on the hydrological response in the River Kelantan catchment. The conversion of forest to built-up land had the most significant effect on peak discharge and runoff volume, followed by conversion of forest to built-up land and agricultural land jointly. The forest is important to reduce runoff since it provides greater rainfall interception and transpiration due to broader leaves compared to crop vegetation (Bonan, 1997), and deeper rooting which enables more precipitation water to be absorbed into the deeper soil layer (Cornish, 1989; Vertessy, 2000). In contrast, built-up land which is associated with highly impervious areas may cause less water to be absorbed into the soil layer, hence causing high runoff to occur.

The combined land use and precipitation scenario showed that the highest percentage differences in peak discharge and runoff volume were simulated with up to 125.8% and 99.1%, respectively, in the 2080s. This suggests that the magnitude of discharge, and potentially flooding, may intensify if a higher precipitation rate is present in the future coupled with decreases in forest area and increases in built-up and agricultural land area compared to precipitation or land use change alone. Although the simulation managed to show that hydrological response and flooding will intensify due to projected precipitation and land use change, careful interpretation of the result is required. This is due to the limited number of factors in relation to climate change used in the study, whereas, others factors such as change in temperature, atmospheric conditions (i.e. La-Nina and El-Nino events) which are deemed to play significant roles in affecting future hydrological response, are not included in the analysis.

Others factors are important to include in forecasting future hydrological response changes due to climate change. For example, a study of rainfall and temperature pattern in Malaysia by the Meteorological Department showed that the past (and future) climate changes were largely influenced by the relationship between rainfall, temperature and the ENSO phenomenon. For example, dry years observed from 1975 to 2005 were associated with several El-Nino events (MMD, 2009). In particular, the three driest years (i.e 1963, 1997 and 2002) for Peninsular Malaysia have been recorded during EL-Nino events (MMD, 2009). Similarly, wet years observed in 1984,

1988 and 1999 are associated with the La Nina phenomenon. For future climate change scenario assessment nine GCM models were incorporated to study climate change in Malaysia as discussed in Chapter 2 previously. The models projected that an increase in temperature is most apparent towards the late 21st century (i.e 2090 – 2099) (MMD, 2009). However, the same model projected that there is no clear trend shown by all of the selected models due to high variability in precipitation projected for Peninsular Malaysia. Therefore, although this study manages to simulate future climate change scenarios and its impacts on the hydrological response, more climate change factors need to be included such as temperature, evapotranspiration, potential evaporation, sea surface temperature conditions and ENSO to provide more meaningful projections of climate change in the future. Even though this study used annual percentage projection for future event based hydrological model, it does relate to flooding in future. This is because, if using monthly percentage projection for future especially in NE monsoon (October to March) higher intensity of precipitation is usually associated with this monsoon, hence flooding usually happens in this period. So although this study used annual percentage projection for future flooding, the result does reflect reasonably what might happen to flooding in the future.

The Nenggiri sub-basin showed the most interesting results. All of the analyses showed that the station demonstrated the largest difference in peak discharge and runoff volume compared to the other five stations. Moreover, the station which is located in the upstream area experienced the largest land conversion from forest to agricultural land as indicated by the land use change map. It is plausible to suggest that land use change may play the most important role compared to precipitation change in affecting hydrological response in the future for this gauge station, if the percentage of precipitation change was smaller compared to percentage reduction in forest and increase in agricultural and built-up lands as shown by 2020s scenario. This is obviously different to the other five flow gauge stations which showed a positive relationship between precipitation and runoff generation, although the same land use change scenario was used.

The analyses demonstrated that precipitation change and land use change may provide significant effects on runoff generation. The analysis demonstrated that if precipitation decreases within -5% to -10% but with increases in agricultural land of 9.2%, built-up

land of 5.8% and decreases in forested area of 15%, peak discharge still exhibited an increasing trend. However, when precipitation decreased almost by -20%, with the same land use scenario, peak discharge showed a decreasing trend (Table 7-14). A similar result was obtained by Bronstert et al. (2002) who stated that increases of 10 mm to 15 mm (i.e. 50%) of rainfall caused significant differences in peak discharge. Hence using arbitrary values is not an appropriate approach.

Careful consideration of extracting and understanding the result of the impact of climate change on runoff estimation is also important. Although the study was able to demonstrate the influence of precipitation change and land use on runoff generation in the Kelantan catchment, input usage and data used are also important. The first consideration is about uncertainty in the input data. For example, the study extracted precipitation change information from the RCM climate change model which contains uncertainty. It was reported in several studies that RCMs use boundary conditions extracted from GCMs which include systematic errors due to atmospheric dynamics, thus limiting the capability of RCM predictions. In addition, many studies (Bergstrom et al., 2001; Bronstert et al., 2002; Kay et al., 2006) stated that climate change scenarios are derived from various GCM models and each model gives different results in estimating climate conditions for the future. Hence, exploration using multiple models may be necessary to provide insight and understanding on how climate change may affect runoff since it is expected to be a better climate change predictor than individual models (Lambert and Boer, 2001; Prowse et al., 2006; Juckem et al., 2008; Li et al., 2009; Chiew et al., 2010; Chung et al., 2010). However, the disadvantage of using multiple models is solely due to numerical infeasibility. Due to that reason, this study only used single climate change scenarios estimated by a single RCM due to its advantage of relatively high spatial resolution (i.e. 50 km) which is deemed appropriate for the study area. In addition, this study only simulates future changes in hydrological response due to changes in annual precipitation as projected by PRECIS RCM. At this point, there is no climate change model projected for monthly and seasonal precipitation. For that reason, the annual percentage change as projected by PRECIS was used in the HEC-HMS event validated model (i.e. December) for the River Kelantan and hydrological response for the future was discussed (i.e 2020s, 2050s and 2080s).

In addition, the exploration of different storylines under the SRES scenarios may also be appropriate. As presented in this study, only the A1B storyline was used since it provides continued practice of present day standards in regard to socioeconomic activities and fuel type usage and to reduce the complexity of the analysis. Different storylines may be necessary since it may give a broader perspective and expectation in runoff generation. Nevertheless, the real precipitation conditions in the future remain highly uncertain to hydrologists and environmental specialists.

Although the results in this study are not meant to represent actual runoff in the future, the results may be appropriate to be used as useful guidelines for any studies of the implications on society and adaptive requirements for water management practices and land use planning. For an example, policymakers may use the land use scenario approaches for future land use planning and its consequences for hydrological response. According to Kepner et al. (2004) scenario analysis offers several advantages compared to other assessment frameworks since it is able to explore several future projections at one time to facilitate decision making processes. In addition, suitable strategies can be implemented by decision makers, including land use planners, such as controlling rapid urban development, particularly along the river and in floodplain areas, and the implementation of sustainable land use planning involving environmentally-friendly artificial drainage schemes or the development of pervious urban structures. Hence, the risk associated with an increase in the surface runoff hazard can potentially be reduced. This research suggests that future land use planning and development activities should consider the influence of observed and future likely changes in climate (precipitation, temperature and evapotranspiration) on the hydrological response and, thereby, the risk of flooding and plan appropriate mitigation strategies. Futhermore, any development in sensitive areas such as forest reserve areas which are deemed important for water infiltration should be restricted or monitored thoroughly. As mentioned in much research forests can help to reduce runoff water due to infiltration and evapotranspiration capabilities (Moussa et al., 2002; White and Howe, 2004)

The likely projected future land use analysis was derived from several observations of the past land use change, for example, through the temporal land use change map. In addition, due to limited information on spatial land use change in the future for the

study area, this study projected land use change for the future through previous observations of land use change and the possibility of what might happen in the future. Several software packages were deemed suitable and reliable to be used in projecting spatial land use changes such as LULC and *What-if* software. However, the land use prediction using these models requires exhaustive and extensive datasets for topography, physical restriction of the study area to specific land use development, population growth projection, estimation of residential demand, residential density and residential vacancy rate. The scarcity of such data, especially for a developing country, makes it inappropriate, and hence, the simple observation and prediction of future land use scenarios were used.

The study incorporates changes in three particular land use categories which are a decrease in forested land, increase in agricultural land and increase built-up land. This scenario is deemed to be suitable and necessary to be used since land use change analysis in the past showed that these three land use types observed dominated the study area. However, different scenarios may be sufficient to be used to provide greater understanding of natural catchment behaviour changes to policy makers to analyze the extent and magnitude of land use change impacting runoff generation in the future. Greater analysis and understanding of past land use trends might also be possible because it may represent better the trend of land use change over time, and land usage in the future (De Roo et al., 2001; DeFries and Eshleman, 2004; Burns et al., 2005; Yu et al., 2008).

The study used only two images: one to represent previous land use conditions (i.e. 1988) and another one to represent "current" land use conditions (i.e. 2000). However, consideration of the availability and reliability of dynamic temporal images needs to be taken into consideration. For example, frequent temporal images but with high cloud cover may cause error and limitation in analysing land use change analysis over time. As for this study, due to the tropical weather zone thick cloud cover was present in the study area. Hence, this limited the user capability to estimate accurately the land use change. However, to overcome this problem a masking process for cloud cover was adopted to eliminate the affected area so that reliable (i.e. accuracy assessment with higher than 85%) land use change estimation could be done.

The study also used SCS CN to quantify how land use affected the water loss in the chosen runoff model. The method utilized all land use information and also took into account impervious surface area (ISA) because it determines the volume of direct runoff in the area under investigation. The study used Landsat TM images with spatial resolutions of 30 m per pixel to calculate ISA. However, to have more informative representation, different remotely-sensed images from different sensors may be appropriate to use such as IKONOS with a 4 m spatial resolution and to the extreme extent of LiDAR imagery with a 1 m spatial resolution. However, the disadvantage of these kinds of images is cost to acquire these images and moreover, it is time consuming and highly technical image processing is needed to derive the needed information such as land use change map and ISA percentage.

In explaining why trends (i.e. increasing or decreasing) in stream flow are exhibited in the river under investigation, possible links to precipitation and land use might be plausible causes as demonstrated in this study. However, other factors such as temperature and evapotranspiration condition are also plausible in describing changes in discharge and the intensity and magnitude of potential flooding in the future. An increase in temperature will cause increases in precipitation to the catchment. High density of forest area will cause a high evapotranspiration rate at the time of the storm event due to high interception of the forest canopy. A study by Jiang et al. (2007) demonstrated that increases of precipitation by 20% with an increase in temperature by 1^0C, 2^0C and 4^0C have caused annual runoff increases in the range of 15% to 35%. The same study also concluded that runoff changes are more sensitive to precipitation changes than to the temperature changes. Similarly, Chiew et al. (1995) found that in Australia, an increase in temperature from 0.2 to 0.6^0C with summer rainfall increases by up to 6% caused runoff increases of up to 25%. In addition, Yao et al. (2009) simulated that afforestation in the Hiji River basin, Japan caused increases in evapotranspiration (i.e. 37%) and led to reduced annual runoff (i.e. -11%). However, this study in the River Kelantan catchment did not incorporate temperature due to incomplete information in the temperature record for the chosen storm event modelled and evapotranspiration was deemed not to be significant for the shorter storm events due to high moisture conditions related to heavy precipitation.

Although the study managed to demonstrate the future hydrological response and potential flooding in the future by manipulating the climate change scenarios, one potentially limiting simplification is that the same relative changes are assumed for all years and for extreme values as well as for average conditions (Bergstrom et al., 2001).

7.6 SUMMARY

This chapter simulated future changes in runoff for the time slices of 2020s, 2050s and 2080s by incorporating three input conditions which are climate change, land use change and the combination of climate and land use change. Overall, the results estimated that climate change is positively related with the peak discharge and runoff volume. If precipitation is estimated to decrease using the A1B storyline from the SRES scenario, runoff was predicted to decrease and *vice-versa*. In addition, the 2080s period has the highest percentage increase in peak discharge and runoff volume using climate change scenarios as compared to the other two periods. The land use change analysis also indicated significant potential impact on runoff generation in the future. The scenario involved reducing forest area, and increases in agricultural land and built-up land. This caused runoff estimated to increase from the 2020s to the 2080s. In some scenarios, precipitation was predicted to decrease, but with increases in land use types such as built-up and agricultural land, peak flow and runoff volume continued to increase. Finally, the combined scenario demonstrated that precipitation coupled with land use change has a significant impact on both increasing and decreasing peak discharge and runoff volume for the study area compared to climate change and land use change alone. The information derived from this analysis is important for future land use planning as well as water management practices.

Chapter 8

Conclusions and recommendations

8.1   CONCLUSIONS

8.1.1 Analysis 1: Time-series analysis

The main aim of the time-series analysis conducted in Chapter 5 was to identify and quantify historical trends in streamflow for the upstream and downstream parts of the River Kelantan catchment. Further trends in precipitation (or climate change) and land use change were also performed to understand the trends detected in the steamflow data. The streamflow time-series analysis revealed that the Mann-Kendall trend detection was suitable method to detect trends in hydrological data for monsoonal areas such as the River Kelantan catchment.

Streamflow in the upstream area (i.e. River Galas) exhibited increasing trends in the annual, seasonal and monthly analyses. However, precipitation stations associated with the River Galas streamflow station only showed several trends, especially for the October-November-December (OND) season. The streamflow trends result associated with precipitation trends indicated that climate change might have contributed to increasing streamflow in the River Galas, particularly in the wet season. However, the land use change analysis using 1988 and 2000 Landsat TM data revealed more interesting findings. Land use conversion from forest to agricultural areas of about 70% from 1988 to 2000 are a plausible cause of increasing streamflow in the upstream area in addition to climate change.

In the downstream area (i.e. River Kelantan) streamflow trends were apparent for the seasonal and monthly analyses. The streamflow trends were supported by an increasing trend in precipitation for the wet seasons (i.e. JFM and OND) and a decreasing trend for the dry season (i.e. JAS). The land use change analysis revealed that afforestation had occurred in the downstream area due to increases in bamboo forest as reported by the Kelantan Forest Department. The agricultural area also increased, but by only 22.4% compared to the upstream area of 66.2%. It is plausible to infer that land use change analysis may have contributed to increasing streamflow trends in the upstream area compared to the downstream area.

From these preliminary findings, the information on precipitation and land use was used further in the runoff model developed using the HEC-HMS. The runoff model was performed to quantify the effects of climate change and land use change on runoff and potentially flooding events in the River Kelantan catchment. The event runoff model was chosen due to the unavailability and severely missing data of precipitation and temperature gauge stations required for the continuous runoff model. Therefore, an event based model was used to quantify precipitation and land use changes to hydrological response using previous (1988) and 'current' (2004) flooding events. The summary of the findings in the runoff model are explained in the next section.

8.1.2 Analysis II: HEC-HMS rainfall-runoff model

From the first analysis, several trends were detected in streamflow for the upstream and downstream areas. Two factors to study such trends exhibited were the links to precipitation and land use change. However, for the upstream area, land use change was suggested to be a plausible factor in describing observed trends, and in the downstream area streamflow trend observed was suggested as likely caused by precipitation mainly. Although time-series analysis managed to reveal trends exhibited in the River Kelantan catchment, the disadvantage of the technique is that it is unable to quantify how much of each factor contributes to runoff generation. Therefore, a second analysis was conducted to explore and quantify how much climate change and land use change affect the hydrological response in the study area using a semi-distributed rainfall-runoff model based on HEC-HMS.

The runoff model for the River Kelantan catchment was developed and six sub-basins were delineated using the HEC-GeoHMS tools, land use types and soil types. The model used the SCS CN and SCS UH to calculate rainfall losses for pervious surfaces and the transform model to calculate direct runoff transformation for impervious surfaces. The simulated model was able to produce an appropriate hydrograph when compared to the observed hydrograph for the 2004 runoff model. The calibration was performed and the results showed that appropriate model efficiency was achieved. Further, model validation was performed and acceptable hydrographs between simulated and observed hydrographs were obtained. The peak discharge and runoff volume in 1988 were observed to be lower than in the 2004 runoff model. Evapotranspiration was not included because many studies have previously suggested that in a storm event, evapotranspiration is not significant in affecting the hydrological response. The runoff hydrographs that were derived were deemed to represent appropriate hydrographs and were acceptable since the main aims of the runoff model development was to establish a repeatable procedure to simulate land use and climate change effects and not to replicate perfectly the observed hydrographs.

Sensitivity analysis also demonstrated that two parameters caused significant differences in hydrological response which are the SCS CN value and lag time. These two parameters caused larger differences in peak discharge, runoff volume, total direct runoff, total baseflow and total loss. The CN integrates land use as well as soil type information. Therefore, the loss model using the CN was deemed to be appropriate in the study to analyse land use changes that have occurred in the River Kelantan catchment (Hernandez et al., 2000; Kim et al., 2010). The huge forest conversion to agricultural lands was observed particularly in the upstream area. Appropriate representation of land use conditions needs careful consideration, especially when choosing a reliable loss model which is used to quantify effective rainfall and direct runoff in the hydrological model. For example, another loss model such as the initial and constant method (USACE, 2000) was deemed inappropriate in its representation of land use information since this method only considers interception and depression storage.

Subsequently, to quantify the effects of climate variability and land use change on runoff generation, the 2004 runoff model was used as a baseline model to see the

effects on runoff generation. The other parameters were kept constant, while land use and climate change inputs in 2004 were replaced by the 1988 input. The result showed that, in the upstream area, the observed precipitation and land use changes contributed to large increases in peak discharge and runoff volume, with observed precipitation changes causing increases about three-to-four times larger than the observed land use changes. In contrast, in the downstream area, the large observed precipitation changes predicted by the trend analysis were the only cause of increases in the hydrological response, with land use changes leading to a slight decrease in response. It is plausible to suggest that during the monsoon season, with heavy precipitation and the large area involved, the effect of land use change on the hydrological response may reduce and allow precipitation to become the dominant factor in causing changes in peak discharge and runoff volume (Van Deursen and Middlekoop, 2002; Saghafian et al., 2008).

The analysis managed to provide a framework into which to differentiate and quantify the effect of climate and land use change factors in understanding the behaviour of the hydrological system in a monsoon catchment. Individual climate change and land use change factors produced different effects on the hydrological response. It was clearly shown that land use factors may be significant in affecting a sub-basin if the area is dominated by forest as shown in Nenggiri as well as Lebir. On the other hand, for semi-developed or developed sub-basins with a higher percentage of impervious surfaces already dominating, climate change (i.e. precipitation) played the most significant role as observed in the Guillemard Bridge sub-basin.

In a decision-making process, the cause and effects of environmental changes within a certain area need to be known prior to any development planning taking place. The study clearly revealed the effect in the River Kelantan catchment, which hydrological response has changed over time with increases in peak discharge and runoff volume observed. This analysis was done solely to quantify and understand the causal factors of such changes. It was hypothesised that both climate change and land use change may be causes of such increasing trends as revealed in the upstream and downstream areas. The question is how much each of these factors significantly affects the observed trends. To provide an answer, a rainfall-runoff model was performed which calculated the percentage of change in peak discharge and runoff volume due to precipitation and land use changes in the upstream and downstream areas in the River Kelantan

catchment. However, only the event-based model was developed using HEC-HMS. This is solely due to severely missing data on precipitation, streamflow and temperature, recorded by DID. The DID utilizes three methods of precipitation data collection known as manual, chart recording and data logging which are simultaneously used at most precipitation stations. This approach leads to the occurrence of missing data in three patterns (missing data from one recording method or two recording method or all three recording methods) (Malek et al., 2009). In addition, some data records are not reliable. For example, in some rare cases all the data exhibit the same value for a long period. These may due to the failure of instruments or human errors while collecting or downloading the data (Chin, 2007). Therefore, an event based model was used due to the complete data record for the chosen years (i.e 2004). The primary aim of Analysis II or developing an event-based runoff model was solely to quantify the effects of climate variability (i.e precipitation) and land use changes on flooding events in the River Kelantan catchment.

8.1.3   Analysis III: Future simulation scenarios

For water resources planning, understanding of what is currently observed in the catchment and prediction of what might happen in the future is essential in controlling environmental hazards. For this reason, in Chapter 7, what might happen in the future if hypothetical climate change and land use change were to occur was simulated. Climate change scenarios were adopted from the RCM models applied by the Department of Meteorology in Malaysia using the Hadley Centre Climate model. Meanwhile land use estimation was based on land use sensitivity scenarios and likely projection scenarios about future conditions. Climate change projections predict that for the first period (i.e. 2020s) water stress would happen due to decreasing rainfall, hence causing peak discharge and runoff volume to show similar decreasing trends. However, the same model demonstrated that over time, increases in precipitation would occur. Runoff model simulation was calculated from a baseline model in 2004. In general, if precipitation increases it will cause increases in peak discharge and runoff volume as well as potentially in flood magnitude in the future.

Land use change analysis for the future scenario also led to interesting findings. The main findings demonstrated that forest plays an important role in controlling water flow

and subsequently minimizing the flood magnitude in the downstream area. If forest were replaced by different land use types such as agricultural and built-up land, less infiltration would be expected to occur and hence a higher peak discharge and runoff volume would be predicted. The what-if land use change scenario simulated that if forest was converted to built-up and agricultural lands, greater peak discharge and runoff volume were derived. However, if forest was fully converted to urbanization or to agricultural land only, smaller peak discharge and runoff volumes were observed. Secondly, forest conversion through urbanization revealed the second highest changes in hydrological response as compared to forest fully converted to agricultural land. This may suggest that if more urbanization happens in the future higher peak discharge may be expected due to higher direct runoff from increased impervious surfaces. Although future conditions are highly uncertain in terms of land use changes as well as climate change, the potential of each change to impact runoff generation needs to be considered. Predicting the potential impact of climate change and land use changes on peak discharge and runoff volume in the downstream of the River Kelantan catchment is very important since changes in the magnitude of flooding and a greater extent of affected flooding area have been observed (e.g. flooding in 2004, 2006 and 2007). Understanding and quantifying these effects will aid water resource management and land use planners and policy makers to make better decisions, especially to reduce encroachment to highly sensitive areas such as the floodplain.

8.2   Limitations of the study

Several limitations of the study need to be presented. This is due to many factors such as specific climate conditions of the study area (i.e. monsoon catchment, heterogeneous land use types), limitations in data used (i.e. streamflow, precipitation, remotely-sensed images), limitations in climate change factors (i.e. not including temperature, evapotranspiration, ENSO phenomena). Some of the limitations of the study are described as follows.

8.2.1 Variables for time-series trend analysis

Stream flow trends were considered only using the mean annual, seasonal and monthly variables. Hence, no further exploration into other hydrological variables such as

maximum annual, extreme flow or number of rainy days was taken into consideration due to data problems (i.e missing data and incompleted data in streamflow and precipitation for the chosen periods). Many studies indicate that extreme flows need to be studied in order to understand more about potential floods that have occurred or may happen in the future (Frei et al., 2000; Schreider et al., 2000; Buchele et al., 2006; Fowler and Kilsby, 2007).

8.2.2 Land use change

The land use classification was derived from Landsat TM with a 30 m spatial resolution. The land use change map used only using two temporal dates (1988 and 2000) due to the availability of data to represent the entire coverage of the study area. A previous land use map (i.e. before 1980s) would provide more dynamic changes in land use, especially in relation to urbanisation which represents impervious surface area, as well as agricultural lands. Due to the non-existence of Landsat TM images before the 1980s, the study used only two images (i.e. 1988 and 2000) and this was deemed appropriate to represent the land use changes that have occurred in the study area.

Land use changes were projected using a simple approach (i.e. observation of past and current land use changes) and no spatial land use analysis was incorporated such as using LULC what-if scenario software (i.e. *What-if*, SLEUTH, etc.). Furthermore, the land use percentage of change was standardized for all sub-basins within the study area. In reality, not all sub-basins will experience equal development and will normally be subjected to local land use planning policy. However, this method was adopted to provide the potential causes of land use and climate change on the hydrological response and potentially flooding in the future.

8.2.3 Hydrological model

A semi-distributed runoff model (i.e HEC-HMS) was used in this study which can integrate, semi-spatially, the spatial variability within a catchment. However, for a large catchment, it is more appropriate to use a fully distributed runoff model because the hydrologic system in a large catchment often exhibits a large degree of spatial

heterogeneity in its characteristics (Ajami et al., 2004). The distributed model has the ability to explicitly represent the spatial variability in a large catchment (Reed et al., 2004). However, in this study of the River Kelantan catchment, a fully distributed runoff model was not suitable to be use due to limited availability of data such as radar-based precipitation (i.e NEXRAD by US) , high resolution of DEM data (i.e 1 m), high-scale or detailed soil and land use maps (i.e 1/25,000) which are required for use in a distributed runoff model.

This study utilized only medium spatial resolution DEM data of SRTM with 30 m spatial resolution. According to Chaplot (2005), the quality of spatial data may significantly affect the simulation results of hydrological models. The high resolution DEM data are deemed important in sub-basin delineation. High DEM resolution data are useful if such data exist such as DEM derived from Light Detection and Ranging (LiDAR) with spatial resolution of approximately 1 m. Although these data are currently available, they are not suitable for a large catchment area because LiDAR is very costly to acquire for a large area (Burtch, 2002) such as the River Kelantan catchment. Moreover, sophisticated algorithms and complicated post-processing of data are also required (Burtch, 2002). Although this study used a 30 m DEM resolution, acceptable sub-basin delineation was performed.

To understand the causes of changes in observed streamflow in the Kelantan catchment, links to precipitation and land use change were necessary. The relationships between these three conditions reveal a significant result for the historical and current event-based runoff models. The calibration and validation periods used only two events. Each period was calibrated and validated differently because of rapid changes in land use as well as climate changes which can alter the natural behaviour of the system in the catchment such as water travel time, infiltration capacities and capabilities. However, a continuous-based runoff model is suitable to be used. It is because this model is able to include other hydrological components such as temperature, ENSO conditions, and evapotranspiration rate. Hence, inter-seasonal and monthly variations were unable to be projected. This study utilized only an event-based runoff model due to limited data on hydrological components as described above.

The study used climate projections from a dynamically downscaled RCM. Another method (as described in Chapter 2), statistical downscaling, can be use to derive future

projections of precipitation (monthly or seasonal). The RCM (i.e PRECIS HadCM3) precipitation projection was only projected for annual precipitation changes of the future (i.e 2020s, 2050s and 2080s). This annual projection was used in the event-based model (i.e. December storm event) of the River Kelantan catchment. Therefore, different result from different downscaling methods may suitable to be used to provide more meaningful future flooding scenarios. In addition, the study used only climate change projections from the UK Hadley Centre and the model was not integrated with different SRES emissions scenarios (i.e. 1A, 1B, A1F1 scenarios, etc.) or different GCM or RCM climate change models. Several studies as discussed in Chapter 7 found that different models will give different precipitation scenarios for any particular region. Therefore, due to the uncertainty in future projections of climate change, different emissions scenarios should be incorporated when evaluating future hydrological response to help water resource managers or policy makers in decision making processes.

8.3 Recommendations

- In projecting land use for the future, a land use dynamics model may be deemed suitable for use. This will integrate spatial and temporal considerations, and hence differences in land use change rates between sub-basins rather than using standard development rates for all sub-basins.

- In this research, land use change was standardized for all sub-basins using the same percentage of increasing and decreasing values. Different proportions of changes in land use and projected precipitation (i.e. if such data are available) may be appropriate to be used since in land development sub-basins may have different land use projections and different precipitation amounts that fall within a sub-basin.

- Finer spatial resolution images such as provided by IKONOS with a 1 m spatial resolution may provide a more detailed classification of land use. In the research, the Landsat TM image caused interruptions to land surface mapping due to cloud cover as observed in the images.

- Further research using a continous rainfall-runoff model instead of an events based model may be appropriate to provide insights and understanding into

changes that happen in a catchment behaviour system. Temperature and evapotranspiration changes may be deemed appropriate to be included.

- Time-series studies can be carried out to explore the linkages of streamflow trends to temperature as well as ENSO conditions, apart from precipitation and land use changes. This will provide a comprehensive understanding and representation of reliable rainfall-runoff in the study area. In addition, in future time-series studies exploration into other hydrological variables such as maximum annual, extreme flow or number of rainy days should be taken into consideration.

- The RCM used by MMD known as PRECIS HadCM3 model is a dynamic downscaling model from GCM. The dynamic approach has some limitations and disadvantages as discussed in Chapter 2. Therefore, projections of future climate from different methods such as statistical downscaling should be used for forecasting hydrological responses due to climate change.

- As described earlier, this study used only annual precipitation changes (in percentage) for an event based runoff model. The future projection of climate change for monthly and seasonal periods should be used, where the information is available, to provide more meaningful representations of future hydrological response projections.

8.4   CONCLUDING REMARKS

The research explored the trends in streamflow in the Kelantan catchment, which is highly influenced by the monsoonal weather. Two factors were considered to associate such detected trends in streamflow which are climate change (i.e. precipitation) and land use change. Both factors were demonstrated to play an important role in causing such detected trends. Changes in precipitation, as expected given the high intensity of monsoonal rainfall, caused greater changes in peak discharge and runoff volume compared to land use changes in the River Kelantan catchment. However, land use changes, particularly increases in urbanization and agricultural lands caused intensification in runoff volume in the upstream part of the catchment.

From the new understanding of what affects hydrological response, the research demonstrated what might happen in the future if predicted climate changes and land

use changes take place. If precipitation increases it will cause increases in the hydrological response (i.e. peak discharge and runoff volume) and land use scenarios demonstrated that forest plays an important role in controlling water flow and subsequently minimizing the flood magnitude. The knowledge gathered from this analysis can lead to improve management policies, especially to mitigate changes in hydrological response and their consequences. Based on such information, suitable strategies can be implemented by decision makers, including land use planners, such as controlling rapid urban development, particularly along the river and in floodplain areas. As suggested earlier in Chapter 7, the policymakers may use the land use scenario approaches for future land use planning and forecasting its consequences on the hydrological response. In addition, suitable strategies can be implemented by decision makers, including land use planners, such as an implementation of sustainable land use planning involving environmentally-friendly artificial drainage schemes or the development of pervious urban structures. Hence, the risk associated with an increase in the surface runoff hazard can potentially be reduced. This research also suggests that future land use planning and development activities should consider the influence of observed and future likely changes in climate (precipitation, temperature and evapotranspiration) on the hydrological response and, thereby, the risk of flooding and plan appropriate mitigation strategies.

Appendices

APPENDIX 1: MAXIMUM LIKELIHOOD (ML) ACCURACY ASSESSMENT RESULT

Table 1 The confusion matrix table (i.e. accuracy assessment) of the 1988 ML classification.

Overall Accuracy	0.89495639	**89.50%**
Kappa Coefficient	0.8084	

	Ground Truth (Pixels)									
Class	**Forest**	**Built-up**	**Paddy**	**Mangrove**	**Oil palm**	**Rubber**	**Mixed-agriculture**	**Water**	**Bare-soil**	**Total**
Forest	1664	0	34	0	0	0	0	0	0	1698
Built-up	0	80	0	0	0	0	0	0	0	80
Paddy	0	0	40	0	0	0	0	0	0	40
Mangrove	0	0	28	206	0	0	0	0	0	234
Oil palm	116	0	0	0	129	0	0	0	0	245
Rubber	0	0	0	0	0	121	0	0	0	121
Mixed-agriculture	0	0	0	0	0	0	40	0	0	40
Water	0	0	0	0	0	0	0	25	0	25
Bare soil	0	0	99	0	0	0	0	0	55	154
Total	**1780**	**80**	**201**	**206**	**129**	**121**	**40**	**25**	**55**	**2637**

	Ground Truth (Percent)									
Class	Forest	Built-up	Paddy	Mangrove	Oil palm	Rubber	Mixed-agriculture	Water	Bare-soil	Total
Forest	93.48	0	16.92	0	0	0	0	0	0	64.39
Built-up	0	100	0	0	0	0	0	0	0	3.03
Paddy	0	0	19.9	0	0	0	0	0	0	1.52
Mangrove	0	0	13.93	100	0	0	0	0	0	8.87
Oil palm	6.52	0	0	0	100	0	0	0	0	9.29
Rubber	0	0	0	0	0	100	0	0	0	4.59
Mixed-agriculture	0	0	0	0	0	0	100	0	0	1.52
Water	0	0	0	0	0	0	0	100	0	0.95
Bare soil	0	0	49.25	0	0	0	0	0	100	5.84
Total	100	100	100	100	100	100	100	100	100	100

Class	Commission (Percent)	Omission (Percent)	Commission Pixels)	Omission (Pixels)	Producer Accuracy (Percent)	User Accuracy (Percent)	Producer Accuracy Pixels)	User Accuracy (Pixels)
Forest	2	6.52	34/1698	116/1780	93.48	98	1664/1780	1664/1698
Built-up	0	0	0/80	0/80	100	100	80/80	80/80
Paddy	0	80.1	0/40	161/201	19.9	100	40/201	40/40
Mangrove	11.97	0	28/234	0/206	100	88.03	206/206	206/234
Oil palm	47.35	0	116/245	0/129	100	52.65	129/129	129/245
Rubber	0	0	0/121	0/121	100	100	121/121	121/121
Mixed-agriculture	0	0	0/40	0/40	100	100	40/40	40/40
Water	0	0	0/25	0/25	100	100	25/25	25/25
Bare soil	64.29	0	99/154	0/55	100	35.71	55/55	55/154

Table 2 The confusion matrix table (i.e. accuracy assessment) of the 2000 ML classification.

Overall Accuracy	0.96913137	96.91%
Kappa Coefficient	0.9632	

	Ground Truth (Pixels)									
Class	Forest	Built-up	Bare-soil	Oil palm	Paddy	Mangrove	Rubber	Mixed-agriculture	Water	Total
Forest	407	0	0	0	0	0	42	0	0	449
Built-up	0	122	0	0	0	0	0	0	0	122
Bare-soil	0	0	152	0	0	0	0	0	0	152
Oil palm	1	0	0	77	0	0	0	0	0	78
Paddy	0	0	0	0	112	0	0	0	0	112
Mangrove	0	0	0	0	0	185	0	0	0	185
Rubber	0	0	0	0	0	0	126	0	0	126
Mixed-agriculture	0	0	0	0	0	0	0	133	0	133
Water	0	0	0	0	0	0	0	0	36	36
Total	408	122	152	77	112	185	168	133	36	1393

	Ground Truth (Percentage)									
Class	**Forest**	**Built-up**	**Bare-soil**	**Oil palm**	**Paddy**	**Mangrove**	**Rubber**	**Mixed-agriculture**	**Water**	**Total**
Forest	99.75	0	0	0	0	0	25	0	0	32.23
Built-up	0	100	0	0	0	0	0	0	0	8.76
Bare-soil	0	0	100	0	0	0	0	0	0	10.91
Oil palm	0.25	0	0	100	0	0	0	0	0	5.6
Paddy	0	0	0	0	100	0	0	0	0	8.04
Mangrove	0	0	0	0	0	100	0	0	0	13.28
Rubber	0	0	0	0	0	0	75	0	0	9.05
Mixed-agriculture	0	0	0	0	0	0	0	100	0	9.55
Water	0	0	0	0	0	0	0	0	100	2.58
Total	**100**	**100**	**100**	**100**	**100**	**100**	**100**	**100**	**100**	**100**

Class	**Commission (Percent)**	**Omission (Percent)**	**Commission (Pixels)**	**Omission (Pixels)**	**Producer Accuracy (Percent)**	**User Accuracy (Percent)**	**Producer Accuracy (Pixels)**	**User Accuracy (Pixels)**
Forest	9.35	0.25	42/449	1/408	99.75	90.65	407/408	407/449
Built-up	0	0	0/122	0/122	100	100	122/122	122/122
Bare-soil	0	0	0/152	0/152	100	100	152/152	152/152
Oil palm	1.28	0	Jan-78	0/77	100	98.72	77/77	77/78
Paddy	0	0	0/112	0/112	100	100	112/112	112/112
Mangrove	0	0	0/185	0/185	100	100	185/185	185/185
Rubber	0	25	0/126	42/168	75	100	126/168	126/126
Mixed-agriculture	0	0	0/133	0/133	100	100	133/133	133/133
Water	0	0	0/36	0/36	100	100	36/36	36/36

APPENDIX 2: THE PRECIPITATION FUTURE SCENARIO RESULTS OF PEAK DISCHARGE AND RUNOFF VOLUME USING PRECIS PROJECTIONS

Table 3 The baseline and simulated peak discharge and runoff volume using HadHCM AIB precipitation scenario for the 2020s.

Station	2004 (m^3s^{-1}) Current	Future 2020 (m^3s^{-1}) Low	Medium	High
Nenggiri				
Peak discharge	*2055.0*	1903.5	1753.7	1501.2
Runoff volume	*145.36*	136.2	127.14	111.95
Pergau				
Peak discharge	*863.7*	819	772.3	692.3
Runoff volume	*359.4*	346.34	332.64	309.23
Galas				
Peak discharge	*3010.5*	2886.5	2762.4	2546.4
Runoff volume	*595.9*	584.08	572.28	551.78
Lebir				
Peak discharge	*1724.2*	1618.5	1513.6	1333.3
Runoff volume	*261.64*	248.12	234.76	211.96
Kuala Krai				
Peak discharge	*1243.7*	1185.4	1127	1025.7
Runoff volume	*461.21*	445.98	430.79	404.52
Guillemard Bridge				
Peak discharge	*12615.2*	12003.5	11392.1	10327.9
Runoff volume	*3440.23*	3289.77	3139.85	2879

Table 4 Peak discharge and runoff volume estimation using HadHCM AIB scenario for the 2050s.

Station	2004 (m^3s^{-1})	Future 2050 (m^3s^{-1})		
	Current	Low	Medium	High
Nenggiri				
Peak discharge	*2055.0*	1873.3	2370.9	2532.1
Runoff volume	*145.36*	134.37	164.65	174.51
Pergau				
Peak discharge	*863.7*	809.6	961.7	1009.9
Runoff volume	*359.4*	343.59	388.38	402.66
Galas				
Peak discharge	*3010.5*	2861.7	3258.5	3382.4
Runoff volume	*595.9*	581.72	619.57	631.42
Lebir				
Peak discharge	*1724.2*	1597.5	1937.6	2045
Runoff volume	*261.64*	254.44	289.09	303
Kuala Krai				
Peak discharge	*1243.7*	1173.7	1360.5	1418.9
Runoff volume	*461.21*	442.94	491.82	507.18
Guillemard Bridge				
Peak discharge	*12615.2*	11881.2	13836.3	14447
Runoff volume	*3440.23*	3259.79	3739.6	3889.59

Table 5 Peak discharge and runoff volume estimation using HadHCM AIB scenario for the 2080s.

Sub-basin	2004 (m^3s^{-1})	Future 2020 (m^3s^{-1})		
	Current	Low	Medium	High
Nenggiri				
Peak discharge	*2055.0*	2184.1	2415.4	2861.3
Runoff volume	*145.36*	153.24	167.09	194.75
Pergau				
Peak discharge	*863.7*	905.1	1002	1107.3
Runoff volume	*359.4*	371.7	400.29	431.53
Galas				
Peak discharge	*3010.5*	3112.2	3382.4	3629.9
Runoff volume	*595.9*	605.6	631.42	655.15
Lebir				
Peak discharge	*1724.2*	1811.4	2045	2264.2
Runoff volume	*261.64*	272.83	303	331.15
Kuala Krai				
Peak discharge	*1243.7*	1291.6	1418.9	1535.8
Runoff volume	*461.21*	473.74	507.18	537.99
Guillemard Bridge				
Peak discharge	*12615.2*	13115.6	14447	15668.1
Runoff volume	*3440.23*	3562.67	3889.59	4189.55

References

Abbott M, Bathurst JC, Cunge JA, O'Connell PE, Rasmussen J. 1986. An introduction to the European Hydrological System SHE. II: Structure of a physically-based, distributed modelling system. *Journal of Hydrology* **87**: 61-77.

Abdullah N. 2002. Measurement of technological change biases and factor substitutions for the Malaysian rice farming. *IIUM Journal of Economics and Management* **10**(2): 1-19.

Abdullah R. 2003. Short-term and long-term projection on Malaysian palm oil production. *Oil Palm Industry Economic Journal* **3**(1):32-36.

ADB. Asian Development Bank. 2009. Economics of climate change in Southeast Asia: A Regional Review. Economics and Research Department, Jakarta.

Adnan NA, Atkinson PM. 2010. Exploring the impact of climate and land use changes on streamflow trends in a monsoon catchment. *International Journal of Climatology* **30**. (Published online).

Ajami NK, Gupta H, Wagener T, Sorooshian S. 2004. Calibration of a semi-distributed hydrologic model for stream flow estimation along a river system. *Journal of Hydrology* 298: 112–135.

Ahmad S, Simonovic SP. 2005. An artificial neural network model for generating hydrograph from hydro-meteorological parameters. *Journal of Hydrology* **315** (1-4): 236-251.

Al-Abed N, Abdulla F, Abu Khyarah A. 2004. GIS-hydrological models for managing ater resources in the Zarga River basin. *Environmental Geology* **47**: 405-411.

Al-Abed N, Whitely HR. 2002. Calibration of the hydrological simulation program fortran (HSPF) model using automatic calibration and geographical information systems. *Hydrological Processes* **16(6):** 3169-3188.

Anderson JR, Hardy EE, Roach JT, Witmer RE. 1976. A land use and land cover classification system for use with remote sensor data. U.S. Geological Survey, Professional Paper 964:28.

Anderson TW, Darling DA. 1952. Asymptotic theory of certain "goodness-of-fit" criteria based on stochastic processes. *Annals of Mathematical Statistics* **23**: 193–212.

Arnell NW, Reynard NS. 1996. The effects of climate change due to global warming on river flows in Great Britain. *Journal of Hydrology* **183**: 397-424.

Arora VK. 2001. Streamflow simulations for continental-scale river basins in a global atmospheric general circulation model. *Advances in Water Resources* **24**: 775–791.

Ashagrie AG, De Lat PJM, de Wit MJM, Tu M, Uhlenbrook S. 2006. Detecting the influence of land use changes on disharge and floods in the Meuse River Basin - The predictive power of a ninety-year rainfall-runoff relation? *Journal of Hydrologic and Earth System Sciences* **10**: 691 - 691.

Atan MJ. 2005. Rancangan Fizikal Negara: Pelaksanaan dan Pemantauan, Senior Planners Meeting, Department of Urban and Country Planning, Malaysia, 25 -26 July, Penang, Malaysia.

Awadalla S, Noor IM. 1991. Induced climate change on surface runoff in Kelantan Malaysia. *International Journal of Water Resources Development* **7**: 53 – 59.

Bae DH, Jung IW, Chang H. 2008. Long-term trend of precipitation and runoff in Korean river basins. *Hydrological Processes* **22**: 2644–2656.

Bahar MM, Ohmori H, Yamamuro M. 2008. Relationship between river water quality and land use in a small river basin running through the urbanizing area of central Japan. *Limnology* **9**: 19–26.

Bates PD, Horritt MS, Smith CN, Mason D. 1997. Integrating remote sensing observations of flood hydrology and hydraulic modelling. *Hydrological Processes* **11**(14): 1777-1795.

Bergström S, Carlsson B, Gardelin M, Lindström G, Pettersson A, Rummukainen M. 2001. Climate change impacts on runoff in Sweden- Assessments by global climate models, dynamical downscaling and hydrological modeling. *Climate Research* **16**: 101–112.

Berne A, Delrieu G. 2004. Temporal and spatial resolution of rainfall measurements required for urban hydrology. *Journal of Hydrology* **299**(3-4): 166 - 179.

Beven K. 1997. TOPMODEL: A critique. *Hydrological Processes* **11**(9): 1069-1085.

Bingeman AK, Kouwen N, Soulis ED. 2006. Validation of the hydrological processes in a hydrological model. *Journal of Hydrologic Engineering* **11**(5): 451- 463.

Birsana MV, Molnara P, Burlandoa P, Pfaundler M. 2005. Streamflow trends in Switzerland. *Journal of Hydrology* **314**: 312–329.

Boegh E, Thorsen M, Butts MB, Hansen S, Christiansen JS, Abrahamsen P, Hasager CB, Jensen NO, van der Keur P, Refsgaard JC, Schelde K, Soegaard H, Thomsen A. 2004. Incorporating remote sensing data in physically based distributed agro-hydrological modelling. *Journal of Hydrology* **287**(1-4): 279-299.

Boer R, Dewi RG. 2008. Indonesian Country Report—A Regional review on the economics of climate change in Southeast Asia. Report submitted for RETA 6427: A Regional Review of the Economics of Climate Change in Southeast Asia. Asian Development Bank, Manila. Processed.

Bonan G. 1997. Effects of land use on the climate of the United States. *Climatic Change* **37:** 449–486.

Booij MJ. 2005. Impact of climate change on river flooding assessed with different spatial model resolutions. *Journal of Hydrology* **303**: 176–198.

Bourletsikas A, Baltas E, Mimikou M. 2006. Rainfall-runoff for an experimental watershed of western Greece using extended time-area method and GIS. *Journal of Spatial Hydrology* **6**(1): 93 - 104.

Box GEP, Jenkins GM. 1976. Time series analysis: Forecasting and control, Rev. ed. San Francisco: Holden-Day.

Brivio PA, Colombo R, Maggi M, Tomasoni R. 2002. Integration of remote sensing data and GIS for accurate mapping of flooded areas. *International Journal of Remote Sensing* **23**(3): 429 - 441.

Bronstert A, Niehoff D, Bürger G. 2002. Effects of climate and land-use change on storm runoff generation: Present knowledge and modelling capabilities. *Hydrological Processes* **16**(2): 509-529.

Bronstert A. 2003. Floods and climate change: Interactions and impacts. *Society for Risk Analysis* **23**: 545 - 557.

Buchele B, Kreibich H, Kron A, Thieken A, Ihringer J, Oberle P, Merz B, Nestmann F. 2006. Flood-risk mapping: contributions towards an enhanced assessment of extreme events and associated risks. *Natural Hazards and Earth System Sciences* **6**: 485–503.

Burn DH, Hag Elnur MA. 2002. Detection of hydrologic trends and variability. *Journal of Hydrology* **255**: 107 - 122.

Burtch R. 2002. LiDAR principles and applications. IMAGIN Conference, Traverse City, Mississippi.

Campbell JB. 1996. Introduction to Remote Sensing. The Guildford Press: New York, London.

Chahinian N, Moussa R, Andrieux P, Voltz M. 2005. Comparison of infiltration models to simulate flood events at the field scale. *Journal of Hydrology* **306** (1-4): 191- 214.

Chan NW, Parker DJ. 1996. Response to dynamic flood hazard factors in Peninsular Malaysia. *The Geographical Journal* **162**: 313 - 325.

Chan NW. 1995. Flood disaster management in Malaysia: An evaluation of the effectiveness of government resettlement scheme. *Journal of Disaster Prevention and Management* **4**: 22 - 29.

Chan NW. 1997. Institutional arrangement for flood hazard management in Malaysia: An evaluation using the criteria approach. *Disasters* **21**: 206 - 222.

Chan NW. 2002. Reducing flood hazards exposure and vulnerability in Peninsular Malaysia floods (Edited by Dennis J. Parker). Taylor & Francis Publisher: London.

Chang H. 2007. Comparative streamflow characteristics for urbanizing basins in the Portland metropolitan area, Oregon, USA. *Hydrological Processes* **21**(2): 211–222.

Changnon S, Demissie M. 1996. Detection of change in streamflow and floods resulting from climate fluctuations and land use drainage changes. *Journal of Climate Change* **32**: 411 - 421.

Chaplot V. 2005. Impact of DEM mesh size and soil map scale on SWAT runoff, sediment, and NO3–N loads predictions. *Journal of Hydrology* **312**: 207–222.

Chappell NA, Stewart WF, Larenus J. 1998. Multi-scale permeability estimation for a tropical catchment. *Hydrological Processes* **12**(9): 1507-1523.

Chen Y, Xu Y, Yin Y. 2009. Impacts of land use change scenarios on storm-runoff generation in Xitiaoxi basin, China. *Quaternary International* in Press, Corrected Proof.

Chen YN, Takeuchi K, Xu CC, Chen YP, Xu ZX. 2006. Regional climate change and its effects on river runoff in the Tarim Basin, China. *Hydrological Processes* **20**(10): 2207–2216.

Chen ZQ, Kavvas ML, Ohara N. 2006. Regional hydroclimate model of Peninsular Malaysia. Seminar-Impact of Climate Change on Water Resources, NAHRIM, Kuala Lumpur, July, 2006.

Cheng H, Ouyang W, Hao F, Ren X, Yang S. 2007. The non-point source pollution in livestock-breeding areas of the Heihe River basin in Yellow River. *Stochastic Environmental Research and Risk Assessment* (*SERRA*) **21**(3): 213-221.

Cheng CT, Zhao MY, Chau KW, Wu XY. 2006. Using genetic algorithm and TOPSIS for Xinanjiang model calibration with a single procedure. *Journal of Hydrology* **316**: 129–140.

Cherkauer KA, Sinha T. 2010. Hydrologic impacts of projected future climate change in the Lake Michigan region. *Journal of Great Lakes Research* **36**(2): 33-50.

Cheung WH, Senayb GB, Singha A. 2008.Trends and spatial distribution of annual and seasonal rainfall in Ethiopia. *International Journal of Climatology*. (Published online).

Chiew FHS, Kirono DGC, Kent DM, Frost AJ, Charles SP, Timbal B, Nguyen KC, Fub G. 2010. Comparison of runoff modelled using rainfall from different downscaling methods for historical and future climates. *Journal of Hydrology* **387**: 10–23.

Chiew FHS, Whetton PH, McMahon TA, Pittock AB. 1995. Simulation of the impacts of climate change on runoff and soil moisture in Australian catchments. *Journal of Hydrology* **167**(1-4): 121-147.

Chinvanno S. 2007. Current research on impact, vulnerability and adaptation to climate change in Thailand. URL: http://research.start.or.th/climate index.php?option=com_remository&Itemid=26&func=fileinfo&id=44. Accessed on: 06 August, 2010.

Chinvanno S. 2008. Climate simulation and the impacts on Thailand and the adjeacent areas. Seminar materials for Thailand Research Fund Meeting on Climate Change and the Impacts on Thailand, March 14, 2008. Siam City Hotel, Bangkok.

Chong AL, Chan AL. 1994. Climate change in the East Asian Seas Region in Implications of expected climate changes in East Asian Seas Regions; An overview. Chou LM (eds), RCU/EAS Technical Reports Series No. 2. UNEP 1994 (pp 29-60).

Chow VT, Maidment DR, Mays LW. 1988. Applied Hydrology. McGraw-Hill. New York.

Chu X, Steinman A. 2009. Event and continuous hydrologic modeling with HEC-HMS. *Journal of Irrigation and Drainage Engineering* **135**(1): 119-124.

Chung, ES, Park K, Lee KS. 2010. The relative impacts of climate change and urbanization on the hydrological response of a Korean urban watershed. *Hydrological Processes* (Published online).

Cingolani AM, Renison D, Marcelo RZ, Marcelo RC. 2004. Mapping vegetation in a heterogeneous mountain rangeland using landsat data: An alternative method to define and classify land-cover units. *Remote Sensing of Environment* **92**(1): 84 - 97.

Clark M J. 1998. Putting water in its place: a perspective on GIS in hydrology and water management. *Hydrological Processes* **12**(6): 823-834.

Coleman RA, McAvaney BJ, Wetherald BT. 1994. Sensitivity of the Australian surface hydrology and energy budgets to a doubling of CO2. *Australian Meteorological Magazine* **43**: 105-116.

Collins WD and Coauthors. 2004: Description of the NCAR Community Atmosphere Model (CAM3.0). Technical Note TN-464+STR, National Center for Atmospheric Research, Boulder, CO: 214. [Accessed from: http://www.ccsm.ucar.edu/models/atm-cam.].

Collins WD, Bitz CM, Blackmon ML, Bonan GB, Bretherton CS, Carton JA, Chang P, Doney SC, Hack JJ, Henderson TB, Kiehl JT, Large WG, Mckenna DS, Santer BD, Smith RD.2006: The Community Climate System Model: CCSM3. Journal of Climate 19: 2122–2143.

Cornish PM. 1989. The effect of radiata plantation establishment and management on streamflows and water quality - A review. Forestry Commission of NSW, Technical Paper 49: 1-53.

Croke BFW, Merritt WS, Jakeman AJ. 2004. A dynamic model for predicting hydrological response to land cover changes in gauged and ungauged catchments. *Journal of Hydrology* **291**: 115 - 131.

Crooks S, Davies H. 2001. Assessment of land use change in the Thames catchment and its effect on the flood regime of the river. *Physics and Chemistry of the Earth, Part B: Hydrology, Oceans and Atmosphere* **26**(7-8): 583-591.

Cunderlik JM, Simonovic SP. 2007. Inverse flood risk modelling under changing climatic conditions. *Hydrological Processes* **21**(5): 563-577.

Cuo L, Lettenmaier DP, Alberti M, Richey JE. 2009. Effects of a century of land cover and climate change on the hydrology of the Puget Sound basin. *Hydrological Processes* **23**: 907–933.

Cuong N. 2008. Viet Nam Country Report—A Regional Review on the Economics of Climate Change in Southeast Asia. Report submitted for RETA 6427: A regional review of the economics of climate change in Southeast Asia. Asian Development Bank, Manila. Processed.

Dahlan T, Abdullah SS. 2006. Gunung Stong State Forest Park-Towards the best managed state park. Proceeding Seminar On The Stong State Forest Park Management Plan Towards The Best Managed State Park. Jabatan Perhutanan Negeri Kelantan: 23-39.

Dalzell BJ, Filley TR, Harbor JM. 2005. Flood pulse influences on terrestrial organic matter export from an agricultural watershed. *Journal of Geophysical Resources* **110**: 1 - 14.

De Roo A, Odijk M, Schmuck G, Koster E, Lucieer A. 2001. Assessing the effects of land use changes on floods in the Meuse and Oder Catchment. *Physics and Chemistry of the Earth, Part B: Hydrology* **26**(8): 593-599.

De US, Dube RK, Prakasa Rao GS. 2005. Extreme weather events over India in the last 100 years. *Journal of the Indian Geophysical Union* **9**(3): 173-187.

DeFries R, Eshleman KN. 2004. Land-use change and hydrologic processes: a major focus for the future. *Journal of Hydrological Processes* **18**: 2183–2186.

Delgado JM, Apel H, Merz B. 2010. Flood trends and variability in the Mekong River. *Journal of Hydrology and Earth System Sciences* **14**: 407–418.

DID. 2008. Managing the flood problem in Malaysia [online]. Accessed from: http://www2.water.gov.my/division/drainage/Khidmat%20Kami/Kertas%20Pembentangan/M_Flood/ManagingFlood.htm [Accessed 12 March 2009].

DID. Drainage and Irrigation Department. 1992. Annual flood report of DID for Peninsular Malaysia. Unpublished report. Kuala Lumpur: DID.

DID. Drainage and Irrigation Department. 1995. Annual flood report of DID for Peninsular Malaysia. Unpublished report. Kuala Lumpur: DID.

DID. Drainage and Irrigation Department. 1997. Annual flood report of DID for Peninsular Malaysia. Unpublished report. Kuala Lumpur: DID.

DID. Drainage and Irrigation Department. 2000. Annual flood report of DID for Peninsular Malaysia. Unpublished report. Kuala Lumpur: DID.

DID. Drainage and Irrigation Department. 2003. Annual flood report of DID for Peninsular Malaysia. Unpublished report. Kuala Lumpur: DID.

DID. Drainage and Irrigation Department. 2004. Annual flood report of DID for Peninsular Malaysia. Unpublished report. Kuala Lumpur: DID.

DID. Drainage and Irrigation Department. 2006. Annual flood report of DID for Peninsular Malaysia. Unpublished report. Kuala Lumpur: DID.

DID. Drainage and Irrigation Department. 2008. Annual flood report of DID for Peninsular Malaysia. Unpublished report. Kuala Lumpur: DID.

Dooge JCI. 1992. Hydrologic models and climate change. *Journal of Geophysical Research* **97**(D3): 2677–2686.

Durand P, Gascuel OC, Cordier MO. 2002. Parameterisation of hydrological models : A review and lesson learned from studies of an agricultural catchment (Naizin, France). *Journal of Agronomie* **22**: 217 - 228.

Eckhardt K, Bruer L, Frede HG. 2003. Parameter uncertainty and the significance of simulated land use change effects. *Journal of Hydrology* **273**: 164-176.

Esteban-Parra MJ, Rodrigo FS, Castro-Diez Y. 1998. Spatial and temporal patterns of precipitation in Spain for the period 1880–1992. *International Journal of Climatology* **18**: 1557 - 1574.

FAO. 2005. Global Forest Resources Assessment 2005—Progress towards sustainable forest management. FAO Forestry Paper No. 147. Food and Agriculture Organization, Rome.

Flato GM. 2005. The Third Generation Coupled Global Climate Model (CGCM3). Accessed from: http://www.cccma.bc.ec.gc.ca/models/cgcm3.shtml. [Acessed on 12 June 2010].

Fleming M, Neary V. 2004. Continuous hydrologic modeling study with the hydrologic modeling system. *Journal of Hydrologic Engineering* **9**(3): 175-183.

Fohrer N, Haverkamp S, Eckhardt K, Frede HG. 2001. Hydrologic response to land use change on the catchment scale. *Physical Chemical Earth* **26**: 577- 582.

Foody GM, Ghoneim EM, Arnell NW. 2004. Predicting locations sensitive to flash flooding in an arid environment. *Journal of Hydrology* **292**(1-4): 48-58.

Fowler HJ, Ekström M. 2009. Multi-model ensemble estimates of climate change impacts on UK seasonal precipitation extremes. *International Journal of Climatology* **29**(3): 385-416.

Fowler HJ, Blenkinsop S, Tebaldi C. 2007. Linking climate change modelling to impacts studies: recent advances in downscaling techniques for hydrological modelling. *International Journal of Climatology* **27**: 1547 – 1578.

Fowler HJ, Kilsby CG, O'Connell and PE. 2003. Modeling the impacts of climatic change and variability on the reliability, resilience and vulnerability of a water resource system. *Water Resources Research* **39** (8): 10-1 – 10-11.

Francisco O, Maidment DR. 1999. GIS tools for HMS modeling support. 19th Annual ESRI International User Conference. San Diego, California.

Franke J, Goldberg V, Eichelmann U, Freydank E, Bernhofer C. 2004. Statistical analysis of regional climate trends in Saxony, Germany. *Climate Research* **27**: 145 – 150.

Frei C, Davies HC., Gurtz J, Schär C. 2000. Climate dynamics and extreme precipitation and flood events in Central Europe. *Integrated Assessment* **1**(4): 281-300.

Garbrecht J, Martz LW. Eds. 2000. Hydrologic and hydraulic modeling support with Geographic Information Systems. Digital elevation model issues in water resources modeling, ESRI Inc.

Ghosh S, Mujumdar PP. 2008. Statistical downscaling of GCM simulations to streamflow using relevance vector machine. Advances in Water Resources **31**: 132 – 146.

Githui F, Mutua F, Bauwens W. 2009. Estimating the impacts of land-cover change on runoff using the soil and water assessment tool (SWAT): Case study of Nzoia catchment, Kenya. *Hydrological Science Journal* **54**(5): 889-908.

Goh KJ. 2000. Agronomic requirements and management of oil palm for high yields in Malaysia. Proceeding of the seminar on managing oil palm for high yields: agronomic principles (Goh KJ ed.). Malaysia Society of Soil Science and Param Agriculture Soil Surveys: 39-73.

Gordon HB, Rotstayn LD,McGregor JL, Dix MR, Kowalczyk EA, O'Farrell SP, Waterman LJ, Hirst AC, Wilson SG, Collier MA, Watterson IG, Elliott TI. 2002. The CSIRO Mk3 climate system model. CSIRO Atmospheric Research Technical Paper No. 60, Commonwealth Scientific and Industrial Research Organization Atmospheric Research, Aspendale, Victoria, Australia..Accessed from: http://www.cmar.csiro.au/e-print/ open/gordon_2002a.pdf.[Acessed on 12 June 2010].

Gosling SN, Bretherton D, Haines K, Arnell NW.2010. Global hydrology modelling and uncertainty: running multiple ensembles with a campus grid. *Philosophical Transactions of The Royal Society* **368** (1926): 4005 – 4021.

Grapes TR, Bradley C, Petts GE. 2006. Hydrodynamic of floodplain wetlands in a chalk catchment : The River Lambourn, UK. *Journal of Hydrology* **320**: 324 - 341.

Grothmann T, Reusswig F. 2006. People at risk of flooding: Why some residents take precautionary action while others do not. *Natural Hazards* **38**(1): 101-120.

Gumbricht T, Wolski P, Frost P, McCarthy TS. 2004. Forecasting the spatial extent of the annual flood in the Okavango delta, Botswana. *Journal of Hydrology* **290**:178-191.

Guo QH, Ma KM, Yang L, He K. 2010. Testing a dynamic complex hypothesis in the analysis of land use impact on lake water quality. *Water Resources Management* **24** (7): 1313-1332.

Hai TC. 2000. Land use and the oil palm industry in Malaysia. Abridged report produced for the WWF Forest Information System Database.

Hamby DM. 1994. A review of techniques for parameter sensitivity analysis of environmental models. *Environmental Monitoring and Assessment* **32**(2): 135-154.

Hamzah H. 2005. Roadmap toward effective flood hazard mapping in Malaysia. Ampang, Kuala Lumpur, Department of Irrigation & Drainage. Unpublished report.

Hassan AAG. 2004. Growth, structural change and regional inequality in Malaysia. Ashgate Publishing Ltd: Malaysia.

Haylock MR, Peterson TC, Alves LM, Ambrizzi T, Anunciacao YMT, Baez J, Barros VR, Berlato MA, Bidegain M, Coronel G, Corradi V, Garcia VJ, Grimm AM, Karoly D, Marengo JA, Marino MB, Moncunill DF, Nechet D, Quintana J, Rebello E, Rusticucci M, Santos JL, Trbejo I, Vincent LA. 2005. Trends in total and extreme South

American rainfall in 1960-2000 and links with sea surface temperature. *Journal of Climate* **19**: 1490 - 1512.

Hejazi MI, Markus M. 2009. Impacts of urbanization and climate variability on floods in Northeastern Illinois. *Journal of Hydrologic Engineering* **14**(6): 606-616.

Hellweger FL, Maidment DR. 1999. Definition and connection of hydrologic elements using geographic data. *Journal of Hydrologic Engineering* **4**(1): 10-18.

Hernandez M, Miller SN, Goodrich DC, Goff BF, Kepner WG, Edmonds CM, Jones KB. 2000. Modeling runoff response to land cover and rainfall spatial variability in semi-arid watersheds. *Environmental Monitoring and Assessment* **64**: 285–298.

Hewitson BC, Crane RG. 1996. Climate downscaling: techniques and applications. *Climate Research* **7**: 85 -95.

Hoblit BC, Curtis DC. 2001. Integrating radar rainfall estimates with digital elevation models and land use data to create an accurate hydrologic model. Floodplain Management Association Spring Conference. San Diego, California.

Horritt MS, Bates PD. 2001. Predicting floodplain inundation: Raster-based modelling versus the finite-element approach. *Hydrological Processes* **15**(5): 825-842.

Horritt MS, Mason DC, Luckman AJ. 2001. Flood boundary delineation from Synthetic Aperture Radar imagery using a statistical active contour model. *International Journal of Remote Sensing* **22**(13): 2489–2507.

Imhoff M, Vermillion C, Story MH, Choudhury AM, Gafoor A. 1987. Monsoon flood boundary delineation and damage assessment using space borne imaging radar and Landsat data. *Photogrammetric Engineering and Remote Sensing* **53**: 405-413.

IPCC. 1992. Climate Change: The supplementary report to the IPCC Scientific Assessment. Houghton JT, Callander BA, Varney SV (eds). Cambridge University Press, UK.

IPCC. 1995. Climate Change 1995: The science of climate change, contribution of WGI to the second assessment report of the IPCC, Houghton, JT, Filho LGM, Callander BA, Harris N, Kattenberg A, Maskell K. Cambridge Univ. Press, UK.

IPCC. 1996. Climate Change 1995. Impacts, adaptations and mitigation of climate change: Scientific Technical Analyse*s*, Cambridge University Press, UK.

IPCC. 2001. Climate Change 2001: Impacts, adaptation and vulnerability. A contribution of working groups II to the third assessment report of the Integovernmental Panel on Climate Change [Watson, R.T. and the Core Writing Team (eds.)]. Cambridge University Press, Cambridge, United Kingdom, and New York: New York.

IPCC. 2007. Climate Change 2007: Impacts, adaptation and vulnerability. M. L. Parry, O. F. Canziani, J. P. Palutikof, P. J. van der Linden and C. E. Hanson, eds. Contribution of Working Group II to the Fourth Assessment Report of the Intergovernmental Panel on Climate Change. Cambridge: Cambridge University Press,UK.

Ippoliti-Ramilo GA, Epiphanio JCN, Shimabukuro YE. 2003. Landsat-5 Thematic Mapper data for pre-planting crop area evaluation in tropical countries. *International Journal of Remote Sensing* **24**(7): 1521-1534.

Islam MDR. 2004. A review on watershed delineation using GIS tools. Department of Civil Engineering, University of Manitoba, Winnipeg. www.wrrc.dpri.kyoto-u.ac.jp [Accessed on 15 July 2010].

Islam MM, Sado K. 2000. Development of Flood hazard maps of Bangladesh using NOAA/AVHRR images with GIS. *Journal of Hydrology Science* **45**(3): 337-355.

Ivanov V Y, Vivoni ER, Bras RL, Entekhabi D. 2004. Preserving high-resolution surface and rainfall data in operational-scale basin hydrology: A fully-distributed physically-based approach. *Journal of Hydrology* **298**: 80 - 111.

Jain MK, Singh VP. 2005. DEM-based modelling of surface runoff using diffusion wave equation. *Journal of Hydrology* **302**: 107 - 126.

Jamaliah J. 2007. Emerging trends of urbanization in Malaysia [online]. Acessed from http://www.statistics.gov.my/eng/images/stories/files/journalDOSM/V104_Article_Jam aliah.pdf [Acessed 20 January 2009].

Jensen JR. 1996a. Introductory digital image processing: A remote sensing perspective New Jersey, USA: Prentice-Hall.

Jeyaseelan AT. 2003. Droughts and floods assessment and monitoring using remote sensing and GIS. Satellite remote sensing and GIS applications in agricultural meteorology: 291-313.

Jiang H, Strittholt JR, Frost PA, Slosser NC. 2004. The classification of late seral forests in the Pacific Northwest, USA using Landsat ETM$^+$ imagery. *Remote Sensing of Environment* **91**(3-4): 320-331.

Jiang T, Chen YD, Xu C, Chen X, Chen X, Singh VP. 2007. Comparison of hydrological impacts of climate change simulated by six hydrological models in the Dongjiang Basin, South China. *Journal of Hydrology* **336**(3-4): 316-333.

Jiang T, Zhang Q. 2004. Climatic changes driving on floods in the Yangtze Delta, China during 1000-2002. *Cybergeo: Revue European de Geographie* **296**: 1 − 21.

Johar Z. 2010. Climate change: Potential impacts on water resources and adaptation strategies in Malayis. The first water environment partnership in Asia (WEPA) International Workshop Hanoi Horizon Hotel, Hanoi, Vietnam, 8 − 9 March 2010.

Johns TC and Coauthors. 2006. The new Hadley Centre climate model HadGEM1: Evaluation of coupled simulations. *Journal of Climate*, **19**: 1327–1353.

Jonkman SN, Kelman I. 2005. An analysis of the causes and circumstances of flood disaster deaths. *Disasters* **29**(1): 75-97.

Juckem PF, Hunt RJ, Anderson MP, Robertson DM. 2008. Effects of climate and land management change on streamflow in the driftless area of Wisconsin. *Journal of Hydrology* **355**: 123–130.

Jungclaus JH and Coauthors. 2006. Ocean circulation and tropical variability in the AOGCM ECHAM5/MPI-OM. *Journal of Clim*ate **19**: 3952–3972.

Junk WJ. 1997. The Central Amazon Floodplain: Ecology of a Pulsing System, Springer.

Jusoff K, Senthavy S. 2003. Land use change detection using remote sensing and geographical information system (GIS) in Gua Musang district, Kelantan, Malaysia. *Journal of Tropical Forest Science* **15**(2): 303-312**.**

Kahya E, Kalayci S. 2004. Trend analysis of streamflow in Turkey. *Journal of Hydrology* **289**: 128 - 144.

Kang B, Ramirez JA. 2007. Response of Streamflow to weather variability under climate change in the colorado rockies. *Journal of Hydrologic Engineering* **12**(1): 63-72.

Karabork MC. 2007. Trends in drought patterns of Turkey. *Journal of Environment Engineering Sciences* **6**: 45 - 52.

Kardoulas NG, Bird AC, Lawan AI. 1996. Geometric correction of spot and landsat imagery: A comparison of map and GPS-derived control points. *Photogrammetric Engineering & Remote Sensing* **62**(10): 1173-1177.

Kavvas ML, Chen ZQ, Ohara N, Shaaban AJ, Amin MZM. 2007. Impact of climate change on the hydrology and water resources of Peninsular Malaysia. International Congress on River Basin Management, Turkey, 22-24 March 2007.

Kavvas ML, Chen ZQ, Tan L, Soong ST, Terakawa A, Yoshitani J, Fukami K. 1998. A regional-scale land surface parameterization based on areally-averaged hydrologic conservation equations. *Hydrological Sciences Journal* **43**(4): 611-631.

Kay AL, Jones RG, Reynard NS. 2006. RCM rainfall for UK flood frequency estimation II. Climate change results. *Journal of Hydrology* **318**: 163–172.

Kendall MG. 1975. Rank correlation methods. Griffin London: England.

Kepner WG. Semmens D J, Bassett SD, Mouat DA, Goodrich DC. 2004. Scenario analysis for the San Pedro River, analyzing hydrological consequences of a future environment. *Environmental Monitoring and Assessment* **94**: 115–127.

KFD. Kelantan Forest Department. 2006. Ringkasan awam untuk rancangan pengurusan hutan 2006-2015 bagi negeri Kelantan Darul Naim. Unpublished report. Kelantan.

Kim NW, Lee JW, Lee J, Lee JE. 2010. SWAT application to estimate design runoff curve number for South Korean conditions. *Hydrological Processes* **24**: 2156–2170.

Kim SJ, Flato GM, Boer GJ, McFarlane NA. 2002. A coupled climate model simulation of the Last Glacial Maximum, Part 1: Transient multi-decadal response. *Climate Dynamics* **19**: 515–537.

Knebl MR, Yang ZL, Hutchison K, Maidment DR. 2005. Regional scale flood modeling using NEXRAD rainfall, GIS and HEC-HMS/RAS: A case study for the San Antonio River Basin Summer 2002 storm event. *Journal of Environmental Management* **75**(4): 325-336.

Koutsoyiannis D, Manetas A. 1998. A mathematical framework for studying rainfall intensity-duration-frequency relationships. *Journal of Hydrology* **206**:118-135.

Krause P, Boyle DP, Base F. 2005. Comparison of different efficiency criteria for hydrological model assessment. *Advances in Geosciences* **5**: 89–97.

Kundzewicz Z, Takeuchi K. 1999. Flood protection and management: quo vadimus? *Journal of Hydrological Sciences* **44**(3): 417 − 432.

Lahmer W, Pfutzner B, Becker A. 2001. Assessment of land use and climate change impacts on the mesoscale. *Physics and Chemistry of the Earth, Part B: Hydrology, Oceans and Atmosphere* **26**(7-8): 565-575.

Lambert SJ, Boer GJ. 2001. CMIP1 evaluation and intercomparison of coupled climate models. *Climate Dynamics* **17**: 83–106.

Lawton RO, Nair US, Pielke SRA, Welch RM. 2001. Climatic impact of tropical lowland deforestation on nearby montane cloud forests. *Science* **294**: 584-587.

Legesse D, Christine VC, Françoise G. 2003. Hydrological response of a catchment to climate and land use changes in Tropical Africa: Case study South Central Ethiopia. *Journal of Hydrology* **275**(1-2): 67-85.

Li Z, Liu W, Zhang X, Zheng F. 2009. Impacts of land use change and climate variability on hydrology in an agricultural catchment on the Loess Plateau of China. *Journal of Hydrology* **377**: 35–42.

Lillesan TM, Kiefer RW. 2000. Remote sensing and image interpretation (4th Edition). New York: Wiley.

Lin YP, Lin YB, Wang YT, Hong NM. 2008. Monitoring and predicting land-use changes and the hydrology of the urbanized Paochiao watershed in Taiwan using remote sensing data, urban growth models and a hydrological model. *Sensors* **8**(2): 658-680.

Lipscomb WH. 2001. Remapping the thickness distribution in sea ice models. *Journal of Geophysical Resources* **106**: 13989–14000.

Liu QQ, Singh VP. 2004. Effect of microtopography, slope length and gradient and vegetative cover on overland flow through simulation. *Journal of Hydrologic Engineering* **9**(5): 375 -382.

Longobardi A, Villani P. 2009. Trend analysis of annual and seasonal rainfall time series in the Mediterranean area. *International Journal of Climatology*. Published online.

López-Moreno JI, Beguería S, García-Ruiz JM. 2006. Trends in high flows in the Central Spanish Pyrenees: Response to climatic factors or to land-use change? *Journal of Hydrological Sciences* **51**(6): 1039 – 1050.

Mahasim NW, Saat A, Hamzah Z, Sohari RR, Khali KHA. 2005. Nitrate and Phosphate Contents and Quality of well water in North-Eastern Districts of Kelantan. Simposium Sains Analisis Malaysia ke-18 (SKAM18), 12-14 September 2005, Johor Bharu, Malaysia. (Unpublished report).

Malaysia Department of Statistics. 2000. 2000 population and housing cencus of Malaysia: Preliminary count report. Unpublished report. Kuala Lumpur, Malaysia.

Malaysia Department of Statistics. 2006. Labour force survey report: Malaysia *2003*. Unpublished report. Kuala Lumpur, Malaysia.

Malaysia National Committee. 1979. Flood control in Malaysia, in Framji KK and Garg BC (Eds). Flood control in the world: A global review. International Commission on Irrigation and Drainage, New Delhi 2: 561 - 569.

Malaysian Water Association (MWA). 2004. Malaysian water industry guide 2004. Unpublished report. Kuala Lumpur.

Malek MA, Harun S, Shamsuddin SM, Mohamad I. 2009. Reconstruction of missing daily rainfall datausingunsupervised artificial neural network. *International Journal of Electrical and Computer Engineering* **4**(6): 340 – 345.

Mann HB. 1945. Non-parametric tests against trend. *Econometrica* **13**: 245 – 259.

Marengo JA, Jones R, Alves LM, Valverde MC. 2009. Future change of temperature and precipitation extremes in South America as derived from the PRECIS regional climate modeling system. *International Journal of Climatology* **29**(15): 2241-2255.

Marengo J, Ambrizzi T. 2006. Use of regional climate models in impacts assessments and adaptations studies from continental to regional and local scales: The CREAS (Regional Climate Change Scenarios for South America) initiative in South America. *Proceedings of 8 ICSHMO*, Foz do Igua¸cu, Brazil, April 24–28, 2006, 291–296.

Mays LW. 2001. Stormwater collection systems design handbook, McGraw-Hill. New York.

Maurer EP, Duffy PB. 2005. Uncertainty in projections of streamflow changes due to climate change in California. *Geophysical Research Letters* **32**: 1 − 5.

Mbano D, Chinseu J, Ngongondo C, Sambo E, Mul M. 2009. Impacts of rainfall and forest cover change on runoff in small catchments: A case study of Mulunguzi and Namadzi catchment areas in southern Malawi. *Malawi Journal of Sciences & Technology* **9**(1): 11-17.

McColl C, Aggett G. 2007. Land-use forecasting and hydrologic model integration for improved land-use decision support. *Journal of Environmental Management* **84**(4): 494-512.

McCuen RH. 1982. A guide to hydrologic analysis using SCS methods. Prentice Hall, Englewood-Cliffs, NJ.

Mitchell JFB. 1989. The greenhouse effect and climatic change. *Reviews of Geophysics* **29**: 115-139.

Meehl GA, Zwiers F, Evans J, Knutson T, Mearns L, Whetton P. 2000. Trends in extreme weather and climate events: Issues related to modeling extremes in projections of future climate change. *Bulletin of the American Meteorological Society*: 427 - 436.

Mertes LAK. 2000. Flood processes and effects: Inundation hydrology. Inland flood hazards: human, riparian and aquatic. Wohl EE, Cambridge University Press, UK.

Miller NS, William GK, Megan H, Mehaffey MH, Ryan CM, David CG, Kim KD, Daniel TH, Miller WP. 2002. *Integrating Landscape Assessment and Hydrologic Modeling for Land Cover Change Analysis* **38**(4): 915-929.

MMD. 2007. Malaysian Meteorological Department (MMD). Report on heavy rainfall that caused floods in Kelantan & Terengganu. Unpublished report. Kuala Lumpur : MMD.

MMD. 2009. Malaysian Meteorological Department (MMD). Climate change scenarios for Malaysia 2001-2099. Scientific report January 2009. Unpublished report. Kuala Lumpur : MMD.

Modarres R, Paulo RSV. 2007. Rainfall trends in Arid and semi-arid regions of Iran. *Journal of Arid Environment* **70**: 344 - 355.

Moghadas S. 2009. Master of Science Thesis in Water Resources Division of Water Resources. Lund Institute of Technology, Lund University.

Moliová H, Grimaldi M, Bonell M ,Hubert P. 1997. Using TOPMODEL towards identifying and modelling the hydrological patterns within a headwater, humid, tropical catchment. *Hydrological Processes* **11**(9): 1169-1196.

Montanari L, Sivapalan M, Montanari A. 2006. Investigation of dominant hydrological process in a tropical catchment in monsoonal climate via the download approach. *Journal of Hydrology and Earth System Sciences* **10**: 769 - 782.

Moriasi DN, Arnold JG, Van Liew MW, Bingner RL, Harmel RD, Veith TL. 2007. Model evaluation guidelines for systematic quantification of accuracy in watershed simulations.*Transactions of the American Society of Agricultural and Biological Engineers* **50**(3): 885-900.

Moussa R, Voltz M, Andrieux P. 2002. Effects of the spatial organization of agricultural management on the hydrological behaviour of a farmed catchment during flood events. *Hydrological Processes* **16**(2): 393 - 412.

Murphy JM. 2000. Predictions of climate change over Europe using statistical and dynamical downscaling techniques. *International Journal of Climatology* **20**: 489 – 501.

Murphy JM. 1999. An evaluation of statistical and dynamical techniques for downscaling local climate. *Journal of Climate* **12**: 2256 – 2284.

Mustafa YM, Amin MSM. 2005. Evaluation of land development impact on a tropical watershed hydrology using remote sensing and GIS. *Journal of Spatial Hydrology* **5**(2): 16 - 30.

Nash JE, Sutcliffe JV. 1970. River flow forecasting through conceptual models part I — A discussion of principles. *Journal of Hydrology* **10**(3): 282–290.

Nawaz F. 2001. Data integration for flood risk analysis by using GIS/RS as tools. Map India 2001, New Delhi, India, 7 – 9 February 2001.

Nearing MA, Jetten V**,** Baffaut C, Cerdan O, Couturier A, Hernandez M, Bissonnais YL, Nichols MH, Nunes JP, Renschler CS, Souchere V, Oost KV. 2005. Modeling response of soil erosion and runoff to changes in precipitation and cover. *Catena* **61**: 131-154.

Ng HYF, Marsalek J. 1992. Sensitivity of streamflow simulation to changes in climatic inputs. *Nordic Hydrol.* **23**: 257–272.

Niehoff D, Fritsch U, Bronstert A. 2002. Land-use impacts on storm-runoff generation: scenarios of land-use change and simulation of hydrological response in a meso-scale catchment in SW-Germany. *Journal of Hydrology* **267**: 80 - 93.

Nik AR. 1988. Water yield changes after forest conversion to agricultural landuse in Peninsular Malaysia. *Journal of Tropical Forest Science* **1**(1): 67 - 84.

Ntegeka V, Willems P. 2007. Climate change impact on hydrological extremes along rivers and urban drainage systems in Belgium. Interim Report of Royal Meteorological Institute of Belgium.

Nurmohamed R, Naipal S De Smedt F. 2006. Hydrologic modeling of the Upper Suriname River basin using WetSpa and ArcView GIS. *Journal of Spatial Hydrology* **6**: 1-17.

Nyarko BK. 2002. Application of a rational model in GIS for flood risk assessment in Accra, Ghana. *Journal of Spatial Hydrology* **2**(1): 14-28.

O'Connell PE, Ewan J, O'Donnell G, Quinn PF. 2007. Is there a link between agricultural land-use management and flooding? *Hydrology and Earth System Sciences* **11**: 96–107.

Olivera F, Bao J, Maidment DR. 1997. Geographic information system for hydrologic data development for design of highway drainage facilities. Research Report 1738(3). Center for Transportation Research - University of Texas at Austin, TX.

Olivera F, Maidment DR. 1998a. HEC-PrePro v. 2.0: An ArcView pre-processor for HEC's hydrologic modeling system. Proceedings of the 18th ESRI Users Conference, San Diego, CA.

Onoz B, Bayazit M. 2003. The power of statistical tests for trend detection. *Turkish Journal of Engineering and Environmental Sciences* **27**: 247–251.

Ormsby JP, Blanchart BJ, Blanchard AJ. 1985. Detection of lowland flooding using active microwave systems. *Journal of Photogrammetric Engineering and Remote Sensing* **51**: 317-328.

Oudin L, Andreassian V, Lerat J, Michel C. 2008. Has land cover a significant impact on mean annual streamflow? An International Assessment using 1508 Catchments. *Journal of Hydrology* **357**: 303 - 316.

Paramanthan S. 2000. Soil requirements of oil palm for high yields. Proc. of the Seminar on Managing Oil Palm for High Yields: Agronomic Principles. Malaysian Society of Soil Science & Param Agriculture Soil Surveys: 18-38.

Parry ML, Magalhaes AR, Nih NH. 1992. The potential socio-economic effects of climate change: A summary of three regional assessments. Nairobi, Kenya: United Nations Environment Programme (UNEP).

Perez R. 2008. Philippines country report—A regional review on the economics of climate change in Southeast Asia. Report submitted for RETA 6427: A regional review of the economics of climate change in Southeast Asia. Asian Development Bank, Manila. Processed.

Perrin C, Michel C, Andréassian V. 2001. Does a large number of parameters enhance model performance? Comparative assessment of common catchment model structures on 429 catchments. *Journal of Hydrology* **242**(3-4): 275-301.

Pielke RA, Marland SG, Betts RA, Chase TN, Eastman JL, Niles JO, Niyogi DS, Running SW. 2002. The influence of land-use change and landscape dynamics on the climate system: Relevance to climate-change policy beyond the radiative effect of greenhouse gases. *Philosophical Transactions of the Royal Society* **360**: 1705-1719.

Pinter N, van der Ploeg RR, Schweigert P, Hoefer G. 2006. Flood magnification on the River Rhine. *Journal of Hydrological Processes* **20**: 147–164.

PPLRNK. 2007. Oil Palm Estates [online]. Acessed from: http://www.pplrnk.gov.my/index.php?option=com_content&task=view&id=17&Itemid =31[Accessed 10 February/2009].

Pramanik MAH, Murai S. 1992. Flood studies in Asia by Remote Sensing. Asia Conference in Remote Sensing, Ulaanbaatar, Mongolia, 7 – 11 October 1992.

Price K, Guo X, Stiles JM. 2002. Optimal Landsat TM band and vegetation indices for discrimination of six grassland types in eastern Kansas. *International Journal of Remote Sensing* **23**: 5031 - 5042.

Pope VD, Stratton RA. 2002. The processes governing horizontal resolution sensitivity in a climate model. Climate Dynamics 19: 211–236.

Prowse TD, Beltaos S, Gardner JT, Gibson JJ, Granger RJ, Leconte R,Reters DL, Pietroniro A, Romolo LA, Toth B. 2006. Climate change, flow regulation and land-use effects on the hydrology of the Peace-Athabasca-Slave system: Findings from the northern rivers ecosysteminitiative. *Environmental Monitoring and Assessment* **113**: 167–197.

Prudhomme C, Reynard N, Crooks S. 2002. Downscaling of global climate models for flood frequency analysis: Where are we now? *Hydrological Processes* **16**: 1137 -1150.

Prudhomme C, Davies H. 2005. Comparison of different sources of uncertainty in climate change impact studies in Great Britain. Workshop of Climatic and Anthropogenic Impacts on Water Resources Variability, Montpellier, 22 – 24 November 2005.

Quinn P, Beven K, Chevallier P, Planchon O. 1991. The prediction of hillslope flow paths for distributed hydrological modelling using digital terrain models. *Hydrological Processes* **5**: 59-79.

Rahimzadeh F, Asgari A, Fattahi E. 2008. Variability of extreme temperature and precipitation in Iran during recent decades. *International Journal of Climatology*. Published online.

Rango A, Anderson A. 1974. Flood hazard studies in the Mississippi River basin using remote sensing. *Water Resources Bulletin* **10**(5): 1060-1081.

Razi MAM, Ariffin J, Tahir W, Arish NAM. 2010. Flood estimation studies using Hydrologic Modelling System (HEC-HMS) for Johor River, Malaysia. *Journal of Applied Sciences* **10**(11): 930-939.

Reed S, Koren V, Smith M, Zhang Z, Moreda F, Seo D-J. Overall distributed model intercomparison project results. *Journal of Hydrology* **298**: 27–60.

Reynard NS, Prudhomme C, Crooks SM. 2001. The flood characteristics of large U.K. Rivers: Potential effects of changing climate and land use. *Climatic Change* **48**(2): 343-359.

Riaño D, Chuvieco E, Salas J, Aguado I. 2003. Assessment of different topographic corrections in Landsat-TM data for mapping vegetation types. *IEEE Transactions on Geoscience and Remote Sensing* **41**(5): 1056 – 1061.

Roeckner E and Coauthors. 2003. The Atmospheric General Circulation Model ECHAM5. Part I: Model Description. MPI Report 349, Max Planck Institute for Meteorology, Hamburg, Germany: 127.

Rumman N, Lin G, Li J. 2005. Investigation of GIS-based surface hydrological modelling for identifying infiltration zones in an urban watershed. *Environmental Informatics Archives* **3**: 315 – 322.

Saghafian B, Farazjoo H, Bozorgy B, Yazdandoost F. 2008. Flood Intensification due to Changes in Land Use. *Water Resources Management* **22**(8): 1051-1067.

Saghafian B. 1996. Implementation of a distributed hydrologic model within GRASS in GIS and environmental modeling: Progress and research issues. (Editted by Goodchild MF, L. T. Steyaert, B. O. Parks, C. Johnston, D. Maidment, M. Crane, and S. Glendinning. GIS World Books, Fort Collins, Colo.

Salmi T. 2002. Trend analysis of air quality monitoring data using Mann-Kendall tests [online]. http://www.nilu.no/projects/ccc/tfmm/geneva3/reports/TSalmi.ppt. [Accessed 20 January 2009].

Saltelli A, Tarantola S, Campolongo F, Ratto M. 2004. Sensitivity analysis in practice: A guide to assessing scientific models. John Wiley &Sons, Chicester.

Samat N. 2006. Applications of Geographic Information Systems in urban land use planning in Malaysia. The 4th Taipei International Conference on Digital Earth, 25-26 May 2006, Taipei.

Scawthorn C, Flores P, Blais N, Seligson H, Tate E. 2006. HAZUS-HM flood loss estimation methodology. 1: Overview and flood Hazard Characterization. *Natural Hazards Review* **7**(2): 39-103.

Schmidli J, Frei C, Vidale PL. 2006. Downscaling from GCM precipitation : A benchmark for dynamical and statistical downscaling methods. *International Journal of Climatology* **26** (5): 679 – 689.

Schmugge TJ, Kustas WP, Ritchie JC, Jackson TJ, Rango A. 2002. Remote sensing in hydrology. *Advances in Water Resources* **25**(8-12): 1367-1385.

Schultz G. 1988. Remote Sensing in hydrology. *Journal of Hydrology* **100**: 239-265.

Schulze RE. 2000. Modelling hydrological responses to land use and climate change: A Southern African perspective. AMBIO: *Journal of the Human Environment* **29**(1): 12-23.

Segond ML, Wheater HS, Onof C. 2007. The significance of spatial rainfall representation for flood runoff estimation: A numerical evaluation based on the Lee catchment, UK. *Journal of Hydrology* **347**(1-2): 116-131.

Seth SM. 1999. Physically based hydrological modelling. Map India Conference, New Delhi, India, 24-26 August 1999.

Shaaban AJ. 2008. Climate change for Malaysia scenario. Second National Conference on Extreme Weather and Climate Change: Understanding Science and Risk Reduction. Putrajaya International Convention Centre, Kuala Lumpur, Malaysia.

Shafiee M, Ahmad A, Hassan F, Yaakub MA, Sing LK, Fatt CS, Dom NM, Samsinar NA, Osman S, Hashim Z, Amin MZM, Aun TS. 2004. Development of an operational monsoon flood management system. The 3rd National Microwave Remote Sensing Seminar. MACRES, Kuala Lumpur.

Shaw G, Wheeler D. 1985. Statistical techniques in geographical analysis. John Wiley & Son.

Shibasaki R, Ochi S. 1998. Development of I km drainage model based on GTOPO 30 and global data sets. Asia Conference on Remote Sensing, Manila, 16 – 20 November 1998.

Smith LC. 1997. Satellite remote sensing of river inundation area, stage, and discharge: a review. *Hydrological Processes* **11**(10): 1427-1439.

Smith D, Gent PR. 2002. Reference Manual for the Parallel Ocean Program (POP), Ocean Component of the Community Climate System Model (CCSM2.0 and 3.0). Technical Report LA-UR-02-2484, Los Alamos National Laboratory, Los Alamos, NM, Accessed from:http://www.ccsm.ucar.edu/models/ccsm3.0/pop/.[Acessed on 12 June 2010].

Soil Conservation Service. 1986. Urban hydrology for small watersheds. Technical Report 55, U.S. Department of Agriculture Soil Conservation Service. Springfield, VA.

Song C, Woodcock CE, Seto KC, Lenney MP, Macomber SA. 2001. Classification and change detection using Landsat TM data: When and how to correct atmospheric effects? *Remote Sensing of Environment* **75**(2): 230-244.

Sooryanarayana V. 1988. Floods in Malaysia. The working group on tropical climatology and human settlements, the 26th Congress of The International Geographical Union, New South Wales, Australia, 21–26 August 1988.

Tangang FT, Juneng L, Ahmad S. 2007. Trend and interannual variability of temperature in Malaysia: 1961-2002. *Theoretical and Applied Climatology* **89**: 127 - 141.

Tapsell SM, Penning-Rowsell EC, Tunstall SM, Wilson TL. 2002. Vulnerability to flooding: Health and social dimensions. *Philosophical Transactions of the Royal Society of London. Series A: Mathematical, Physical and Engineering Sciences* **360**(1796): 1511-1525.

Tholey N, Clandillon S, Fraipont PD. 1997. The contribution of spaceborne SAR and optical data in monitoring flood events: Examples in northern and southern France. *Hydrological Processes* **11**(10): 1409-1413.

Thompson JP, Polet G. 2000. Hydrology and land use in a Sahelian floodplain Wetland. *Wetlands* **20**(4): 639-659.

Tollan A. 2002. Land-use change and floods: what do we need most, research or management? *Water Science and Technology* **45**(8): 183–190.

Toutin T. 2004. Review article: Geometric processing of remote sensing images: models, algorithms and methods. *International Journal of Remote Sensing* **25** (10): 1893-1924.

Townsend PA, Walsh SJ. 1998. Modeling floodplain inundation using an integrated GIS with radar and optical remote sensing. *Journal of Geomorphology* **21**(3): 295-312.

Trigo RM, Palutikof JP. 2001. Precipitation scenarios over Iberia: A comparison between direct GCM output and different downscaling techniques. *Journal of Climate* **14**: 4422–4446.

Tso BCK, Mather PM. 1999. Classification of multisource remote sensing imagery using agenetic algorithm and Markov random fields. *Geoscience and Remote Sensing IEEE* **37**(3): 1255-1260.

UNEP/GRID-Arendal. 2005. Climate change: processes, characteristics and threats. UNEP/GRID-Arendal Maps and Graphics Library. http://maps.grida.no/go/graphic/climate_change_processes_characteristics_and_threas [Accessed 15 July 2010].

United States Department of Agriculture (USDA). 1986. Urban Hydrology for Small Watersheds. Technical Release 55 (TR-55) - Soil Conservation Service, Engineering Division. USDA, Washington, DC, USA.

USACE. 2000. HEC-HMS hydrologic modeling system user's manual. Hydrologic Engineering Center, Davis, California.

USACE. 2000b. Geospatial Hydrologic Modeling Extension HEC-GeoHMS. User's Manual, Version 1.0.US Army Corps of Engineers, Hydrologic Engineering Center, Davis, California.

USACE. 2008. HEC-HMS hydrologic modeling system user's manual. Hydrologic Engineering Center, Davis, California.

Van Deursen WPA, Middelkoop H. 2002. Development of flood management strategies for the Rhine and Meuse basins in the context of integrated river management. Executive summary of the IRMA-SPONGE project 2. In IRMA-SPONGE. Towards Sustainable Flood Risk Management in the Rhine and Meuse River Basins, Hooijer A, van Os A (eds). NCR Publication 18-2002.

Vandaele K, Poesen J. 1995. Spatial and temporal patterns of soil erosion rates in an agricultural catchment, central Belgium. *CATENA* **25**(1-4): 213-226.

Verma AK, Jha MK, Mahana RK. 2009. Evaluation of HEC-HMS and WEPP for simulating watershed runoff using remote sensing and geographical information system. *Paddy Water Environment* (Published online).

Vertessy RA. 2000. Impacts of Plantation Forestry on Catchment Runoff Proceedings of a National Workshop, Melbourne, 20-21 July 2000.

Walsh CL, Kilsby CG. 2007. Implications of climate change on flow regime affecting Atlantic salmon. *Hydrology and Earth System Science* **11**(3): 1127-1143.

Wan I. 1996. Urban growth determinants for the state of Kelantan of the state's policy makers. Penerbitan Akademik Fakulti Kejuruteraan dan Sains Geoinformasi. *Buletin Ukur* **7**: 176 - 189.

Wang S, Kang S, Zhang L, Li F. 2008. Modelling hydrological response to different land-use and climate change scenarios in the Zamu River basin of northwest China. *Hydrological Processes* **22**: 2502-2510.

Wang X, Yin ZY. 1998. A comparison of drainage networks derived from digital elevation models at two scales. *Journal of Hydrology* **210**: 221-241.

Ward PJ, Renssen H, Aerts JCJH, Van Balen RT, Vandenberghe J. 2007. Strong increases in flood frequency and discharge of the River Meuse over the late Holocene: Impacts of long-term anthropogenic land use change and climate variability. *Hydrology and Earth System Sciences* **4**: 2521-2560.

Whetton PH, Pittock AB. 1991. Australian region intercomparison of the results of some general circulation models used in enhanced greenhouse experiments. CSIRO Division of Atmospheric Research, Aspendale, Vic. Technical Paper 21: 73.

White I, Howe J. 2004. The mismanagement of surface water. *Applied Geography* **24**: 261 - 280.

Wilby RL, Wigley TML. 1997. Downscaling general circulation model output: a review of methods and limitations. *Progress in Physical Geography* 21: 530–548.

Wilson MD. 2004. Evaluating the effect of data and data uncertainty on predictions of flood inundation. School of Geography, Faculty of Engineering, Science and Mathematics. Southampton, University of Southampton. Doctor of Philosophy: 251.

Winsemius HC, Savenije HHG, Gerrits AMJ, Zapreeva EA, Klees R. 2005. Comparison of two model approaches in the Zambezi river basin with regard to model realibility and identifiability. *Journal of Hydrologic and Earth System Sciences* **10**: 339-352.

Wohl EE. 2000. Inland flood hazards: human, riparian, and aquatic communities. Cambridge University Press.

Wooldridge S, Kalma J, Kuczera G. 2001. Parameterisation of a simple semi-distributed model for assessing the impact of land-use on hydrologic response. *Journal of Hydrology* **254**: 16-32.

Wright SJ. 2005. Tropical forests in a changing environment. *Trends in Ecology & Evolution* **20**(10): 553-560.

Wurbs R, Toneatti S, Sherwin J. 2001. Modelling uncertainty in flood studies. *International Journal of Water Resources Development* **17**(3): 353-363.
Xia J, Wang ZG, Wang GS, Tan G. 2004. The renewability of water resources and its quantification in the Yellow River basin, China. *Hydrological Processes* **18**(12): 2327-2336.

Xiaoming Z, Xinxiao Y, Manliang Z, Jianlao L. 2007. Response of land use/coverage change to hydrological dynamics at watershed scale in the Loess Plateau of China. *Acta Ecologica Sinica* **27**: 414-421.

Xu ZX, Takeuchi K, Ishidaira H, Li JY. 2005. Long-term trend analysis for precipitation in Asian Pacific FRIEND river basins. *Hydrological Processes* **19**: 3517-3532.

Yao H, Hashino M, Xia J, Chen X. 2009. Runoff reduction by forest growth in Hiji River basin, Japan. *Journal of Hydrological Sciences* **54**(3): 556-570.

Yimer G, Jonoski A, Griensven AV. 2009. Hydrological response of a catchment to climate change in the Upper Beles River Basin, Upper Blue Nile, Ethiopia. *Nile Basin Water Engineering Scientific Magazine: Special Issue on Climate and Water* **2**: 49-59

Yu DS, Shi XZ, Wang HJ, Zhang XY, Weindorf DC. 2008. Function of soils in regulating rainwater in southern China: Impacts of land uses and soils. *Pedosphere* **18**(6): 717-730.

Yu PS, Yang TC, Chen SJ. 2001. Comparison of uncertainty analysis methods for a distributed rainfall-runoff model. *Journal of Hydrology* **244**(1-2): 43-59.

Yu YS, Zou S, Whittemore D. 1993. Non-parametric trend analysis of water quality data of river in Kansas. *Journal of Hydrology* **150**(1): 61-80.

Yukimoto S, Noda A. 2003. Improvements of the Meteorological Research Institute Global Ocean-Atmosphere Coupled GCM (MRIGCM2) and its climate sensitivity. CGER's Supercomputing Activity Report, National Institute for Environmental Studies, Ibaraki, Japan

Yusop Z, Chan CH, Katimon A. 2007. Runoff characteristics and application of HEC-HMS for modelling stormflow hydrograph in oil palm catchment. *Journal of Water Science & Technology* **56**(8): 41–48.

Zakaria AS. 1975. The geomorphology of Kelantan delta (Malaysia). *CATENA* **2**: 37-350.

Zakaria S, San LY. 2008. Climate change and water resources management in Malaysia. 2nd National Conference on Extreme Weather and Climate Change, PICC, Putrajaya, 14-15 October 2008.

Zehe E, Singh AK, Bardossy A. 2006. Modelling of monsoon rainfall for a mesoscale catchment in North-West India II: stochastic rainfall simulations. *Journal of Hydrology & Earth System Sciences* **10**: 807-815.

Zorita E, Storch HV. 1999: The analog method as a simple statistical downscaling technique: Comparison with more complicated methods. *Journal of Climate* **12**: 2474–2489.

Zulkarnain MAR, Alkema D. 2006. Digital Surface Model (DSM) construction and flood hazard simulation for development plans in Naga City, Philippines. Map Asia 2006, Queen Sirikit National Convention Center, Bangkok, Thailand, 29 August – 1 September 2006.

Zwenzner H, Voigt S. 2009. Improved estimation of flood parameters by combining space based SAR data with very high resolution digital elevation data. *Hydrology and Earth System Sciences* **13**(5): 567-576.